AFML-TR-69-244
PART I

add - 14.

A QUANTITATIVE EVALUATION OF TEST METHODS FOR BRITTLE MATERIALS

C. D. PEARS

H. S. STARRETT

ROY E. BICKELHAUPT

DAN W. BRASWELL

Southern Research Institute

TECHNICAL REPORT AFML-TR-69-244, PART I

MARCH 1970

AIR FORCE MATERIALS LABORATORY
AIR FORCE SYSTEMS COMMAND
WRIGHT-PATTERSON AIR FORCE BASE, OHIO

229

DISCLAIMER NOTICE

THIS DOCUMENT IS BEST QUALITY PRACTICABLE. THE COPY FURNISHED TO DTIC CONTAINED A SIGNIFICANT NUMBER OF PAGES WHICH DO NOT REPRODUCE LEGIBLY.

NOTICES

When Government drawings, specifications, or other data are used for any purpose other than in connection with a definitely related Government procurement operation, the United States Government thereby incurs no responsibility nor any obligation whatsoever; and the fact that the Government may have formulated, furnished, or in any way supplied the said drawings, specifications, or other data is not to be regarded by implication or otherwise as in any manner licensing the holder or any other person or corporation, or conveying any rights or permission to manufacture, use, or sell any patented invention that may in any way be related thereto.

This document is subject to special export controls and each transmittal to foreign governments or foreign nationals may be made only with prior approval of the Metals and Ceramics Division (MAM), Air Force Materials Laboratory, Wright-Patterson Air Force Base, Ohio 45433.

Protection of Technical Know-How relating to materials manufacturing processes.

Copies of this report should not be returned to the Air Force Systems Command unless return is required by security considerations, contractual obligations, or notice on a specific document.

A QUANTITATIVE EVALUATION OF TEST METHODS FOR BRITTLE MATERIALS

C. D. PEARS

H. S. STARRETT

ROY E. BICKELHAUPT

DAN W. BRASWELL
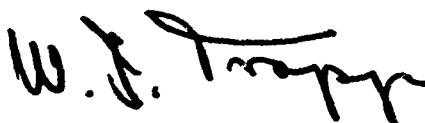
Southern Research Institute

FOREWORD

This report was prepared by Southern Research Institute under USAF Contract No. AF 33(615)-3265. This contract was initiated under Project No. 7350, "Refractory Inorganic Nonmetallic Materials," Task No. 735003, "Theory and Mechanical Phenomena." The work was administered under the direction of the Air Force Materials Laboratory, Air Force Systems Command, Wright-Patterson Air Force Base, Ohio, with Mr. G. R. Atkins (MAMD), acting as project engineer.

This report covers work conducted from 15 April 1966 to 1 July 1969.

The manuscript of this report was released by the authors August 1969 for publication.

This technical report has been reviewed and is approved.

W. J. TRAPP
Chief, Strength and Dynamics Branch
Metals and Ceramics Division
Air Force Materials Laborabory

ABSTRACT

This report covers the work completed under a preliminary phase of a program to perform a quantitative evaluation of test methods for brittle materials. This phase involved a production control study to demonstrate that a ceramic material produced in a variety of specimen configurations has uniform strength, microstructure, and density. This report includes most of the data generated to date and some preliminary analysis. More extensive analyses will be conducted and additional data generated where required.

Of the 13 blank types investigated, 10 demonstrated acceptable uniformity and reproducibility, one requires minor modifications, and two require additional work.

The only variables which correlated with strength on first inspection were fired density and a production figure of merit. There was not sufficient data to determine whether a strength-grain size correlation existed. Micro specimen fractology showed that the stronger specimens usually had the rougher, more undulating fracture surfaces.

With this material it should be possible to conduct an effective analysis of test methods; however, some additional definition of the material is required.

TABLE OF CONTENTS

TABLE OF CONTENTS-(Continued)

TABLE OF CONTENTS-(Continued)

LIST OF ILLUSTRATIONS

vii

LIST OF ILLUSTRATIONS-(Continued)

LIST OF ILLUSTRATIONS-(Continued)

ix

LIST OF ILLUSTRATIONS-(Continued)

LIST OF ILLUSTRATIONS-(Continued)

LIST OF ILLUSTRATIONS-(Continued)

LIST OF TABLES

A QUANTITATIVE EVALUATION OF TEST METHODS
FOR BRITTLE MATERIALS

INTRODUCTION

This is the summary progress report under Contract No. AF 33(615)-3265 to perform a quantitative evaluation of test methods for brittle materials and includes an exploration of the relationship between tensile and compressive properties and the flexural response. This report covers the work completed under Phase I of this program. Phase I involved a production control study to demonstrate that a ceramic material as produced for various specimen configurations is uniform in strength, microstructure, and density. To evaluate for uniformity of strength, tensile and flexural evaluations were used.

BACKGROUND

Many, if not most, brittle materials exhibit a somewhat different response to tensile, flexural, and compressive loads as well as when loaded as a disc (Brazil test), a thick ring or a thin ring. For example, the tensile and compressive fracture strengths often differ by a factor of 2 and can differ by a factor of 10 or more. Modulus of Rupture values of $1\frac{1}{2}$ to 3 times the measured tensile strengths are frequently reported in the literature. It is possible to conceive physical models to explain the difference in response of a material to tensile and compressive loads; however, it is more difficult to conceive a model that will explain any gross departure of MOR values from ultimate tensile strength. Generally, brittle materials are characterized as being governed by a weakest link fracture mechanism such that cracks initiate and/or propagate to fracture as soon as the stress in any localized region of the stressed material reaches the ultimate value. Evidence thus far obtained indicates that brittle materials are weakest in tension; consequently, one would expect flexural specimens to fracture when the extreme outer fibers reached the ultimate in tension.

For quite some time Southern Research Institute has been interested in determining the causes for the discrepancies in reported strengths. We have felt that at least a portion of the discrepancy is due to experimental error caused by the inability of the standard tensile facility to apply truly uniaxial tensile loading.

1

The presence of bending moments during a test will result in a lower "apparent" tensile strength. Interestingly enough, most cases where gross discrepancies in MOR and tensile values are reported, the tensile values are the lower of the two. Also data obtained in Southern's gas-bearing tensile facility indicate that good agreement between tensile and flexural strengths can be obtained on most materials.

Thus while it appears that non-uniform loading of tensile specimens is a major factor in the reported discrepancies, present indications are that other parameters are also exerting influences. For example, tensile values for some materials differ significantly from MOR values even when truly uniaxial loads are applied. In addition, even where good agreement between tensile and MOR values have been obtained, there appears to be a tendency for the MOR to show slight increase in strength with temperature after the tensile strength begins decreasing. Part of this effect at elevated temperature may be caused by plastic deformation and subsequent stress relief at the outer fibers of flexural specimens; however, plastic deformation is hardly the mechanism causing discrepancies observed at room temperature.

One explanation is that errors result from calculating MOR values from classical beam equations. One assumption in the derivation of these equations is that the tensile and compressive moduli are equal to fracture; hence, the neutral axis coincides with the centroidal axis. According to an analysis developed by Simon if a material has a higher compressive modulus than tensile modulus the neutral axis will shift to the compressive side of the beam and reduce the peak tensile stress. For a material that fails in tension, the calculated MOR values would give "apparent" tensile ultimates higher than can be observed in a uniaxial tensile test.

Other conditions which could cause the difference between tensile and flexural strengths include surface condition and the volume under stress. Unfortunately the nature of the effects of these condtions would be different for tensile and flexural evaluations. Surface finish would be very active in setting the strength of a flexural specimen since the peak stress occurs only at the surface, whereas in a tensile specimen the entire volume of the gage section is subjected to the same peak stress as the surface.

It is known that the strength of brittle materials depends on the volume under stress. This has been demonstrated effectively with tensile specimens; however, the effect is not easily defined when using flexural specimens chiefly because of the stress gradient.

2

We have mentioned some of the difficulties encountered in relating tensile and flexural results. Similar difficulties occur when one considers test methods besides these two, particularly the indirect tensile tests such as the Brazil Test and others.

Having mentioned some of the difficulties in testing brittle materials, consider the plight of the designer. He needs information that will permit him to proceed from specimen data to the proper design of a structure. This information includes the effects of (1) surface finish, (2) stress concentrations, (3) volume, (4) skin discontinuties, (5) Weibull coefficients, (6) biaxial stress, and other physical behavior such as those already mentioned. Before the designer can make this step, the various mechanisms and behaviors must be understood with reference to the test methods.

The solution to the problem is the ordered study of these natural phenomena. However, before this type of study can proceed, a uniform and reproducible material which can be manufactured in large quantities must be found. Otherwise the effects being investigated may be masked by anomalous material behavior. For instance in a recent program in which volume effects were studied, some of the material was found to have anomolously large grains and areas of incomplete sintering which yielded low strength specimens. If all small volume specimens had been manufactured from this material and all large volume specimens had been made from better material, in all likehood the volume effect would have been missed. Fortunately, the specimens were located randomly in the several tiles so that the volume effect was not masked. This is merely one example of why a uniform material is needed.

The scope of this program includes obtaining a uniform and reproducible material and then conducting a quantitative comparison of several test methods. The study is primarily phenomenological and analytical in scope, concentrating on the effects of size, surface finish variations, stress-strain response under different types of loadings, and applying the proper analysis to the specimen. These will, in turn, be treated in terms of statistical fracture criteria.

The criteria for the material has been established as "the material is acceptable if it is statistically describable in terms of certain properties between the different blanks even though there may be some differences in structure." Thus, reproducibility (piece to piece) in key properties is the vital point. Uniformity (within a piece) is necessary to good reproducibility since it is doubtful a material can be reproducibly non-uniform. Then, with an adequate material one could be able to control the range of certain variables and compare different tests by (1) volume normalizing (2) control of test conditions, and proper analysis.

3

SCOPE

Phase I

As already discussed, Phase I was a study to determine whether or not a current material could be made uniform and reproducible enough to carry out the overall objectives of the program. To this end Southern Research subcontracted with Coors Porcelain Company to perform a production control feasibility study. The primary production parameters included in this study were powder characteristics, forming techniques, green density, and sintering procedures.

Specimen blanks for 13 different specimen configurations were manufactured by Coors during the control study. These blanks were then evaluated to determine the uniformity and reproducibility of the material with respect to strength, structure, and fractography. This report deals with the evaluation of the material starting from the specimen blanks.

Phase II

Phase II as originally defined involves the purchase of a sufficient number of specimens to conduct the comparison of test methods and the actual comparison of the methods.

Present Status

We have completed most of the preliminary work on evaluating the specimen blanks obtained from the production control study and have established the general ranges that interrelate strength, grain size, density, and porosity with some degree of confidence. To complete Phase I requires a "finer" look at these relations to extract as much information as possible before proceeding on to Phase II.

4

MATERIALS AND SPECIMEN PREPARATION

MATERIAL

The material for this program was a high purity alumina manufactured by Coors Porcelain Company of Golden, Colorado. The material and its production were developmental as opposed to the state-of-the-art, but all parts were manufactured on a production basis rather than using research facilities. The emphasis was on the optimization of the material from the standpoint of uniformity and reproducibility with respect to strength and its physical characteristics.

The material was manufactured in 13 different blank shapes, each representing a particular specimen configuration. The number of blanks of each type were based on the number of macro specimens deemed necessary for the study of uniformity and reproducibility. All blanks received are listed in Table 1. The number of macro specimens (tensile and flexural) removed from each blank is also listed in columns seven and eight of the table. Note that all parts were not used and this must be kept in mind in reviewing the results; however, we feel we have taken representative samples in all cases. There were several Type A11 blanks shipped which are not listed in the table. These blanks were sent by Coors for experimental machining purposes and were not considered to be representative of the production material for the study.

Review of Coors' Reports

The success to be obtained in the subject program is very much related to the quality of the brittle body used. The Coors Porcelain Company was selected to produce an alumina body which would meet the major requirements of uniformity and reproducibility of character. Although the specific data which define this character were of quantitative interest, the main concern was centered on the degree with which properties of interest could be repeatedly produced.

The object was to have available for study a body demonstrating minimal variation in character within a given object (uniformity) and a minimal variation in character among objects of both similar and dissimilar geometry (reproducibility). Since some of the required parts were large and the nature of the program would necessitate production over an extended time period, it was desired to have the material produced using a well-documented production procedure. To do this mechanics study with a material which might be defined later as a "laboratory curiosity" was to be strictly avoided.

The specific character of the body was only loosely specified with regard
to density and grain size. Although the body selected to be used in the program
was not a standard production item, it was one which Coors believed could be
made in quantity over a period of time with suitable uniformity and reproducibility.
No preconceived limits of homogeneity existed. As is obvious from this report
on the initial phase of the program, it was hoped to be able to readily discern
deviations from uniformity or reproducibility by review of physical measurements,
microstructure, fractography, and mechanical data acquired from specimens
taken from larger shapes.

To secure the desired uniformity and reproducibility, Coors spent considerable
effort in establishing and documenting the processing parameters. Likewise, the
parts produced for Phase I of this program were closely observed during processing
and their features were also documented. The Coors' reports related this
information in an informal manner on a monthly basis. No attempt will be made
to discuss these data. This review will merely point out the areas of processing
which were investigated and controlled during production. Those persons interested
in the specific details of the processing are referred to the sponsor of this work
for a copy of the original information.

The following outline will describe the various steps taken by the manufacturer
to establish the process.

Body Preparation - Since the body used was one which had been previously
designed by Coors, this portion of the work was largely concerned with the
documentation of initial particle size, specific surface, body chemistry, and
spray-dry pellet size distribution.

Preliminary Kiln Study - This study was made to select a production kiln
in which to fire the parts for this program. Longitudinal, transverse, and
vertical thermal profiles were established using traveling thermocouples and
pyrometric cones. The kiln performance was evaluated based on these measure-
ments and a study of kiln losses (camber and cracking) versus position in the kiln.

Pressing Study - The parts used in this program were isostatically pressed
(some parts had restraint on one axis) and optimum conditions regarding fill
control, rate of pressure rise, ultimate pressure, dwell time, and rate of
pressure fall were investigated. Conditions yielding maximum green density
with minimal varation were established.

6

Firing Study - The objective of the firing study was to determine the correct firing parameters to obtain a density of 96.5 percent ±1.5 percent of the theoretical at a maximum grain size of less than 25 microns for all six geometries produced. The factors considered in this study included: kiln temperature, car schedule, car load, preheat, soak and cooling profile, cone deformation, etc. Optimization of these factors was established by repeated firings utilizing density and grain size measurements for judgment.

After establishing the production procedures, the parts for Phase I of the program were produced. Green density and fired density were recorded for each part. Cone deformation and grain size determinations were recorded for representative part geometries and kiln positions.

Nomenclature

Due to the large number of specimens and types of specimens involved in this work, it will be convenient to clearly define the nomenclature early in the report.

The material initially was pressed isostatically into basic shapes using different tool sets. There were six basic shapes (or tool sets) for this program. These basic shapes were then green machined into parts which were fired. These parts (or near-shapes) were machined oversize as tensile, compressive, flexural, diametral compression, brittle ring, and pressurized ring specimens and remained about 0.020 to 0.050 inch oversize after firing. They are referred to as specimen blanks. When these specimen blanks were machined to final dimensions in Phase II, they then will be called specimens and hence are loosely called specimens in this report.

In order to evaluate the material to determine whether or not it was uniform with respect to strength it was necessary to examine the material taken from the gage sections of the specimen blanks. To do this it was mandatory to adopt a test method, or methods, that was common to all specimen blanks. For our purposes the tensile and flexural evaluations were used. Thus, small tensile and flexural specimens were removed from the potential gage sections of the specimen blanks. These small specimens have been called macro specimens.

To summarize thus far, we have mentioned the following categories of parts:

1. basic shapes
2. specimen blanks
3. specimens
4. macro specimens

In Phase I we have been concerned primarily with macro specimens.

7

For each specimen type (large tensile, small flexure, etc.) several specimen blanks were manufactured. Each piece was assigned a specimen number by Coors. This number is referred to as the Coors specimen number. As Coors completed various stages of production control study and as the parts were manufactured, firing data were kept for each part. These data are presented in a Firing Analysis Data Table (Table 1). In this table the specimens were also assigned an Item Number. The item numbers are in ascending order and give easy access to the firing data.

From the above discussion we see that with each macro specimen we can associate the following information.
1. Tensile or Flexural strength
2. The particular specimen blank from which the macro specimen was removed.
3. The type of specimen blank from which the macro specimen was removed.
4. The basic shape (tool set) from which the specimen blank was derived.

In order to convey all of this information and to provide easy access to the firing data a numbering system as follows was used. Consider the macro specimen number

| 1 | A02 | - | 023 | - | 01 | F |

1 Designates the basic shape number. This number ranges from 1 to 6.

A02 Signifies the type of specimen blank. A02 is a small tensile specimen blank.

023 is the Coors item number. This identifies a particular blank and lets one look up the firing data in Table 1.

01 is the macro specimen number. In most cases more than one macro specimen was removed from each specimen blank.

F flexure. Identifies the macro specimen as to whether it was a tensile or flexural specimen.

8

There were 13 different types of specimen blanks manufactured by Coors for evaluation. These are listed below with their identifying number.

A02 Small Tensile Specimen
A04 Intermediate Tensile Specimen
A05 Large Tensile Specimen
A06 Small Compressive Specimen
A07 Intermediate Compressive Specimen
A08 Large Compressive Specimen
A09 Small Flexural Specimen
A10 Intermediate Flexural Specimen
A11 Large Flexural Specimen
A12 Intermediate Diametral Compressive Specimen
A13 Large Diametral Compressive Specimen
A14 Pressurized Ring Specimen
A17 Brittle Ring Specimen

Specimen Preparation

The mechanical evaluations for Phase I of the program were preceded by an inspection of the alumina parts received from Coors Porcelain Company. The parts were inspected for cracks and other anomolies which would affect the testing program.

The testing requirements for Phase I included running twenty flexural tests and eight tensile tests on material from each type of specimen blank as received from Coors to determine material uniformity and reproducibility. Because of the limited amount of material available in the gage sections, it was necessary to develop the testing under Phase I around miniature test config-urations (macro specimens). These were taken to be of such size that the required number could be removed from the gage sections of the specimen blanks where practical. The flexural macro specimen selected has dimensions of 0.100 inch x 0.200 inch x 2.0 inches as shown in Figure 1. The tensile macro specimen selected was 0.125 inch in diameter x 2.0 inches long with a gage section of 0.094 inch diameter x 0.188 inch long as shown in Figure 2. These were removed from the blanks according to the cutting plans shown in Figures 3 through 17. The distribution of the macro specimens is shown in columns 7 and 8 of the Firing Analysis Data (Table 1). The distribution was established by distributing the required number of test specimens from each blank config-uration in such a manner that the test specimens would be from along both sides and across a section of the kiln car. This distribution is shown in Figure 18. Note that an even distribution according to kiln car location was not att__ned.

9

Bulk density measurements were made on all of the macro specimens. Dimensions were measured with micrometers, and weights were measured with an analytical balance which has a sensitivity of 0.0001 gram. Density measurements for the flexural specimens were made on the final specimens. Density measurements for the tensile macro specimens were made on square blanks prior to grinding them to cylindrical form. These densities are referred to as those of the Mechanics Section. There are also those of the Inorganic Materials section and those from Coors. There are systematic differences in the measurement not considered critical at this point.

There were some problems associated with the mechanical density measurements which need to be clarified at this stage. It will be noted in the tables later on that there were some differences between the densities determined on the macro tensile and flexural specimens. These differences do not appear to be systematic, but are believed to be associated with the accuracy of the measurement. For instance on the small flexural specimen, if the measurement is in error by 0.0005 in. on the nominal dimension of 0.100 then the density value can be off by as much as 0.02 gm/cm^3. This is most apparent for the A13 macro flexural specimens where the density of the macro flexural specimens from one cutting averaged 3.78 gm/cm^3 and from the second cutting averaged 3.81 gm/cm^3. We are currently pursuing this matter and making more accurate measurements on the specimens.

Because of the small size of the macro tensile specimens, adequate gripping area for tensile testing was not available. This was overcome by gluing steel shanks to both ends of the specimens. The steel shanks are shown in Figure 19. Three grooves three mils wide were ground on each end of the cylindrical macro tensile blanks for the purpose of providing a better gripping area for the glue. The blanks were then glued into the shanks with an epoxy glue consisting of a 10:1 mixture by weight of Shell Epon Resin 815 and Trienthylene Tetramine hardener. The resin-hardener combination was mixed 4:1 by volume with a 1:1 mixture of alumina powder and Cahosil for reinforcement. The shank-blank combinations were placed in vee-blocks and cured in an oven at about 170° F for two hours. The composite macro specimen blanks were then ground to final size and shape. Grinding the gripping surfaces and gage sections about the same center line insured good alignment which is critical in the tensile testing of brittle materials. A completed macro tensile specimen is shown in Figure 20.

10

Note that no macro tensile specimens could be removed from specimen blanks 1831-A06 because the reduced length did not provide adequate surface area for gluing the steel shanks due to the limited shear strength of the epoxy cement. This length limitation of SRI part 1831-A06 also required that the macro flexural specimens be shorter than the usual two inches. This necessitated relocation of the load points in the flexural apparatus for these specimens.

Machining- The cutting and grinding operations were performed with diamond wheels of No. 100 grit. These proved to be efficient, and they produced a surface finish of from 14 to 18 RMS. The cooling fluid used was a water soluble cutting oil. Preliminary experiments showed that Stuart 4567 water soluble oil mixed about 25 to 1 was a good compromise between wheel wear and labor costs.

The final grinding operation on the macro tensile specimens required the use of steady-rests to insure against accidental breakage of the delicate gage sections. Even with the precautions taken, several were broken in machining and handling and are noted in the data tables. Gage sections were checked by way of a 20 to 1 optical comparitor for accuracy of shape.

We have adopted as standard procedure the removal of sharp corners on the tensile side of all flexural specimens for the purpose of eliminating nicks and small cracks which might initiate a premature failure. This procedure was used on the macro flexural specimens by grinding off a few mils at 45° to the faces.

APPARATUS AND PROCEDURES

Use of the macro specimens for the material evaluations required that special techniques be employed for loading the specimens. The adaptation of the macro tensile specimens to standard grips was discussed in the preceding section.

Flexure

For the flexural evaluations of the macro specimens a precision miniature flexural apparatus was developed which employs rollers for load points and is constructed so that parasitic stresses are minimized. Figure 21 is a schematic of the apparatus.

11

Much has been said and written about the practical limitations of the tensile test, and this is probably one of the main reasons for substituting flexural tests. However, there are certain practical limitations to the flexural tests. Chiefly, these are frictional forces at the load points, superimposed torsion, and inaccurate placement of the load points. The miniature flexural apparatus used for these evaluations was designed to overcome these limitations in so far as was possible.

· Note in Figure 21 that the loading points are rods which are mounted on heavier pieces of drill rods (loading beams). V-grooves have been accurately machined into the loading beams to provide true placement of the loading points. The loading points were held in place on the loading beams with RTV Silastic Adhesive which remained flexible after curing and allowed relative rotation between the loading rods and loading points. The RTV also allowed the loading points to rotate around their own axis to some extent and thus to minimize frictional effects.

Specimen and upper and lower loading rod alignment was maintained by mechanical stops incorporated in an alignment jig. These stops held everything in place until a slight preload could be applied after which the stops were removed. Loading was accomplished in a Tinius Olsen Universal Testing Machine. The load at fracture was read directly from the load dial on the testing machine.

Tension

The tensile specimens were loaded in tensile frames equipped with gas bearings in the load train to eliminate bending stresses. A typical tensile facility is shown in the photograph in Figure 22 and in the schematic in Figure 23. The primary components are the gas bearings, the load frame, the mechanical drive system and associated instrumentation for measurement of load. The load capacity is 15,000 pounds.

The load frame and mechanical drive system are similar to those of many good facilities. The upper crosshead is positioned by a small electric motor connected to a precision screw jack. This crosshead is stationary during loading and is moved only when assembling the load train. The lower crosshead is used to apply the load to the specimen through a precision screw jack chain driven by a variable speed motor and gear reducer.

12

Nonuniaxial loading, and therefore bending stresses, may be introduced in tensile specimens not only from (1) misalignment of the load train at the attachment to the crossheads, but also from (2) eccentricity within the load train, (3) unbalance of the load train, and (4) external forces applied to the load train by such items as electrical leads and clip-on extensometers. Although the bending moments from some of these sources may seem relatively slight, the resulting stress distortions are quite significant in the evaluation of the extremely sensitive brittle materials. Now consider each individually.

To confirm that the gas bearings had eliminated nonuniaxial loading at the point of attachment of the load train to the crossheads, the frictional moment was determined at a load of 5000 pounds by measuring the torque required to produce initial motion within the system with the bearings in operation. This torque was found to be a maximum of 6.6×10^{-3} inch pounds. The equation

$$M_O = \frac{2\mu P}{3} R_2 \left[\frac{R_2^3 - R_1^3}{R_2^2 - R_1^2} \right] \qquad (1)$$

was then applied to the system to calculate the kinetic friction where M_O was the resisting moment due to kinetic friction and μ represented the coefficient of kinetic friction. The calculated value of μ was then equal to a maximum of only 4.5×10^{-7}.

The bending stress equation

$$S = \frac{Mc}{1} \qquad (2)$$

was then employed to obtain the stress that could be induced in the specimen due to this bending moment. This value was 0.16 psi, or less than 0.002 percent of the tensile stress produced within a typical tensile specimen. These low values clearly indicate the elimination of problems of bending stress in the specimen imposed by misalignment at the crosshead attachments, either initially or during loading.

Emphases in the design of the load train were placed on (1) large length-to-diameter ratios at each connection, (2) close sliding fits (less than 0.005 inch) of all mating connection, (3) the elimination of threaded connections, (4) the use of pin connections wherever possible, and (5) increasing the size of

13

components to permit precise machining of all mating surfaces. All members were machined true and concentric to within 0.0005 inch, and the entire load train was checked regularly to ensure overall alignment following assembly of the individual members. This process ensures the concentricity and no kinks in the system.

The problem of unbalance within the load train and of external forces applied to the load train have been explored and corrected. The entire load train is statically balanced to less than 0.01 inch pound for normal operation.

The configuration of the tensile specimen has been shown in Figure 19. This specimen provides a relatively large L/D ratio in the gripping area to ensure good alignment. All surfaces in the gripping area are cylindrical in order to make precision machining easier and repeatable from specimen to specimen.

A schematic of the precision tensile grip is shown in Figure 24. The design is much like the jaws of a lathe head or the chuck of a drill motor made with precision. Observe from the figure the long surface contact of the mating parts and the close fits to establish precise alignment with the specimen. As the load is applied, the wedges maintain alignment to fracture.

Instrumentation includes primarily a stress measurement system composed of a 1000-pound SR-4 Baldwin load cell, constant d.c. voltage power supply and an X-Y recorder. The load cell receives a constant d.c. voltage input from the power supply and transmits a millivolt signal (directly proportional to load) to the X-Y recorder. During loading, the loading rate is adjusted manually so that the recorder pen follows a load-time line of pre-determined slope. This establishes the stress rate, and the ultimate load can be read from the curve.

NDT Measurements

Ultrasonic Velocity measurements were made on most of the macro specimens. This was accomplished by introducing a burst of high frequency energy from the pulse unit of Sperry UM 721 Reflectoscope into one end of the specimen and timing the wave propogation to the opposite end by means of a Tektronix oscilloscope which has a time-base precision of one percent. The sending and pick-up units were ten megacycle transducers.

14

A number of other NDT testing techniques were also employed. Cracks and porous regions found visually were enhanced by <u>dye penetrants</u> as shown in Figure 25. In this figure two cross sections of an earlier A11 blank are shown after treatment by the penetrant. The edges of the cracks and the porous region are apparent. These figures were more obvious under ultraviolet light. The cause of fluorescence was not explained but most of the fracture faces of the flexural specimens were scanned with ultraviolet light. Minute fluorescent spots were observed occasionally, but no correlations were noted. Again, the cause of the fluorescence is not known.

<u>Ultrasonic pulse-echo</u> examinations were also made on the macro specimens. The porous area mentioned above was initially found by pulse echo indication; however, most of the specimens gave indications of being "clear".

DATA AND RESULTS

Flexural Data

The flexural data for the material evaluation are presented in Table 2. The SRI run number shown in column 1 indicates the order in which the specimens were loaded to failure. Initially, specimens were loaded in the order of their specimen numbers but, starting with specimens from SRI part number A11 the remaining specimens were loaded in random order.

There were a total of 314 flexural evaluations excluding those used for the brief surface finished study. Of these 314, 14 were from specimen blanks A06 which were shorter and were evaluated using a slightly different loading setup. Thus, there were 300 flexural evaluations under the same conditions with respect to the loading fixture and set-up. Five of the 300 specimens failed outside of the gage section. Several of the specimens fractured in two places, and it was not possible to determine which fracture occurred first. In those cases where two fractures occurred the data were included for only those specimens where both fractures were located equidistance from the midpoint.

15

The distribution of fractures along the gage section was as follows:

Distance from Midspan-in.	No. of Fracture
0-0.025	25
0.025-0.125	74
0.125-0.225	74
0.225-0.325	64
0.325-0.375	51
	288
Fractured out of the gage section	5
Fractured in two places	7
	300

These results are shown plotted in Figure 26. Also plotted are the theoretical values from the uniform distribution. The observed distribution agrees rather closely with the uniform distribution and indicates there was no prejudice or systematic bias in the flexural loadings.

Although five of the specimens fractured out of the gage section this does not create any conflicts when one considers the Weibull Volume Theory. Recall that the risk of rupture includes the stress level and volume and does not depend on the maximum or minimum stress developed in a part.

Figure 27 is a frequency plot for the flexural strengths. All data except those few specimens used for the surface finish studies have been included in this plot. The average flexural strength (MOR) was 48,290 psi with a standard deviation of 4610 psi and a coefficient of variation of 9.5 percent. The maximum and mimum values reported were 58,950 psi and 29,810 psi. The histogram is slightly skewed by several low values. Fifteen out of 314 values or 5 percent fell outside of the 2σ limits. Fourteen of the fifteen were on the low side.

Also shown plotted on the figure is the probability density function for the normal distribution. It appears to fit the data rather well.

The Weibull parameters, calculated using a modification of an iterative graphical technique were: $m = 12.4$ and $\sigma_u = 0$ psi.

Table 3 is a summary of the flexural results broken down by specimen blank type. Included in this table are the number of specimens, average MOR, standard deviation, and coefficient of variation. Blanks of the type A11 and A13

16

gave the lowest average strengths and the A02 and A06's exhibited the highest values. The average strengths were plotted versus specimen blank numbers and minimum fired thickness in Figure 28. A slight negative correlation with fired thickness is apparent. Note that except for the ring configuration, the strength decreased for each type configuration as the size of the fired piece increased. The two weakest sets of flexural specimens are seen to be from Blanks A11 and A13.

This section is only a brief look at the flexural data. Particular data will be discussed in later sections.

Tensile Data

The tensile data for the material evaluation are presented in Table 4.

Because of the configuration of the tensile specimen it was very difficult to locate the exact location of the fracture. However, by using a 20:1 optical comparator we were able to determine whether or not the specimen failed within the uniform diameter gage section. This is noted in Table 4 by a "G" for gage section or an "R" for radius. Where a break occurred in a radius the diameter of the fracture surface has also been noted. Twenty-five out of 141 specimens or about 17 percent fractured outside of the gage. The strength values noted in the tables are based on the minimum cross-sectional dimensions. The stress concentration associated with the breakdown radius is something less than 1.1. It is probably closer to 1.0 than 1.1. It is small enough that most charts and tables do not show it. The value of 17 percent for out of gage breaks is slightly higher than what has been observed in the past, but is consistent with the Weibull theory since it is part of the stressed volume.

Strength distribution for the tensile data is shown in Figure 29. The mean values of fracture stress, standard deviations of fracture stress and coefficients and scatter ranges are plotted versus SRI blank numbers and minimum fired thickness in Figure 30. Three blanks show low average strengths, namely A05, A11, and A13. A closer examination of the data discloses that one extremely weak specimen (22,800 psi) from A05 greatly affects the average value. This particular specimen, 2A05-047-01T, came from a blank which had been fired to a higher than normal temperature. If the extreme value is discarded, the A05 average becomes 44,860 psi and again, as was found in the case of flexure, the A11 and A13 blanks are the low strength pieces.

The average value of strength for the entire population of tensile specimens was found to be 45,180 psi as opposed to 48,290 psi for the total population of flexural specimens. The fact that the flexural test yields higher values has been

17

seen in other materials and may be attributable to the stress gradient in the flexural specimen, an effect of the difference between the tensile and flexural moduli of elasticity or even to the fact that the elementary bending stress equation probably does not accurately describe the stress distribution in the flexural specimen.

It is interesting to note that if the single extremely weak tensile specimen is ignored, the standard deviation for tension for the entire population is 4500 psi which compares quite favorably with the value of 4610 psi for the flexural specimen population. The coefficients of variation compare favorably with the values of 0.098 and 0.095 for tension and flexure, respectively.

Table 9 is a summary table of the tensile and flexural results. Average strength values are shown here for the various types of blanks along with the densities, velocities, number of specimens and extreme values.

Uniformity and Reproducibility

For the purpose of studying uniformity within specimen blanks, it was decided to choose some of the larger parts and remove specimens from a sufficient number of locations to allow profiling of properties. One specific part chosen for the study was Item 88, which was an A10 type blank, the intermediate size flexural configuration. The cutting plan and data have been shown previously (Figure 11 and Table 2 respectively). Figure 31 shows the longitudinal, transverse and cross sectional variations of strength for the piece. These are displayed graphically in Figures 32 and 33. In Figure 32, it is seen that uniformity is relatively good except at section C where the top two layers of specimens are weaker. Figure 33 which shows the strengths at section B, illustrates the trend towards lower strength at interior positions and higher strengths near the surfaces. Figure 34 depicts the longitudinal, transverse and cross sectional variations in density for part A10. These are displayed graphically in Figures 35 and 36. The density values seem to be somewhat scattered longitudinally. Cross sectionally the variation is considerably more uniform except at section B.

Figure 37 and 38 show density profiles for Item 89 (large flexural blank). The values are fairly scattered and there are no definite trends shown. Two longitudinal strips show lower than average densities but there relative positions are not indicative of an particular trends.

18

Reproducibility or piece to piece variation in strength is another important factor which must be considered. Figures 39 and 40 show average flexural strengths versus item numbers for 10 different A02 tensile specimen blanks and 7 different A04 tensile specimen blanks. The maximum deviation from the total mean strength was 11 percent for the A02 blanks and 8 percent for the A04 blanks. For the A02 blanks (Figure 39) it is seen that except for Items 7 and 16 there is only a 3000 psi spread in the average flexural strengths.

Surface Finish

The nominal surface finish on all the specimens discussed to this point was approximately 15 rms. A brief study was undertaken to investigate the effect of surface finish on strength. Flexural specimens from Item 87 were considered along with those from Item 88 for the as-ground examples. Specimens 3A10-088C-11F, 12F, and 13F were cut into two pieces of approximately one inch in length, designated A and B. The three pieces designated "A" were polished and lapped with $\frac{1}{4}$ micron diamond compound. Both one-inch pieces from each specimen were loaded in flexure. The data are presented in Table 6.

Specimens 3A10-088-A4, -B5, -C1, -C2,-C3,-D1,-D2, and D3 were polished to a surface finish of 3 to 4 rms. The data for these specimens are shown in Table 6. Tensile specimens 3A10-088-C4T,-C5T, -C14T,-C15T,-D4T, and -D5T were also polished to a finish of 3 to 4 rms, and their strength values are presented in Table 7.

The polishing procedure employed was as follows:

1. Initial grinding with Norton D100-R50B56-3/32 diamond wheel
2. Lap out grinding scratches with 15 micron diamond compound on wooden paddle.
3. Lap with 5 micron diamond compound
4. Lap with 1 micron diamond compound on wooden lapping disk
5. Final lapping with $\frac{1}{4}$ micron diamond compound.

It was also deemed desirable to consider the influence of an as-pressed-and-fired surface of the SRI part. These as-fired surfaces were positioned as the tensile surfaces when the specimens were loaded. The surface finish was about 150 to 175 rms. Data are presented in Tables 6 and 7.

19

The results of the cursory surface finish investigation are briefly summarized in Table 8. These results show that except for the as fired surface, the surface finish did not affect the strength of the specimens. The ground surfaces, polished surfaces (by machine shop), and metallurgically lapped surfaces all gave essentially the same strength values in both flexure and tension. The nominal flexural strength was about 49,000 psi. The pressed and fired surface gave about a 15 percent lower strength value of 40,820 psi. More discussion of the surface finishes is included later in the report.

Preliminary Statistical Results

The tensile and flexural data were subjected to analysis by way of the Weibull distribution function. The computer program for computing the Weibull distribution is a slight modification of the program written by L. A. Jacobson and reported in AFML-TR-65-176. The essential steps executed in the program are the same in that it is designed to coverge on the most likely value of σ_u which will produce the best straight line fit, by the method of least squares, of log log $[(N + 1) / (N + 1 - n)]$ + versus log $(\sigma - \sigma_u)$ where σ_u is the strength below which the probability of fracture is zero. Due to the fact that a negative value of σ_u would have no physical interpretation, the program restricts the value of σ_u to be not less than zero. In the case where the theoretical value of σ_u is less than zero, this restriction will result in some error in the fitting of the computed probability curve to the experimental values depending on how much less the theoretical value is than zero. Some indication of the magnitude of the error can be obtained from the magnitude of the sum of the squares of the deviations used in the method of least squares. For the tensile and flexural data under consideration here, the values of σ_u were essentially zero. A copy of the computer program is included in the appendix.

The Weibull distribution is very sensitive to extreme values. The tensile data were run with the computer program two times; once with the entire population and once with the extremely low value deleted. The resulting curves are presented in Figure 41 along with the curve for the flexural data. The effect of the single extreme value is quite apparent. Note that the curve for the truncated tensile population has nearly the same character as the flexural curve with nearly identical Weibull parameters. The primary difference in the two curves is that the tensile curve is displaced about 2000 psi to the left or toward lower strengths.

20

Figures 42 through 54 show the experimental strength values for the flexural specimens for the blanks superimposed on the theoretical curve for the entire population. Figures 55 through 66 show the tensile 'rengths for the separate blanks superimposed on the theoretical curve for the total population (truncated) of tensile strengths. In most cases it is seen that a remarkably similar distribution exists between tensile and flexural distribution for corresponding blanks as related to their respective theoretical curves. That is when a given blank falls low on the curve in flexure, it also falls low in tension.

During the course of the work reported herein, the Air Force brought Professor W. Weibull to Southern Research Institute for discussions of various aspects of his statistical distribution theory as applied to this program. Professor Weibull's intuitive remarks regarding the application of his theory to real materials were interesting. He stated that the distribution for the Coors alumina for the various SRI parts with respect to the computed probability curve is what one might expect. He explained that a similar distribution might be expected of a similar group of subsets of numbers taken from a population of random numbers (we checked this and will discuss it later).

Another interesting point discussed by Professor Weibull was that of truncation of extreme data points such as the one extremely low value encountered in the alumina tensile data. Truncation is a legitimate operation if there is some physical basis for it, such as flaws in the material. He mentioned that there are various statistical methods for justifying truncation in some cases. As an extreme example of truncation, it may be proper to treat specimens in a bimodal distribution as two separate groups, particularly if differences in failure mode or criteria were suspected.

Test methods were also discussed, including pressurized rings, Brazil, thick rings, flexural and tensile tests. The point was made that the various indirect tests have the inherent disadvantages of nonuniform and, for many geometries in current use, inadequately defined stress fields.

Certain other aspects of Professor Weibull's Theory of Rupture were discussed, including the interaction of volume and σ_0, the uniqueness of the parameters m and σ_u and stress gradients. σ_0 is a normalizing factor which adjusts with volume changes. Stress gradients such as those present in flexural tests and other indirect techniques were discussed in light of their effect upon the

21

theory. It was brought out that according to the theory the stress gradient has no effect except as it affects the volume of material under consideration.

The influence of other factors encountered in the mechanical evaluation of real materials was discussed. These included the influence of surface finish, crack blunting, the interaction of voids, sample size, and others. The main conclusion seemed to be that these influences might change the shape of the distribution curve but that the results still could be defined statistically if the sample was representative.

A major conclusion of the total conversation was that judgements remain important in the statistical treatment of data. This seems to conflict with some views seen in past work and reported in the literature in this area where the material aspects were ignored and obvious differences in a parameter still grouped.

Out of curiosity and encouraged by Professor Weibull's remark, it was decided to choose a normally distributed population of numbers, draw several random subsets and subject the population to the Weibull computer program. A convenient population was taken from Statistical Methods by Snedecor and is seen plotted versus the computed Weibull curve in Figure 67. Five random subsets were drawn by use of random number tables and four additional random subsets were taken from Statistical Methods by Snedecor. These are plotted separately versus the computed curve for the entire population in Figures 68 through 76. It is interesting to note that, indeed, similar distributions to those encountered with the alumina test data are encountered with the random numbers. Random Subset No. 8 is very much like the group for the A12 tensile data and No. 9 is very similar to the group for the A13 tensile and flexural data. That is, a uniform distribution of smaller sample sizes was not obtained even using random numbers.

Figure 77 shows a comparison of the Phase I flexural and tensile macro specimen data with the alumina data from Technical Report No. AFML-TR-66-228. The original data shown here was obtained on a high purity, hot pressed alumina body. Note the macro tensile data falls fairly well in line with the past tensile results. The flexural data was pretty much off the curve which is not to be unexpected since the materials were different and also the difficulty in defining volume in a flexural specimen. For this plot 50 percent of the tensile volume was used.

22

Microstructural Characterization

This study was made to record the general microstructural characteristics of the Coors' alumina used for this project. If possible, these characteristics were to be related to specific points of interest which might influence the decision regarding the continuation of the program. The areas of interest included an evaluation of material uniformity within a given blank and of reproducibility between blanks made from the same tool set and among all blanks. Also, the relationship between material characteristics and the occurrence of fracture at lower-than-expected stress (weak/strong) was of interest.

The characterization is based on the following determinations. Bulk density was determined on whole mechanical macro specimens and on small pieces from locations near the area of fracture. Microstructural detail, including pore characteristics, grain size and shape, and the identification of micro-constituents, was obtained by metallographic and microprobe analyses. Fracture mode was examined by macro and microfractography. Surface conditions were photographically recorded by replication techniques.

In all, seven specimens from flexural tests and eight specimens from tensile tests were examined. The specimens were selected based on strength-density relationships and on those factors concerned with uniformity and reproducibility, that is, fired volume and specimen location in a given volume.

Summary

Within a given blank and among identical blanks, uniformity, with respect to microstructural features, was good. One must include specific features such as the maximum grain size or maximum pore size as shown by a single photo-micrograph to demonstrate differences.

Within the limits of present knowledge, one can also say that reproducibility is good for all blanks produced by a given tool set. For example, the blanks making up Groups A9 and A10 produced from Tool Set 3 are quite similar. This point is somewhat difficult to judge for Tool Set 2 since five different blank shapes of great size difference were made from this tool set.

When all the blanks produced are considered, a detectable degree of non-reproducibility is apparent. The Groups A11 and A13 are similar in characteristics to each other, but differ from the other groups. This difference is manifested by lower average fracture stress, lower density, greater total porosity, and larger maximum pore size for those specimens from Groups A11 and A13.

23

Efforts to relate specific microstructural detail to failure at lower-than-average stress (weak/strong studies) for specific specimens within a group failed. Only fractography correlated with fracture stress for this part of the study. Low stress fracture resulted in a more or less planar fracture surface, while fractures at high stress developed an irregular surface. Although it has not quantitatively established, microfractography indicated more intragranular fracture for the high fracture stress parts. Within the effort used, these features could not be related back to the source of fracture.

Procedures for Specimen Preparation and Measurement

The descriptions below are given in the order in which the work was conducted.

Macrofractography - All flexural and tensile specimens examined were photographed at 20X or 50X magnification using oblique lighting. The magnification used was subject to the size of the object. Views of the fracture face and the region of fracture in profile were used.

Density - Density values reported herein came from three sources: Coors' reports, the Institute's Solid Mechanics Section, and the Institute's Inorganic Materials Section. The comments below pertain to the latter's data.

Bulk density values were determined for flexural specimens only. A liquid displacement technique was used, and the data were acquired in duplicate. Pieces approximately 0.1 inch x 0.2 inch x 0.2 inch including the fracture face were used. Saturation was attempted using distilled water under vacuum. Bubbling as a result of water replacing air in the pores subsided after 10 to 20 minutes and the pieces were allowed to remain in the water 24 hours. Since no absorption could be detected, it was concluded that the bubbling action was due to surface pores only. Dry and saturated weights in duplicate never varried more than 0.2 mg. Suspended weights varied from 0.4 to 1.3 mg between successive measurements on the same piece. Since the specimens were very small, about 0.25 gm, this variation in suspended weight data caused differences of as much as 0.05 gm/cc in bulk density. Thus the results reported are averages of two determinations which individually may have differed by as much as 0.05 gm/cc. Insufficient data are available to present a statistical description of the information. The data are self-criticized on two counts: the specimen weight is too small for the variations accompanying suspended weight measurements and the technique excludes the surface porosity from the volume of the specimen.

24

Ceramographic Preparation- Specimens from the flexural tests were prepared using those pieces used in the density determination. The specimen was diamond sawed to expose a longitudinal section at the centerline with the cut perpendicular to the compression and tension surfaces of the mechanical test piece. The specimens were mounted in blue bakelite with the diamond sawed surface exposed. Polishing was done using successively 30, 15, 6, 3, and 1 micron diamond on nylon cloth at slow-to-moderate wheel speeds.

The tensile specimens were handled in much the same way except the section represents a plane perpendicular to the longitudinal direction of the mechanical test piece immediately below the fracture surface. Since the relatively rough fracture face was removed, the polishing procedure included the use of silicon carbide papers from 240 to 600 grit before final polishing with diamond as above.

When some structural detail was desired without the influence of etchants, a relief polish was used. This was done using 0.1 micron alumina on a high nap cloth at high wheel speeds. This technique revealed portions of the structure useful in the microprobe analysis.

To reveal the alumina grain boundaries, the specimens were etched in 85 percent H_3PO_4 at 240-250°C for 5 minutes. This procedure at 140-150°C was suitable for revealing a phase other than alumina without having much effect on the alumina boundaries.

Microstructural Features- The size of the various microconstituents was measured by a linear intercept method as discussed by Underwood, et al., Part I, Chapter I, Ceramic Microstructives, John Wiley and Sons, Inc., New York. Area determinations to obtain volume fractions were made by visually counting grid openings overlying photomicrographs.

For flexural specimens, three photomicrographs were taken at the following positions: along the mid-point between the compression and tension surfaces 1.3 mm (Position 1), 2.5mm (Position 2), and 3.8mm (Position 3) from the fracture face. These positions were located within about 0.1mm using a mechanical stage. To avoid bias, the location was not altered after microscopic focusing. With respect to grain size and the features of the second phase, no difference could be detected among the three photomicrographs. Therefore, the Position 2 photomicrograph was arbitrarily selected. These photomicrographs were made at 800X

25

after etching at 140°C (second phase) and then after etching at 240°C (alumina boundaries). The total intercept length for grain size was 471 μ and for second phase it was 902 μ. With respect to the area of second phase, this was done as stated above using the same photomicrograph as was used for the intercept count. The total area surveyed was 16×10^3 square microns.

Photomicrographs for the determination of porosity features were taken at 500X in the as-polished condition. Since in some cases the photomicrographs differed visually among the three positions, that position which represented an average of the three was used. If all three were similar, Position 2 was used. Total intercept length used was 902 mm. Total area examined to determine porosity area fraction was about 40×10^3 square microns.

Grain size measurements for tensile specimens were made using single 800X photomicrographs taken at the center of the polished section.

Microprobe- Qualitative chemical constitution concerning a second phase was examined using normal microprobe techniques. The specimens were in a relief-polished condition and had been lightly coated with carbon. A Materials Analysis Company Model 400 microprobe was used.

Microfractography and Surface Characterization- Fracture and external surfaces were examined by light and electron microscopy. Suitable specimens for examination were prepared by a two-stage replication technique. Cellulose acetate was used to make the negative impression. This was dry stripped, shadowed at 45° with chromium, and replicated with carbon. Acetone-water mixtures were used to dissolve the plastic. The electron microscopy was done on a Siemens Elmiskop 1A microscope.

General Description of Microstructural Characteristics

In this discussion the information for both tensile and flexural specimens is included. The data for individual specimens are listed in Table 10. The information presented in this section is primarily directed toward material uniformity and reproducibility.

Density and Porosity Features- The greatest manifestation of deviation from uniformity and/or reproducibility can be seen from the data for density and porosity. Four sets of information are available with which to judge the degree of variation. The Solid Mechanics Section of the Institute obtained bulk density values for all macrospecimens. The weight and physical dimensions of

26

the entire macrospecimen were used in this determination. The Inorganic Materials Section of the Institute determined bulk density of small fractions of specific flexural specimens by liquid displacement method and also obtained porosity data from photomicrographs. Coors' reports furnished bulk density values determined by liquid displacement. The Coors' data were obtained from end pieces of blanks from which the mechanical specimens were obtained. If no data were available for the specific blank in question, then data for a blank fired in a nearby or equivalent kiln position were used.

Considering the differences in measurement procedures, the amount of material examined and the variety of techniques used, one would not expect absolute agreement between all the values. Indeed, when one examines these data, the values are found to differ depending on the source of data. If one converts the density data to porosity data for the 15 individual specimens of Table 10, a comparison of the ranges of porosity becomes apparent depending on the measuring technique:

Data Source	Porosity Range
Coors' Data	3-5 percent
SRI Inorganic Materials Section	3-5 percent
SRI Solid Mechanics Section	3-7.5 percent
From Photomicrographs	5-10.6 percent

Two important points should be noted: (a) the relative agreement of data is good, that is, the specimens with lowest or highest porosity occupy that position regardless of data source, and (b) the principal concern in this program involves material uniformity and reproducibility, not the specific level of any given property or characteristic. Comments will appear below concerning certain data; however, the general merits of the density-porosity data will not be discussed. It is believed that a significant difference in material and porosity exists which is relateable to the average fracture stress, and it really makes little difference whether the porosity range is 3-5 percent, 4-7 percent, or some other range.

The data of Table 10 show that the density is lower and porosity higher for the A11, A12, and A13 specimens than for the specimens of the other "A" groups. The data for flexural Specimen 7 of Table 10 are quite obvious in this respect, regardless of the source of information used. The photomicrographs of Figures 78 through 88 illustrate the nonuniformity of pore volume among the 15 specimens examined. Figures 78 through 84 show longitudinal sections of the flexural specimens starting at the fracture face and continuing into the specimen for a

27

depth of about 0.2 of an inch. The top of each picture represents the compressive surface and the bottom is the tensile surface. Figures 85 and 88 reveal the cross-sectional view of the tensile specimens near the plane of fracture. It is believed that these low power photomicrographs generate an impression of the relative magnitude of porosity which is in agreement with the data displayed in Table 10. From these photomicrographs, it can be seen that the pore volume is greater for the A11 (Figures 84, 87a, 88b), A12 (Figures 82, 85b), and A13 (Figures 81, 85a) specimens.

When the data of Table 10 and the remaining density information acquired by the Solid Mechanics Section are considered together, the lack of reproducibility with respect to density or porosity over the entire collection of blanks produced is seemingly related to the size of the part fabricated. Items made from Tool Sets 4(A11) and 5(A13) seem to have the highest porosity. Items made from Tool Sets 1(A02 and A06), 3(A09 and A10), and 6(A14 and A17) have the lowest porosity. Those items (A04, A05, A07, A08, A12) made from Tool Set 2 are somewhat ill-defined with respect to porosity. It is difficult to present data on this point since five different sizes of parts were cut from a rather large master form. For example referring to Table 10, the A12 blanks would indicate the lower limit of density while the A05 blanks would indicate high density. Although the specific tensile specimen listed for A05 was fired at a higher than normal temperature, the group average density is greater than A12.

It is believed that the higher porosity of the A11 and A13 parts is associated with a greater frequency of pores of all sizes and that the maximum pore size is greater. Figure 89 illustrates this point. These data were obtained from pore size frequency counts, using the low magnification photomicrographs of Figures 78, 81, 83, and 84. The smallest pore area that could be conveniently measured was 1 square mil. Therefore, this figure only compares the pore size-frequency distribution at the large pore end of the spectrum. Figure 89 shows that the increased frequency of occurrence of large size pores for specimens of higher total porosity is uniform with respect to pore size. Furthermore using the density values acquired by the Solid Mechanics Section, it can be shown that the porosity represented by these distributions represents about 30 percent of the total porosity for each pair of specimens. Therefore, it is apparent that the higher total porosity does not come exclusively from pores of large size.

28

The specimens used to develop the information shown in Figure 89 illustrate a second point. On the basis of weak/strong studies of the individual mechanical specimens, the amount of total porosity (within the range of porosity of the specific material used in this study) and the frequency or occurrence of large pores does not apparently affect the strength. The effect of porosity on strength is only correlatable when average fracture stress for groups of mechanical specimens is considered.

In theoretical sintering studies using specimens of equal green consolidation, one expects total porosity to decrease with increased thermal input and for the frequency of large pores to increase. However, in the present study involving the data for Figure 89, there is no evidence of advanced sintering (advanced grain growth) and the specimens of greatest porosity contained the larger pores; therefore, one concludes that items such as A13 and A11 were not consolidated in the green state to the same extent as the other parts. This is suggested also by an inspection of the green densities in Table 1.

The porosity features listed in the last four columns of Table 10 were obtained from the 500X photomicrographs shown in Figures 90, 91, 92, and 93. These photomicrographs were taken at one of three positions along the centerline of Figures 78 through 84. The percentage porosity by area values are not in very good agreement with density values on an absolute basis, but are in agreement on a relative basis. (It is believed that the porosity value for Flexural Specimen 5 (2A12-096-11F) is too low.) The area count method in general yields high porosity values because of grain pullout, rounding and enlarging of the pores during polishing, and an apparent tendency to trace the pore to larger-than-true size on the light table. There seems to be little difference in average pore size. The percentage porosity and average pore size were determined from the photomicrograph which appeared to be an average of the three taken. The maximum pore size was taken from the largest pore shown on the three 500X photomicrographs. It is questionable as to the definitive value of this maximum size data. Another set of photomicrographs would probably given an entirely different set of data. The information of Figure 89 and the 50X pictures of Figures 78 through 84 give a better picture of maximum pore size.

To summarize the above observations, it would seem that there are at least two levels of porosity existing. The denser parts have a porosity of approximately 3-4 percent with a maximum size of 50 microns, while the less dense parts have about 4-7 percent and a maximum size of 125 microns. Parts from Tool Sets 4 and 5 seem to be different with respect to porosity features from those parts made with Tool Sets 1, 3, and 6. Judgment is reserved with regard to blanks from Tool Set 2. This point will be discussed later.

29

Within the limited examination described above, no indication on non-uniformity within a given blank or nonreproducibility within a group of identical blanks was found.

The less dense blanks, A11 and A13, possess a lower average fracture stress, but 1:1 correlation between fracture stress and density for individual mechanical specimens was not detected.

Second Phase- In the course of this characterization, an unknown micro-constituent was detected. It differs from α alumina with respect to polishing, chemical etching, morphology, and chemical constitution. If relief polishing is used to reveal microstructure, this material appears readily, while tne alumina grain boundaries do not. In this study, 85 percent H_3PO_4 acid was used as an etchant. This reagent at 150°C brings out the detail of the "second phase" without extensively developing the appearance of the alumina grain boundaries. At 250°C, this etchant reveals alumina grain boundaries and takes the unknown phase into solution. The photomicrographs of Figure 94 show the grain shape to be prismatic rather than the more-or-less equiaxed structure expected of alumina. Since the volume present and size of these grains varied little among the specimens examined, only two photomicrographs are presented. These two specimens were from the same type of blank and exhibited high and low strength.

Various pieces of evidence from a microprobe analysis of this material were also obtained. When compared with adjacent alumina grains, the unknown phase indicates the presence of magnesium, calcium, sodium, and silicon, in addition to aluminum. This was shown by stationary beam-spectral scanning and by line traverses for the specific elements which had been qualitatively identified. Scanning-beam technique searching for magnesium also revealed these areas of unknown material, both on polished and fracture faces. Figure 95 shows one piece of microprobe evidence. This is a reproduction of stripchart from a spectral scan using a beam sufficiently small so that the X-ray output was coming exclusively from the unknown phase. Peaks associated with sodium, magnesium, aluminum, and silicon are visible. Other scans were made which more prominently displayed the silicon peak and showed the presence of calcium. Similar scans on areas immediately adjacent to the unknown phase, revealed only aluminum.

One unsuccessful attempt was made to identify the material by X-ray diffraction. Only the pattern for α alumina appeared. Although only the alumina pattern was present, the "d" spacings calculated were not in as good agreement with ASTM values as one might expect.

30

At present, one can only speculate regarding the identity of the micro-constituent. It could be suggested that the questionable phase is an impure spinel or an alumino-silicate. The microprobe analysis indicated about the correct amount of aluminum in the unknown for it to be a spinel. However, the raw count data were not corrected so the other elements of lesser concentration are quantitatively in doubt. If this questionable phase is spinel, it should be noted that only about 1 percent RO would be sufficient to create the quantity seen. Since the measured volume percentage present may be in error to the high side and the density of the unknown lower than alumina, a weight percentage too low for detection by diffraction may be present. On the other hand, one might suggest that the area represents an alumina solid solution which has had its lattice spacing altered by the foreign ions and its crystal morphology modified due to the initial reaction state which may have been a spinel formation. Finally, existence of an amorphous phase.

Whether the cations other than aluminum which have been qualitatively identified occur as inherent impurities or intentional additions, their presence was noted only in isolated positions (the unknown phase). These elements were not detected within alumina grains. No specific effort was made to examine alumina grain boundaries. The line traverses made with the probe adjusted to detect magnesium did not delineate alumina grain boundaries but showed dramatic response when the beam crossed the unknown phase. Obviously grain boundary impurity may have been overlooked using a rather rapid line traverse.

In any event, the amount and size of this phase seems to be equal in all specimens examined. For the seven flexural specimens examined, Table 10 shows that the volume percentage present varied from 5.1 to 7.7, and the average size varied from 1.7 to 2.4 microns. As in the case of the data on porosity, the volume percent may be a little high, and the largest crystal dimension is considerably greater than the average size.

An electron photomicrograph is shown in Figure 96 to indicate more clearly the morphology of the grains and their size. Tensile specimen 3(2A05-047-2T) Table 10 was used for this photomicrograph. The surface was polished and etched at 150°C with H_3PO_4 before replication. No evidence was obtained that micro-cracks developed at the interface between the unknown phase and the alumina matrix. To examine this point more closely, additional electron microscopy would be in order using a direct replication technique.

At present, it would be impossible to say that this unknown microconstituent contributes in any way either to failure at stress levels well below the expected average value or to the primary failure criterion. Its potential role in the mode of fracture will be mentioned in the section on fractography.

31

Grain Size - Among the nine specimens fired under "standard conditions" for which grain size was measured, little difference could be detected. The average size varied from 2.8 to 3.4 microns, and the maximum size was about 15 to 25 microns; see Table 10. No indication of nonuniformity or nonreproducibility was found with respect to grain size and shape. Tensile Specimen 3(2A05-047-2T) and 4(2A05-047-1T) in Table 10 possessed a 6.9 micron average grain size and a 30-35 micron maximum size. However, these specimens came from a blank intentionally fired to a temperature 80°C above the standard temperature. Figure 97 shows the microstructure for Flexural Specimens 4(5A13-102-6F) and 6(3A09-085-1F) from Table 10. All specimens fired under "standard conditions" possessed a grain structure similar to these examples. The black angular areas are not pores. These positions were occupied by the unknown microconstituent which was taken into solution by the etchant when used at 250°C.

From the standpoint of grain size, material uniformity and reproducibility were good and no relationship between grain size and strength was detected.

Fractography - A correlation seems to exist between the appearance of macrofractographs and the stress required for fracture. Specimens which required a higher stress to fracture developed a rough undulating fracture face, while those fracturing at a lower stress revealed an almost planar fracture face. Although it was most obvious for flexural specimens, this was also true for tensile specimens.

The macrofractrographs of Figures 98 and 99 illustrate this observation. These figures show a comparison of Flexural Specimens 1(3A09-085-2F) and 6(3A09-085-1F) of Table 10, respectively, high and low (weak/strong) strength mechanical specimen from the same blank. Figure 98 compares the fracture paths for the two mechanical specimens viewed in profile, with the top of the picture representing the region of compression. Note the irregular fracture path of the stronger specimen and the rather classic relation to the stress fields on the tensile and compressive sides. A comparison of the fracture faces of these two specimens at low magnification is shown in Figure 99. It is apparent that the stronger specimen possesses a rougher, more undulating fracture face.

That the stronger specimen reveals the creation of more new surface in fracture than the weaker one is a rational observation. However, it does not offer direct evidence of explanation for the low and high strength; i.e., it expresses nothing regarding fracture mode or fracture criterion. To examine the fracture surfaces in more detail, electron fractography was employed for several pairs of specimens. From the observations above, it was assumed that electron fractography would reveal a difference in fracture mode between weak and strong specimens.

32

Fracture surfaces were examined for two specimens mentioned above which came from the same blank, but yielded divergent strength values at similar densities. Figures 100 and 101 show typical regions of small and great amounts of transgranular fracture for Specimen 2(3A09-085-2F) (52,000 psi), Flexural Specimen 1 of Table 10. Fractographs of 1(3A09-085-1F) (35,000), Flexural Specimen 6 of Table 10 are shown in Figures 102 and 103.

From many photomicrographs such as those mentioned above, it was found that the primary fracture mode was intergranular. It was estimated that less than 10 to 20 percent of the fracture surface was intragranular and that between the upper and lower limits of strength for a group of specimens, the stronger specimens showed more intragranular fracture. Both the stronger and weaker specimens display what has been tentatively termed "a second phase" or intergranular impurity. Almost all fractographs contain this structure. Since these fractographs were made by a two stage (plastic-carbon) replicating technique, a negative (plastic) impression of the fracture is shadowed. Therefore on those photomicrographs which show an obvious shadowing direction, pores which are projections on the plastic cast a shadow outside their periphery, while an intergranular phase which is a depression in the plastic shows a deficiency of shadowing material on that side of the structure near the shadow source and a build up of shadowing material on the opposite side. With this in mind it will be apparent in these and other fractographs that little porosity can be seen in the fracture surface.

Fractography studies to be made in a continuation of this program will utilize a direct replication technique which should eliminate certain structural ambiguities and reduce the number of artifacts. A direct replication technique has been discribed by Gutshall and Shaw on pages 282 and 283 of the "Proceedings of the Electron Microscopy Society", 25th Annual Meeting, 1967. Artifacts which appear in the electron photomicrographs of this report include tears in the replica, undissolved plastic, round black particles at grain boundaries and other discontinuities, and black bands between specific grains. The black particles have not been identified. They may be due to poor conditions of evaporation or atmosphere pollution during preparation. The black bands are believed caused by replica collapse at points of sharp surface discontinuity.

Two additional specimens were examined which also showed divergent strength values and similar densities. However, these two specimens were of a lower density than the specimens mentioned above. Figures 104 and 105 compared the compression regions of Flexural Specimens 4(5A13-102-6F) (50,000 psi) and 5(2A12-096-11F) (30,000 psi) of Table 10, respectively.

33

Microfractographs for the tensile regions of these specimens are shown in Figures 106 and 107. The observations were essentially the same as those stated with respect to Flexural Specimens 1(3A09-085-2F) and 6(3A09-085-1F) of Table 10. That is, the amount of intragranular fracture was greater for the stronger specimen. It was also noted that the amount of transgranular fracture was less in the compression region for both the stronger and the weaker specimens. Both specimens had an intergranular phase and little porosity within the fracture face.

In this limited fractography study, weak and stronger specimens at two porosity levels were examined. A correlation seems to exist in that for each porosity level the stronger specimen reveals more transgranular fracture and a more tortuous fracture path. However, the stronger of the less dense specimens fractured in about the same manner as did the stronger of the more dense specimens. This is the same as the impression derived from physical density measurements versus strength. Although the presence of an intergranular phase probably contributes to the prominent intergranular fracture, the fractography study did not suggest any nonuniformity or nonreproducibility might contribute to the presence of more transgranular fracture in certain specimens. Consequently, within a given strength and density range, a small difference in fracture topography has been noted but no explanation is available.

Material Characteristics versus Extreme Differences in Strength

In the foregoing sections the characterization was largely concerned with material uniformity or reproducibility and a search for evidence which might explain the variation in strength within a range of values adhering to statistical description. It was also within the purpose of the study to attempt to learn why certain specific specimens failed at a much lower-than-expected stress. This is the weak/strong study. This problem has been referred to in some of the information above, but a concentrated effort was made on this point using Tensile Specimens 3(2A05-047-2T) and 4(2A05-047-1T) of Table 10. These specimens came from the only A05 blank tested which was intentionally fired to a higher temperature than normal. From the gage section of this blank, four specimens were cut: two flexural and two tensile. The two flexural specimens had strengths of 45,140 psi and 45,420 psi, compared with an average strength of 49,050 psi for all A05 specimens tested in flexure. Tensile Specimens 3(2A05-097-2T) and 4(2A05-047-1T) of Table 10 had strengths of 46,540 psi and 22,800 psi, respectively, compared with an average of 45,000 psi for all A05 specimens tested in tension with the exception of the 22,800 psi value. Since these two tensile

34

specimens came from essentially adjacent volumes of material and had such different strengths, it would seem they were excellent candidates for the investigation.

Probably the most obvious difference in these two specimens was recorded in the low magnification inspection of the fracture. The stronger specimen developed a classic fracture plane normal to the outer tensile face and then becoming inclined to the longitudinal specimen axis, while the fracture path of the weaker one was normal to this axis. The fracture surface of the stronger specimen was rougher than that of the weaker one. These observations parallel those previously cited for the flexural specimens.

Polished sections of the entire cross-section of the tensile specimen slightly below the fracture plane were made. Low magnification photomicrographs of these sections are shown in Figures 108 and 109. The cracks and missing areas associated with the periphery of both specimens are related to longitudinal cracks near the specimen surface which propagate more or less normal-to-the-fracture plane. This was observed on almost all tensile specimens. It would seem that the stronger specimen, Figure 108, was less dense, had more porosity striations, and had the larger maximum pore size. However, these observations are highly questionable for two reasons. The polished surface is quite near the fracture surface, so that the evidence may be influenced by the disruptive effect of fracture. Since the two specimens were contained in the same mount, polishing technique may be considered equivalent. However, the initial surfaces were rough, and therefore it is not known whether or not the plane of view is exactly the same distance from the fracture face for both specimens. The visual difference in porosity is also discounted by two sources of density determinations shown in Table 10, which indicate the two specimens are equivalent in this respect. Since all of the stronger tensile specimens seemed to have more damage or more peculiarities in the plane immediately below the fracture face, we intend to pursue this observation.

Typical areas of microstructure for both specimens are shown in Figures 110, 111, and 112 in the as-polished conditions, etched at 150°C, and etched at 250°C, respectively. These photomicrographs indicate that the size, amo ..t, and distribution of pores and second phase are similar for the two specin.. .s. The porosity shown in these photomicrographs may be slightly greater than the 3 percent indicated by density measurements and this is attributed to a certain amount of pullout. Figure 112 shows the similarity of grain size. The black

35

angularly shaped areas in these photomicrographs are positions formerly occupied by the second phase which had been taken into solution by the etchant at 250°C. As is indicated in Table 10, a value of 6.9 microns was determined for the average grain size of both specimens.

Replicas were prepared from the fracture faces of the remaining halves of Tensile Specimens 3(2A05-097-2T) and 4(2A05-047-1T). The fractographic examination revealed information similar to that previously stated for the flexural specimens. That is, the primary mode of fracture was intergranular for both specimens, with the stronger one displaying more intragranular fracture. Figures 113 through 116 illustrate typical comparative fracture areas.

Within the limits of this study, it has been impossible to determine the reason for the unusually low strength displayed by specific specimens. Prior to this examination, it was believed that a disparate flaw contributed to the very low strength. This type of flaw may include any structural detail that is abnormal to the general microstructure; for example, a heterogeneous distribution of porosity, a pre-existing large crack, a large void, etc. Such disparates critically located in the specimen, should produce low strength.

Evidence of disparate flaws was not found during the fractographic examination. However, it is quite possible that: the descriptive detail was overlooked, the evidence is not sufficiently different from the other fractographic structure, or the definitive structure is destroyed during fracture. That disparate flaws exist is a certainty, and the lack of success in finding something of this nature associated with the fracture face of Tensile Specimen 4(2A05-047-1T) does not preclude its existence. On several occasions, cracks were found in noncritical positions away from the fracture zone. These cracks usually enter the specimen at a rather shallow angle and it would seem that a chipped surface would result if the crack were propagated. Such a crack could develop during processing or during grinding as a result of relieved residual stress or due to grinding abuse. One may also argue that such cracks could develope during applied load. Since a meticulous microscopic in inspection of specimen surfaces prior to testing was not part of the procedure, no conclusion is available. However, if this type of flaw critically positioned served as a source of fracture, there is reasonably doubt that one could detect it during post-test fractography. Another disparate that was observed during post-test examination was a very large void probably associated with the bridging of powders during compaction. This void is shown in Figure 117, and in this view the cross section of the void is about 5 x 30 mils. It occurred within the gage length of flexural specimen 2A05-043-3F, which had a strength of 54,000 psi. It was located on the side of the specimen in that half of the tension region nearest to the neutral axis. It is difficult to imagine that a disparate of this magnitude would not play a role in low stress fracture

36

had the volume of material been extracted from the blank in a manner which would have placed the flaw in a critical position. Having examined replications of as-fired surfaces, one would say that evidence of this void within a fracture surface could be overlooked in electron fractography.

Although no positive data associating very low strength with disparates have been produced, the idea that this is probable has not been diminished. It is believed that in the future, suspect fractures should be examined by scanning electron microscopy and that extensive pretest, nondestructive testing should be employed including low power microscopic inspection of the specimen surface.

Characterization of Specimen Surface Condition

Initially, the tensile surfaces of high and low strength flexural specimens were examined by light and electron microscopy using replicas. No distinguishing differences were noted. However, the appearance of these surfaces was much like that of a fracture surface and both contained regions suggesting the presence of cracks.

It can be visualized that this type of surface structure could have diverse effects. For example, the surface may be damaged in a manner which introduces discontinuities and cracks of various sizes which tend to cause not only data scatter but occasional very low strength values. On the other hand, it could be suggested that grinding introduces a rather uniformly flawed surface which tends to normalize the mechanical data.

As a result of this observation, a cursory examination was conducted pertaining to the effect surface finish might have on the strength. The specimens were taken from an A10 blank. This type of blank, when previously examined by flexural and tensile tests, had shown uniform strength and density. The following finishes were evaluated: "as received" (pressed and fired), standard shop grind (15 RMS), standard shop grind plus shop lapping using 15 and $\frac{1}{4}$ micron diamond (3-4 RMS), standard shop grind plus shop lapping using 15, 7, 1, and $\frac{1}{4}$ micron diamond (3-4 RMS), and standard shop grind plus metallurgical lapping (finishing with 3 micron diamond). The results have been reported elsewhere and it need be only reiterated that none of the procedures enchanced the strength over that of the standard shop grind. "As-received" surfaces yielded strengths significantly lower than the ground specimens.

37

To document the surfaces resulting from the above procedures, two series of photomicrographs are presented. The first series was made from plastic replicas using transmitted light. These optical photomicrographs give one a general feel for the differences present. More detail will be obvious from the electron photomicrographs subsequently presented.

Figures 118-120 illustrate the general appearance of the subject surface conditions. The "as-received" surface consisted of a multiplicity of mounds. Their height prevented suitable focusing. The gross irregularity of this surface may have contributed to the lower-than-normal strength of this blank. Standard shop grinding (15 RMS) produced a surface which was reasonably flat, but contained many crevices or cracks. Very little cutting action had taken place since no evidence of areas of smooth surface had developed. The inherent structure of the body is not visible. The two shop lapping procedures (3-4 RMS) tend to smooth the surface produced by grinding but in no way eliminated the deep detail visible after grinding. Metallurgical lapping removed most of the obvious grind damage and exposed the positions of porosity and/or grain pullout. The scratches in evidence are from the last abrasive used, 3 micron diamond. Although these surfaces were not tested, photomicrographs are also included to document a fired surface which had been previously green machined and a surface resulting from refiring after shop grinding. The surface which was refired came from an area adjacent to that shown in Figure 118b, standard shop grind.

Figures 121-127 are electron photomicrographs of the same surface conditions mentioned above. Two-stage (plastic/carbon) replicas shadowed with chromium were used. Obvious artifacts include undissolved plastic and contamination particles. It can be seen that the individual mounds making up the pressed and fired surface, Figure 121, intersect at rather sharp angles and that the individual alumina grains showing a crystallographic growth pattern also present many minor surface discontinuities. Shop grinding, Figure 122, produces a surface not unlike that of a fracture surface. Cracks, grain surfaces, and grain boundaries are visible. Lapping in the shop tends to create islands of smooth material where cutting action has taken place; however, the deep surface distress from the original grind remains, see Figures 123 and 124. Thermal treatment after green machining or after grinding, Figures 125 and 126, produced somewhat similar surfaces. The individual alumina grains are obvious with a certain amount of thermal faceting. The gross surface imperfections of the pressed and sintered part are absent. From these photomicrographs however, it cannot be determined if surface cracks exist when the final treatment is thermal. Surfaces such as these were not part of

38

the mechanical test series so that insight is not available. The specimen used to illustrate the metallurgically lapped surface has been etched at 150°C to reveal some of the structure such as the second phase and polishing scratches. After viewing this photomicrograph, Figure 127, it is not surprising that the metallurgically lapped specimens did not yield greater-than-normal strength values. A large selection of fracture criteria is still available including (1) exposed pores, (2) the interface between the alumina matrix and the second phase, alumina grain boundaries (not visible), (3) fracture surface developed during grinding which was not completely removed by lapping and (4) possibly microcracks.

It is obvious that none of the secondary finishing operations completely eliminate the features developed during the initial grinding step, even though from the standpoint of profilometry the surface was greatly improved. Since the strength was not increased with improved surface finish, one must question the advisability of using conventional surface finish measurements to relate finish to strength for this material. It would seem that the question of the effect that surface finish or damage due to grinding has on strength cannot be answered until only the inherent material characteristics are present on the surface. At the present time, it is not known whether fracture was associated with damage induced during grinding or was initiated by some inherent external or internal structural characteristic.

The tensile surface of one of the shop-ground, metallurgically lapped flexural specimens was photographed before and after testing. The lower picture in Figure 128 shows the mating tensile surfaces after fracture, while the upper picture is of the same region before fracture. This photomicrograph is included to show that fracture, if initiated at this surface, is not necessarily associated with a major surface imperfection. In fact, the fracture path across this surface of maximum tensile stress did not intersect any of the largest surface discontinuities. This is not to say that fracture did not originate at a site of grind damage, for it may well have. However, it would lend support to the idea that simply removing gross surface pits, and thereby improving finish, will not necessarily improve strength.

More work of this type where the fracture is mapped on prior photomicrographs is anticipated, also the middle range of surface finish will be explored. As found on earlier programs, it now appears that strength increases with improved surface finish up to a point and then shows no further increase with further polishing and reduced rms readings.

39

Synopsis

In this summation an attempt has been made to critically digest the information presented in Tables 9 and 10 and the various photomicrographs, and thereby condense the data. This presents an opportunity to state what appears to be the standard or average characteristics of the material, to point out the deviations, and to make comments which otherwise are difficult to introduce in the presentation of results.

Statement of Average Characteristics and Deviations- The standard or average characteristics of this material can be described as follows:

1. Alumina grain size - Average grain size was 3 microns, while the maximum grain size was 15-25 microns. Certain specimens which were intentionally fired to a higher temperature had an average grain size of 7 microns with a maximum size of 30-35 microns. Nothing was found which would suggest a lack of uniformity or reproducibility with respect to grain size within reasonable limits.

2. Second phase - The presence of a phase other than alumina was observed to occur as discrete grains similar in size to the alumina grains and possibly as an intergranular deposit. About 6 volume percent of this phase was present, having an average size of 2 microns. This material was uniformly present in all specimens examined.

3. Features of porosity - The average pore size was 1.3 microns with a maximum size of 50 microns. The maximum pore size value is open to considerable debate. It is quite common to develop artifactual voids on the polished surface of a polycrystalline brittle oxide. Furthermore, the presence of large voids was not detected in fractography studies. On the other hand, voids several mils in size are not impossible, and indeed, evidence of a very large void was presented in a foregoing section. It is felt that the validity of the presence of large pores does not detract from the conclusions of this characterization and judgement of this point is reserved pending additional study.

The amount of porosity was also subject to critical discussion in a previous section. The typical level of porosity was 3 to 5 percent based on the density determinations (3.80 to 3.88 gm/cc) made by the Mechanical Engineering Division. These data are used to state a typical porosity level because they are the only data involving a great number of determinations and also are the only

40

data directly relatable to the specific volume of material from which mechanical test specimens were taken.

Within the examination of porosity features, it was observed that the A11, A12, and A13 specimens were different from the other blanks of different geometry. The porosity was greater than 5 percent, ranging up to 8 percent (density - 3.81 to 3.67 gm/cc), and maximum pore size was 125 microns. All other blanks showed reproducibility with respect to the stated typical values. The blanks stated above which showed deviation will be discussed below.

4. Fracture mode - The predominant fracture mode for all specimens examined was intergranular. Up to about 20 percent transgranular fracture was noted. In all cases, the stronger the specimen, the higher the percentage of transgranular fracture regardless of density level. No evidence of non-uniformity or nonreproducibility was detected within the limited qualitative fractography study.

5. Fracture stress - The average tensile strength was 46,300 psi and the average flexural strength was 48,290 psi. Elsewhere in this report, it has been pointed out that the data for blanks A11 and A13 do not conform to the data of the whole population of specimens. This opinion results from: (1) the comparison between the average strengths for these two groups and the range of average strengths for all other groups, and (2) the comparison of the plots of probability of fracture versus fracture stress.

The comparison of average strengths for each type of blank would also indicate on first glance that the A05 specimens had low strength. Examination of the data for the individual A05 tensile specimens shows that the lower-than-normal average strength is unduly influenced by one very unusual specimen which fractured at a stress which was approximately 50 percent of the average stress for the nine specimen group. Furthermore, the lower-than-normal average tensile strength for the A05 group is not repeated in the flexural results as is the case of the A11 and A13 groups. Finally, the particular specimen which fractured at very low stress was one of the group fired at a higher-than-standard temperature.

Review of Deviations- Within the limitations of this study, no significant observations have been made to question the uniformity of the volume of interest of any given blank. Also, the reproducibility of character among identical blanks seems good. With one exception, the reproducibility among

41

blanks for a given tool set is good. This exception is A12, previously cited as having lower-than-normal density. The A12 blanks were prepared from Tool Set No. 2, also used to produce blanks for A04, 05, 07 and 08. A review of data pertaining to the manufacture of these blanks suggests a possible explanation. The two A12 blanks studied were green machined from the central portion of a Tool Set No. 2 pressing, as were all the other blanks mentioned above. The green densities of the A12 blanks were just slightly below the average for 30 blanks produced from Tool Set No. 2. However, of all the blanks machined from Tool Set No. 2 pressings, the A12 parts present the greatest cross-section exposed to thermal treatment, and the two A12 parts examined received the lowest thermal input of any blanks as measured by cone deformation. If below-normal thermal input is a reasonable explanation, it would seem that the manufacturer could readily rectify the conditions. Since strength for the A12 blanks was not above average and grain size was slightly less than average, one might assume a small increase in thermal input would not develop unwanted side effects.

When one considers the material's reproducibility among blanks made from different tool sets, a deviation from typical or average character is observed. In this program, six tool sets were used to acquire pressed shapes suitable for the preparation of 13 blank geometries. Blanks A11 and A13 were the only geometries produced from Tool Sets 4 and 5, respectively. One A11 blank and three A13 blanks were examined. As pointed out above, the mechanical strength and density data for these blanks did not conform to that for the other blanks in the study.

It is not too surprising that the data for the A11 blank and the A13 blanks differed somewhat from the blanks made from other tool sets. To maintain uniform material characteristics between large and small size ceramic parts is always an arduous task. Although other factors are involved, one can appreciate the problem by considering the ratio of area pressed to volume pressed. Other things being equal, this ratio gives one a feel for the difficulty concerning the development of uniform and reproducible green density between blanks from different tool sets. For example, in this work the area-to-volume-pressed ratio varies from over 6 for Tool Sets 1 and 6 to less than 3 for Tool Sets 4 and 5. Generally, the greater this ratio, the more easily a specific density level may be maintained. This same type of size effect can be visualized having a role in the firing process.

Since it would be undesirable to change blank sizes or to delete certain sizes, it is hoped that the manufacturer's wealth of knowledge pertaining to auxiliary techniques concerned with pressing and firing of this material will be able to overcome the shortcomings observed regarding the A11 and A13 blanks. In the case of the A11 type, it should be reiterated that only one blank was examined. This blank was one of an initial group in which the manufacturer had some confidence in the quality. Since that time, additional A11 blanks have been received at the Institute. The manufacturer believes these to be of superior quality. None of these latter blanks have been examined. It is therefore possible that the deviation from normal character with respect to the A11 type blank has been corrected.

General Opinion Regarding the Characteristics of the Material - The primary objective for the characterization of the material being used in this program was to obtain the assurance that microstructurally the alumina was uniform within individual blanks and reproducible among blanks of a given tool set and between blanks of different tool sets. The character of the material was evaluated with respect to: density, grain size, features of porosity, identification of secondary microconstituents, and fractography. Within the limit of this study, only the density or amount of porosity for blanks A11 and A13 seemed to deviate from what might be termed typical or average. All other characteristics were uniform. There was considerable discrepancy between absolute values regarding density or percent porosity depending on the measuring technique. However, regardless of the technique employed, the data for A11 and A13 specimens fell to the low side of the density spectrum. Also, the average mechanical strength of specimens from these blanks was lower than that of the other groups, and the probability of fracture plots would indicate the strengths of A11 and A13 did not distribute over the general population. If additional examination should show that the manufacturer has the capability to increase the density and strength of these blanks of the required rather small amount without appreciably altering the remaining characteristics, the question of reproducibility would be resolved.

The characterization effort was also concerned with identifying the reason for an individual macro specimen having an unusually low strength. This occurred with respect to several blanks and was not limited to either one of the test methods. For example, one A12 blank had 13 flexural specimens prepared from it; 12 of which failed at 43,590 psi to 51,330 psi, while one specimen failed at 29,810 psi. This same thing occurred during tensile tests. The characterization work associated

43

with specimens from an A05 blank was discussed previously. Although it was repeatedly found that the weak specimen developed a more planar fracture path and showed less transgranular fracture, no specific reason for unusually low strength was determined. The premise has been maintained that a disparate type of flaw contributes to the low stress failure. This type of flaw in the form of cracks and large voids has been observed, but not in association with specimens of low strength during post-test examination. Nothing has been learned which would negate the original premise. It has become apparent that extensive and meticulous nondestructive testing, along with continued post-test examination including techniques not used in this study, may be required to resolve the question.

A small amount of effort was devoted to the characterization of macro specimen surface finish. It was observed that the standard grinding procedure produced a surface not unlike that of a fracture surface. That is, little cutting action takes place and the surface is removed by uniform intergranular fracture. No difference in surface characteristics was noted between specimens which failed at high and low stress. Although lapping procedures using the facilities of the machine shop and the metallographic laboratory increase the percentage of smooth or cut surface, these efforts did not eliminate all the original grinding and no increase in strength was noted. Obviously, other techniques of surface preparation may be used to derive a condition which would present only the material's inherent flaws at the surface but it is quite possible that the procedure would be impractical for this program. The question remains even on the best finishes as to whether the fracture is initiating at the surface or internally particularly on the tensile specimens where stress is constant across the diameter.

Strength Monitors

A cursory examination has been made of several strength monitors, correlators, or descriptors generalized for tensile and flexural observations. An attempt was made to correlate these monitors to both average and individual strengths. Some of the monitors have been mentioned and/or discussed in earlier sections of the report, but will be mentioned again here to provide a summary view. The discussions are in terms of the monitor and average plus individual behavior.

Statistical Behavior- In general the strength distributions for the different blanks followed the pattern of random numbers rather well. That is, almost all of the blank types had strength values which were more or less normally distributed throughout the strength range. Further, the flexural and tensile

44

distributions were similar in character though shifted by about 5 percent. Where there were departures from normal behavior in averages, material differences were found.

Density - Figure 129 is a plot of average density of the macro specimens versus their average flexural strength. A trend of increasing strength with increasing density seems to exist but the relationship is not a tight one. Figure 130 is a similar plot for the macro tensile specimens which shows even less correlation between average strength and density. Some limitations of the density analysis have been mentioned in terms of the representative nature of the samples and the precision of the measurement. About the only definite conclusions would be that in general the low strength blanks were also the low density blanks. Other than that there was no definite trends. Also, there was not a one to one relation between density and single weak specimens from a given blank. Thus the weak/strong study did not reveal density as a monitor of disparate behavior.

Disparates - As previously mentioned, ultrasonic pulse-echo did locate a porous region in the A11 blank. Also, no disparates were found by pulse-echo in the macro specimens. Specimen 3A10-087-19F showed a weak back-echo during inspection. This specimen was weaker than the average from its parent blank and had lower density. No other such observations were made with pulse-echo.

One rather large disparate void was found visually in Specimen 2A08-043-03F, however, the flaw was near the neutral axis of a flexural specimen and it failed at another location. Large cracks and porous regions were observed visually, by penetrant and under ultraviolet light in an A11 specimen.

Fracture and Near Fracture Surface - In general the weak specimens had smooth fracture surfaces and the stronger ones had rougher, undulating surfaces. There appeared to be more intragranular fracture associated with the strong ones. Also for the strong tensile specimen the damage from fracture did not seem to be limited to the fracture surface; usually, several mils away from the fracture surfaces there was some evidence of damage. More detailed investigations may reveal something here.

45

Surface Finish - There were strength increases when progressing from highly irregular as-fired surfaces to shop-machined surfaces, but no differences were detected between the shop-machined, the shop-polished, and laboratory lapped ones. There are still some questions to be answered regarding surface finish. Primarily, the questions concern whether the strength data are being normalized by grinding damage during specimen preparation and whether the fractures are initiating at the surface or internally. These questions are very difficult to answer, but answers will be pursued before proceeding into the final phase of the program.

Griffith Cracks - The relation $\sigma = \sqrt{2ET/\pi c}$ gives a theoretical crack size of about 0.0015 inch using $T = 20,000$ ergs/cm^2. Microscopic examination revealed no cracks of this type in the material. However, the larger void sizes are about 0.002 inch (or bigger) so that, given a crack tip, they could serve as initiators or propagators. The inference is that any crack significantly smaller than this may provide for subsequent crack nucleation but not crack propagation without growth.

Production Figure of Merit - This is a qualitative type of figure which includes such manufacturing considerations as pressing area to volume ratio, firing thickness, cone readings, and others. There was some correlation between a combination of these factors and strength and some evidence that closer control of these factors would bring the data in tighter. A variance analysis may provide additional information in this particular area. An extensive review of the production variables is under way to establish the extent to which grain size and density, for example, are properly monitored in the hardware by tag end pieces and small samples placed nearby during firing.

Ultrasonic Velocity - Some difficulty was encountered in making ultrasonic velocity measurements on the macro specimens due to their small size. This was especially true with some of the tensile specimens because the ends had been chamfered to such an extent that insufficient surface area was available to allow the proper input of the ultrasonic energy. This was corrected later in the program by taking the measurements prior to chamfering the ends. No correlation was noted for average velocities and average strengths nor for individual weak/strong relations.

Grain Size - The average grain size varied from 2.8 to 3.4 microns, and the maximum size was about 15 to 25 microns. There was no indication of non-uniformity or nonreproducibility with respect to grain size or shape. Several blanks were fired purposely to a higher temperature and the grain size for these specimens averaged 6.9 microns with a maximum size of 30-35 microns; however, with only one exception these high-fired pieces had nominal strengths in spite of the larger grain size.

46

Figure **131** shows a plot of grain size versus fracture stress for seven flexural specimens. Also shown are curves using the expression $\sigma = KG^{-a}$ as proposed by Knudsen. The range in grain size for the normal specimen is too small to make a judgement as to the effect of grain size or to make a regression analysis except by normalizing to theory. Grain size measurements on more specimens may provide a greater spread so that better definition can be made. There are possibilities that this additional information could provide better limits for the grain size and thus further eaduce the strength ranges. Single weak specimens were not related to grain size.

Porosity and Pore Nature - Porosity has been discussed in some detail in earlier sections. Only the results will be restated here. The average pore size was **1.3** microns with a maximum size of **50** microns on most blanks. **A11, A12, A13,** were different from the other blanks with respect to porosity. Their porosity was greater than **5** percent and the maximum pore size was **125** microns. All other blanks showed uniformity and reproducibility with respect to the above typical values to the extent they were sampled.

Figure **132** shows the average flexural strength plotted versus porosity based on the average density values. Curves using the expression $\sigma = Ae^{bx}$ are also shown plotted. There are not enough values for definite conclusions. That is, the range of densities for a given grain size is quite small. A regession probably should be to the theoretical curve.

Fracture Mechanisms

Work thus far in this area has been limited, and at present there is no clear evidence as to the source of fracture. Although some intragranular fracture was observed on the stronger specimens the primary mode seems to be intergranular for all specimens. There was some evidence in the micrographs of cracks at the second phase, but we cannot be sure at this time whether or not there were cracks or artifacts from the replication technique. In either event they could have provided nucleation but were too small to provide propagation. There was no evidence of pore to pore fracture. In fact, in a single controlled flexural test the fracture line seemed to avoid surface voids. Also, large pores seemed to be conspicuously absent in the fracture faces.

47

CONCLUSIONS

In the final analysis the material will be judged from two points of view; (1) as a source for providing specimens to study test methods, and (2) as a standard material. The following conclusions are made only with respect to (1).

1. The extent of uniformity and reproducibility is nominally acceptable on all 13 blank types except for three of them, A11, A12, and A13. At least one of these, A12, can be brought up to standards with minor alterations in the production procedure, but the other two will require some additional work.

The grain size did not vary appreciably on any of the blanks except for those which were intentionally fired to a higher temperature. The densities among the several blanks were all reasonably consistent except for A11, A12, and A13, which had low densities. The average strength values were all within acceptable limits except for A11 and A13. There was no uniformity problem within a given piece for the small number of blanks inspected.

2. The only variables which correlated with strength were the density to some extent and a production figure of merit which includes considerations such as pressing area to volume ratio, firing thickness, cone readings, and others. There were not data to determine whether or not strength correlated with grain size. There were no correlations noted with respect to ultrasonic velocity, pulse echo, and others. Macro specimen fractology correlated to some extent. The stronger specimens usually had rougher and more undulating fracture surfaces while the fracture surfaces of the weaker specimens were smooth and more planar.

3. At this point in time perhaps we now could box the strengths at 46,000 psi to 51,000 psi averages if we boxed density between 3.80 to 3.84 gm/cm^3 and grain size within 2-5 microns, and employed certain controls on the production figure of merit.

4. Within the limits of (3) we could probably conduct an effective analysis of test methods, but we would not have a standard material. Hence, it remains a matter of judgement whether the material should be further improved before proceeding with the test methods study. At any rate, A11 and A13 will have to be upgraded.

48

RECOMMENDATIONS

Our recommendations for the next years effort are as follows:

1. Continue the joint effort with Coors, anticipating Phase II starting in perhaps a year, to improve A11 and A13 relative to other blanks.

2. Conduct an analysis of variance and covariance of all data to date. This may require obtaining some additional data to firm up sources of variance. Emphasis of the analysis is to be placed on variables such as the locations of macro specimens within a given blank, etc; however, some effort will need to be placed on the causes of the variances to aid in the discussions when the time comes to purchase the material for Phase II.

3. Based on the above analysis suggest modifications in the fabrication technique to accommodate different blank shapes so that a reasonably tight density range more insensitive to production techniques can be obtained to a common grain size. This infers slightly higher densities and larger grain sizes.

4. Take a considerable look at surface effects. This study may include, but not be limited to:

    a. Using different laboratories to machine specimens to the same finishes

    b. Use of all reasonable surface preparations to determine their effect

These preparations could include machine grinding, shop-laps, metallurgical-laps, thermal surface treatment, chemical surface treatments, others.

5. Investigate chemical and environmental effects. This would require testing several groups of specimens (10-20 specimens/group) which had been exposed to different environments.

6. Conduct a more extensive examination of the fracture faces with particular interest on disparates and second phase.

7. Examination of surface fracture patterns and subsurface damage.

8. Some work in the area of mechanics of fracture to try and determine the causes of fracture and/or sources and to define the weak/strong relationships.

49

9. More fully employ inspection techniques to examine the specimens, particularily prior to testing. We do not mean employ new exotic techniques necessarily, but to use existing techniques more extensively.

20 RMS

0.200"

0.100"

2"
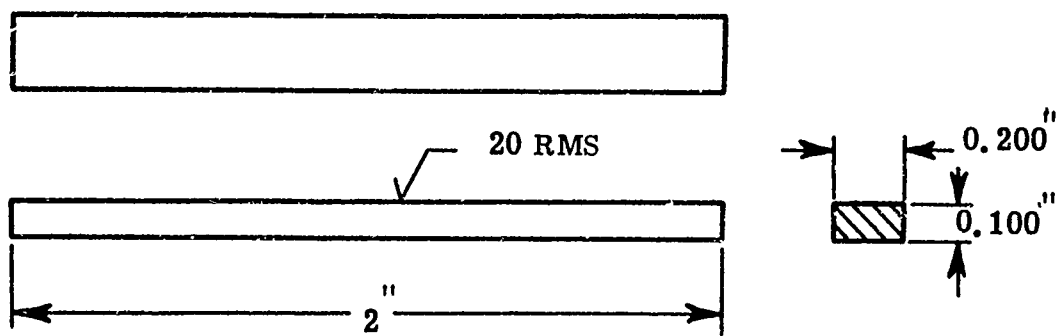
Figure 1. Macro Flexural Specimen

51
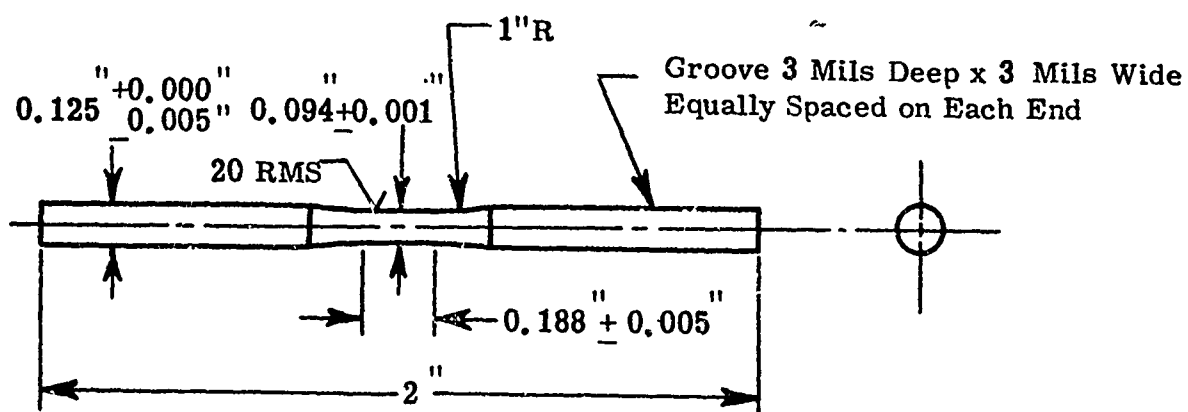
Figure 2. Macro Tensile Specimen
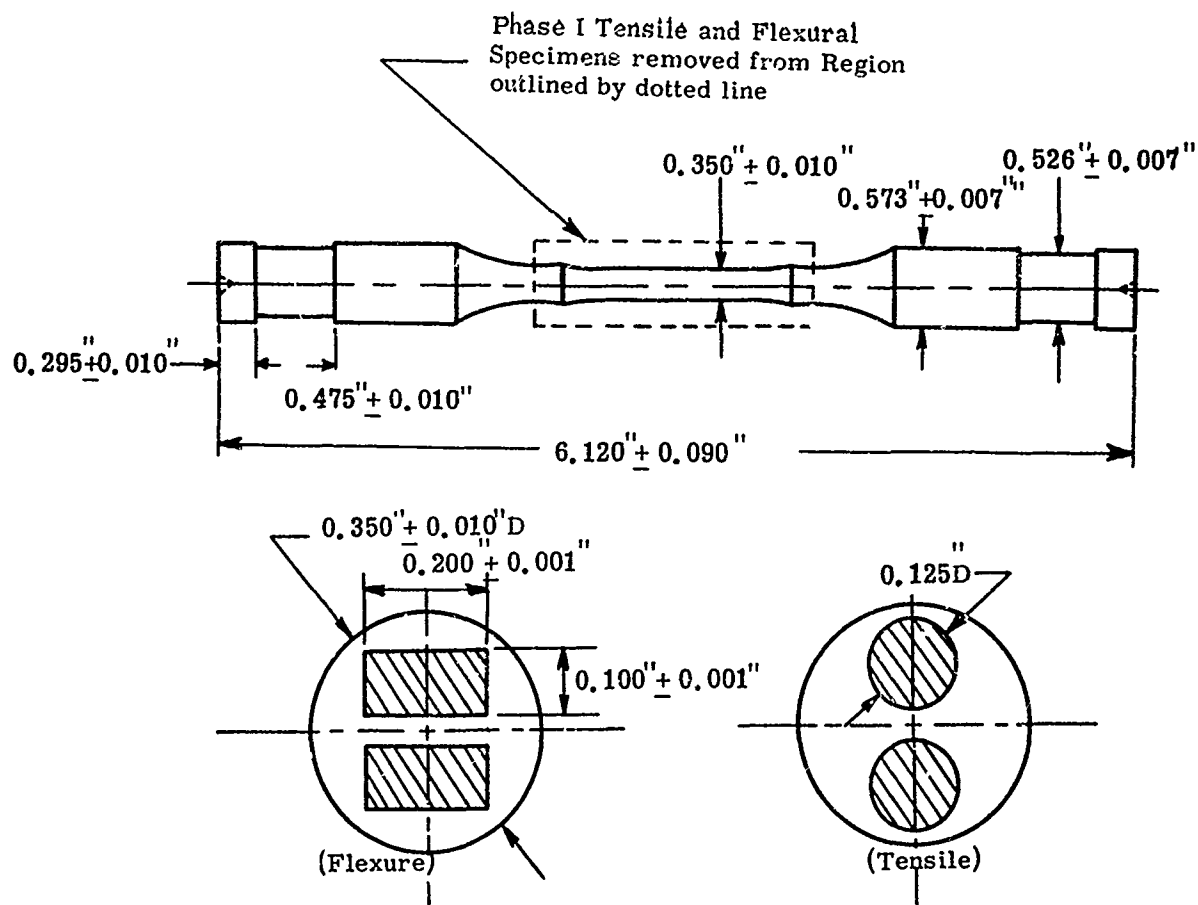
Figure 3. Configuration of Specimen Blank **1831-A-2** as received from Coors and Cutting Plan for Removing Phase I Macro Tensile and Macro Flexural Specimens

53

Phase I Tensile and Flexural Specimen
Specimens removed from Region
outlined by dotted line

0.597 ± 0.007

0.547 ± 0.007

9.925 ± 0.145

1.105 ± 0.015

0.547 ± 0.007

54
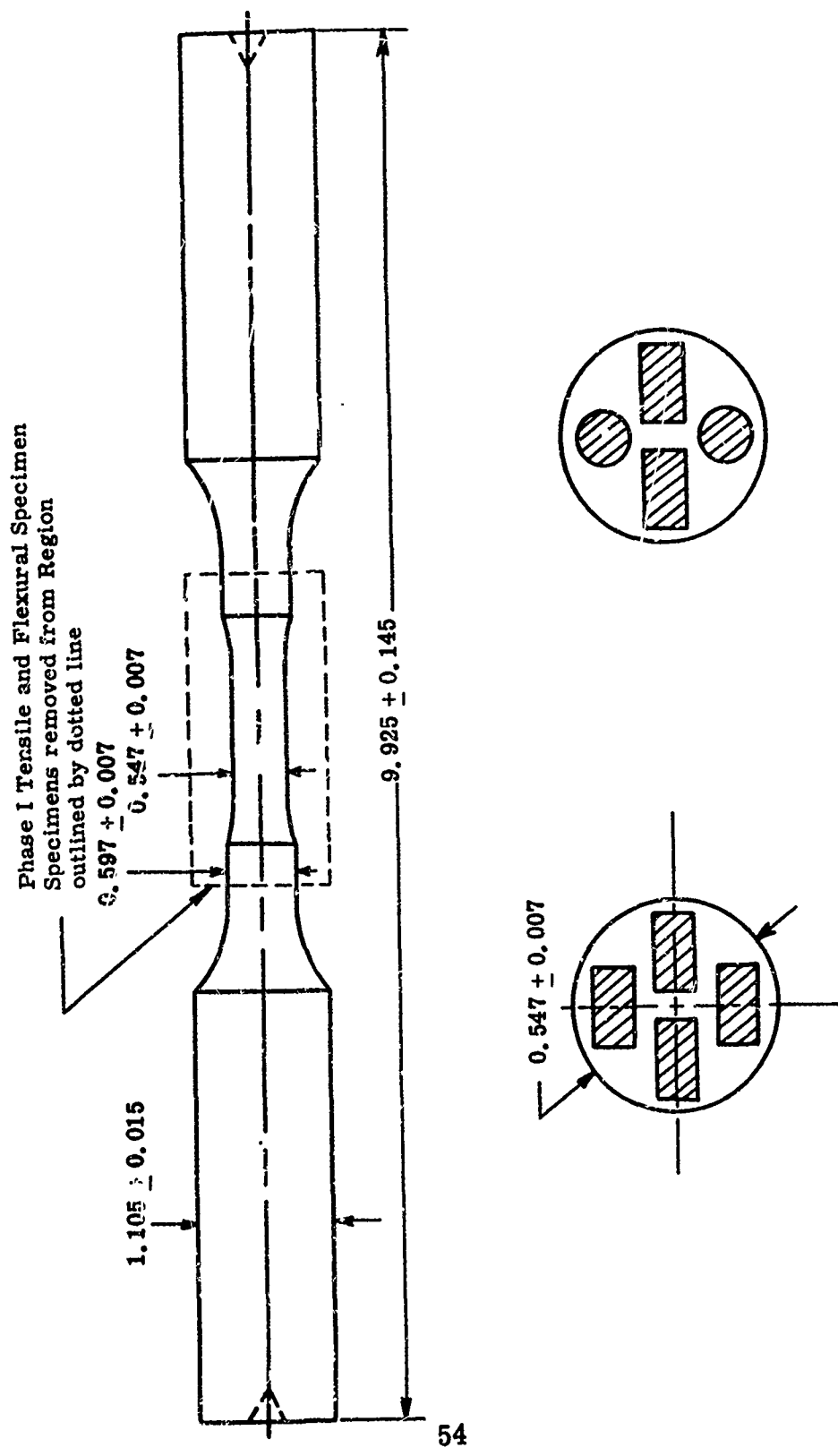
Figure 4. Configuration of Specimen Blank 1831-A-4 as received from Coors
and Cutting Plan for Removing Phase I Macro Tensile and Macro
Flexural Specimens
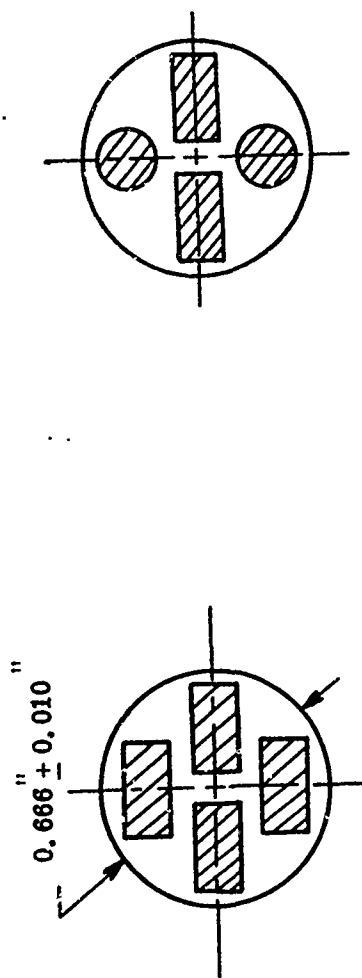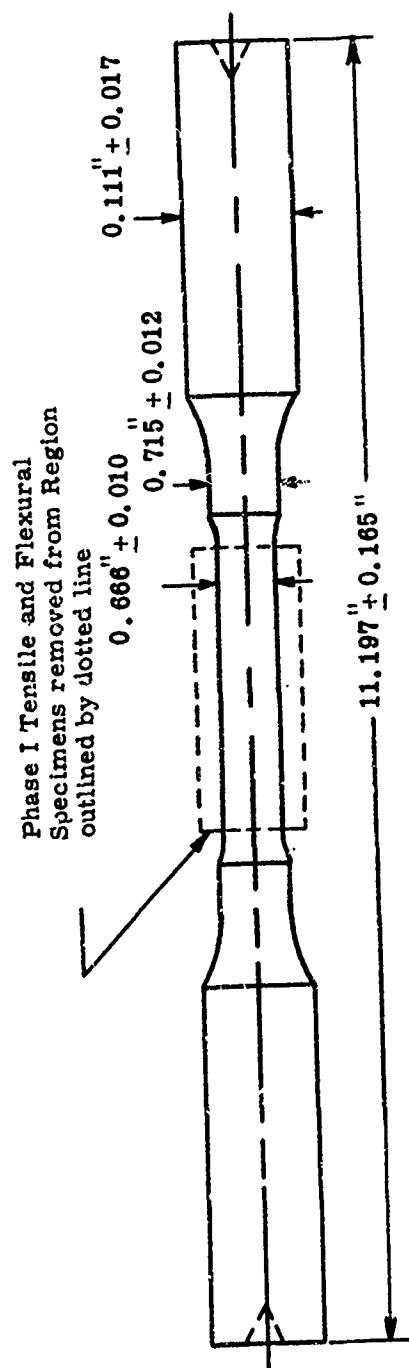
Figure 5. Configuration of Specimen Blank 1831-A-5 as received from Coors and Cutting Plan for Removing Phase I Macro Tensile and Macro Flexural Specimens

55

Phase I Flexural Specimens Removed from Region Outlined by Dotted Line

0.319 + 0.005"

0.547" +0.008"

1.426" +0.020"

56

Figure 5. Configuration of Specimen Blank 1831-A-6 as received from Coors and Cutting Plan for Removing Phase I Macro Tensile and Macro Flexural Specimens

Phase I Tensile and Flexural
Specimens Removed from Region
outlined by dotted line

$1.059\,{}^{+0.015}_{-}{}''$

$0.491\,''\,{}^{+\,0.007}_{-}$

$2.315\,''\,{}^{+0.035}_{-}$

$0.491\,''\,{}^{+\,0.007}_{-}$
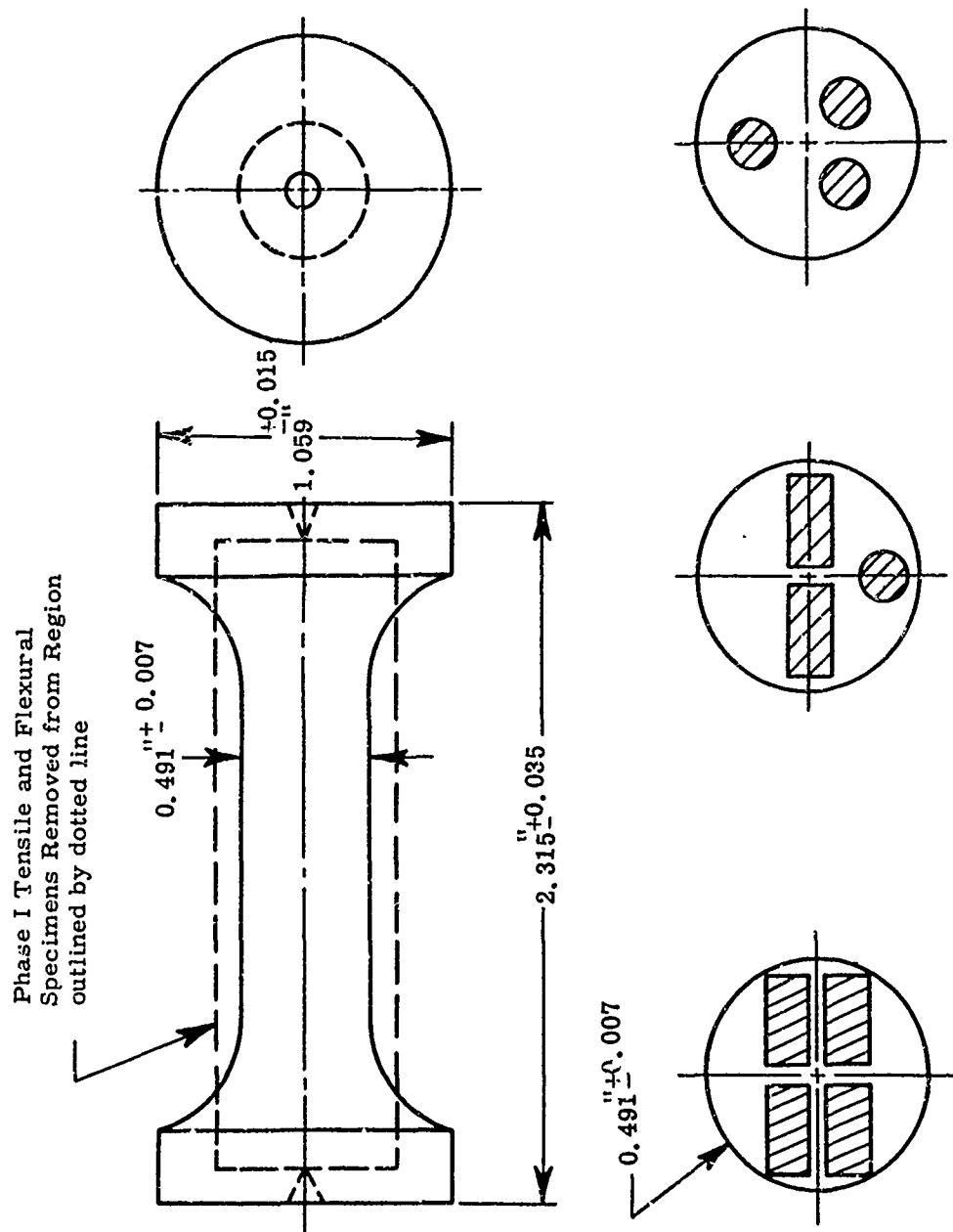
Figure 4. Configuration of Specimen Blank 1831-A-7 as received from Coors
and Cutting Plan for Removing Phase I Macro Tensile and Macro
Flexural Specimens

57
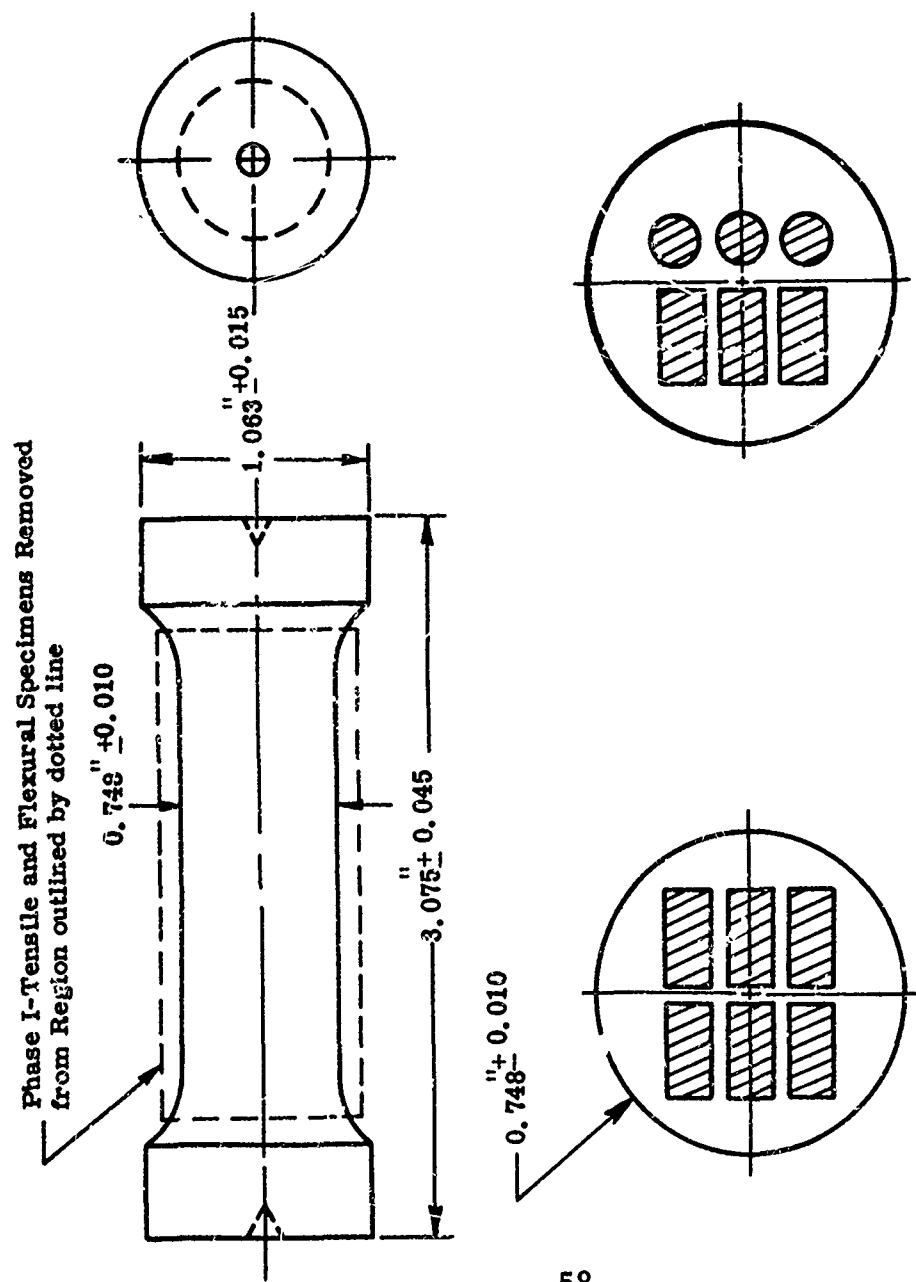
Figure 8. Configuration of Specimen Blank 1831-A-8 as received from Coors and Cutting Plan for Removing Phase I Macro Tensile and Macro Flexural Specimens

58
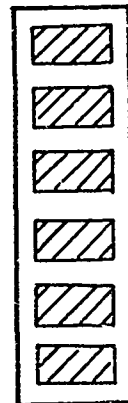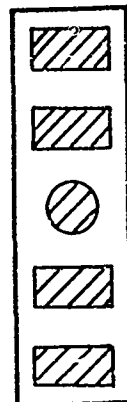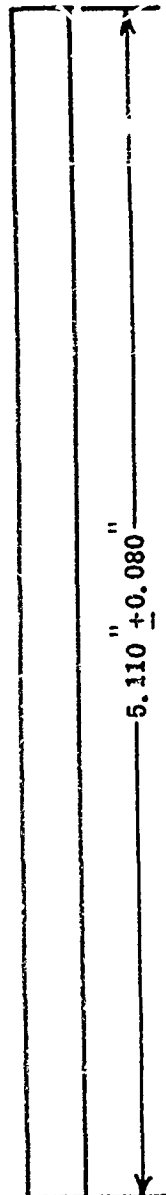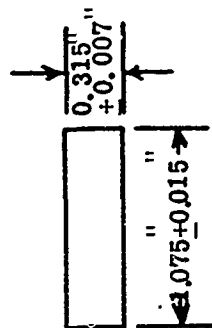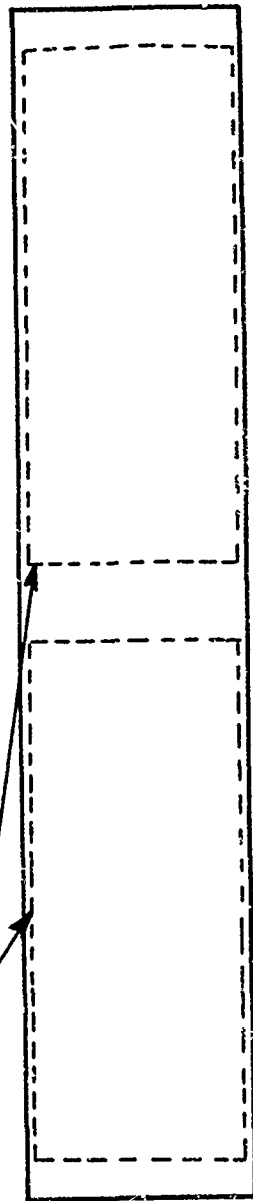
Figure 9. Configuration of Specimen Blank 1831-A-9 as received from Coors and Cutting Plan for Removing Phase I Macro Tensile and Macro Flexural Specimens

Phase I Tensile and Flexural Specimens removed from Regions outlined by dotted lines.

0.315" +0.007"

4.075 ±0.015"

5.110" ±0.080"

59

Phase I Tensile and Flexural Specimens removed from regions
outlined by dotted lines

$1.111"$
$\pm 0.015"$

$1.111"$
$+0.015"$

$11.197" \pm 0.167"$
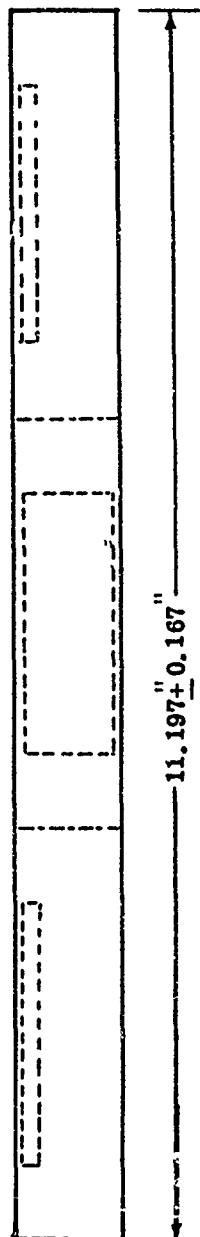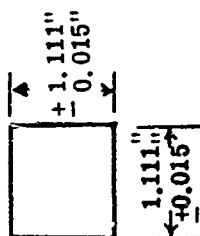
60
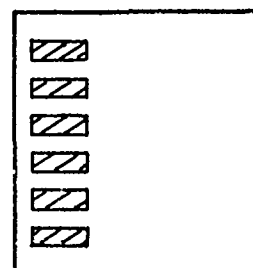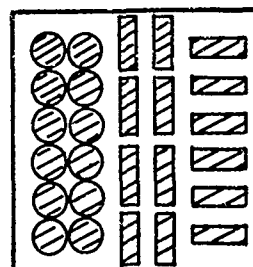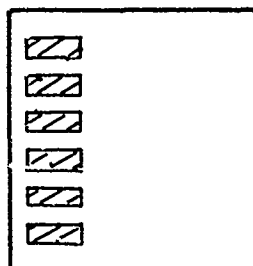
Figure 10.   Configuration of Specimen Blank 1831-A-10 as received from Coors and Cutting Plan for
Removing Phase I Macro Tensile and Macro Flexural Specimens   (Item 87)
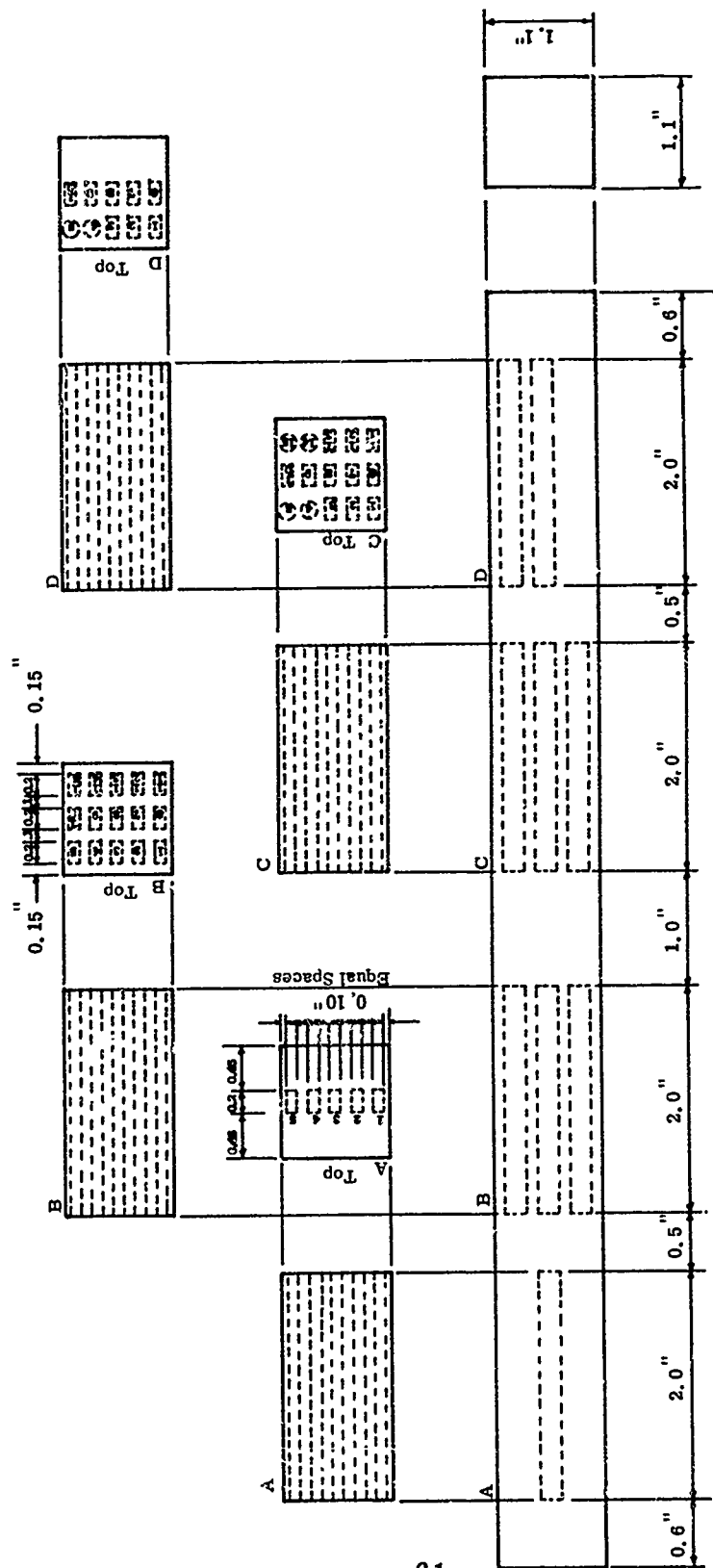
Figure 11. Configuration of Specimen Blank 1831-A-10 as received from Coors and Cutting Plan for Removing Phase I Macro Tensile and Macro Flexural Specimens (Item 86)

61
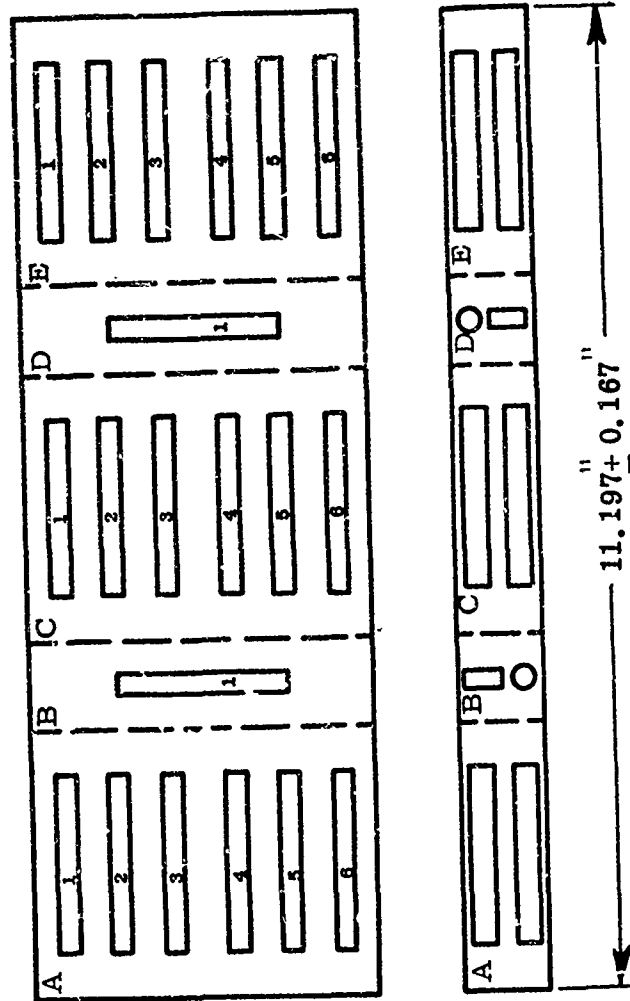
Figure 12. Configuration of Specimen Blank 1831-A-11 as received from Coors and Cutting Plan for Removing Phase I Macro Tensile and Macro Flexural Specimens
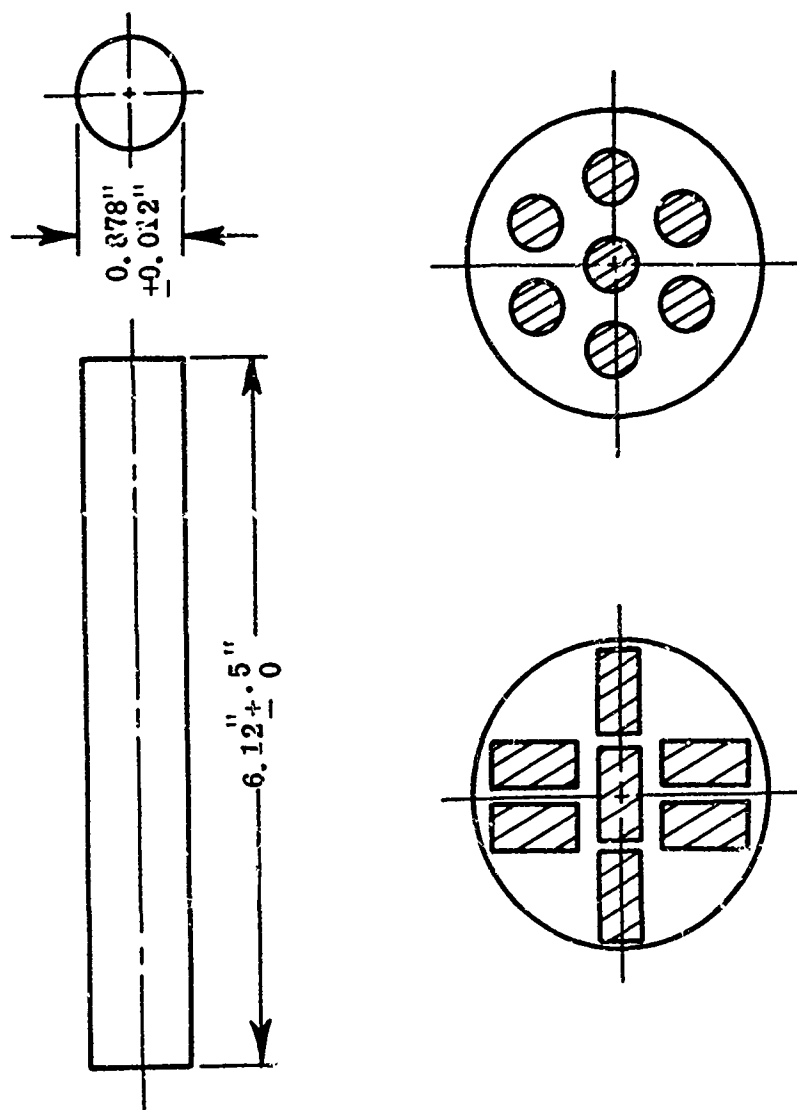
Figure 13. Configuration of Specimen Blank 1831-A-12 as received from Coors and Cutting Plan for Removing Phase I Macro Tensile and Macro Flexural Specimens

63
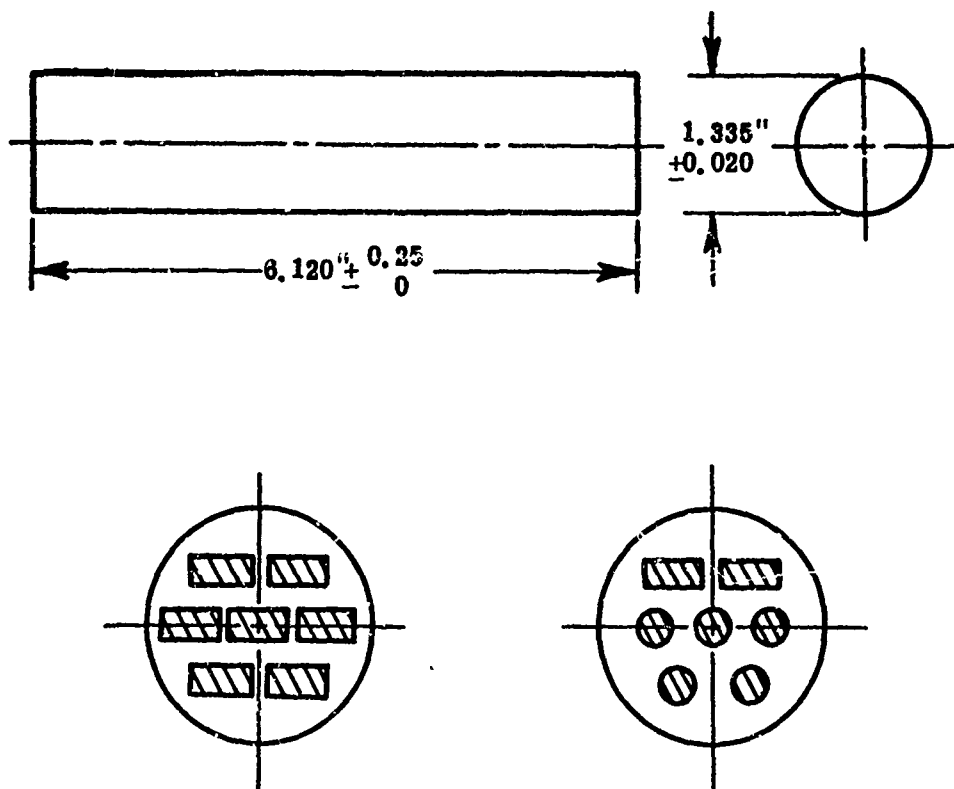
Figure 14. Configuration of Specimen Blank 1831-A-13 as received from Coors and Cutting Plan for Removing Phase Macro Tensile and Macro Flexural Specimens
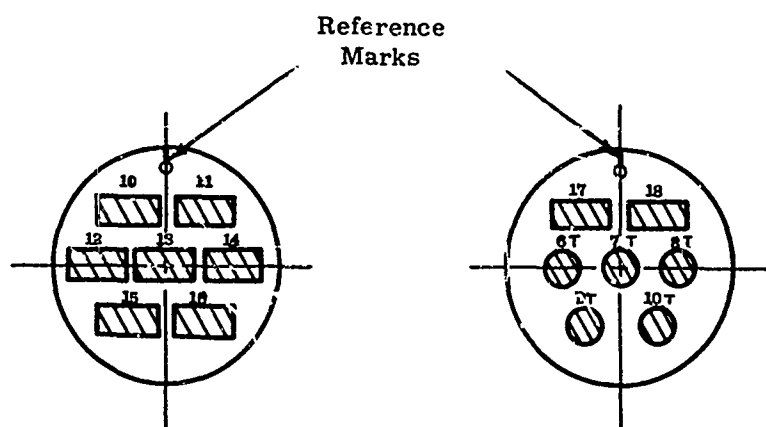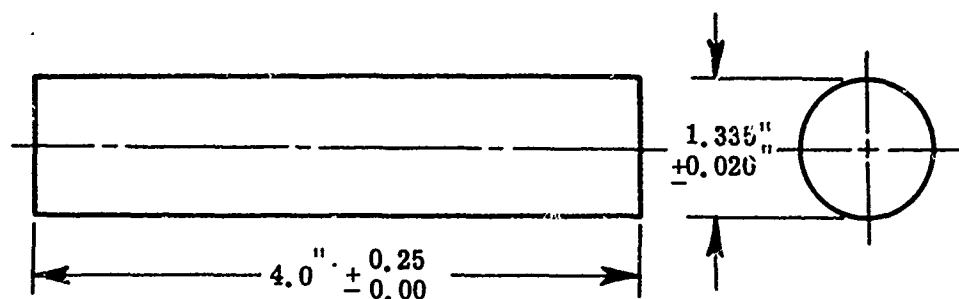
64

Figure 15. Ccnfiguration of Specimen Blank 1831-A-13 as received from Coors and Cutting Plan for Removing Phase I Macro Tensile and Macro Flexural Specimens
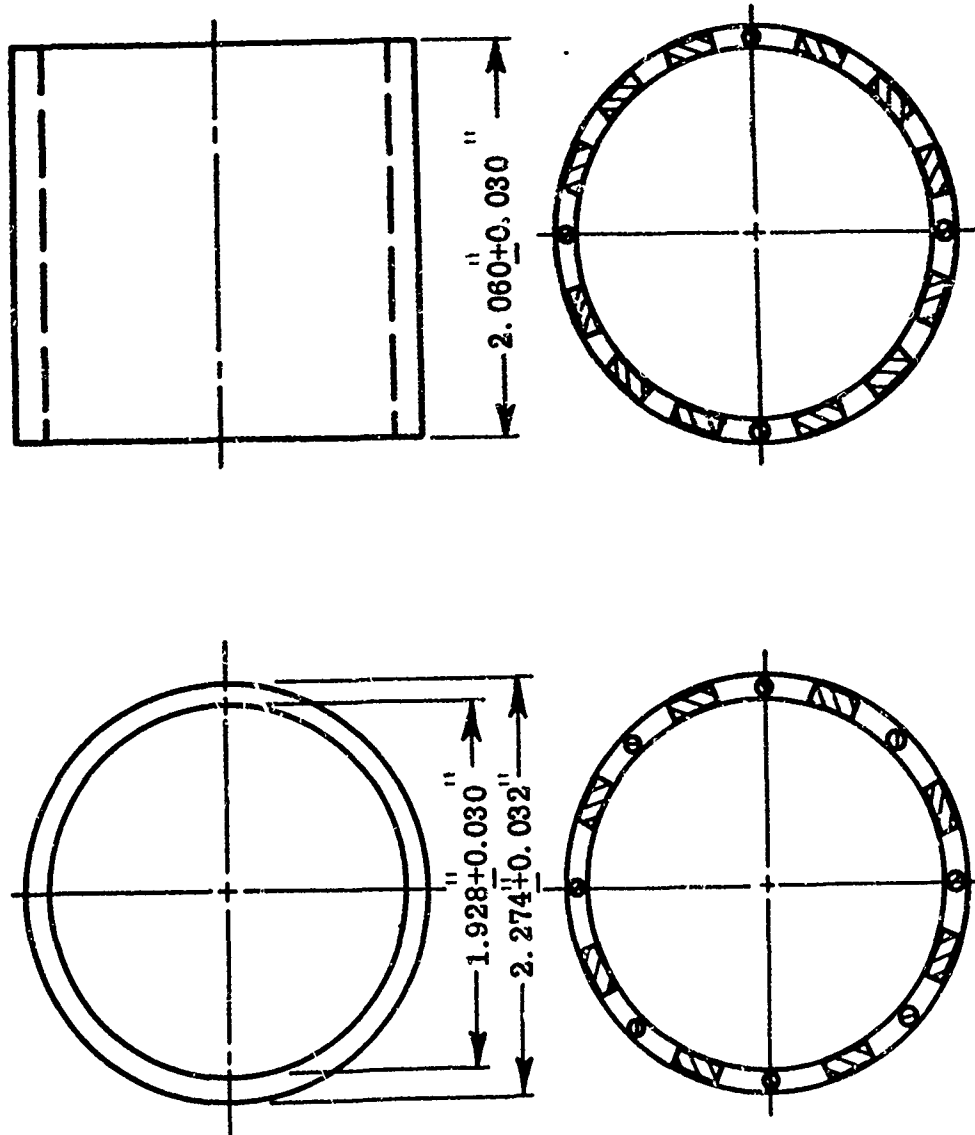
Figure 16. Configuration of Specimen Blank 1831-A-14 as received from Coors and Cutting Plan for Removing Phase I Macro Tensile and Macro Flexural Specimens

66
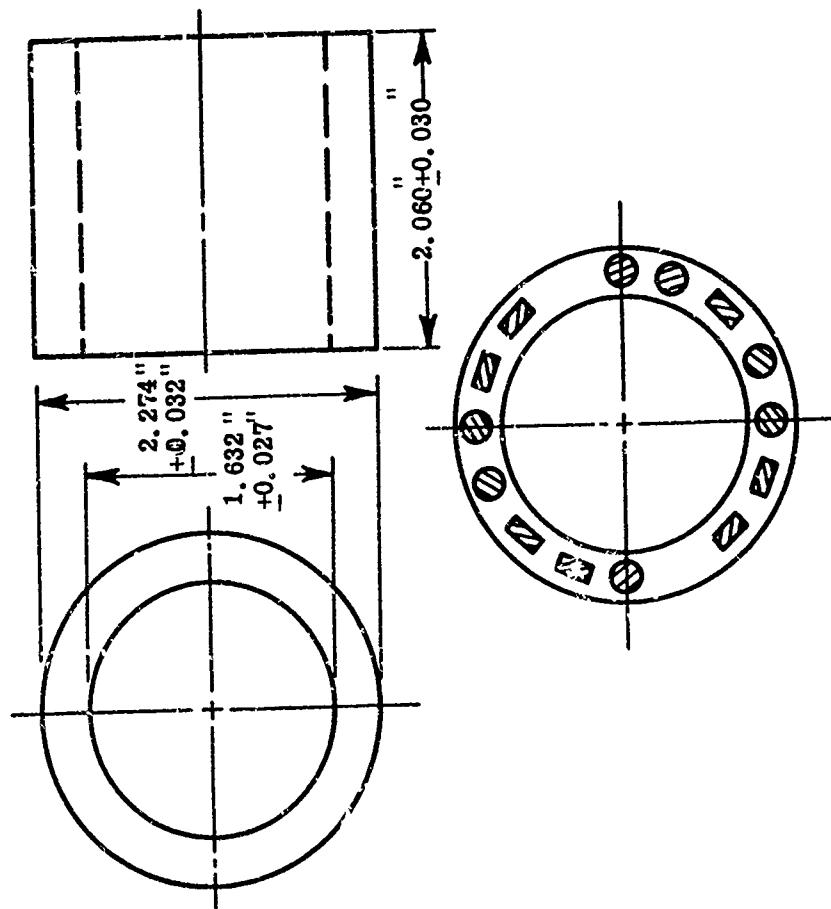
Figure 17. Configuration of Specimen Blank 1831-A-17 as received from Coors and Cutting Plan for Removing Phase I Macro Tensile and Macro Flexural Specimens

67

Number of Tensile and/or
Flexural Specimens Removed
from Blanks Fired in the Bung

Right

	16T 21F 28	15T 8F 29	6T 13F 30	8T 16F 31	--- 2F 32	3T 11F 33	--- 2F 34	
27								35

Front

| 18 | --- 10F 19 | --- 4F 20 | 2T --- 21 | --- 2F 22 | 23 | 24 | 25 | 26 |

20" Rear

| 10 | 7T 15F 11 | 1T 15F 12 | 2T 4F 13 | 3T 12F 14 | 3T 12F 15 | 4T 6F 16 | 17 | |

| 5" 1 | 16T 34F 2 | --- --- 3 | 8T 41F 4 | 13T --- 5 | 9T 9F 6 | 7T 15F 7 | 2T 10F 8 | 9 |

Left

48"

Bung Numbers

Diameter of Bungs

Front

Top

Middle

Bottom

Kiln Car

17" Rear
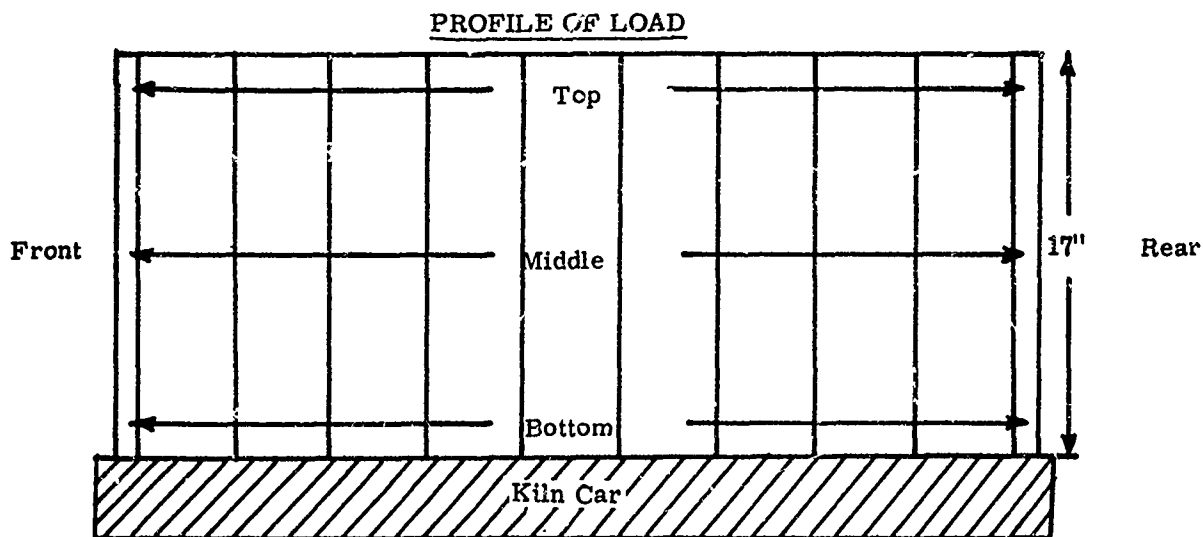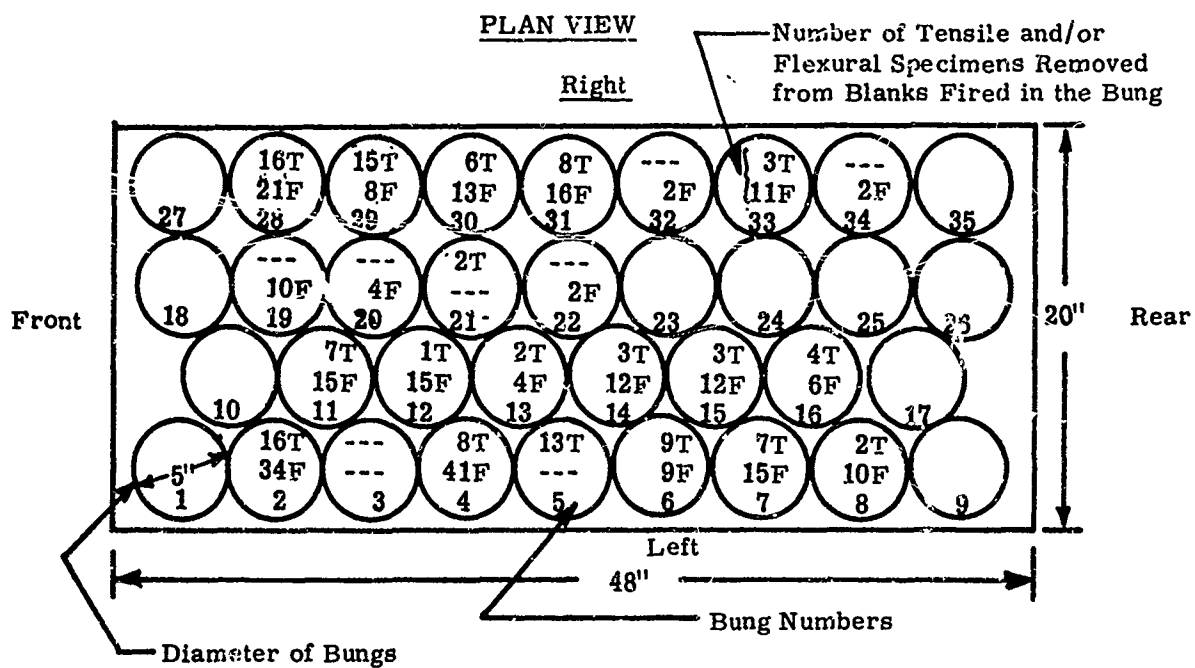
Parts shall be loaded on kiln cars in covered bungs as shown above

Figure 18. Schematic of L-33 Kiln Car Loading Layout

68
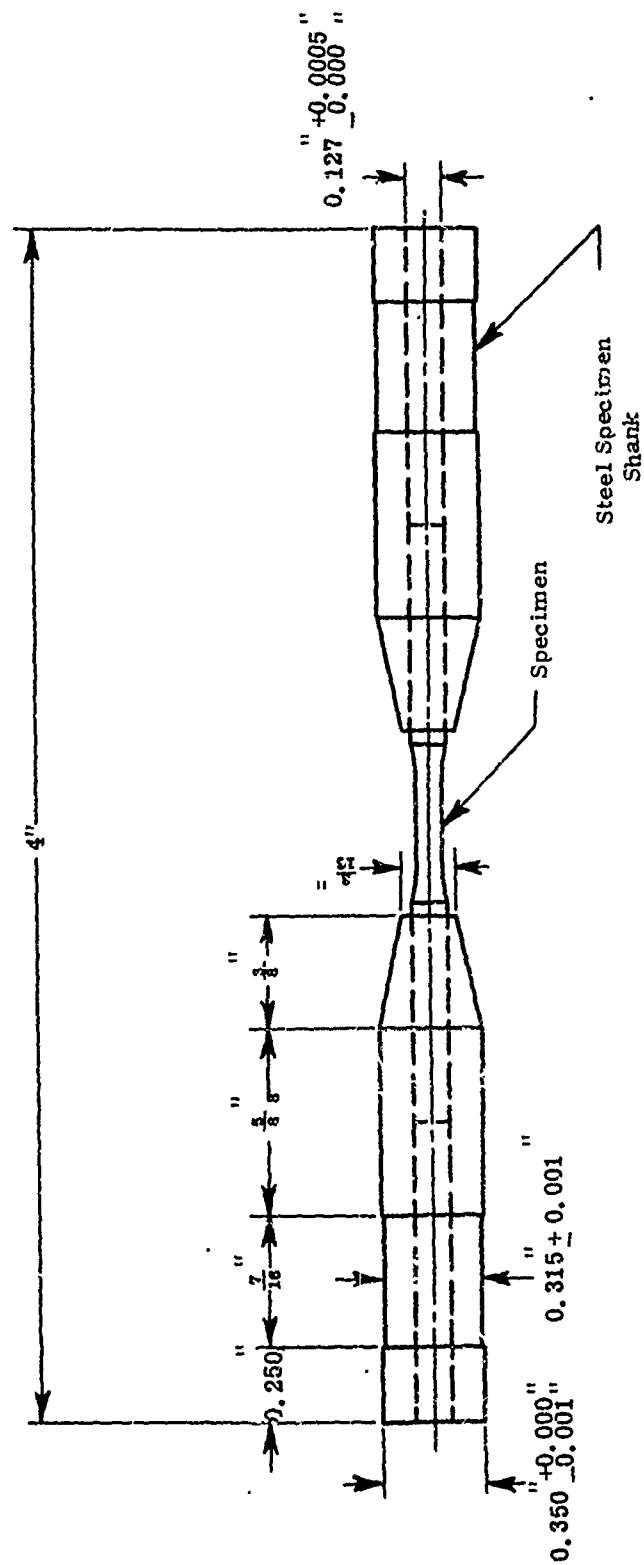
Figure 19. Steel Shanks for Providing a Gripping Surface for Precision Tensile Grips

69
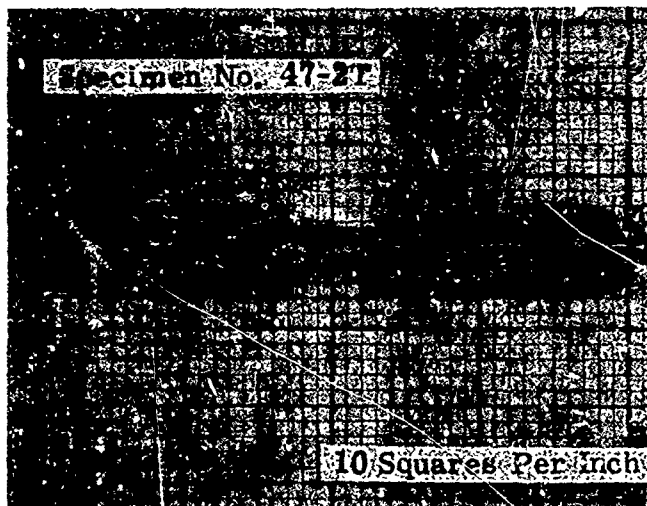
Figure 20. Photograph of Macro Tensile Specimen
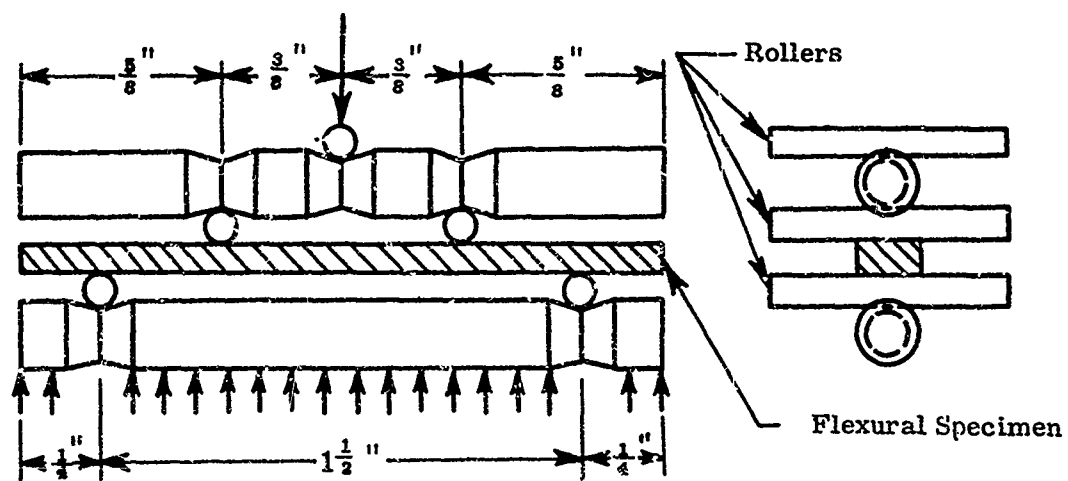
Figure 21. Schematic of Miniature Flexural Load Train
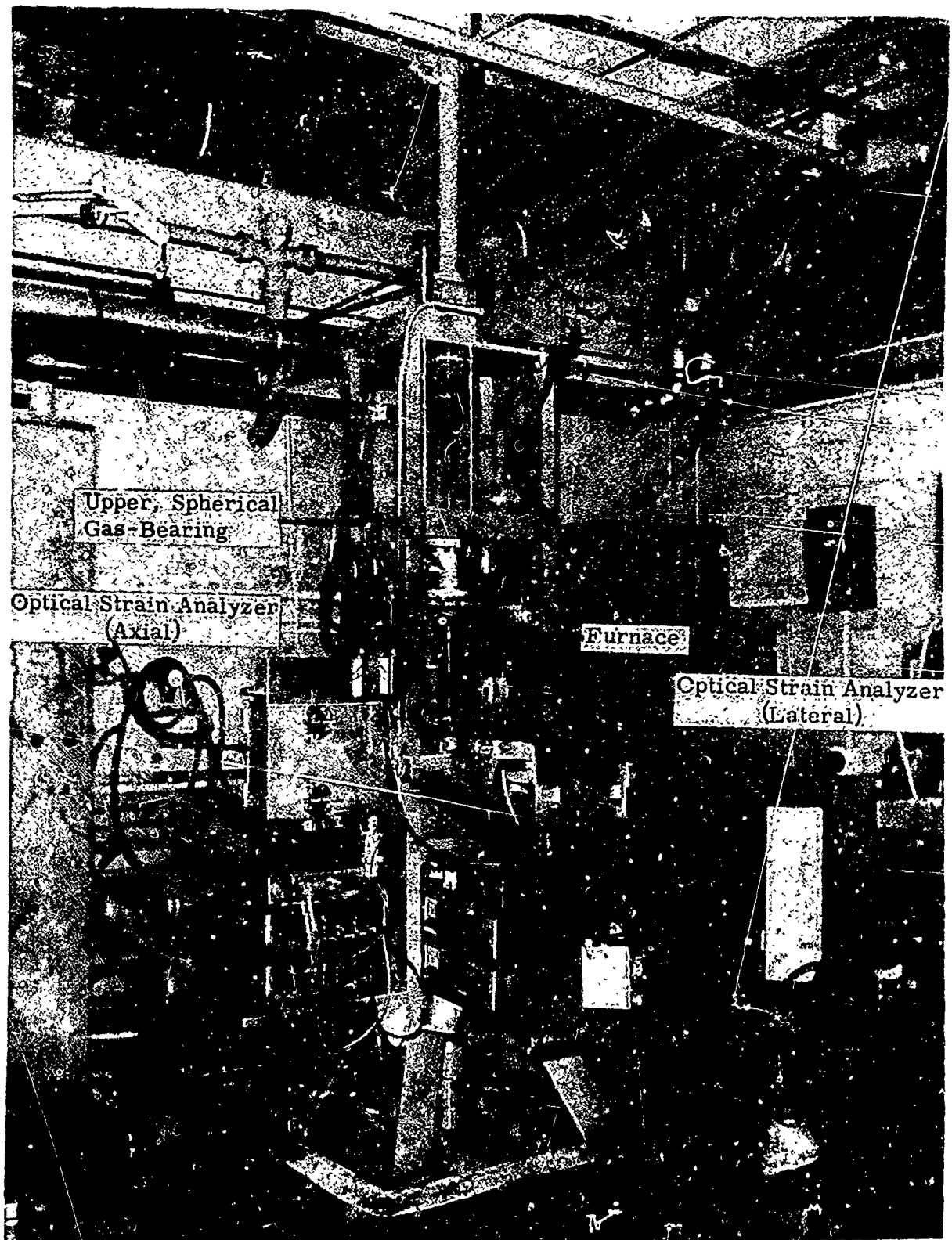
Figure 22. Picture of a Tensile Stress-Strain Facility

72
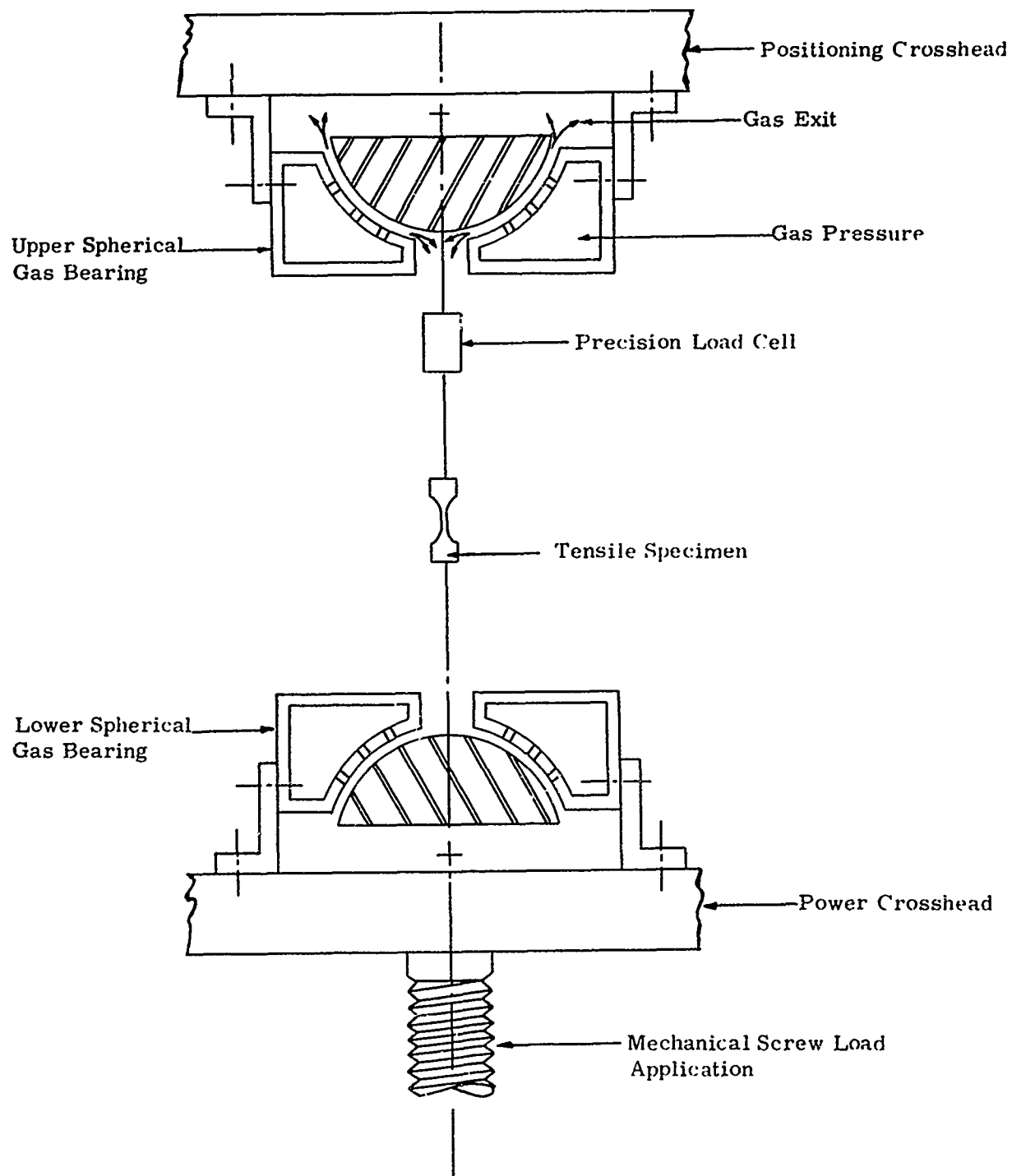
Figure 23. Schematic of the Gas Bearings and Load Train
for the Tensile Apparatus

73
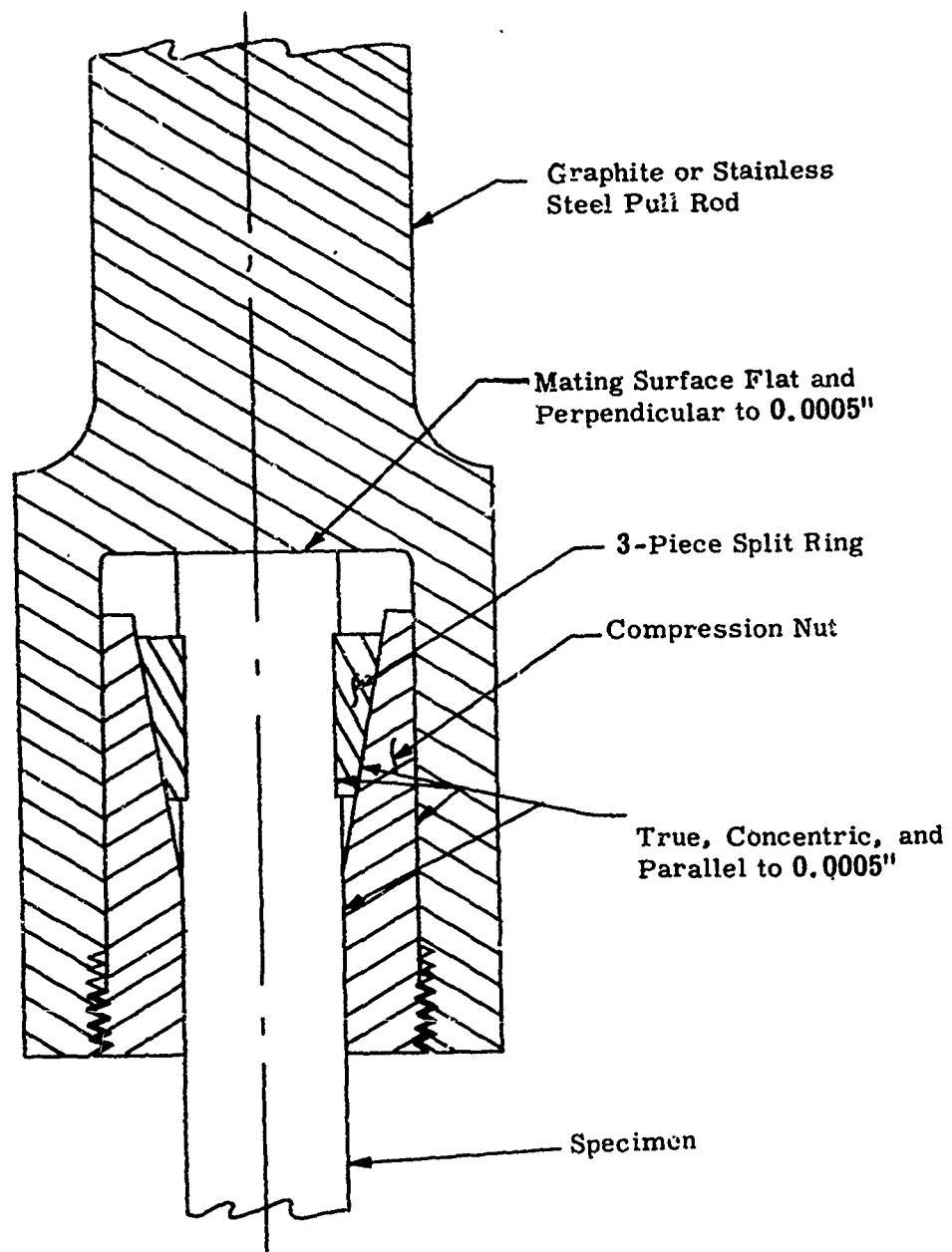
Figure 24. Precision Collet Grip for Tensile Specimens 2:1 Scale

74

Figure 25. Photograph of Crack Enhanced with Dye Penetrant
on an Earlier Type A11 Blank
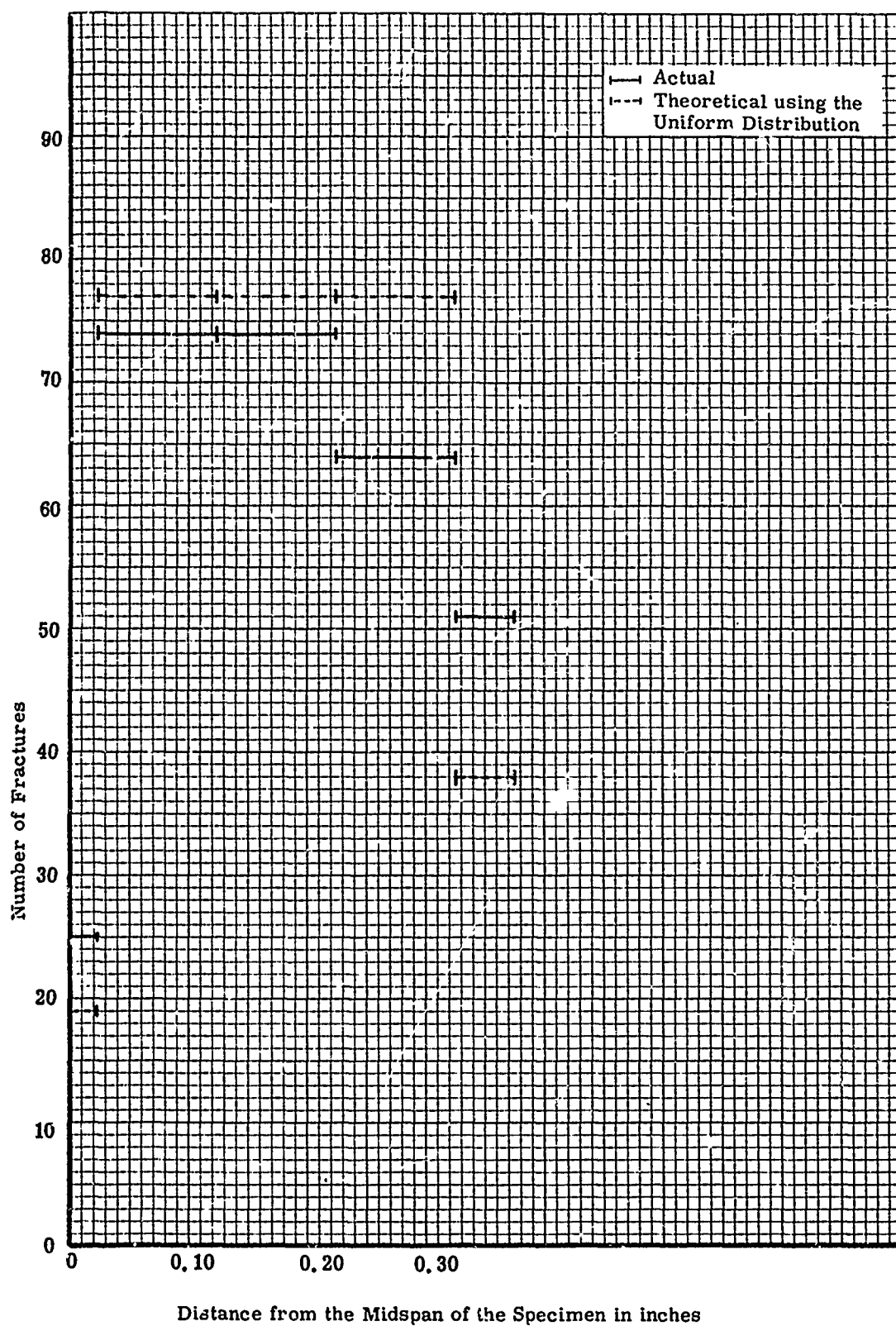
Figure 26. Distribution of the Fracture Locations for the Macro Flexural Specimens
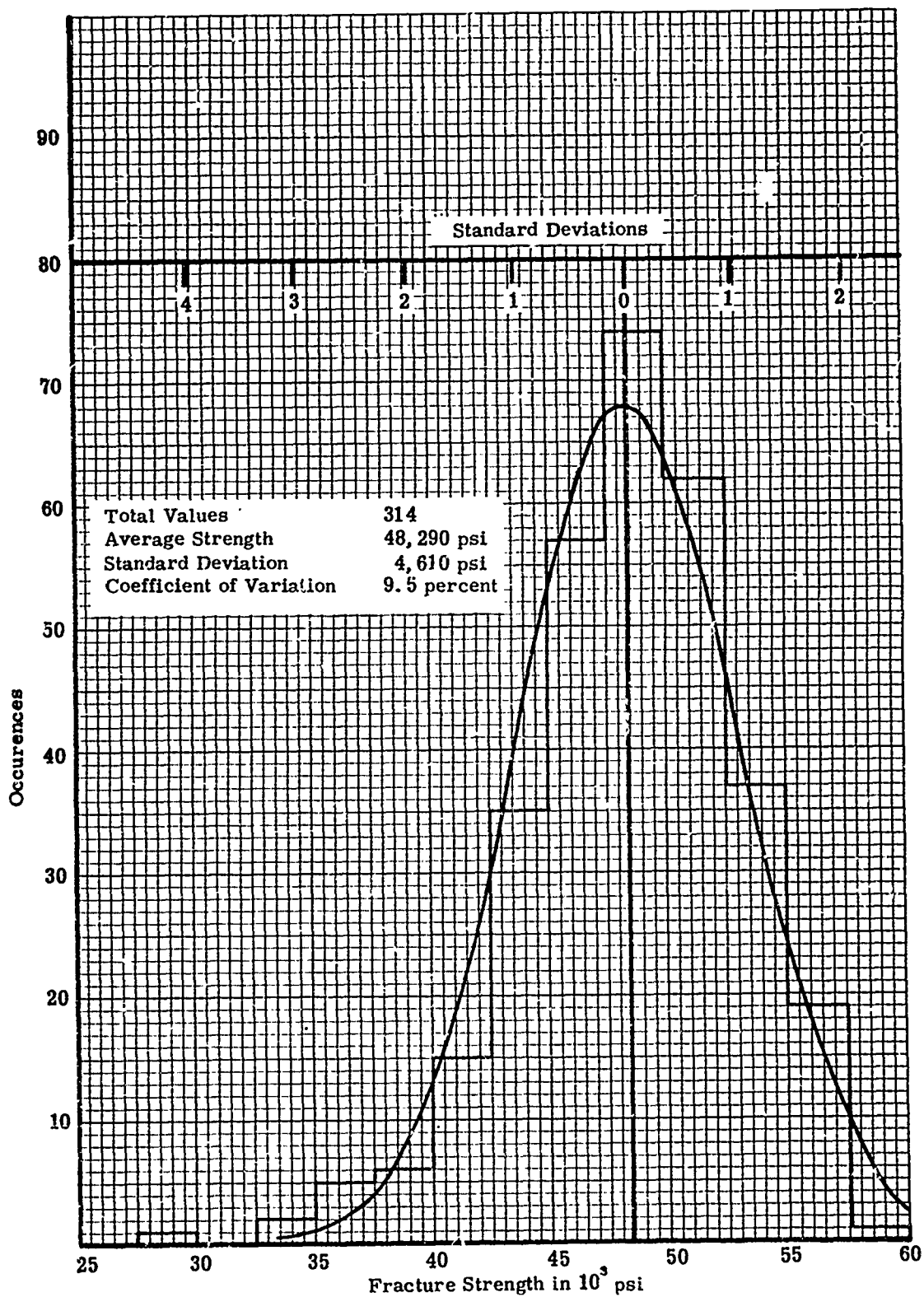
Figure 27. Distribution of the Flexural Strengths of the Macro Specimens
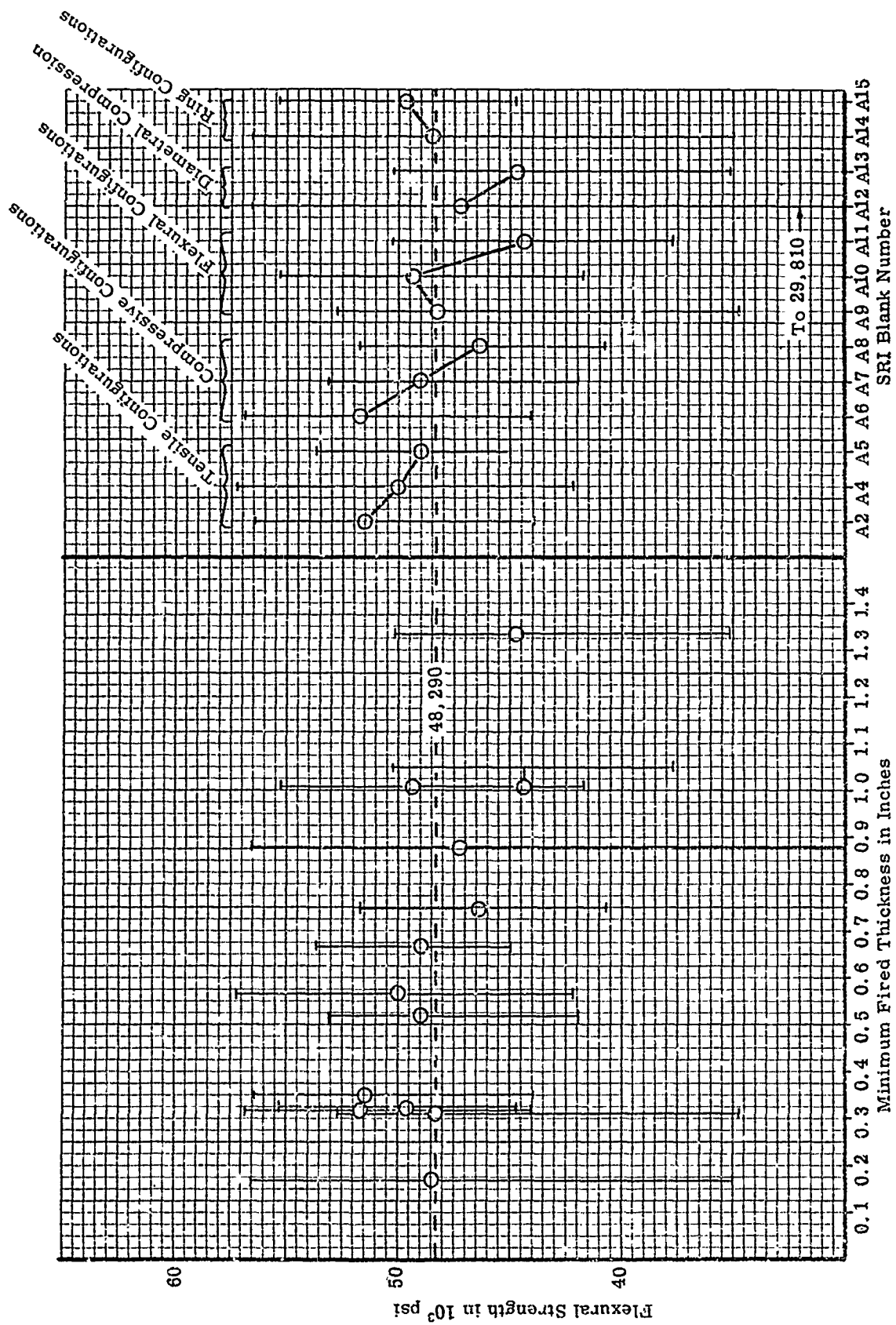
Figure 28. Average Flexural Strengths versus SRI Blank Numbers and Minimum Fired Thickness

78

Total Values 143
Average Strength 46,300 psi
Standard Deviation 4,930 psi
Coefficient of Variation 10.7 percent

Standard Deviation

Occurrences

Fracture Strength in 10^3 psi
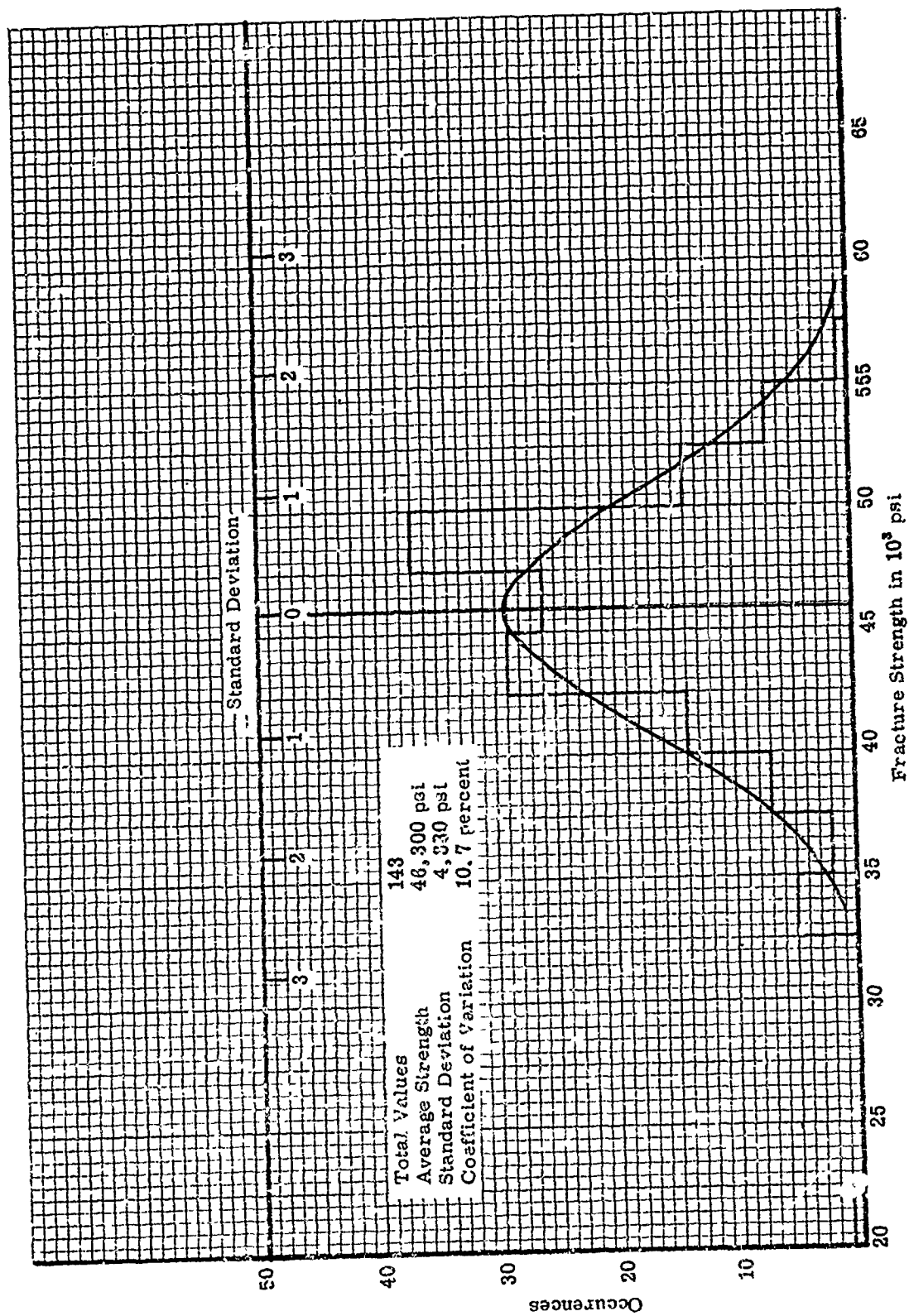
Figure 29. Distribution of the Tensile Strengths of the Macro Specimens
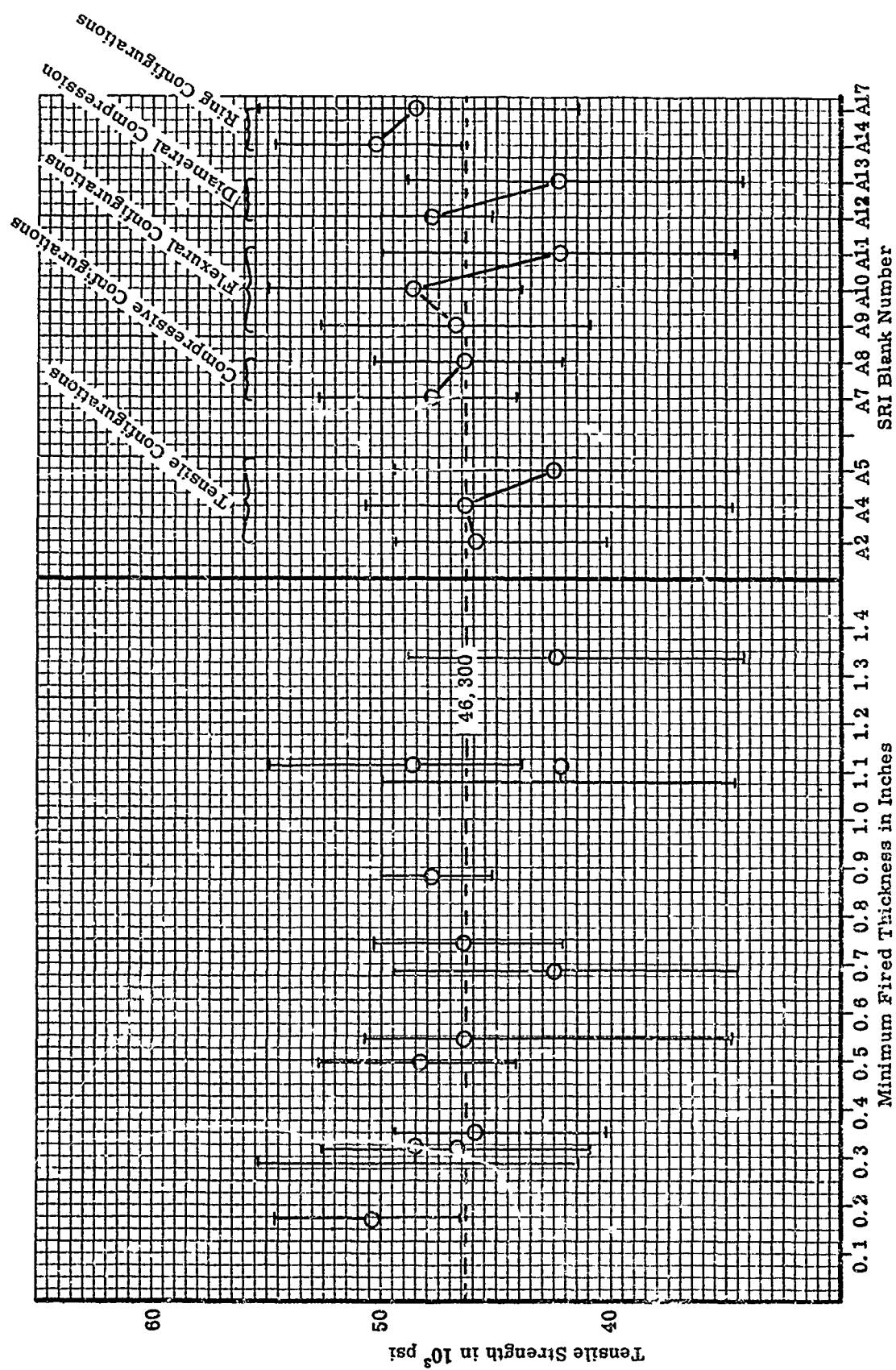
Figure 30. Tensile Strength versus SRI Blank Numbers and Minimum Firing Thickness

80

Longitudinal Variation →

Transverse Variation ↕

A1	56760	B6	53250	C6	36810	D6	57180	(51000)
A2	52550	B7	50130	C7	42990	D7	51420	(49280)
A3	53110	B8	47350	C8	51990	D8	43700	(49040)
A4	48450	B9	50020	C9	52830	D9	53110	(51100)
A5	48610	B10	52410	C10	52970	D10	53110	(51790)
	(51300)		(50640)		(47520)		(51700)	

Cross-sectional Variation

B1	58950	B6	53250	B11	51000	(54400)
B2	53110	B7	50160	B12	52830	(52030)
B3	55620	B8	47350	B13	49740	(50900)
B4	47770	B9	50020	B14	56480	(51420)
B5	50100	B10	52410	B15	48190	(50230)
	(53110)		(50640)		(51650)	

A1
A2
A3
A4
A5

B1 B6 B11
B2 B7 B12
B3 B8 B13
B4 B9 B14
B5 B10 B15

A   B   C   D

Figure 31.   Uniformity of Strength in 3A10 – 088 as determined from Flexural Strength Data
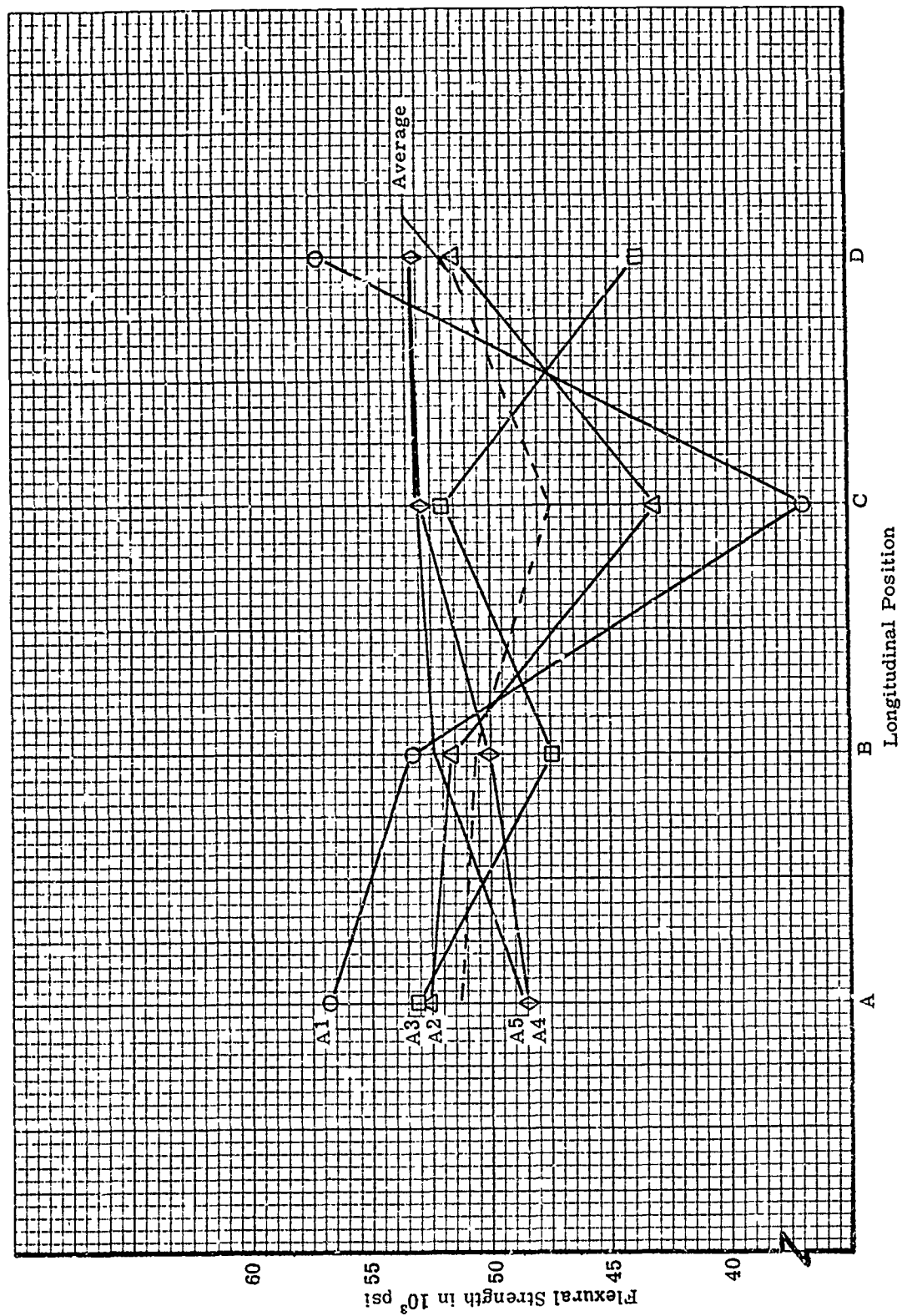
Figure 32. Flexural Strength versus Longitudinal Position at Five Transverse Positions for 3A10-088

82
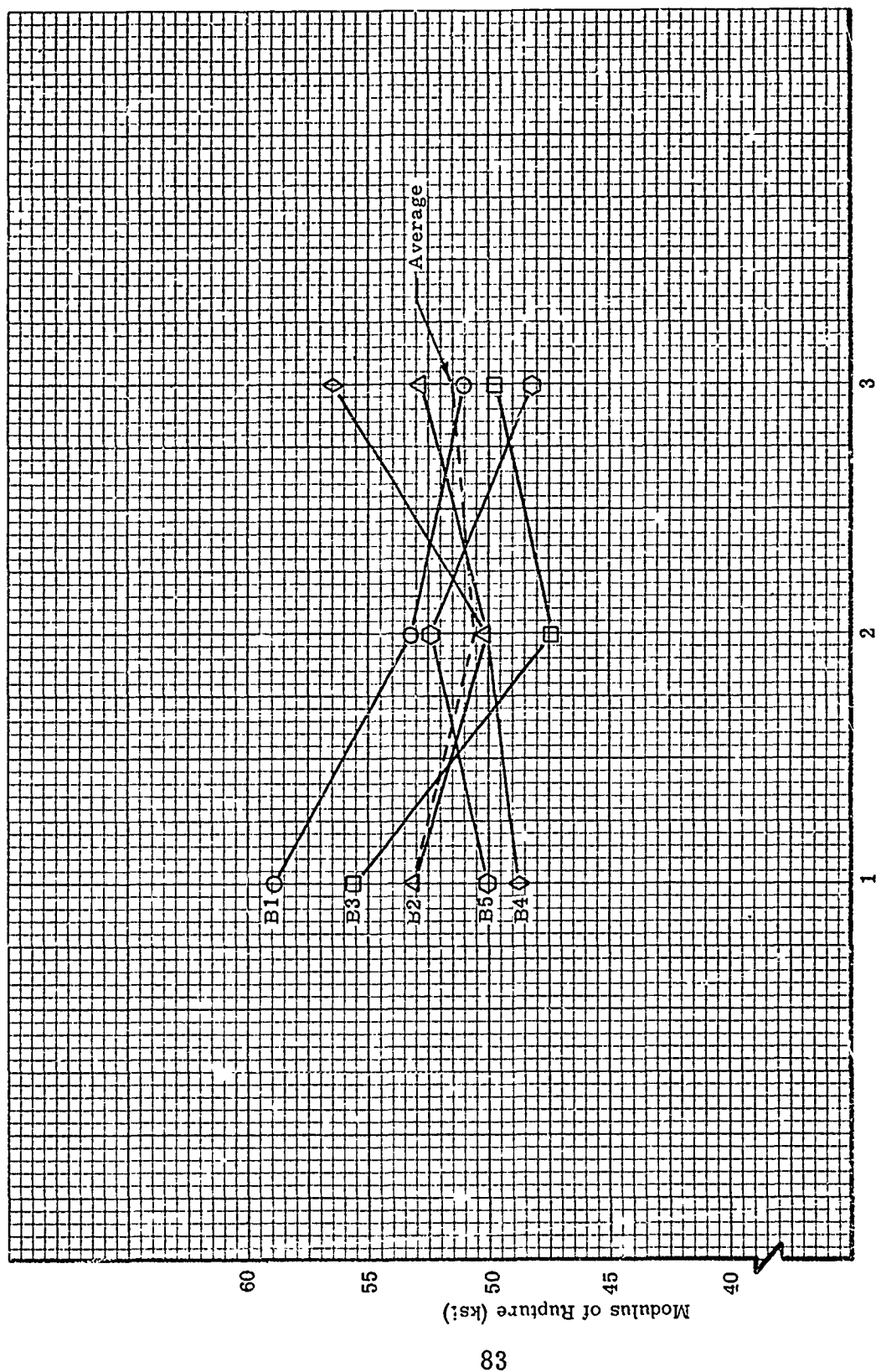
Figure 33. Cross Sectional Variation of Strength for 3A10-088

Longitudinal Variation →

Transverse Variation

A1	3.814	B6	3.852	C6	3.850	D6	3.844	(3.840)
A2	3.834	B7	3.838	C7	3.834	D7	3.835	(3.835)
A3	3.817	B8	3.805	C8	3.831	D8	3.831	(3.823)
A4	3.855	B9	3.842	C9	3.831	D9	3.841	(3.839)
A5	3.855	B10	3.841	C10	3.834	D10	3.821	(3.838)
	(3.832)		(3.836)		(3.836)		(3.836)	

Cross-sectional Variation

B1	3.837	B6	3.852	B11	3.851	(3.847)
B2	3.823	B7	3.838	B12	3.841	(3.834)
B3	3.835	B8	3.805	B13	3.843	(3.828)
B4	3.825	B9	3.842	B14	3.844	(3.837)
B5	3.830	B10	3.841	B15	3.822	(3.831)
	(3.830)		(3.836)		(3.840)	

A1 A2 A3 A4 A5

B1 B6 B11
B2 B7 B12
B3 B8 B13
B4 B9 B14
B5 B10 B15
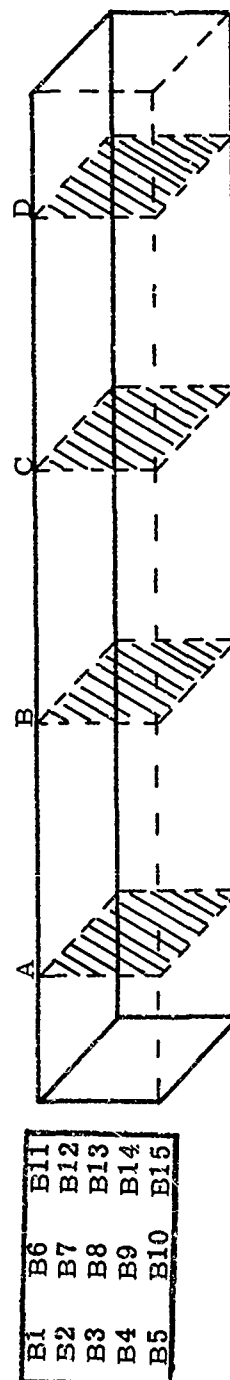
Figure 34. Uniformity of Density in 3A10-088 as determined from Macro Flexural Specimens

84
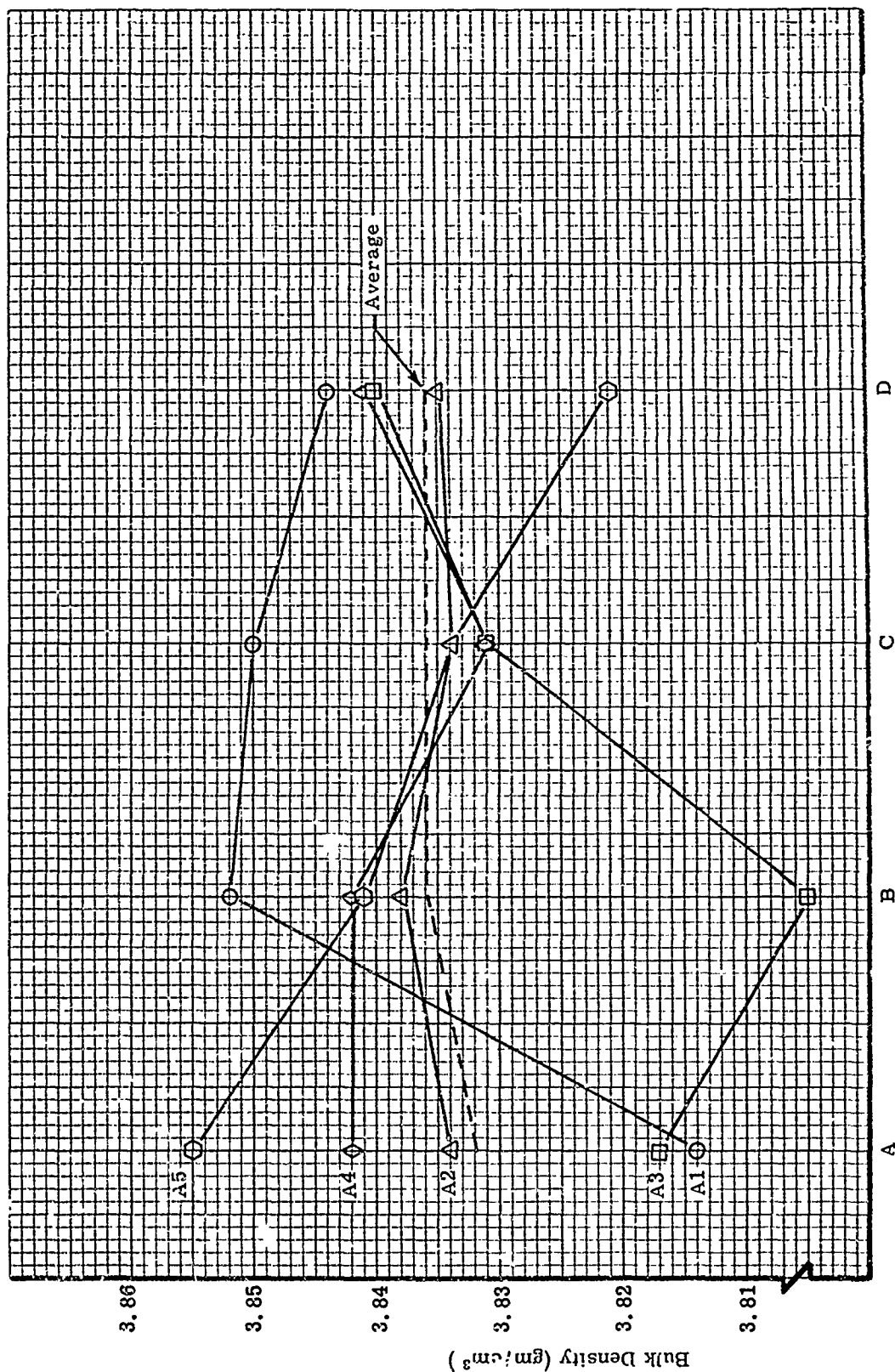
Figure 35. Density versus Longitudinal Position at Five Transverse Positions for 3A10-088

85
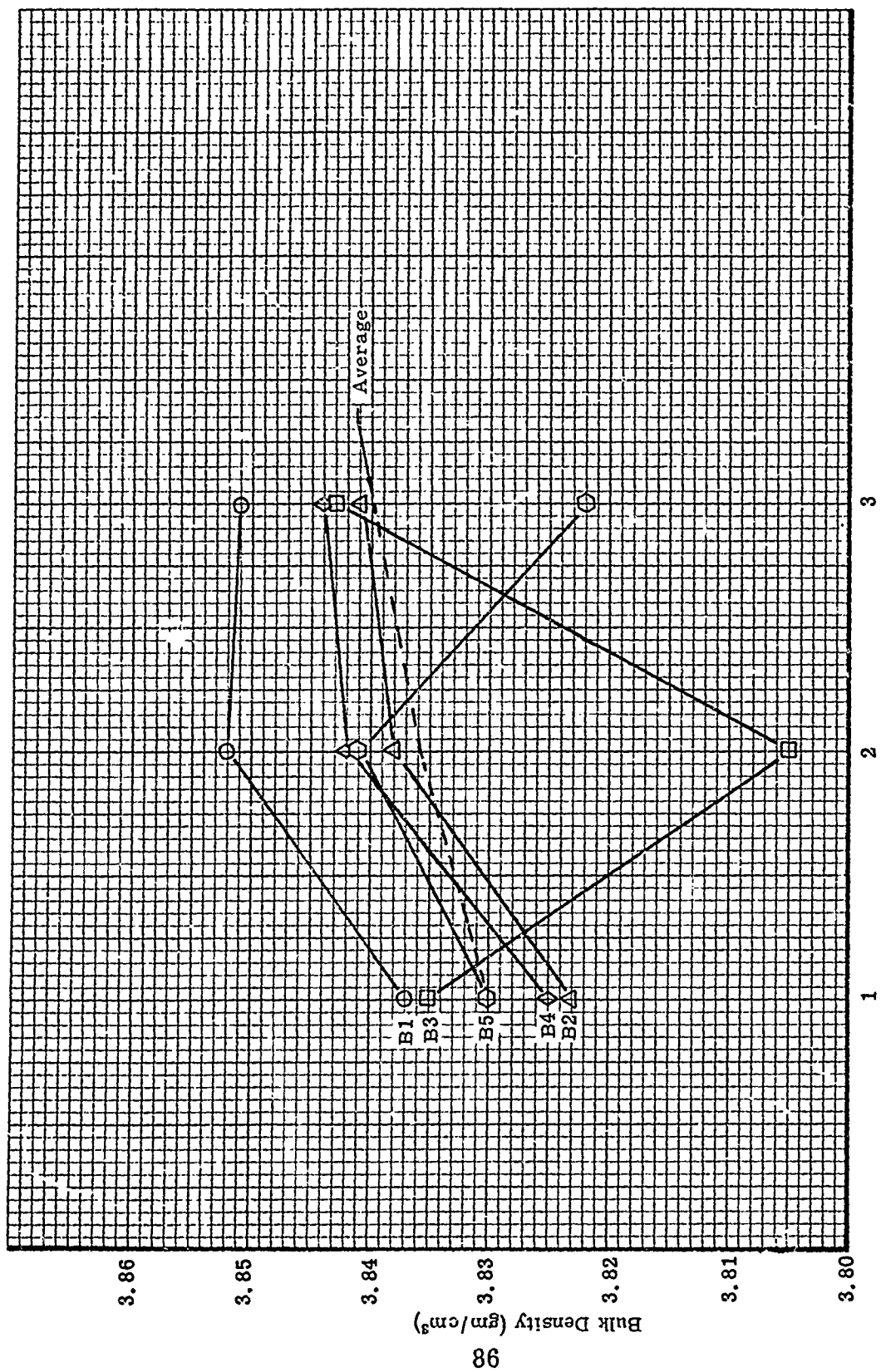
Figure 36. Cross Sectional Variation of Density for 3A10-088

	Longitudinal Variation →		
A1	3.782	C1	3.802	E1	3.791	(3.792)
A2	3.787	C2	3.790	E2	3.768	(3.782)
A3	3.755	C3	3.765	E3	3.768	(3.763)
A4	3.786	C4	3.776	E4	3.789	(3.784)
A5	3.756	C5	3.773	E5	3.775	(3.768)
A6	3.791	C6	3.786	E6	3.787	(3.788)
	(3.776)		(3.782)		(3.780)	

Transverse Variation
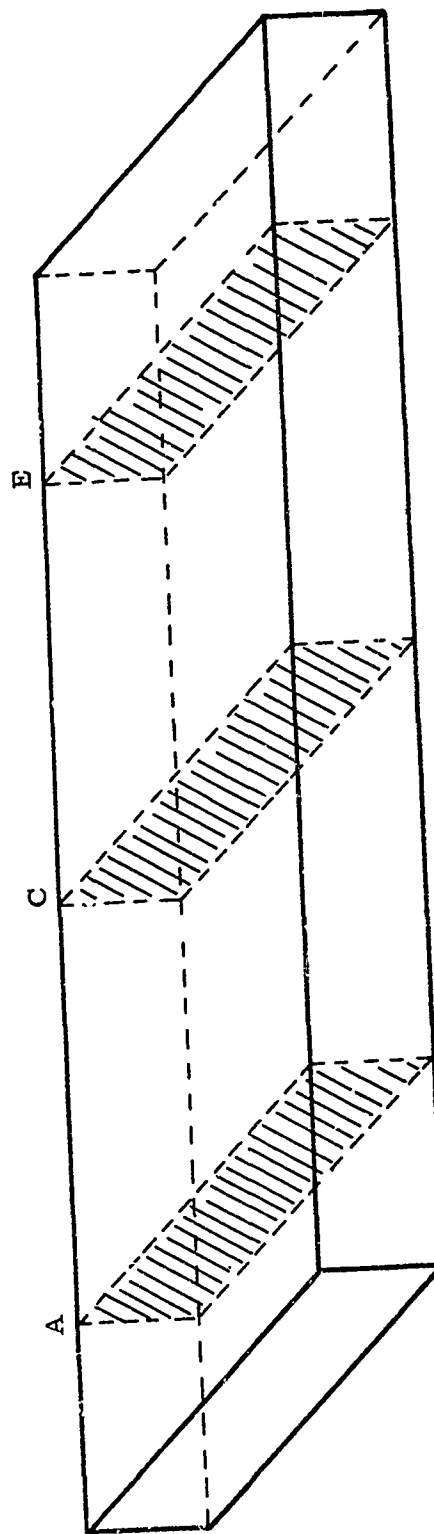
Figure 37. Uniformity of Density in 4A11-089 as determined from Macro Flexural Specimens

87
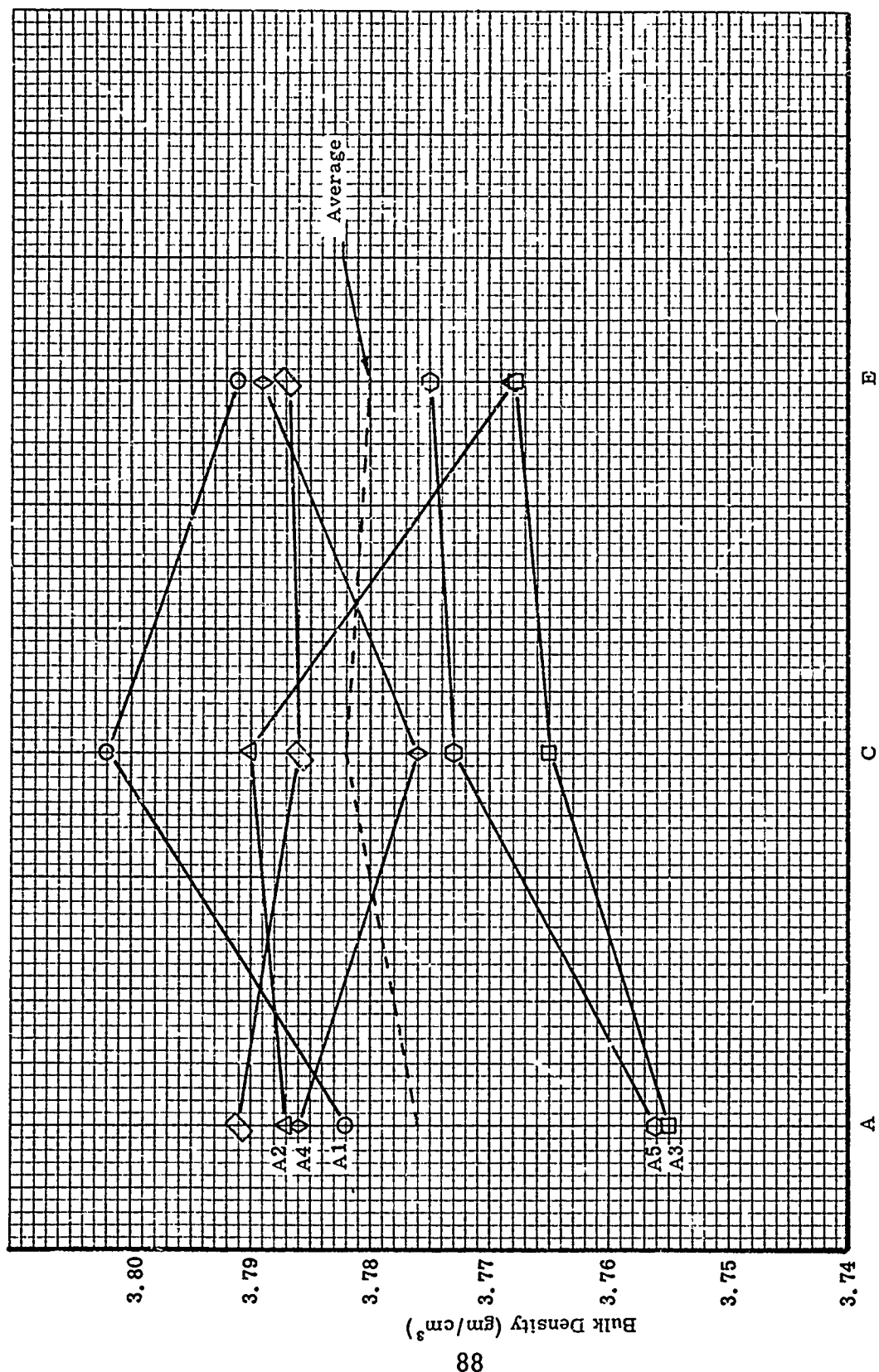
Figure 38. Longitudinal Density Profile for 4A11-089

88
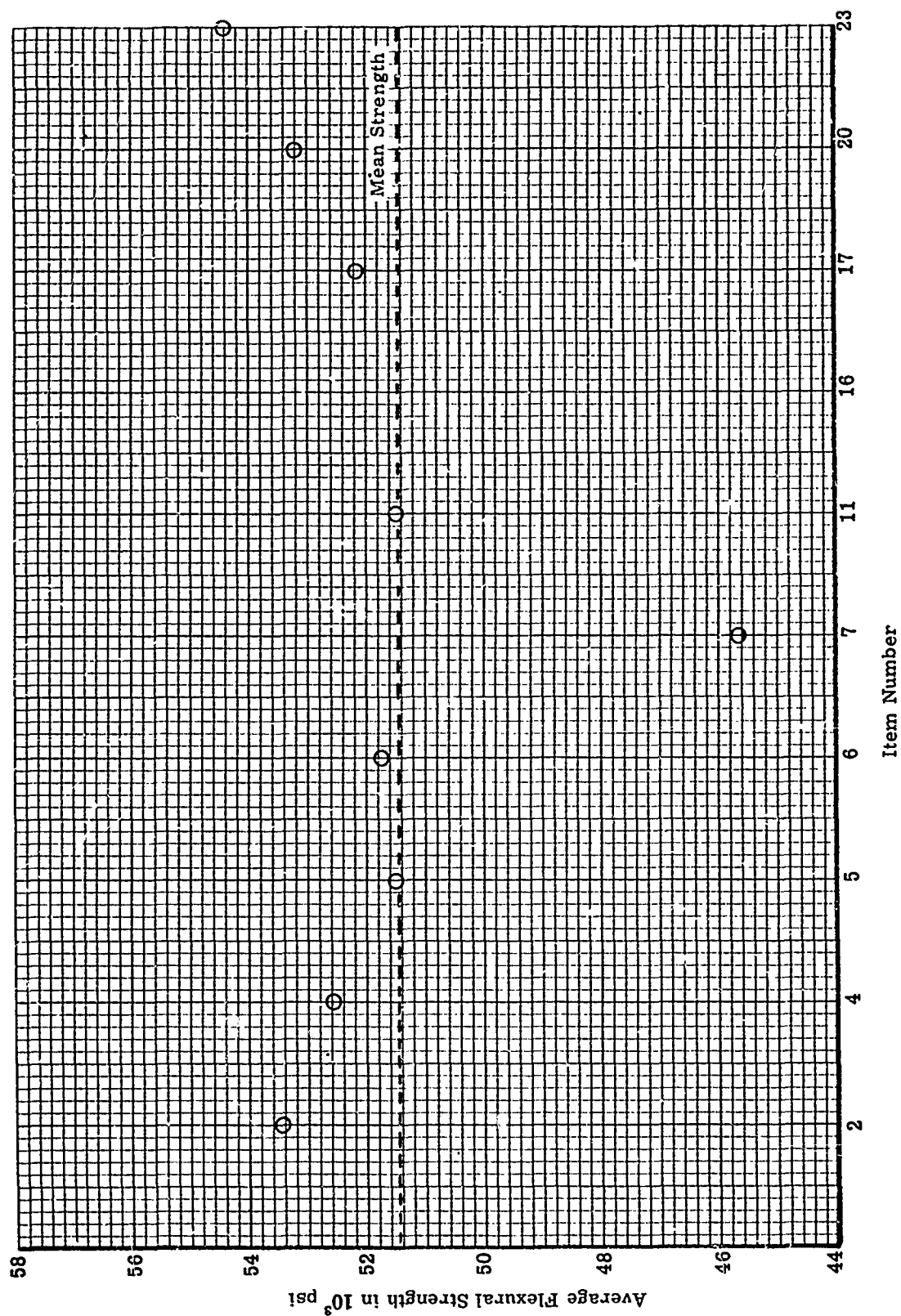
Figure 39. Variation in Average Strengths Among the Several Items of Blank Type A02
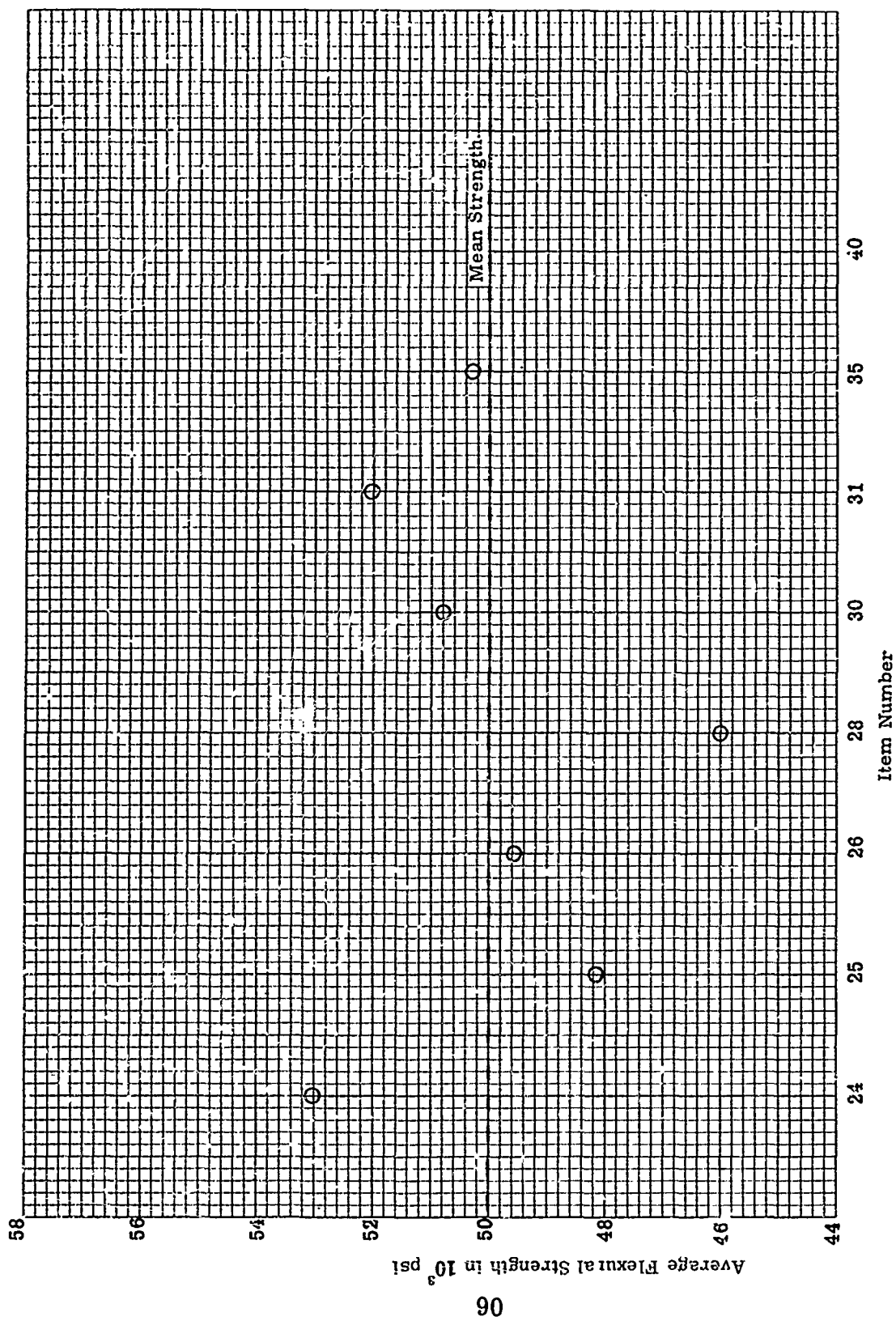
Figure 40. Variation In Average Strengths Among the Several Items of Blank Type A04
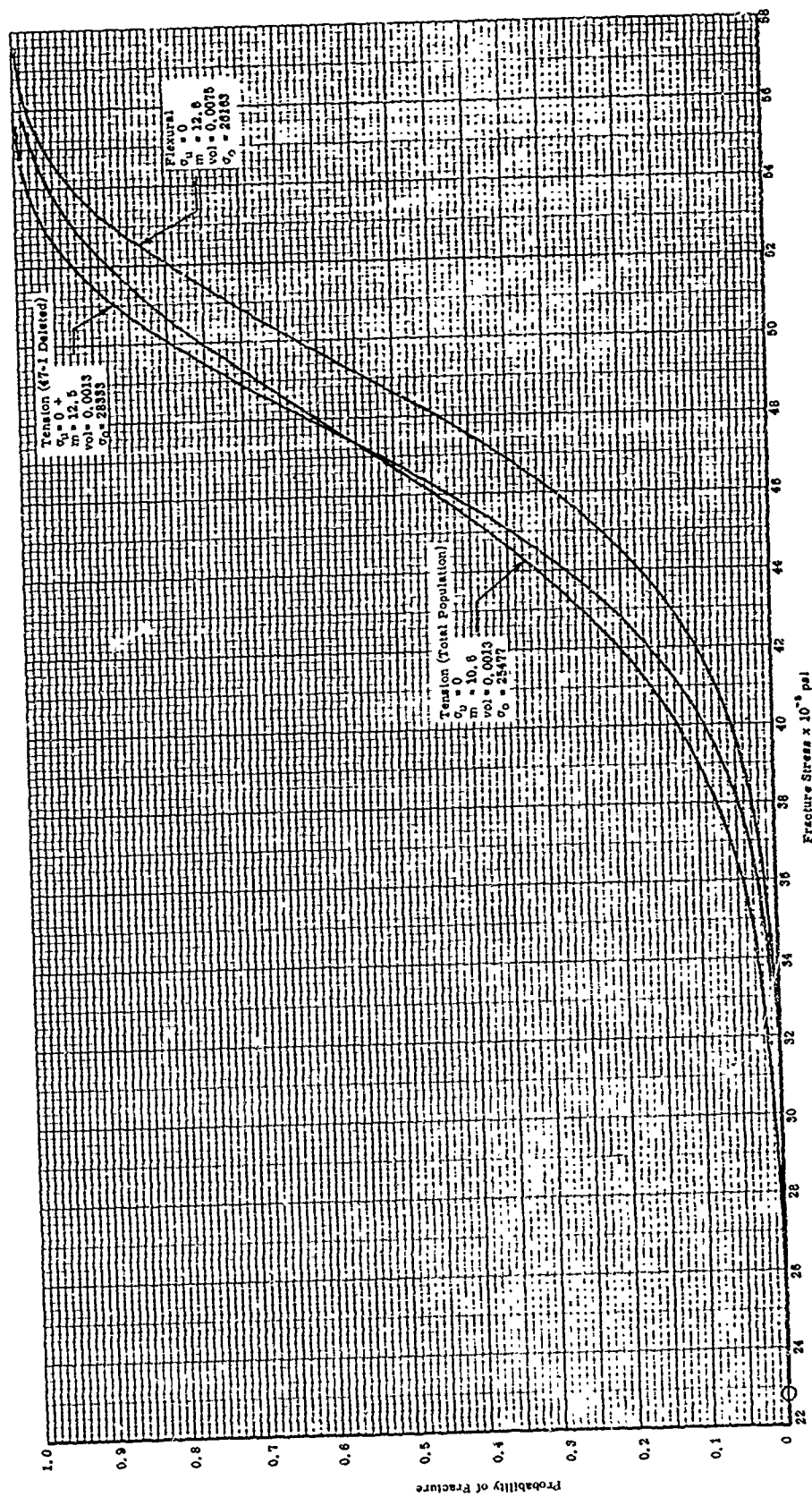
Figure 41. Probability of Fracture versus Fracture Stress for all Phase I Macro Tensile and Macro Flexural Specimens

Tension (47-1 Deleted)
$\sigma_u = 0 +$
$m = 12.5$
$vol = 0.0013$
$\sigma_0 = 28353$

Flexural
$\sigma_u = 0$
$m = 12.6$
$vol = 0.0075$
$\sigma_0 = 20163$

Tension (Total Population)
$\sigma_u = 0$
$m = 10.8$
$vol = 0.0013$
$\sigma_0 = 25477$

Fracture Stress × 10^{-3} psi

Probability of Fracture

91
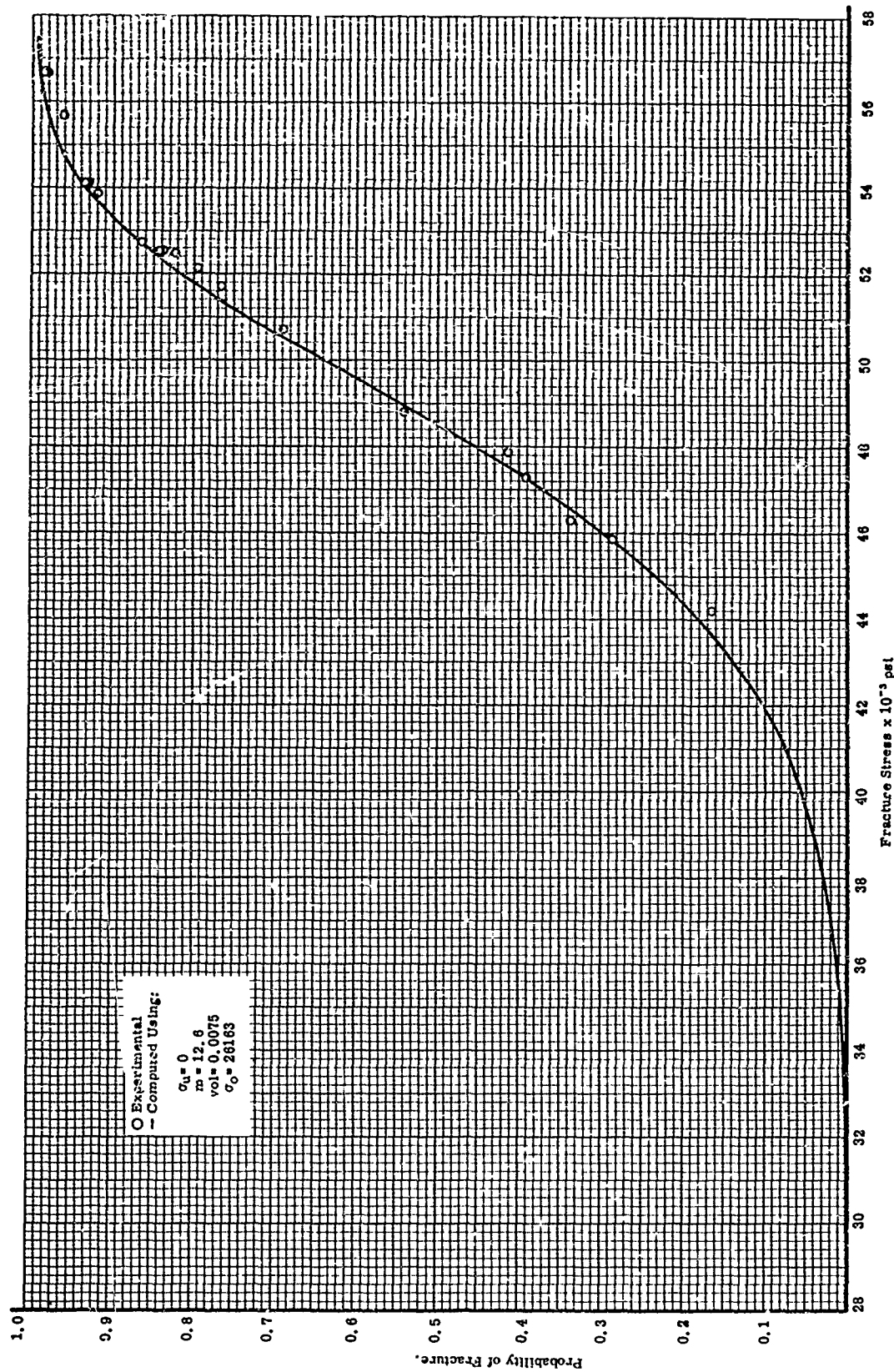
Figure 42. Probability of Fracture versus Fracture Stress for Phase I Macro Flexural Specimens from Specimen Blank A02

Fracture Stress x 10^{-3} psi

Probability of Fracture,

O Experimental
— Computed Using:

$\sigma_u = 0$
$m = 12.8$
vol= 0.0075
$\sigma_o = 28163$

92
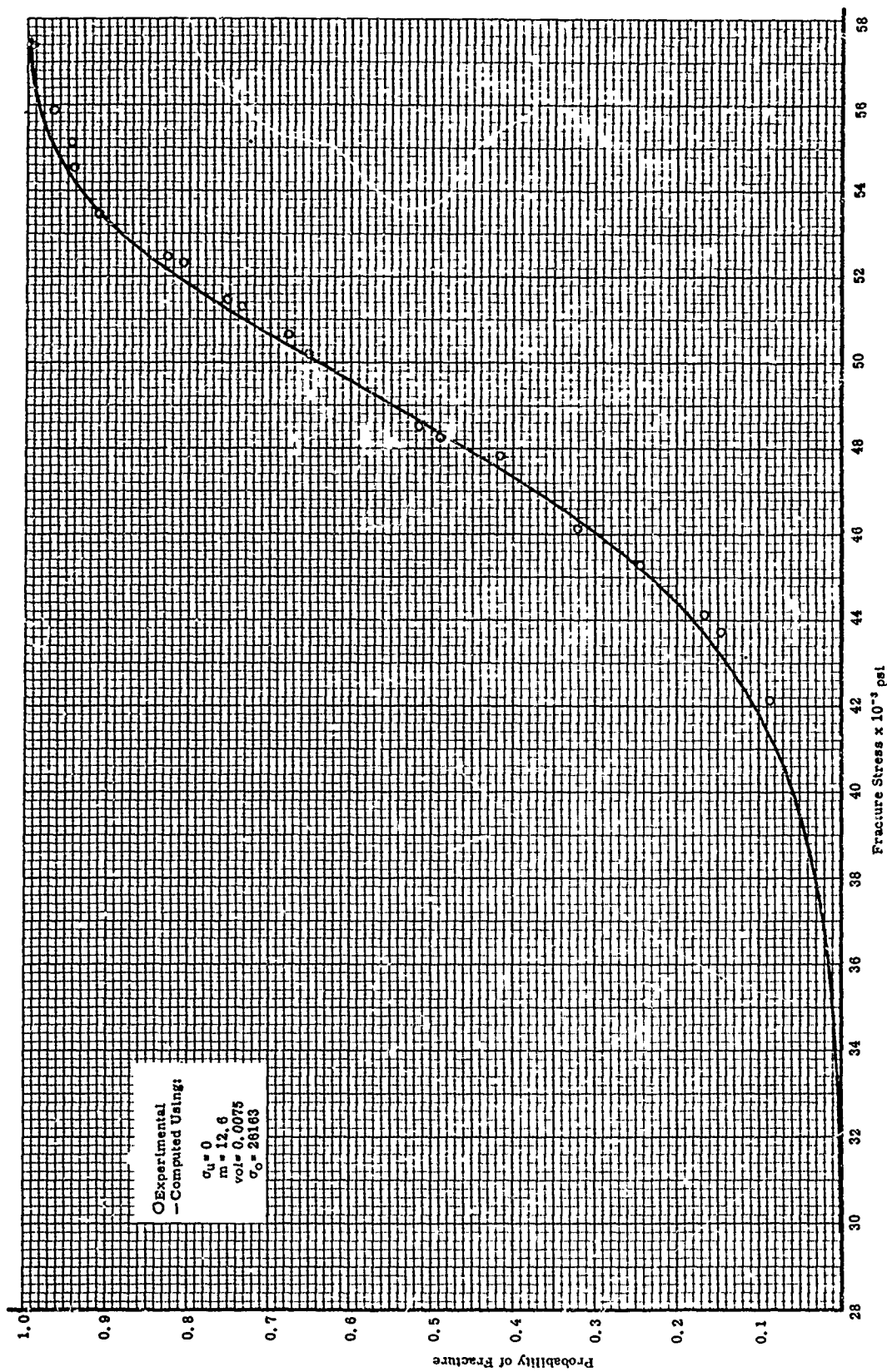
Figure 43. Probability of Fracture versus Fracture Stress for Phase I Macro Flexural Specimens from Specimen Blank A04

O Experimental
— Computed Using:
$\sigma_u = 0$
$m = 12.6$
vol = 0.0075
$\sigma_o = 28163$

Fracture Stress x 10^{-3} psi

Probability of Fracture

93
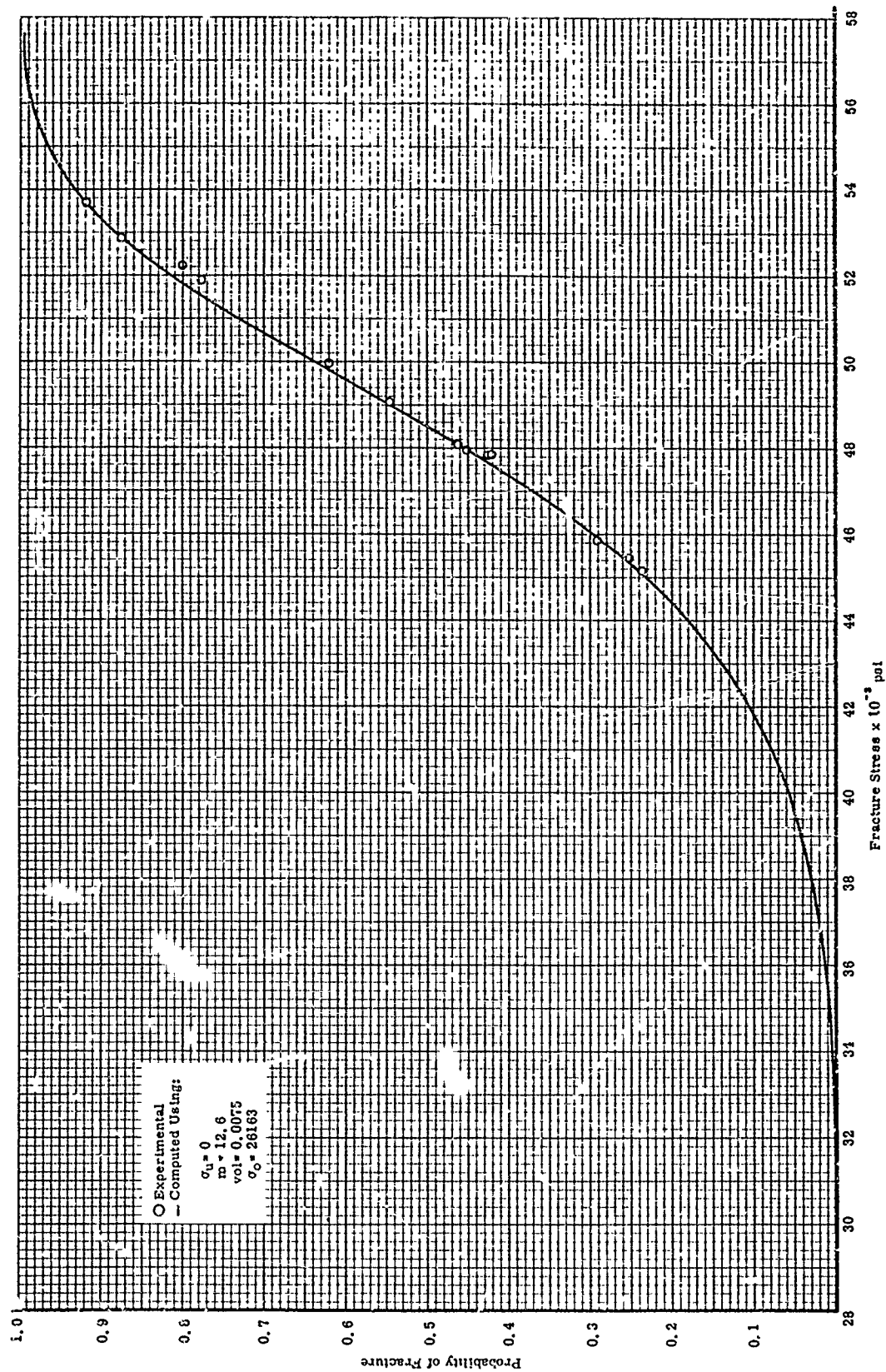
Figure 44. Probability of Fracture versus Fracture Stress for Phase I Macro Flexural Specimens from Specimen Bla. k AC5
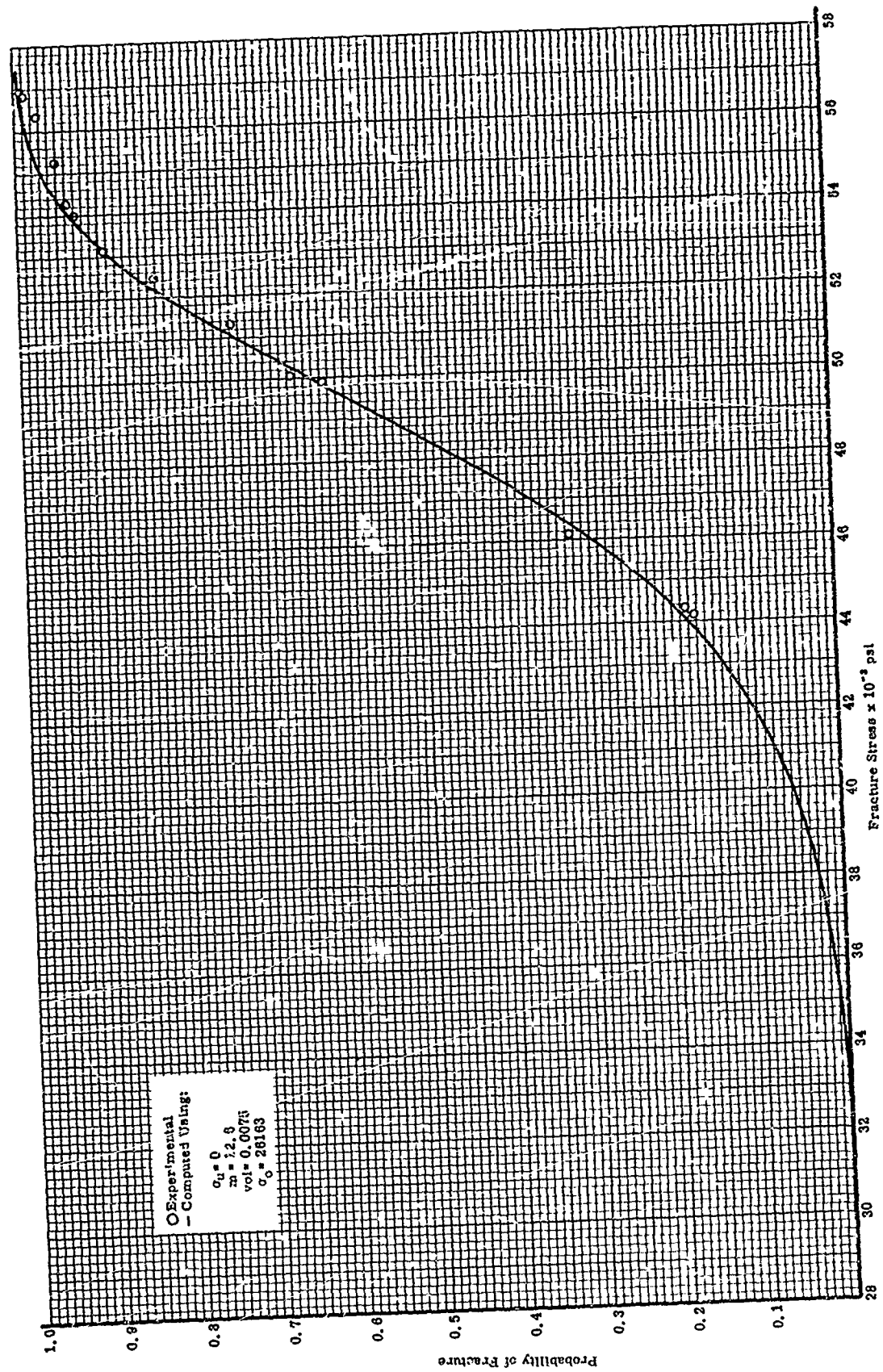
Figure 45. Probability of Fracture versus Fracture Stress for Phase I Macro Flexural Specimens from Specimen Blank A06.

O Experimental
— Computed Using:
$\sigma_u = 0$
$m = 12.8$
vol = 0.0075
$\sigma_o = 28163$

Fracture Stress x 10^{-3} psi

Probability of Fracture

95
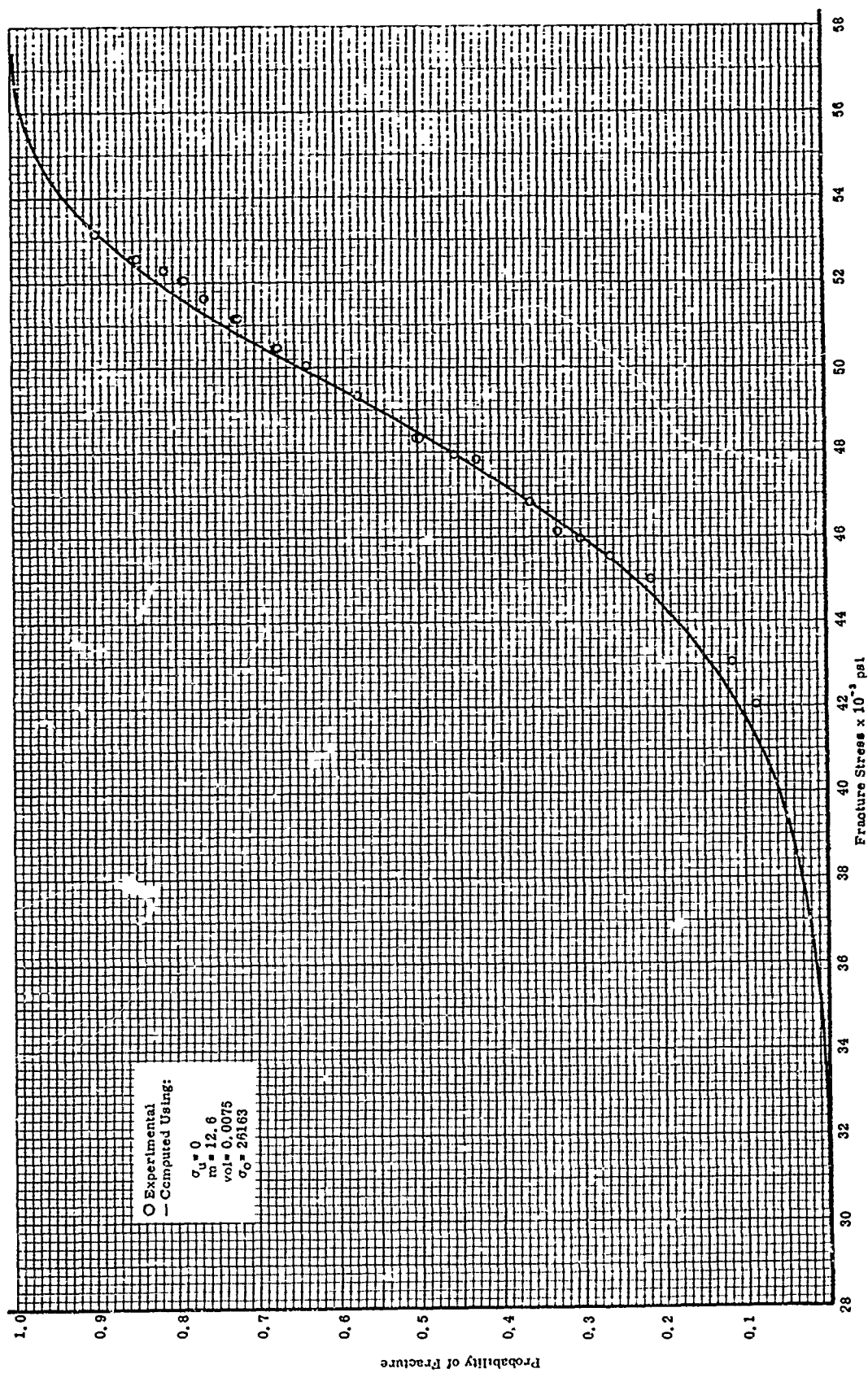
Figure 46. Probability of Fracture versus Fracture Stress for Phase I Macro Flexural Specimens from Specimen Blank A07

Legend:
O Experimental
— Computed Using:
$\sigma_u = 0$
$m = 12.6$
vol = 0.0075
$\sigma_o = 26163$

Y-axis: Probability of Fracture
X-axis: Fracture Stress x 10^{-3} psi
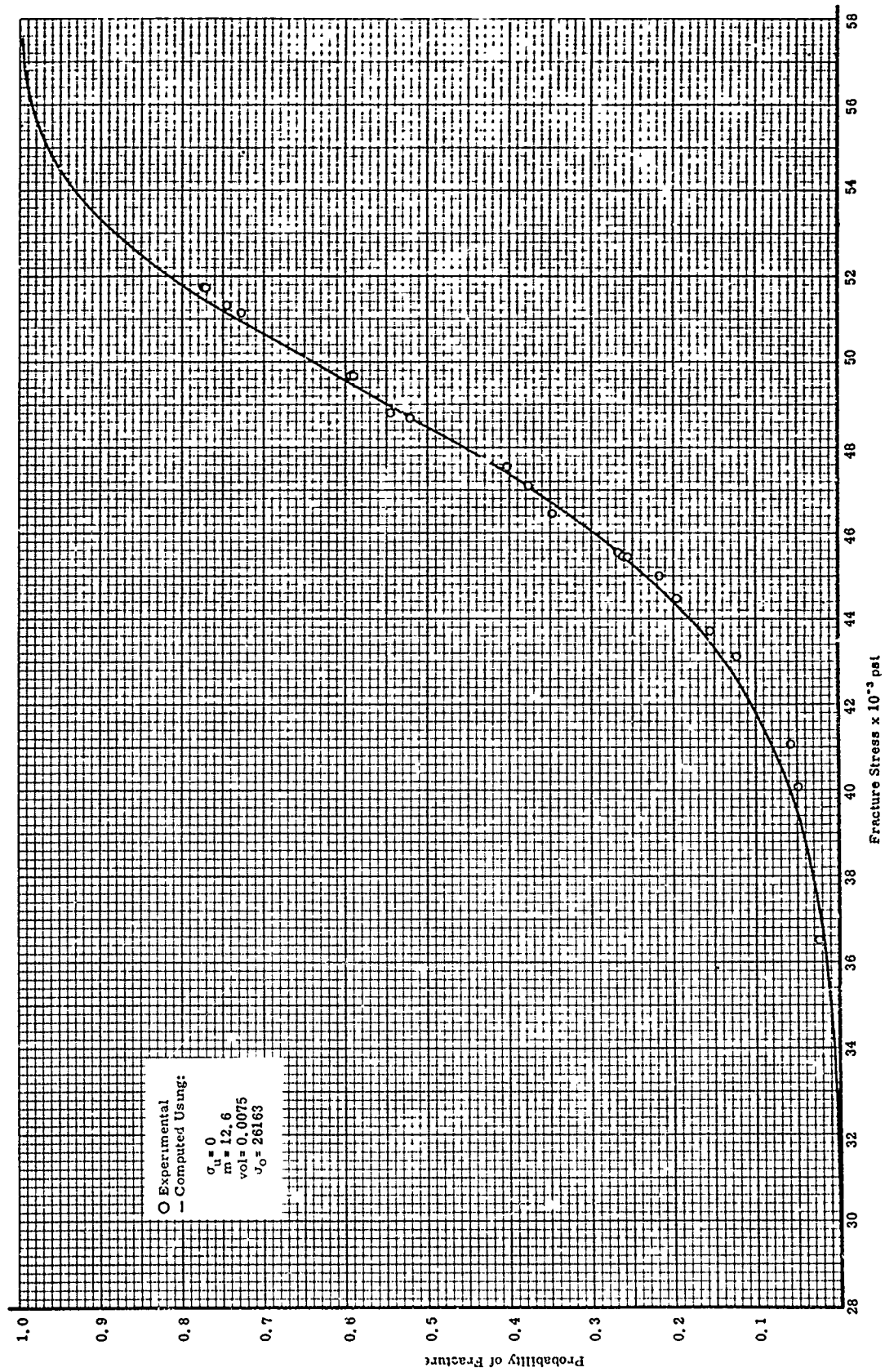
Figure 47. Probability of Fracture versus Fracture Stress for Phase 1 Macro Flexural Specimens from Specimen Blank A08

O Experimental
— Computed Using:
$\sigma_u = 0$
$m = 12.6$
$vol = 0.0075$
$J_o = 26163$

Fracture Stress x 10^{-3} psi

Probability of Fracture

97
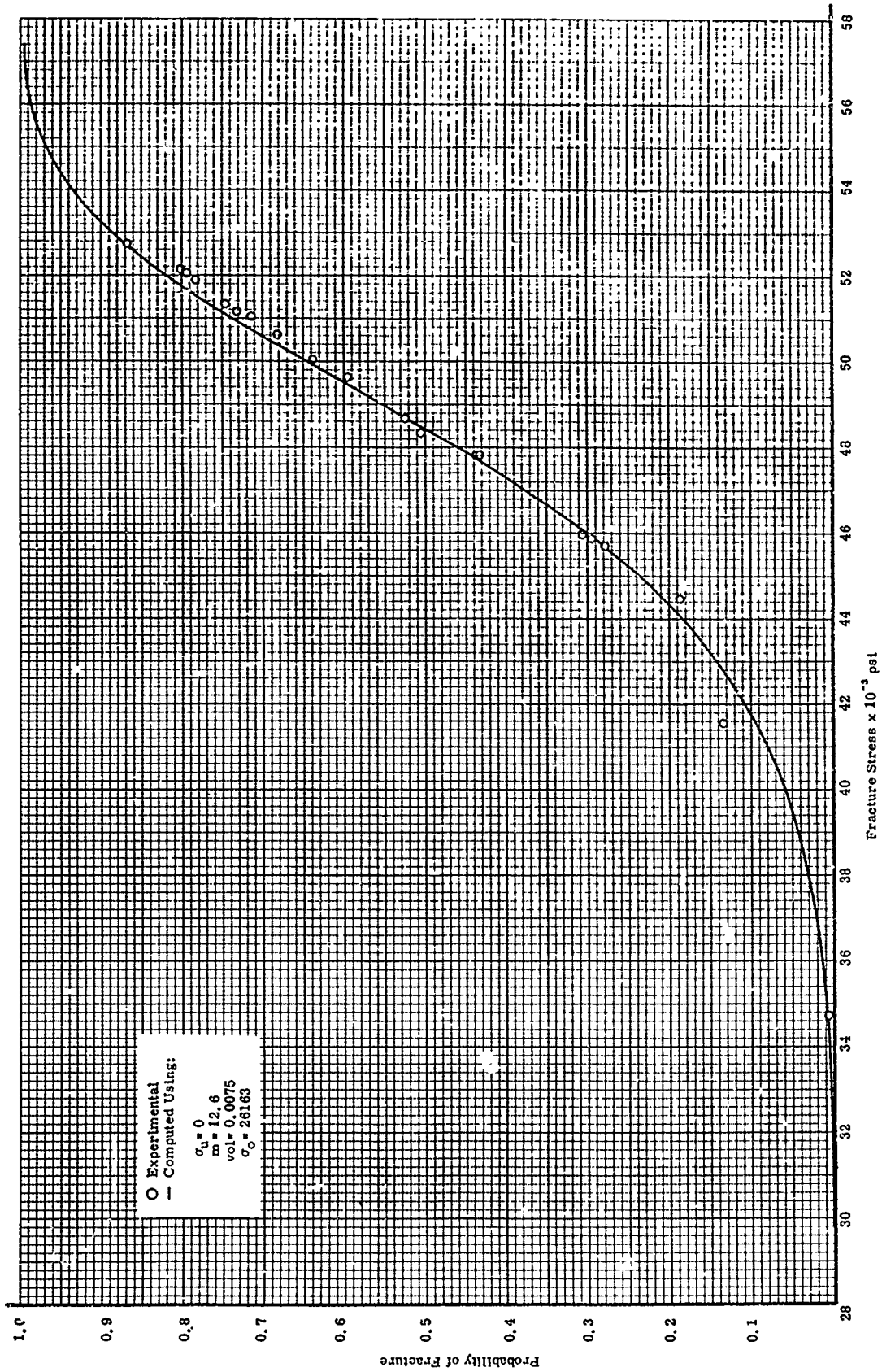
Figure 48. Probability of Fracture versus Fracture Stress for Phase I Macro Flexural Specimens from Specimen Blank A09

98
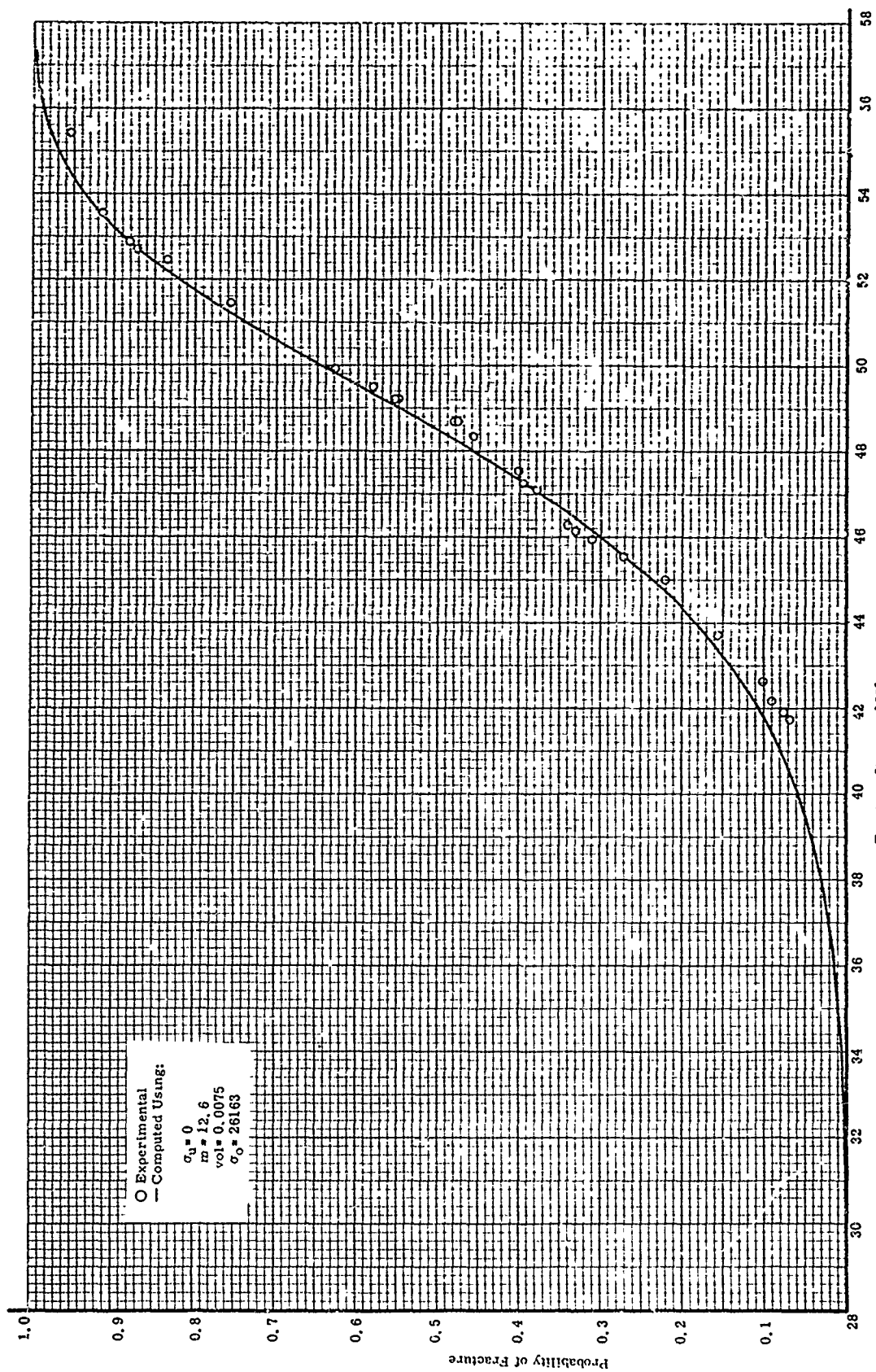
Figure 49. Probability of Fracture versus Fracture Stress for Phase I Macro Flexural Specimens from Specimen Blank A10
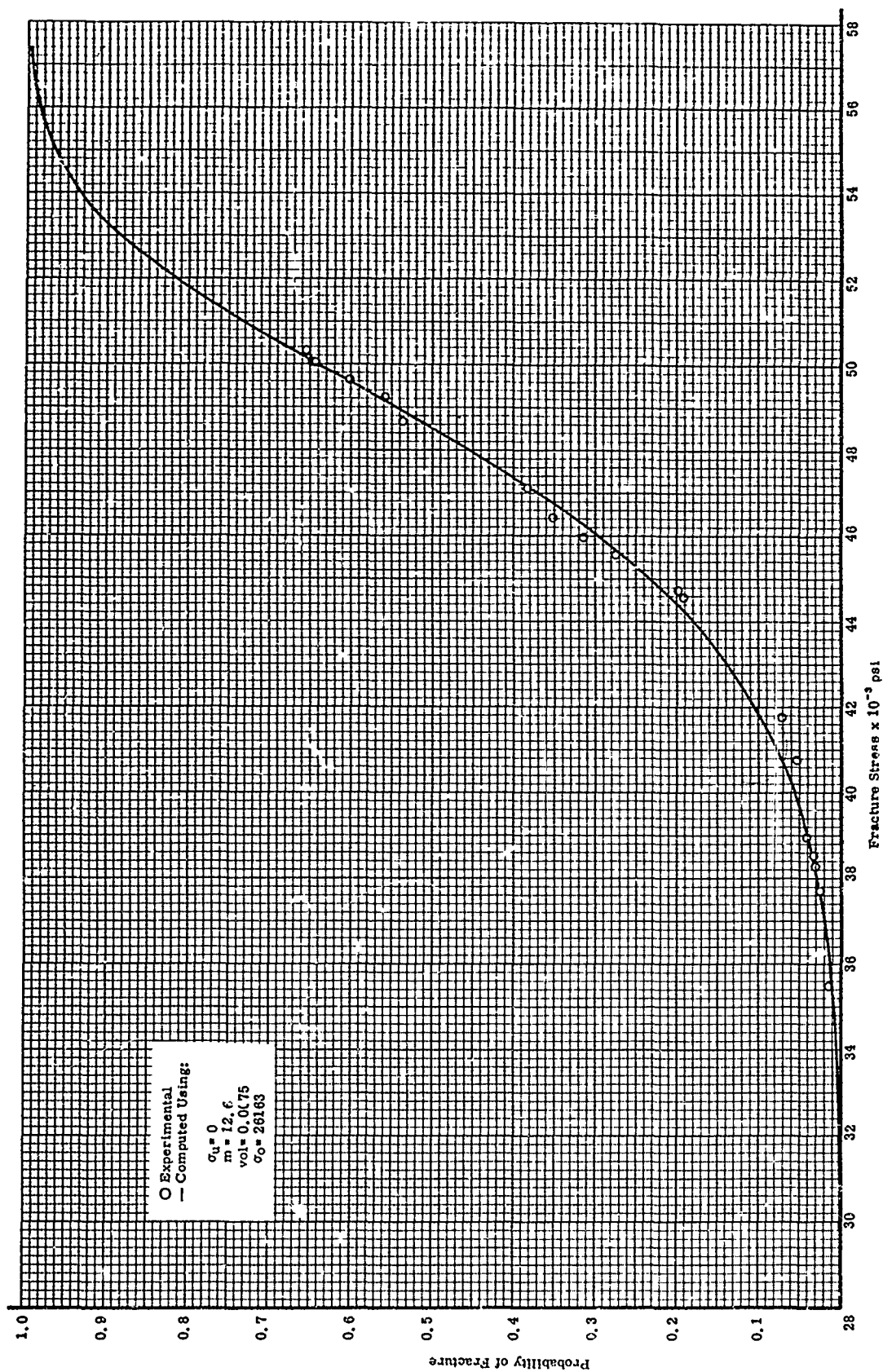
Figure 50. Probability of Fracture versus Fracture Stress for Phase I Macro Flexural Specimens from Specimen Blank Λ 11

O Experimental
— Computed Using:

$\sigma_u = 0$
$m = 12.6$
$vol = 0.0675$
$\sigma_o = 26163$

100
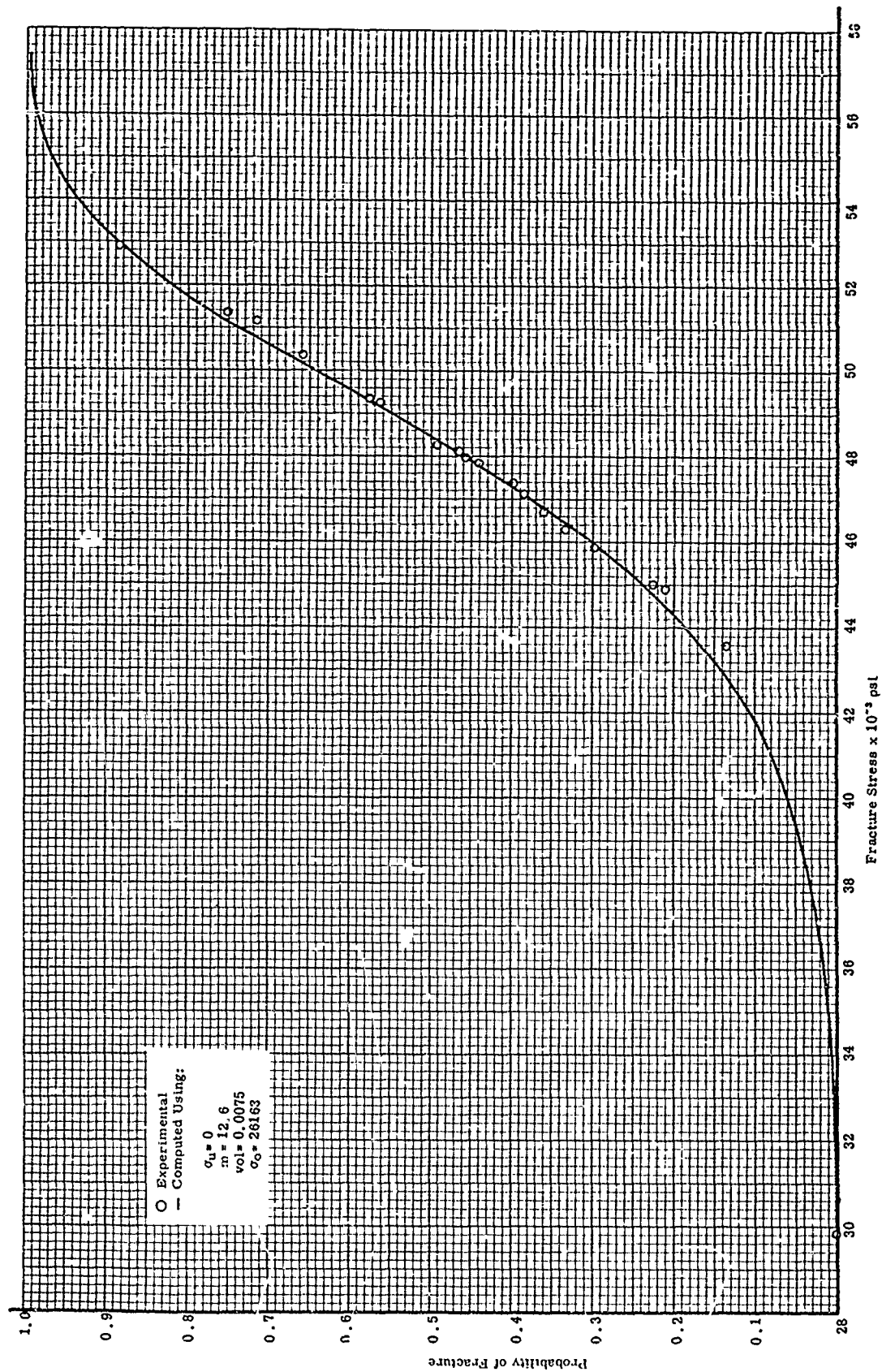
Figure 51. Probability of Fracture versus Fracture Stress for Phase I Micro Flexural Specimens from Specimen Blank A12

101
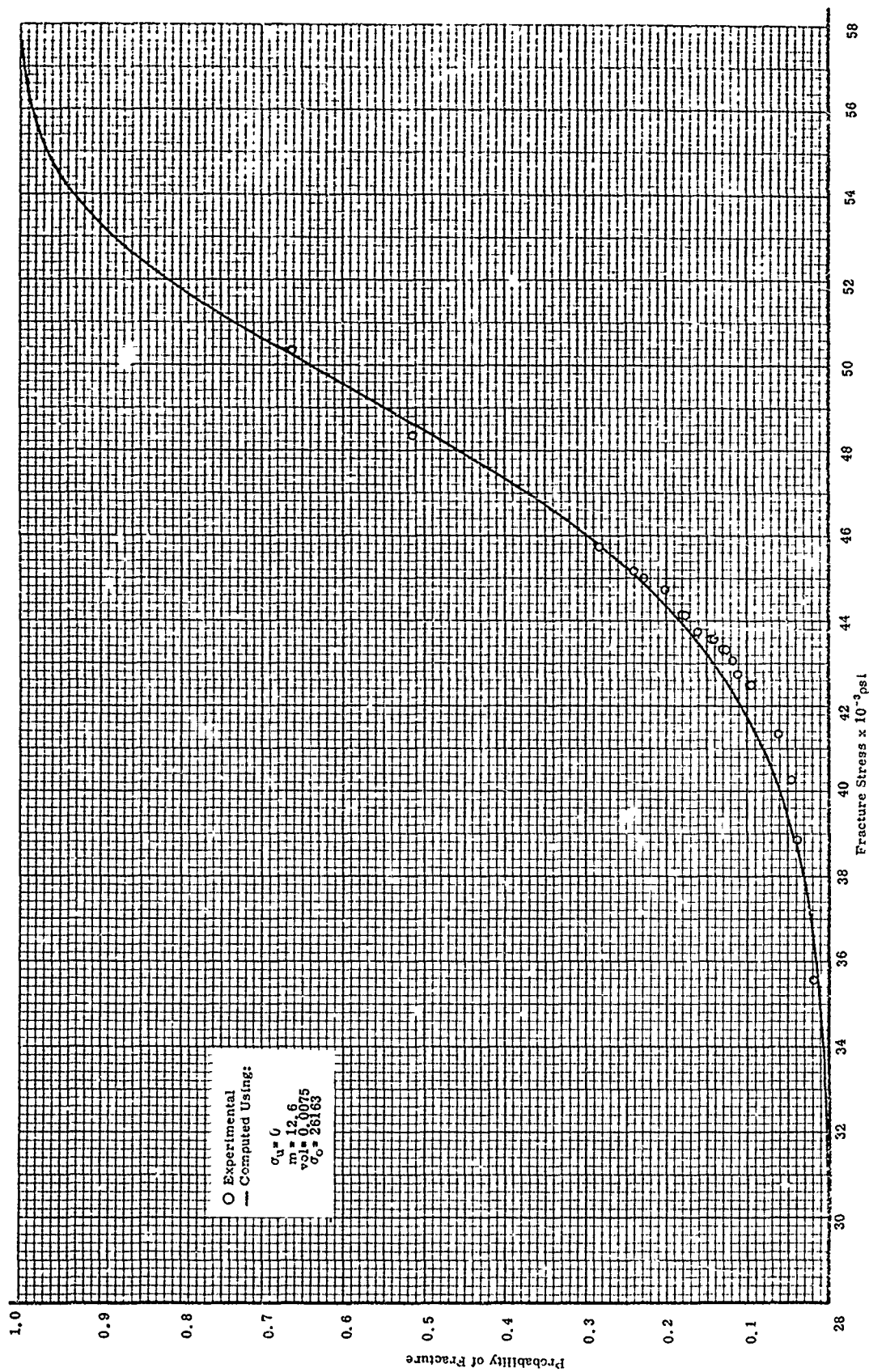
Figure 52. Probability of Fracture versus Fracture Stress for Phase I Macro Flexural Specimens from Specimen Blank A13

102
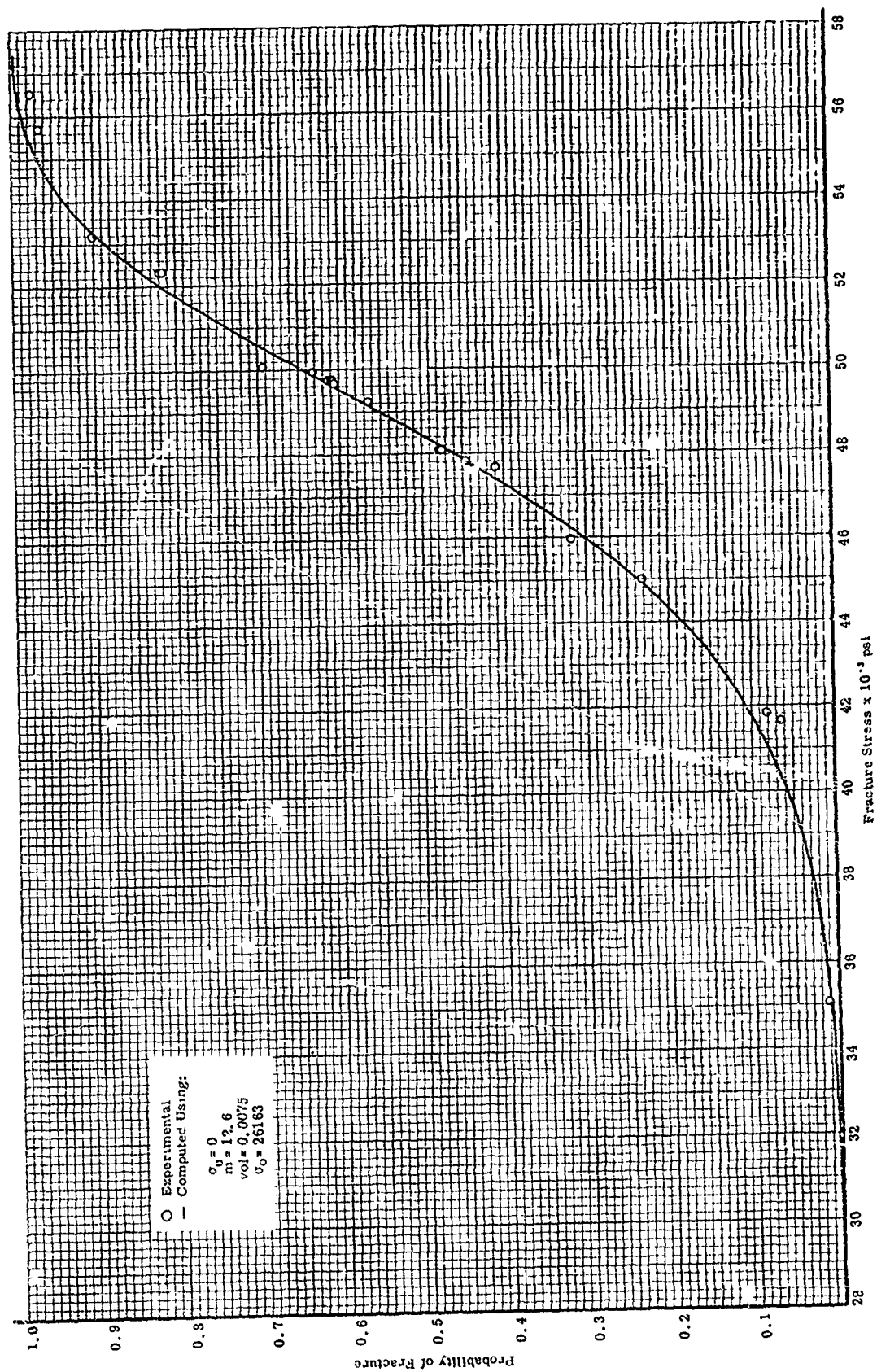
Figure 53. Probability of Fracture versus Fracture Stress for Phase I Macro Flexural Specimens from Specimen Blank A14

Legend (within plot):
O Experimental
— Computed Using:

$\sigma_u = 0$
$m = 12.6$
vol = 0.0075
$\sigma_0 = 26163$

Y-axis: Probability of Fracture

X-axis: Fracture Stress x 10^{-3} psi

103
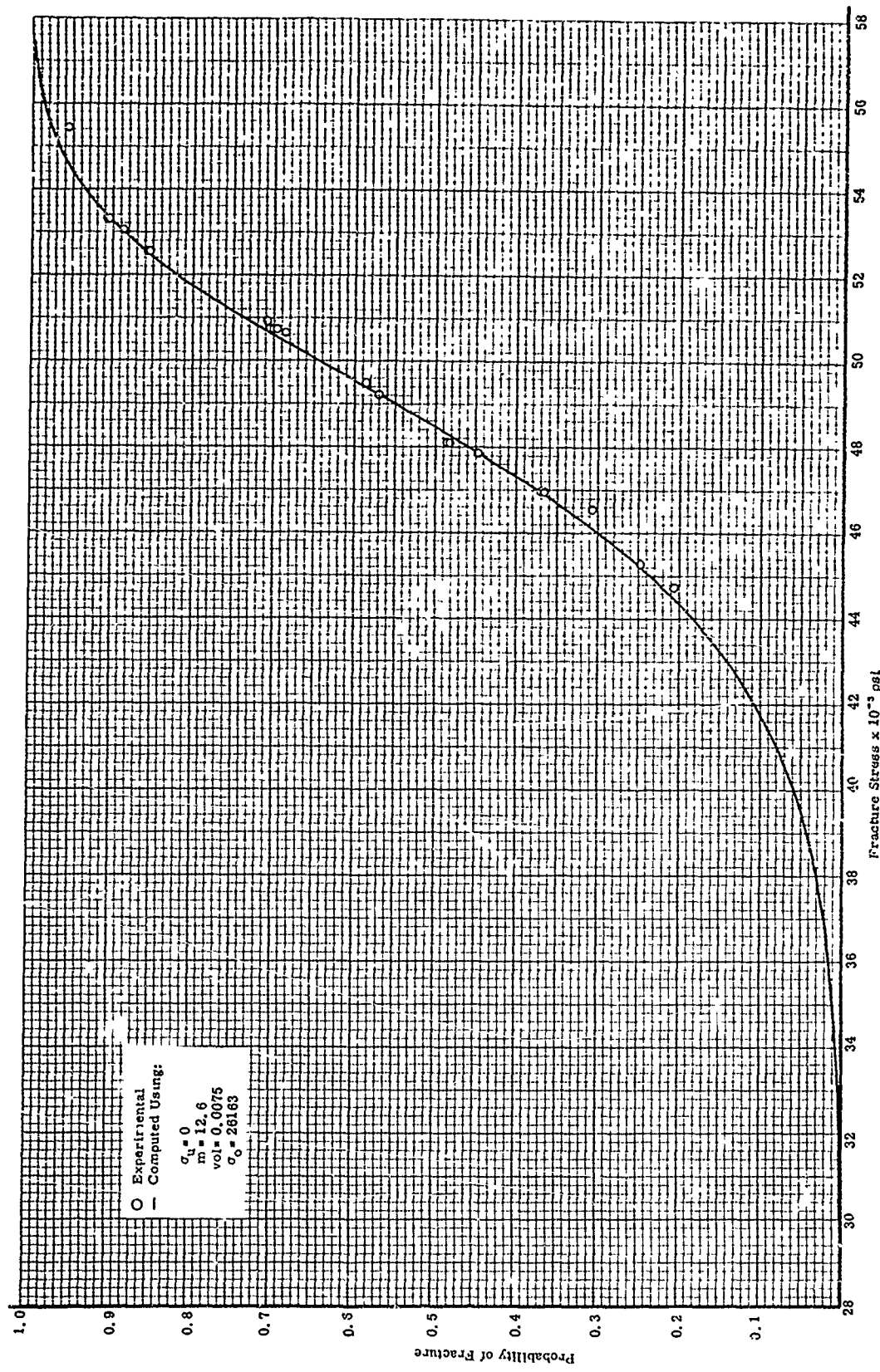
Figure 54. Probability of Fracture versus Fracture Stress for Phase I Macro Flexural Specimens from Specimen Blank A17

104
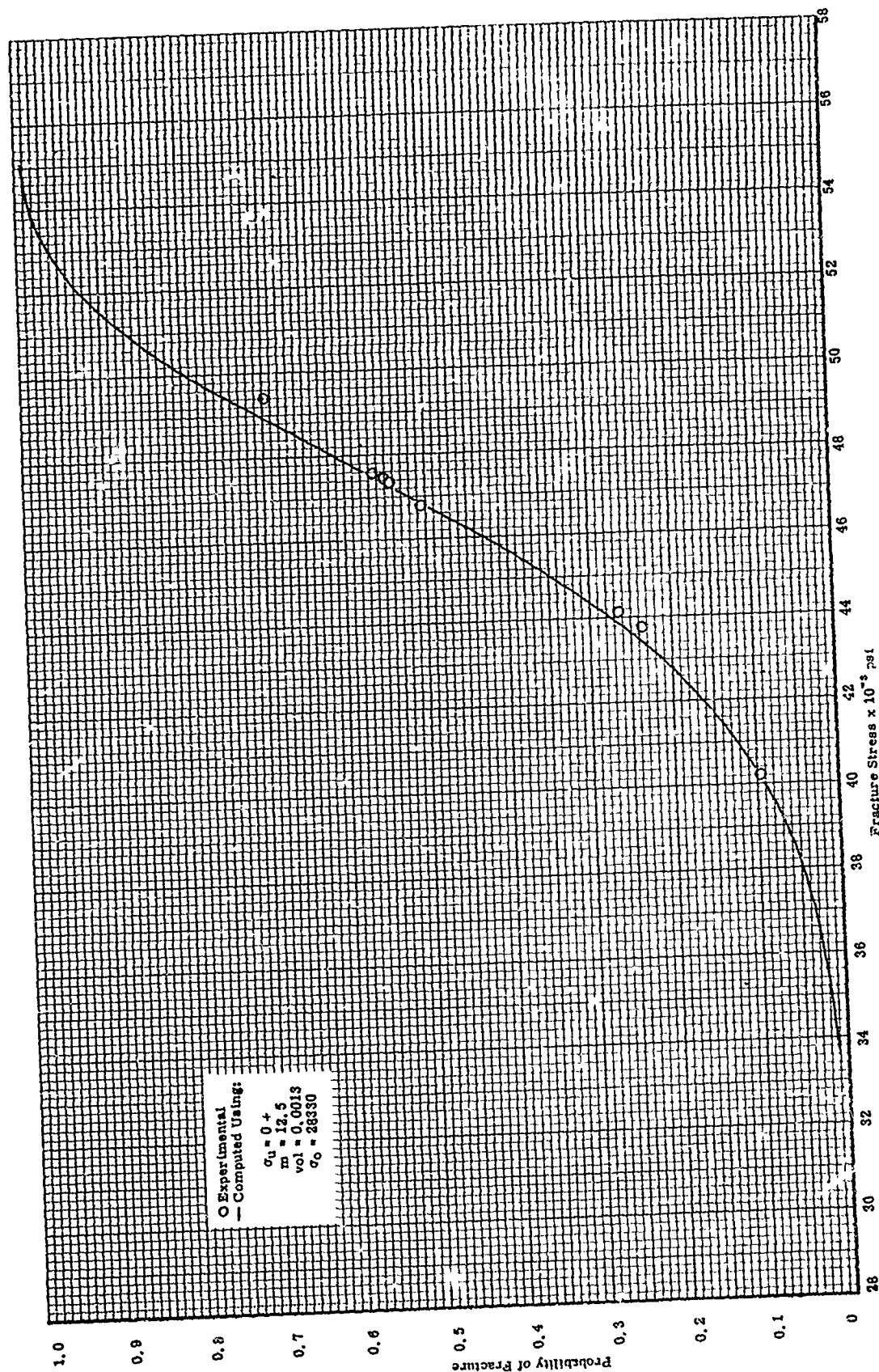
Figure 55. Probability of Fracture versus Fracture Stress for Phase I Macro Tensile Specimens from Specimen Blank A02

O Experimental
— Computed Using:
$\sigma_u = 0 +$
$m = 12.5$
$vol = 0.0013$
$\sigma_o = 28330$

Probability of Fracture

Fracture Stress $\times 10^{-3}$ psi
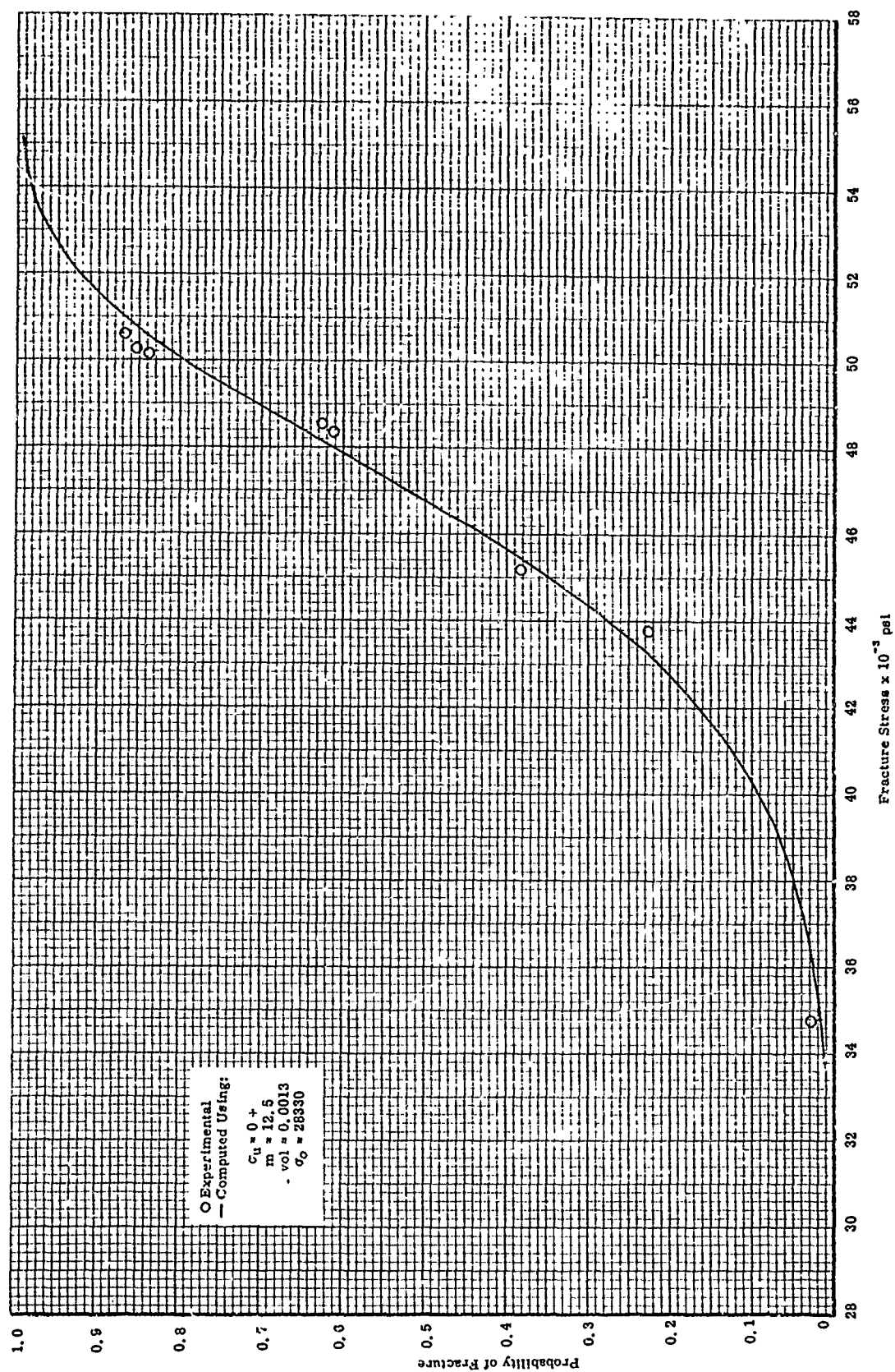
Figure 56. Probability of Fracture versus Fracture Stress for Phase I Macro Tensile Specimens from Specimen Blank A04
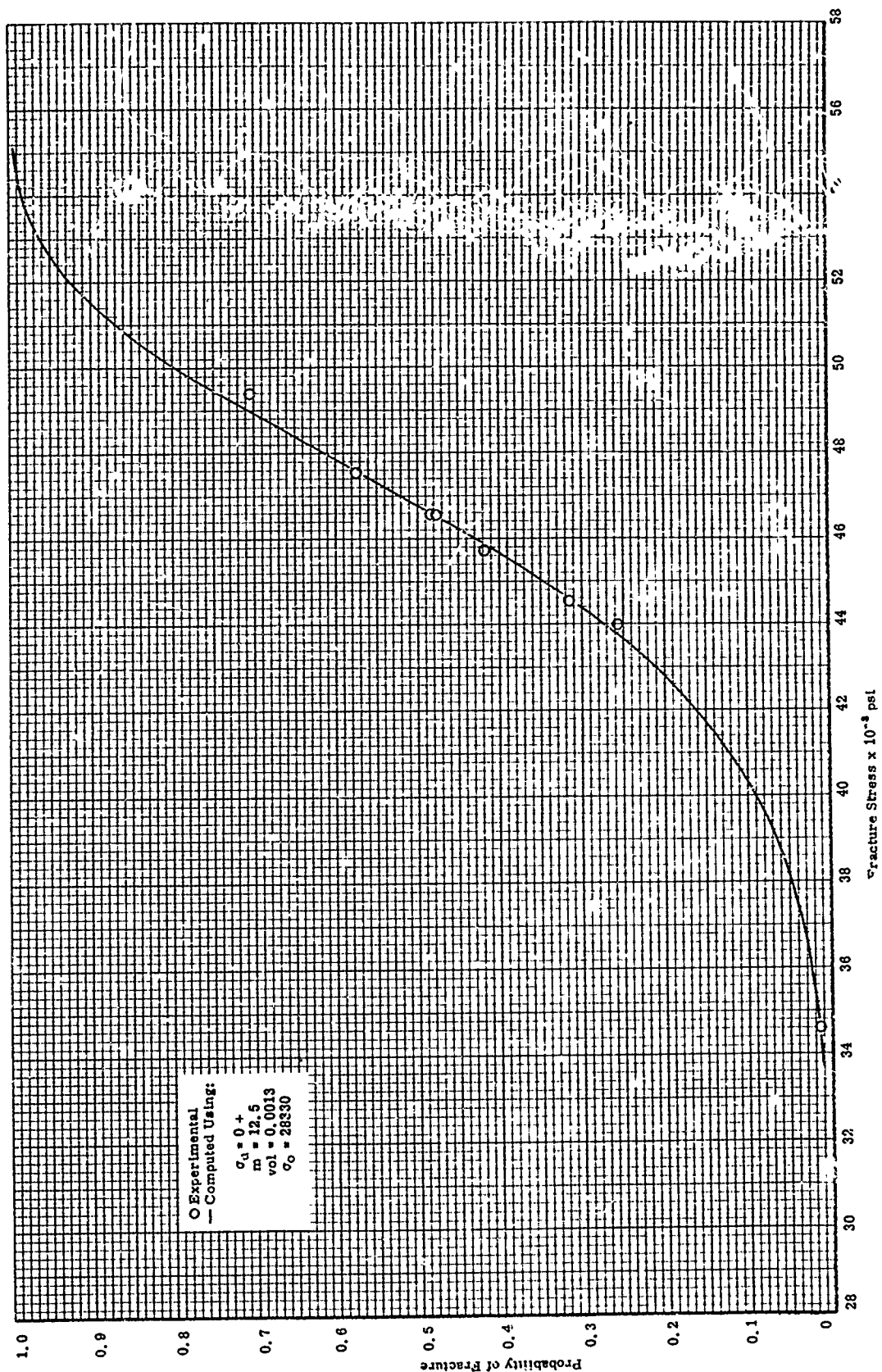
Figure 57. Probability of Fracture versus Fracture Stress for Phase I Macro Tensile Specimens from Specimen Blank A05
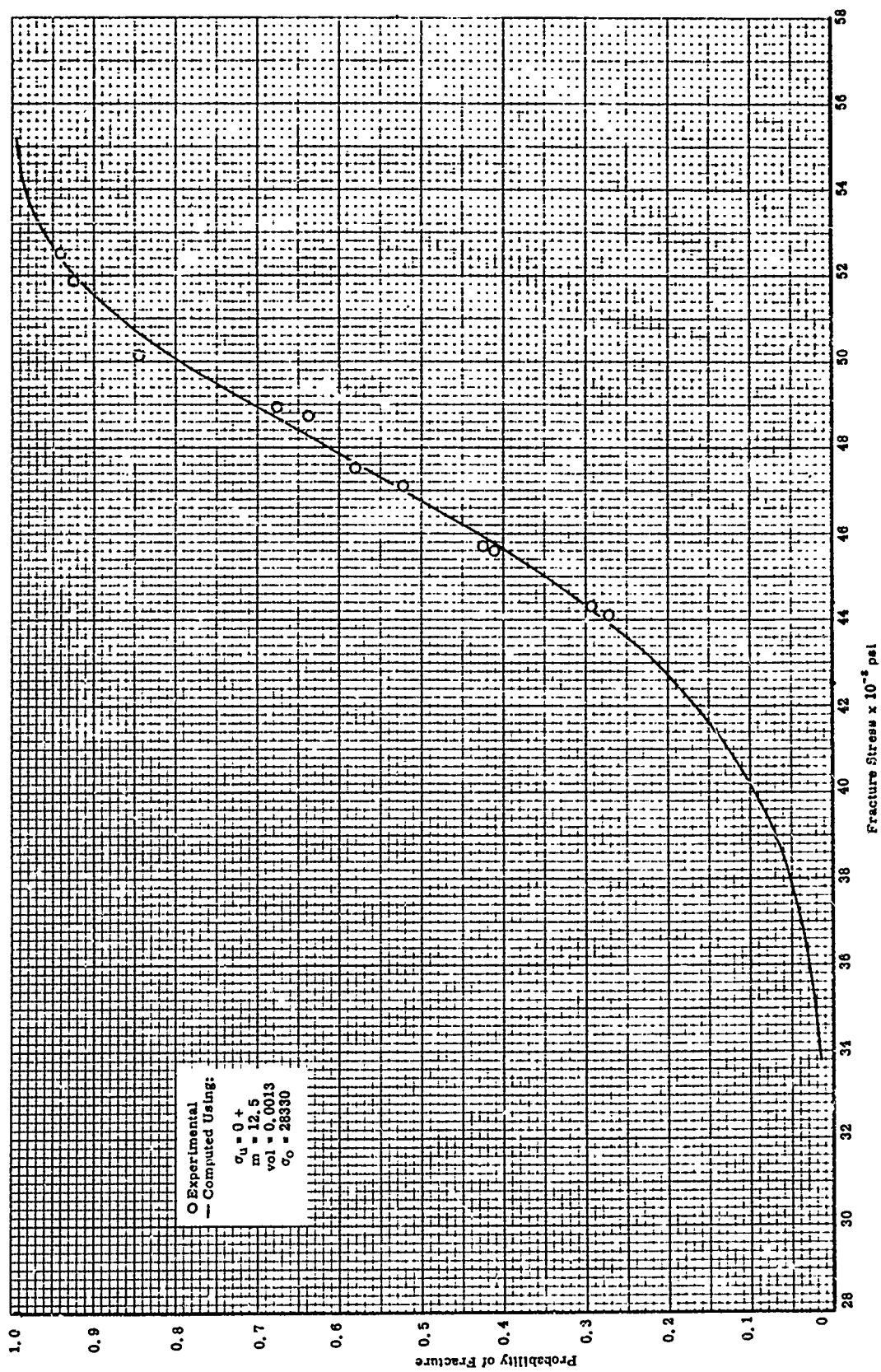
Figure 58. Probability of Fracture versus Fracture Stress for Phase I Macro Tensile Specimens from Specimen Block 107
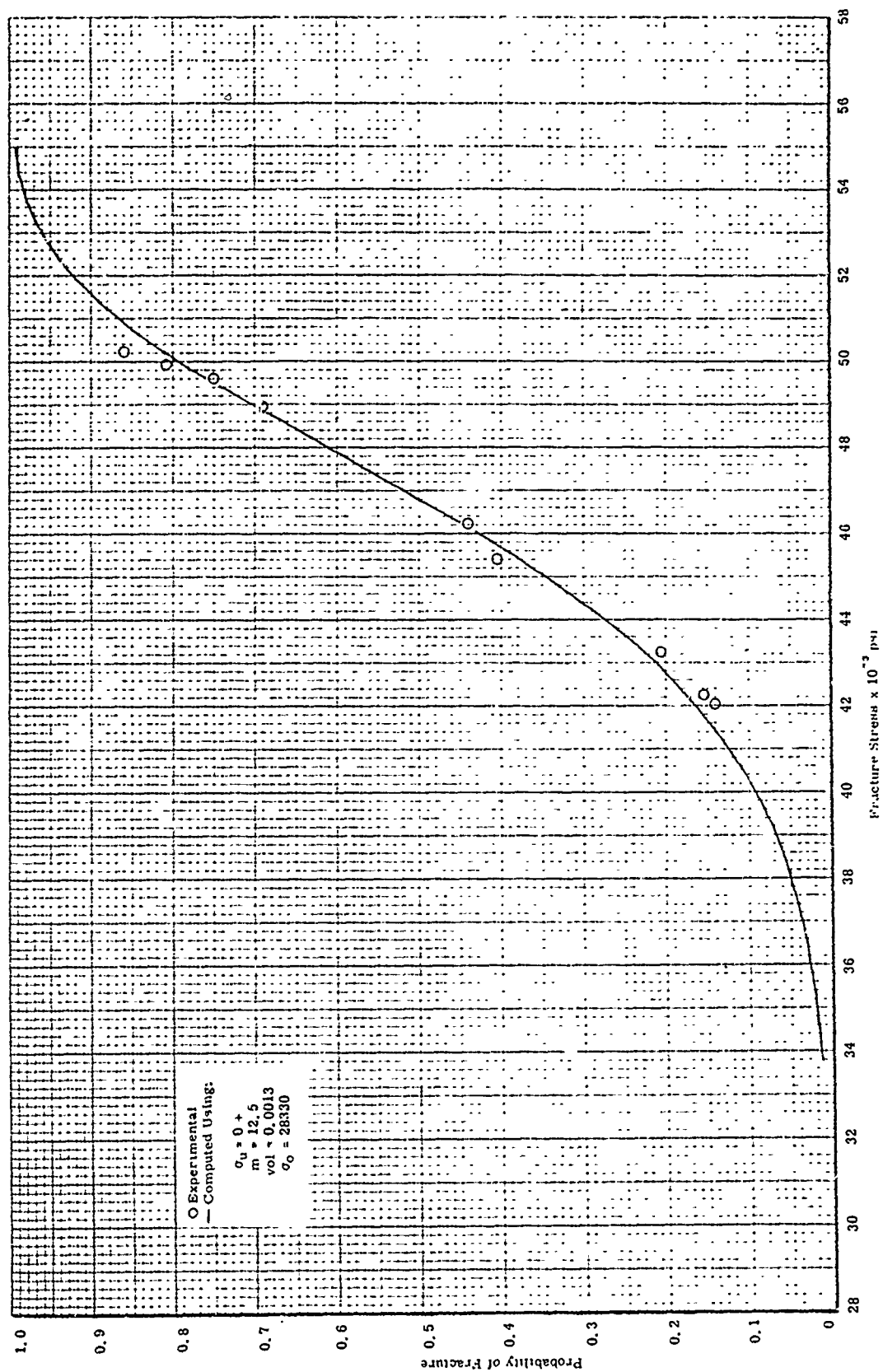
Figure 59. Probability of Fracture versus Fracture Stress for Phase 1 Macro Tensile Specimens from Specimen Blank Λ08
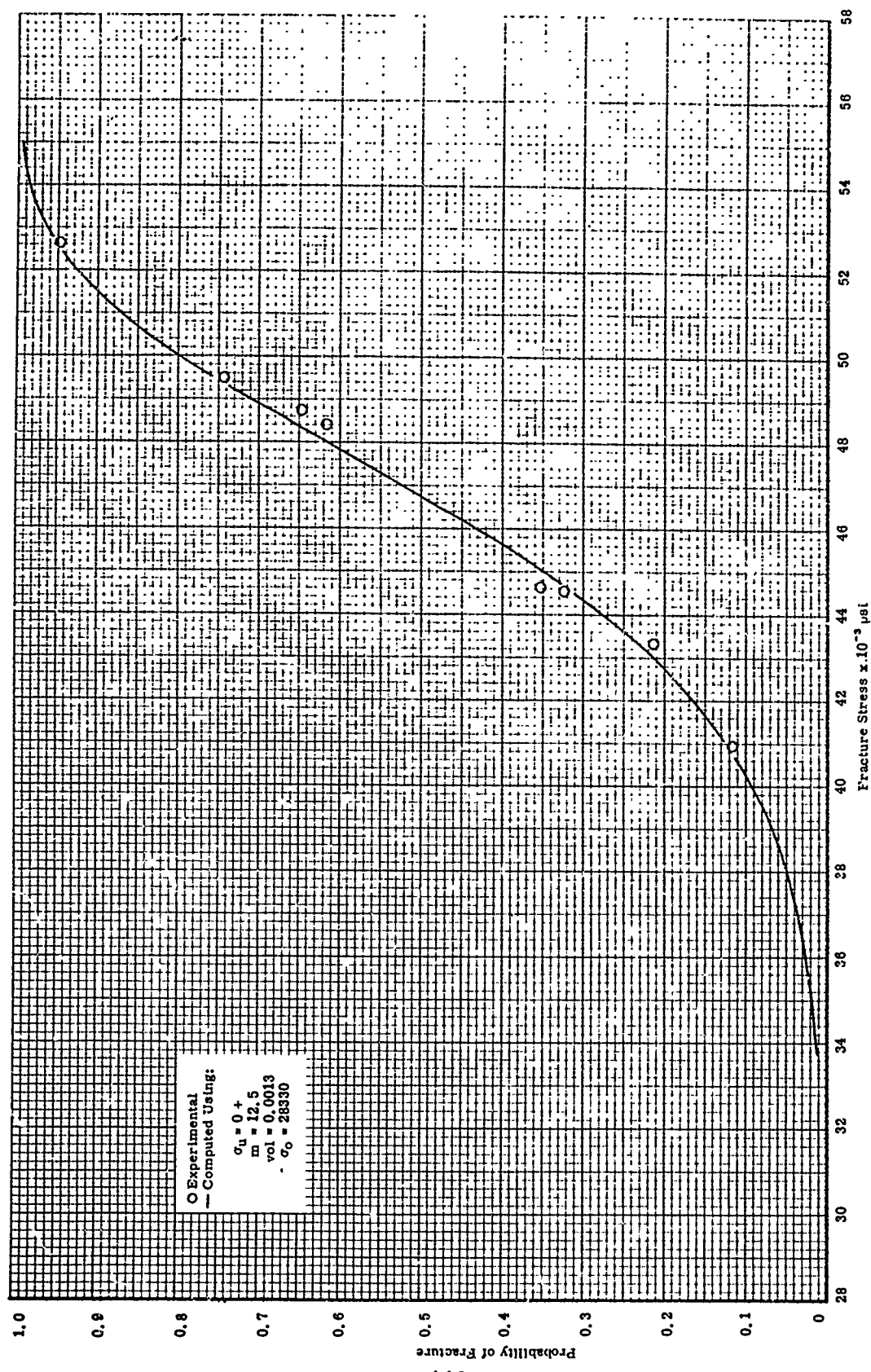
Figure 60. Probability of Fracture versus Fracture Stress for Phase I Macro Tensile Specimens from Specimen Blank A09
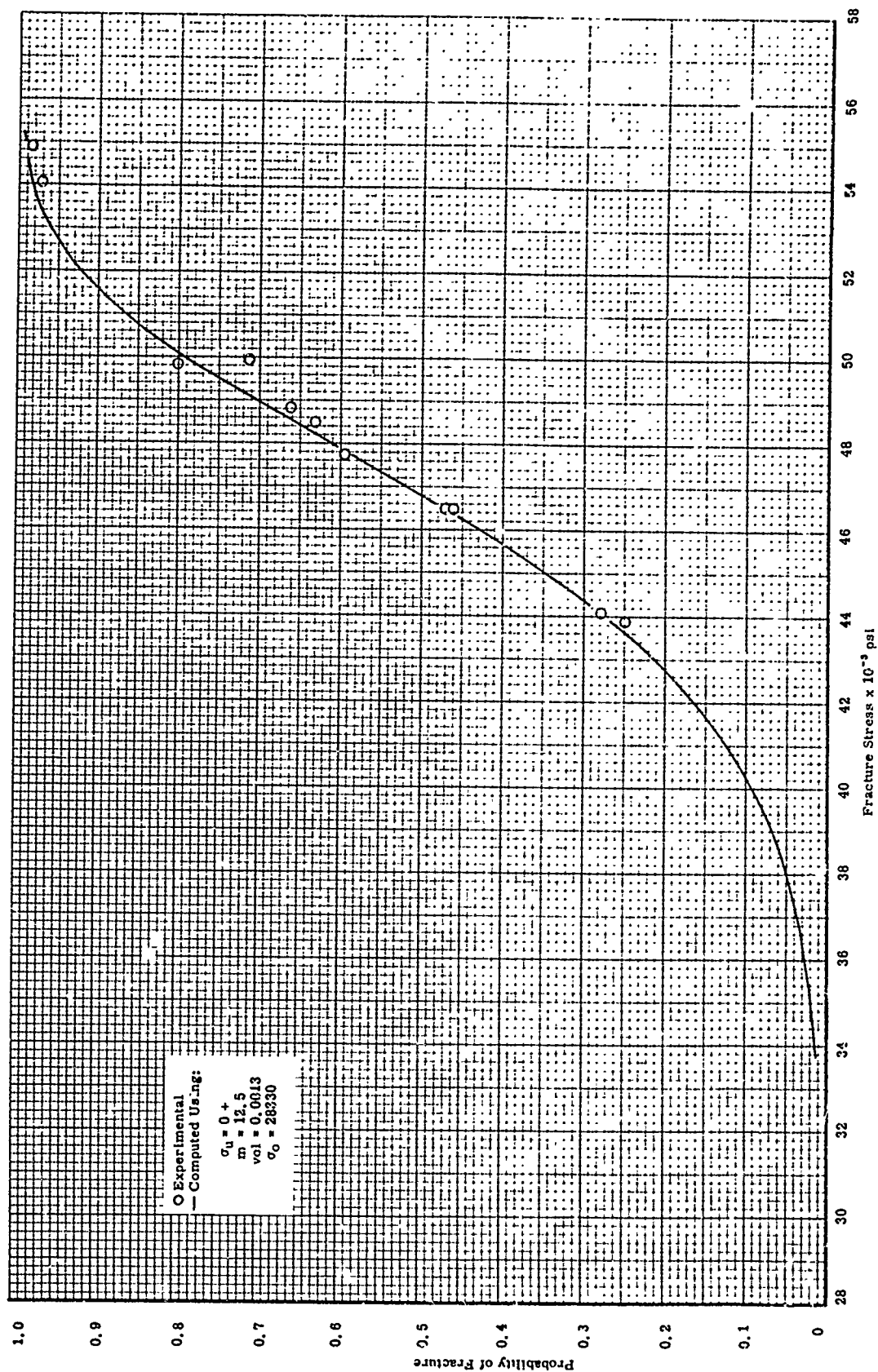
Figure 61. Probability of Fracture versus Fracture Stress for Phase I Macro Tensile Specimens from Specimen Blank AlO

111
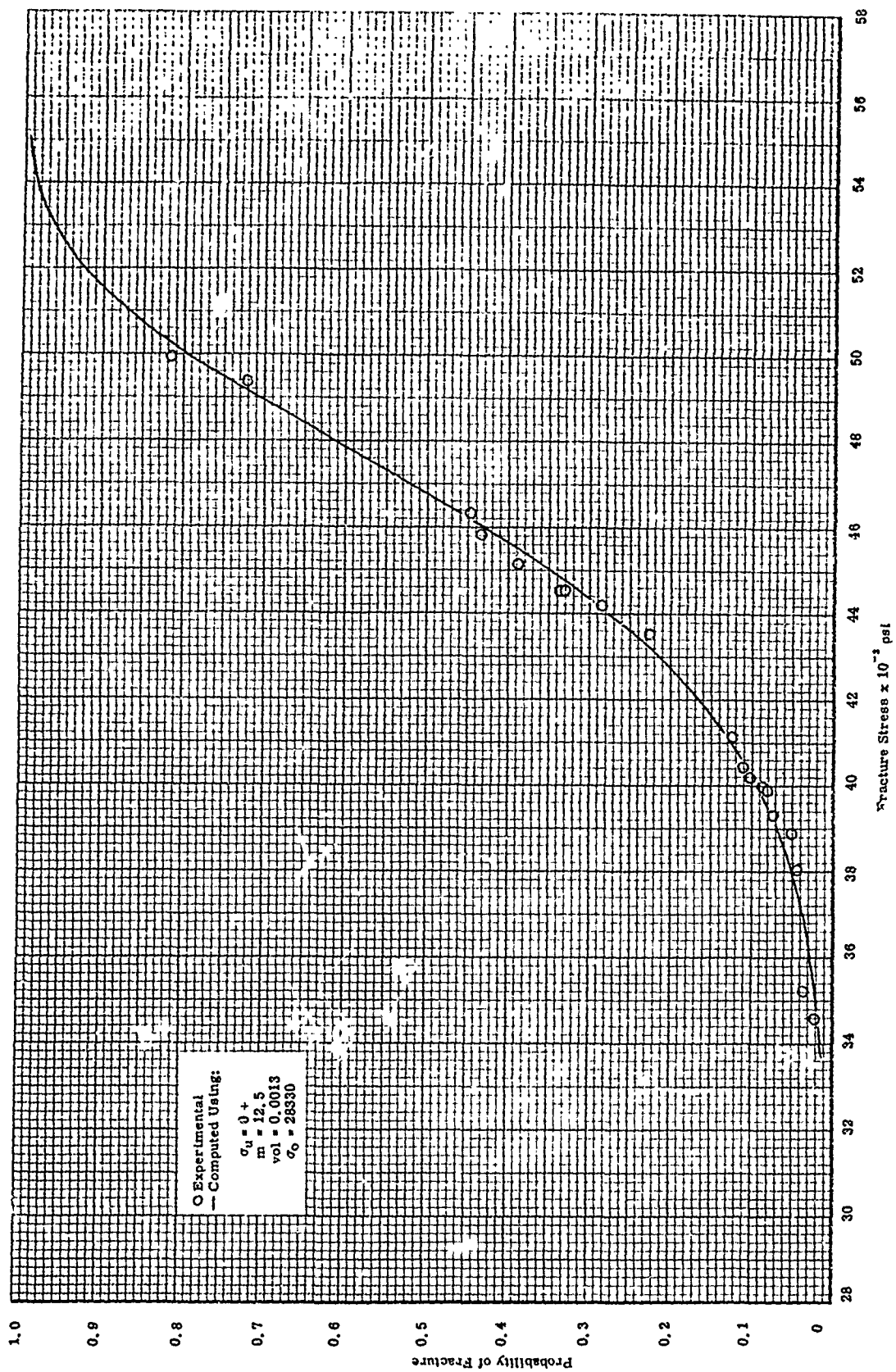
Figure 62. Probability of Fracture versus Fracture Stress for Phase I Micro Tensile Specimens from Specimen Blank A11

112
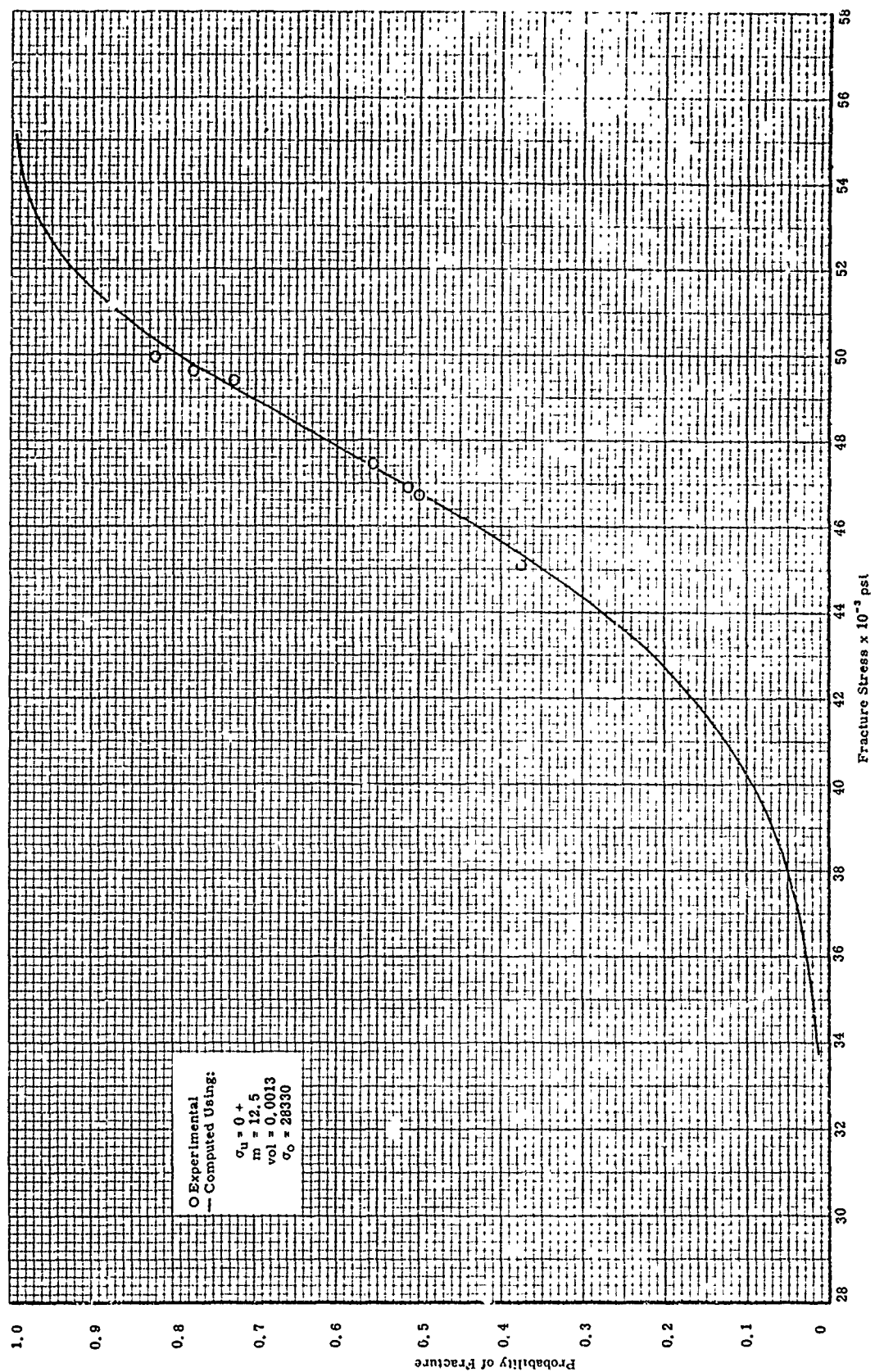
Figure 63. Probability of Fracture versus Fracture Stress for Phase I Macro Tensile Specimens from Specimen Blank A12

113
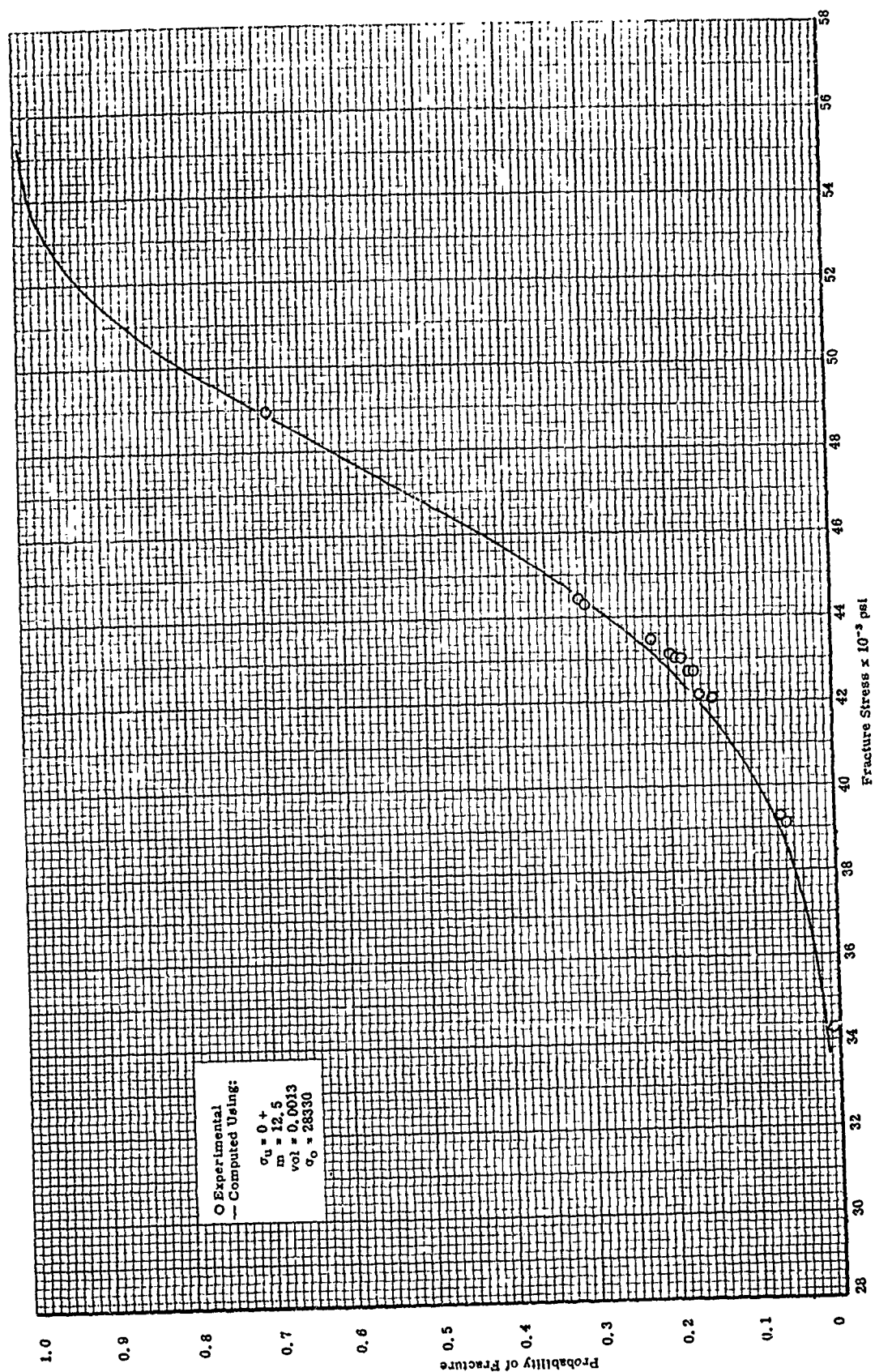
Figure 64. Probability of Fracure versus Fracture Stress for Phase I Macro Tensile Specimens from Specimen Blank A13
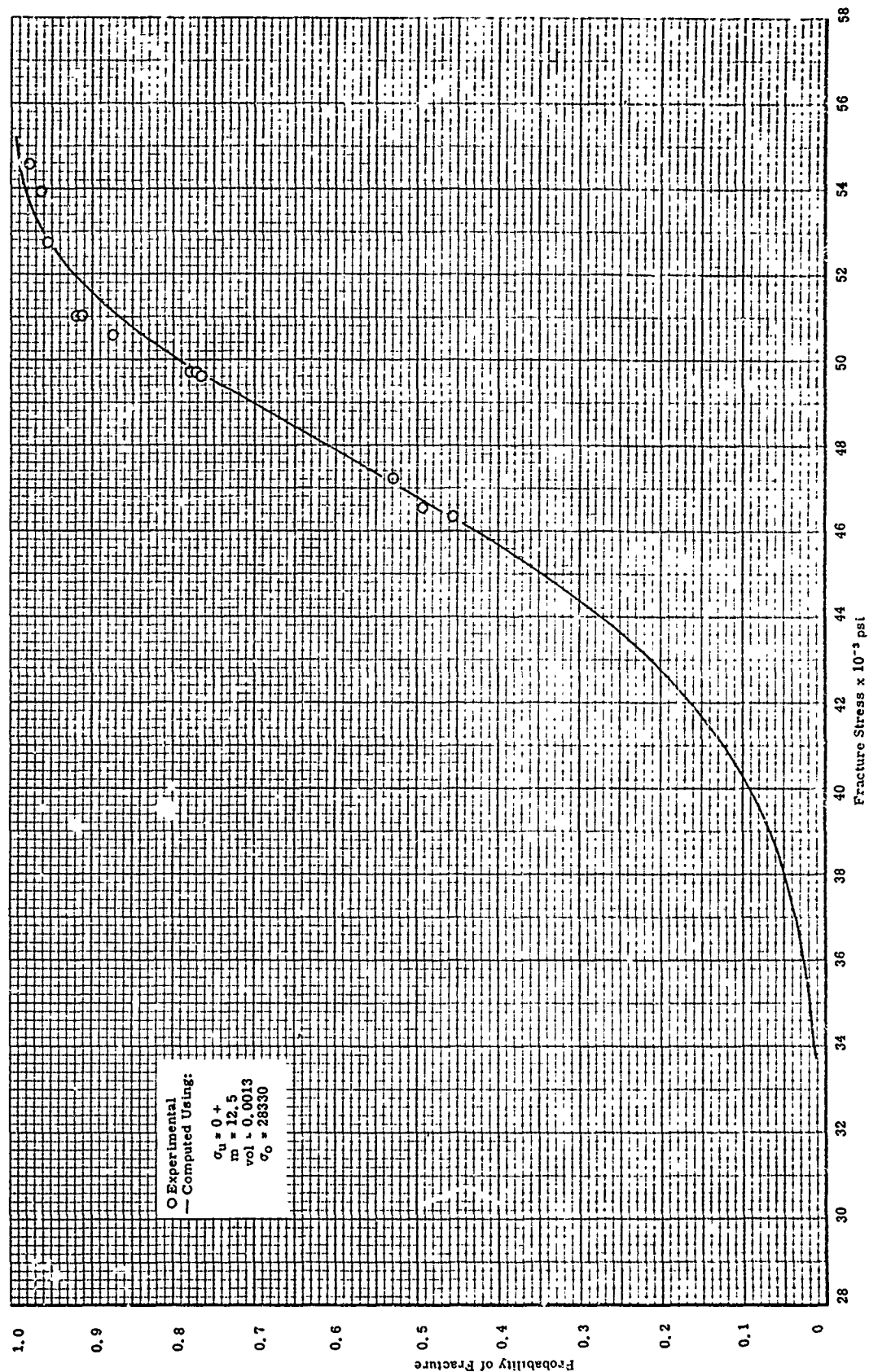
Figure 65. Probability of Fracture versus Fracture Stress for Phase I Macro Tensile Specimens from Specimen Blank A14

Legend (inside plot):

O Experimental
— Computed Using:

$\sigma_u = 0+$
$m = 12.5$
$vol = 0.0013$
$\sigma_o = 28330$

X-axis: Fracture Stress $\times 10^{-3}$ psi

Y-axis: Probability of Fracture

115
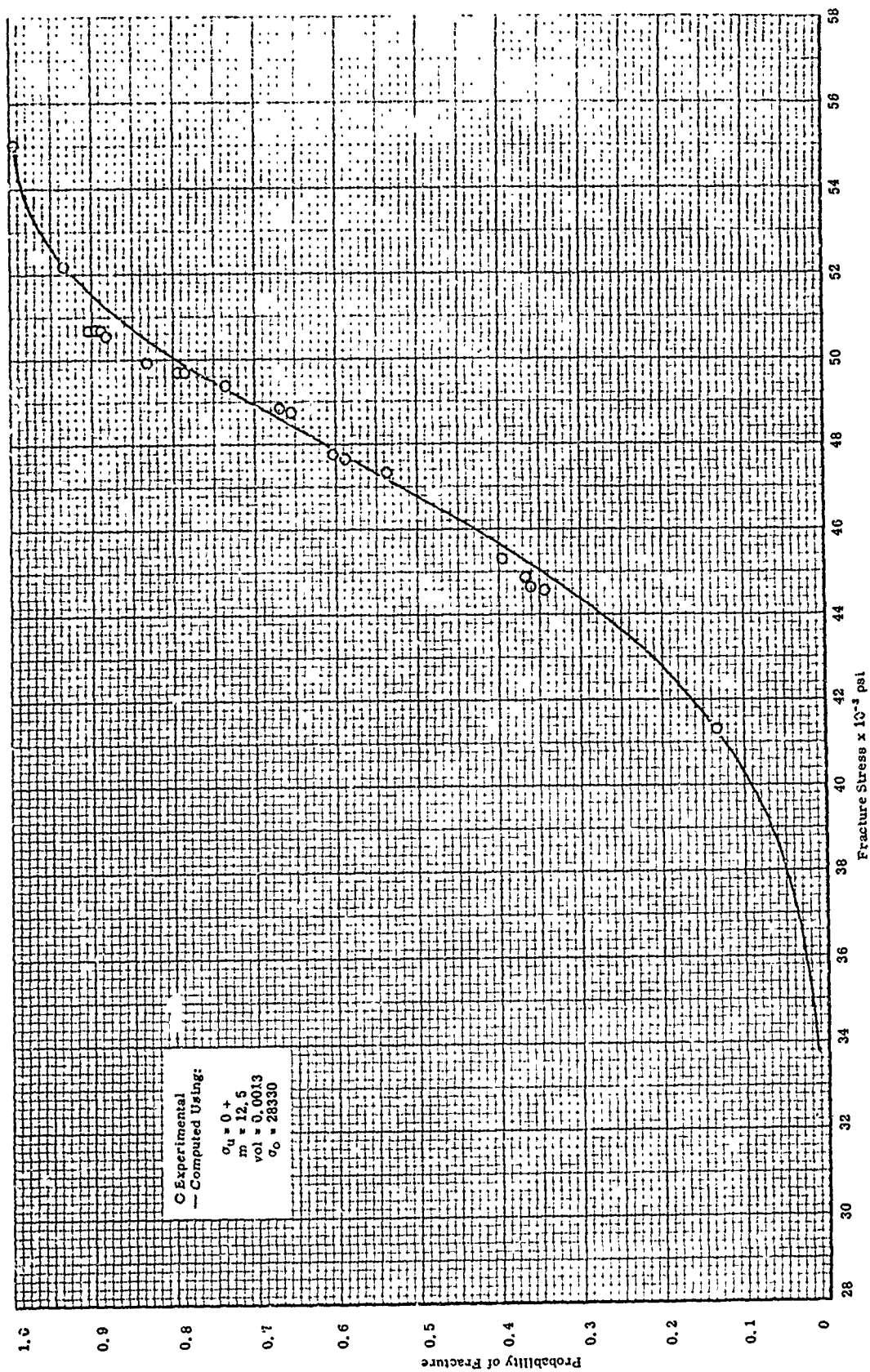
Figure 66. Probability of Fracture versus Fracture Stress for Phase I Macro Tensile Specimens from Specimen Blank A17

116
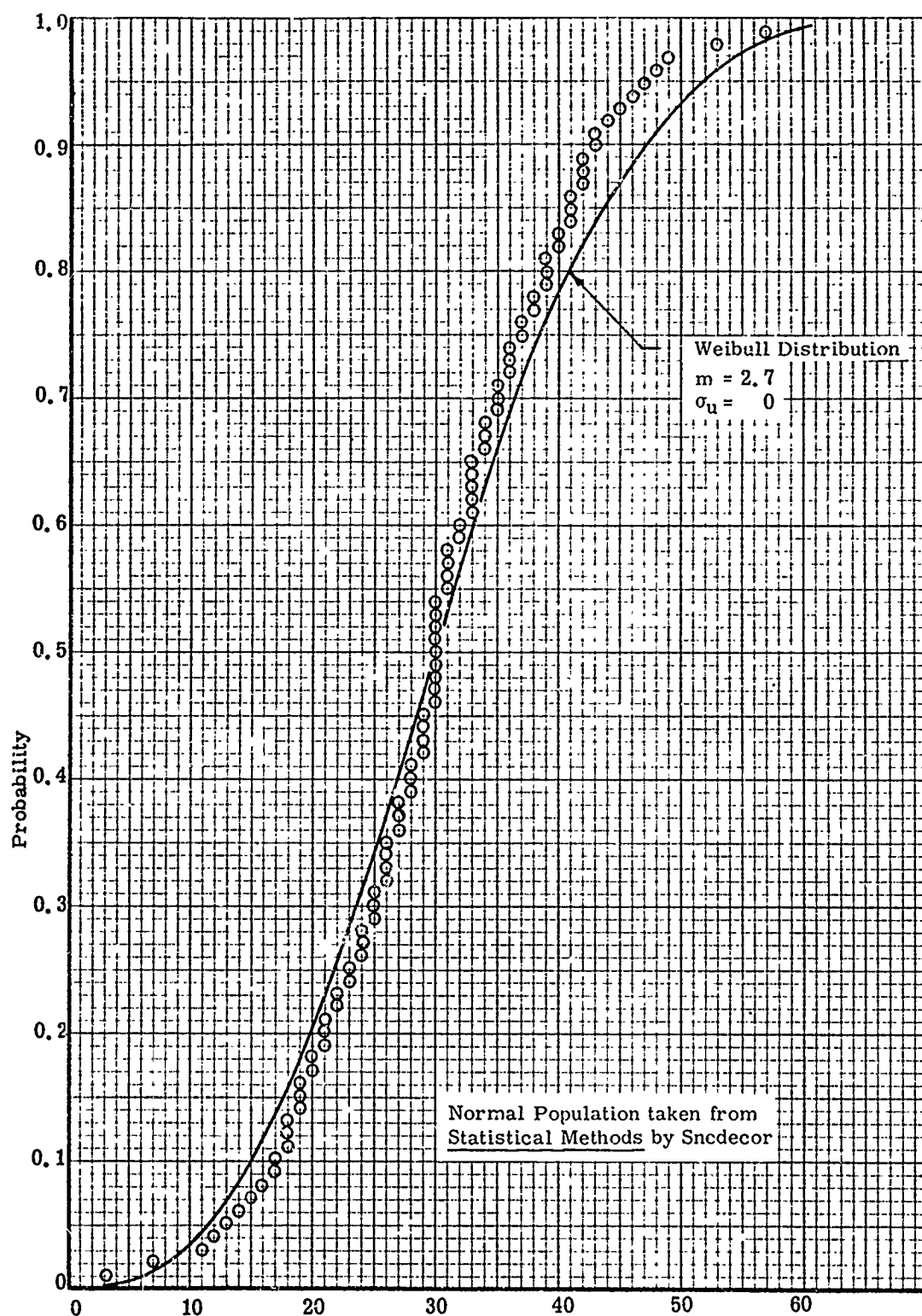
Figure 67. Normally Distributed Population with Weibull Distribution Curve

117
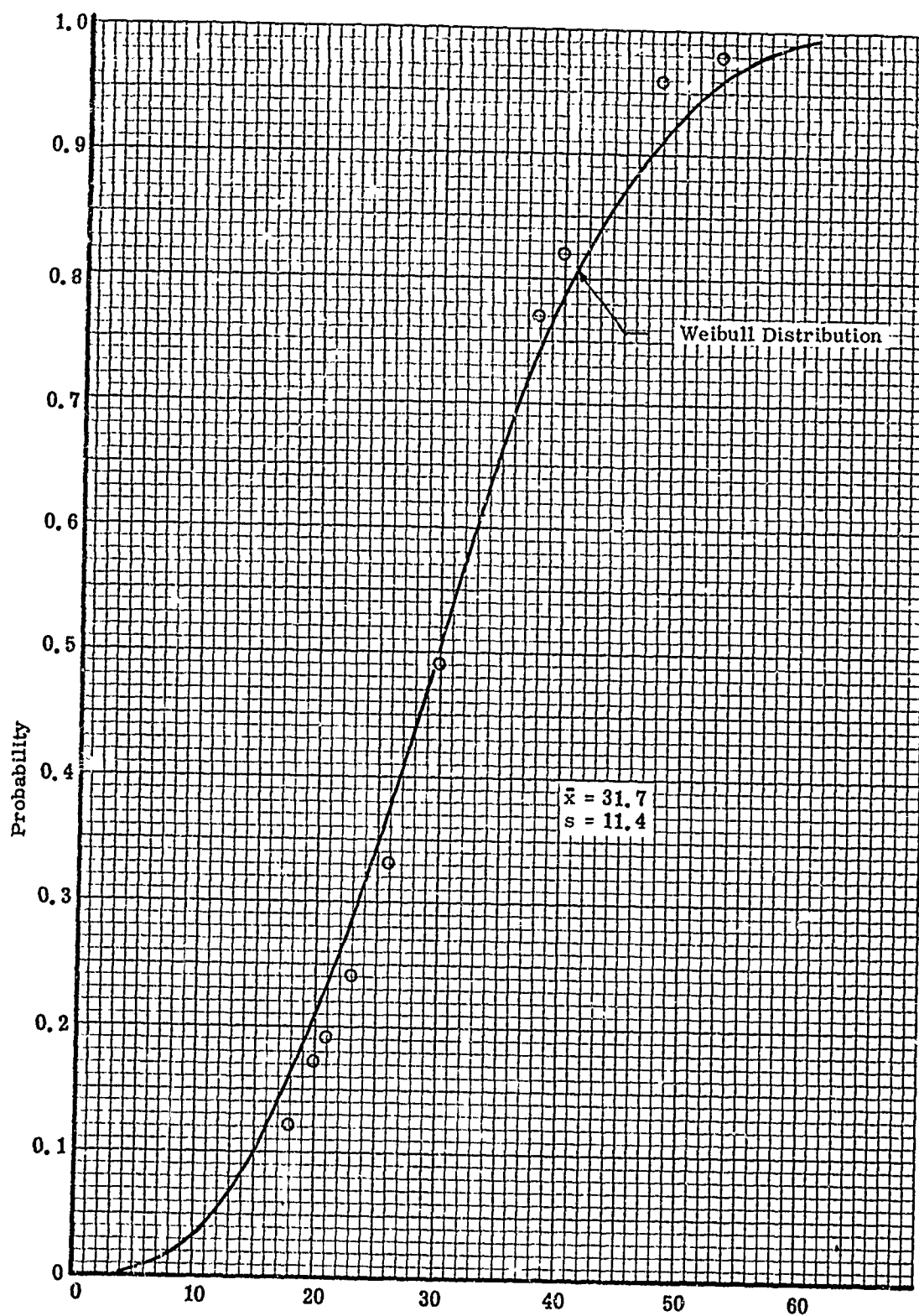
Figure 68. Random Subset No. 1 from Normally Distributed Population

118
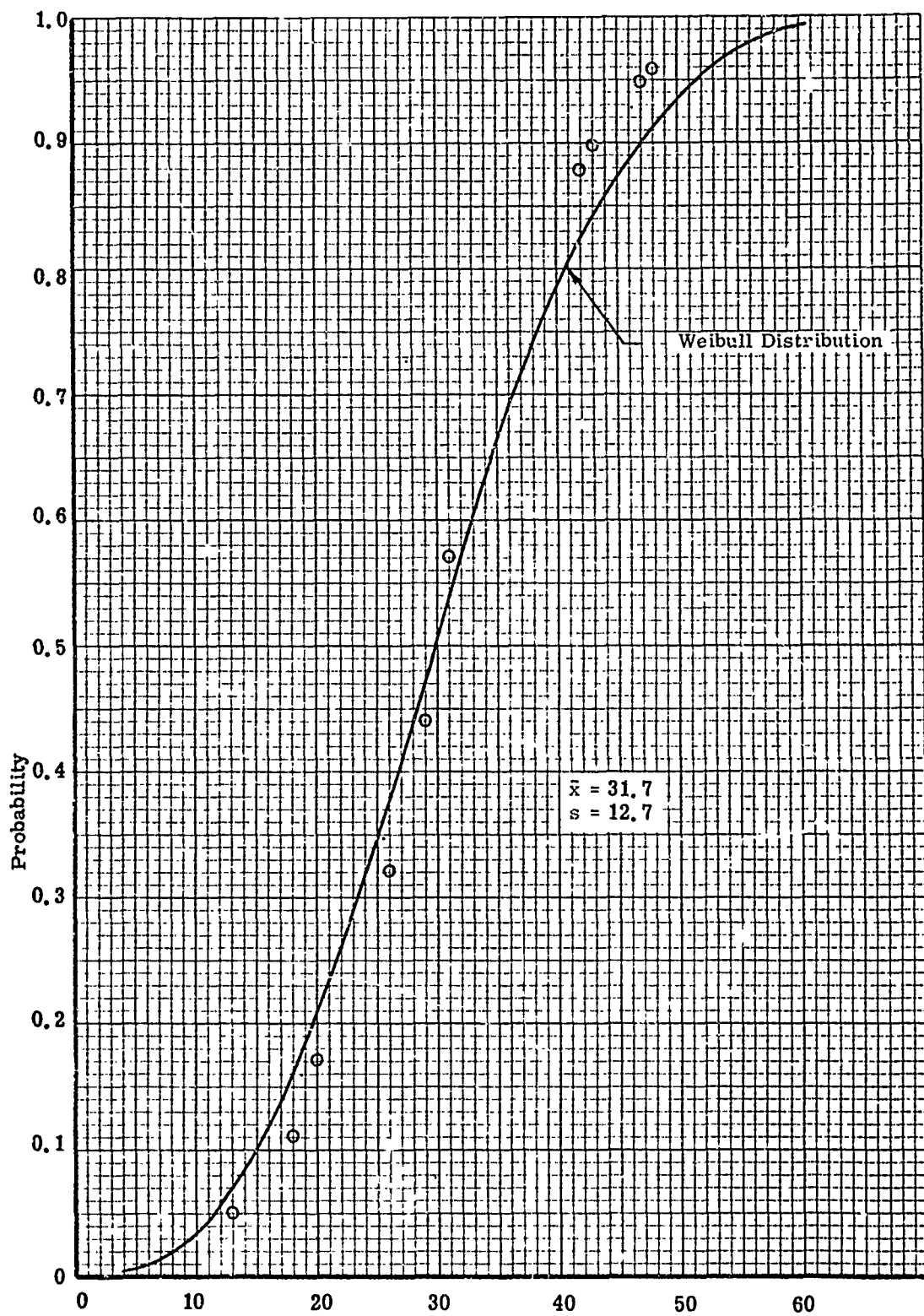
Figure 69. Random Subset No. 2 from Normally Distributed Population

119
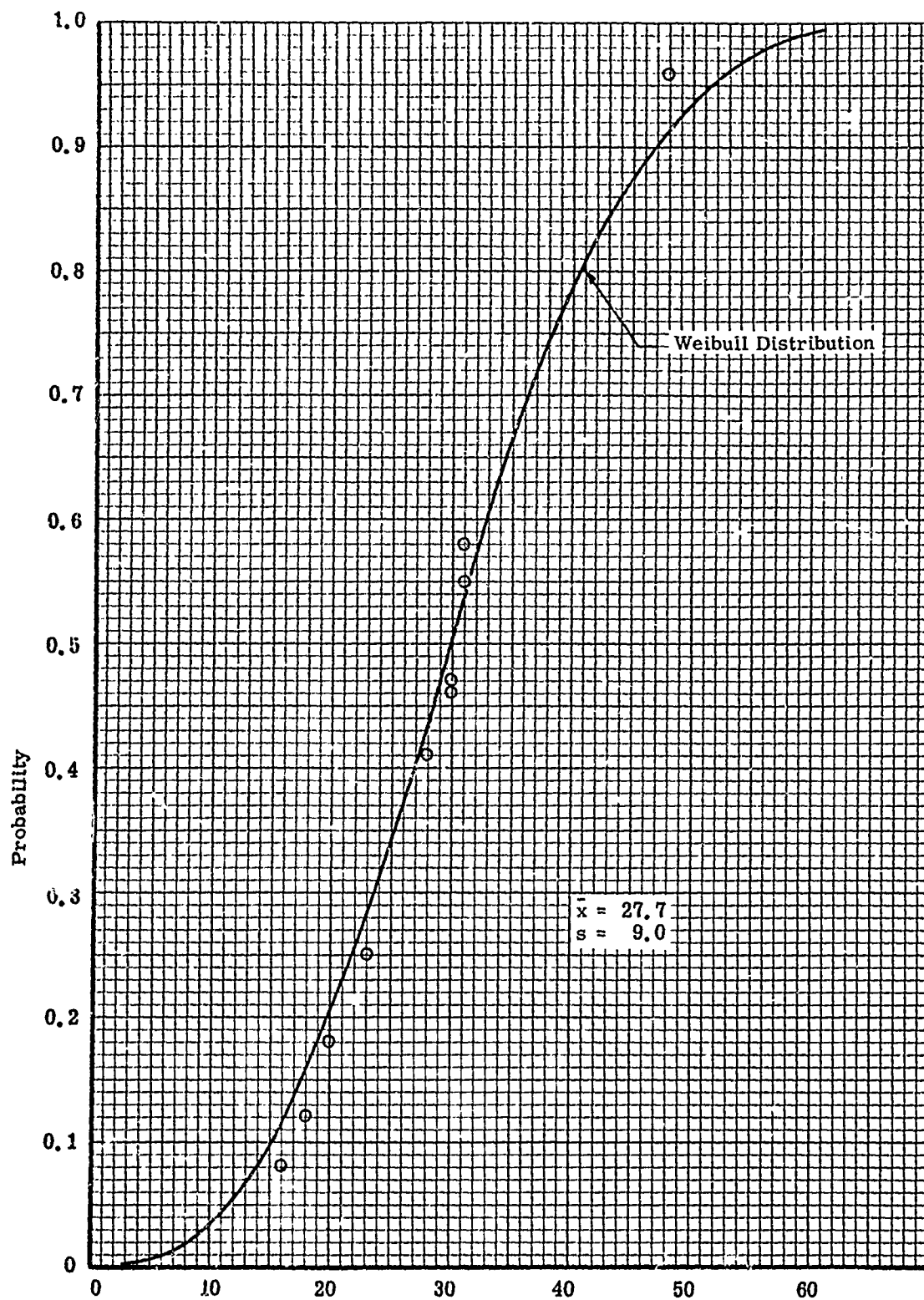
Figure 70. Random Subset No. 3 from Normally Distributed Population

120
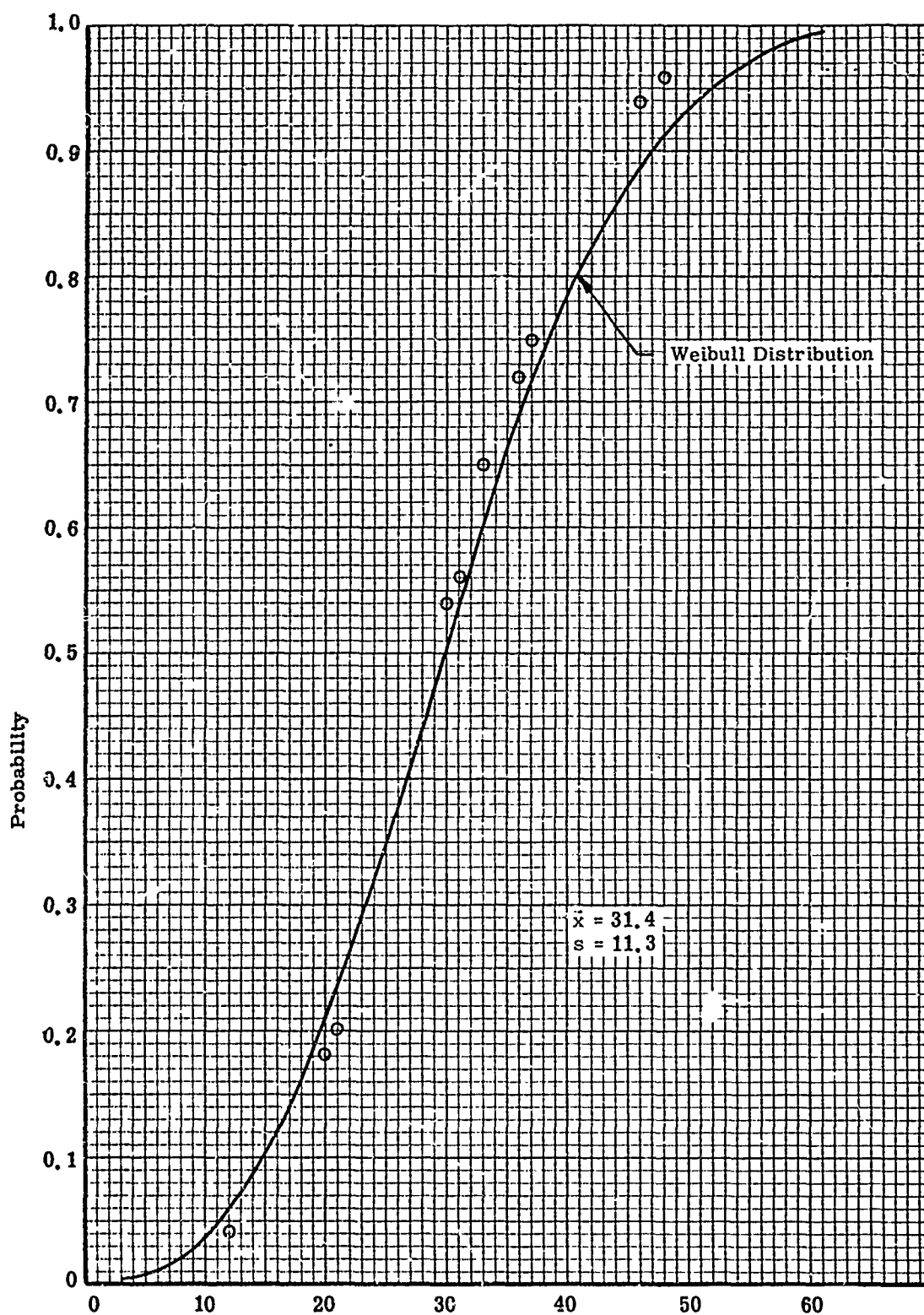
Figure 71. Random Subset No. 4 from Normally Distributed Population

121
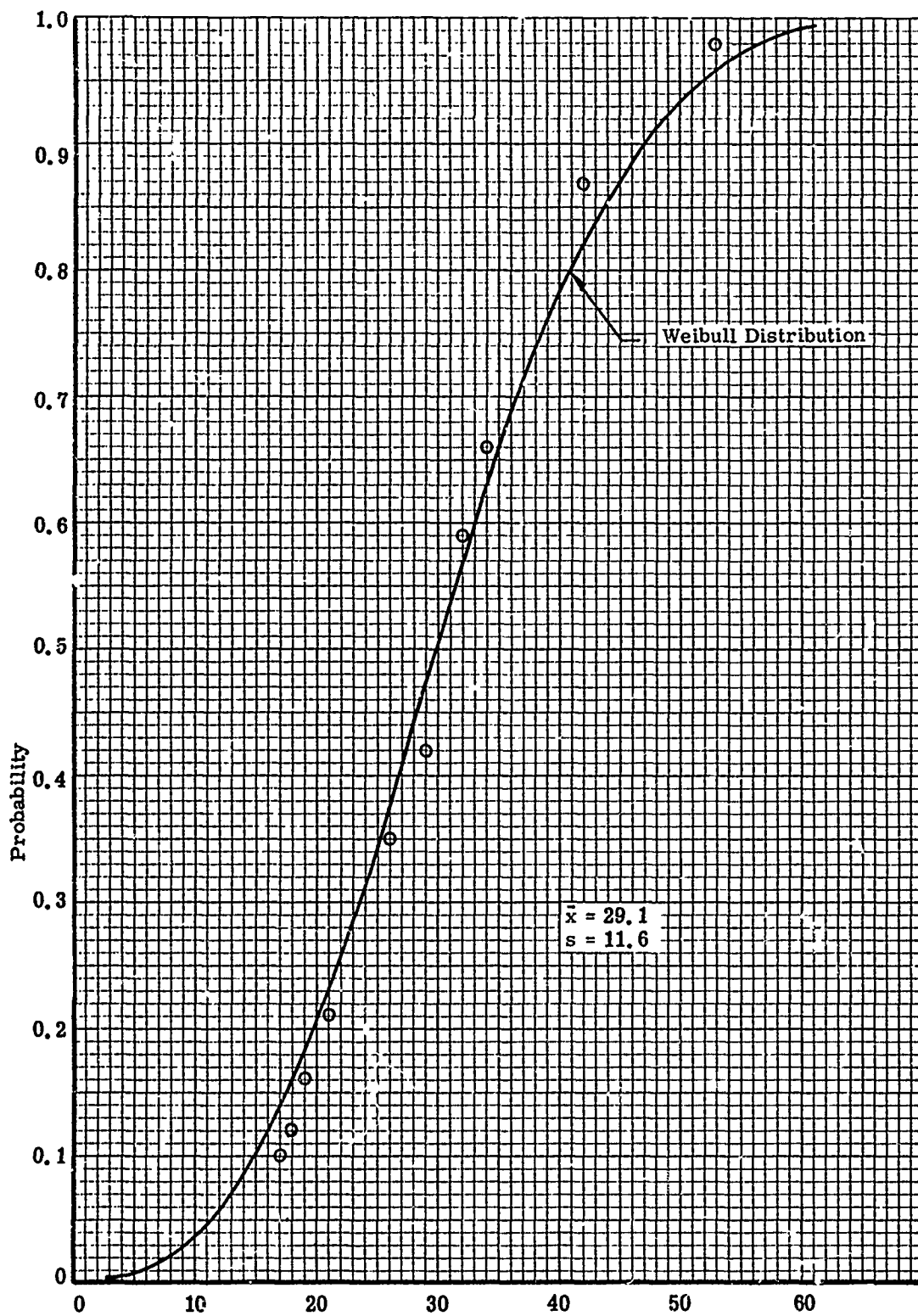
Figure 72. Random Subset No. 5 from Normally Distributed Population

122
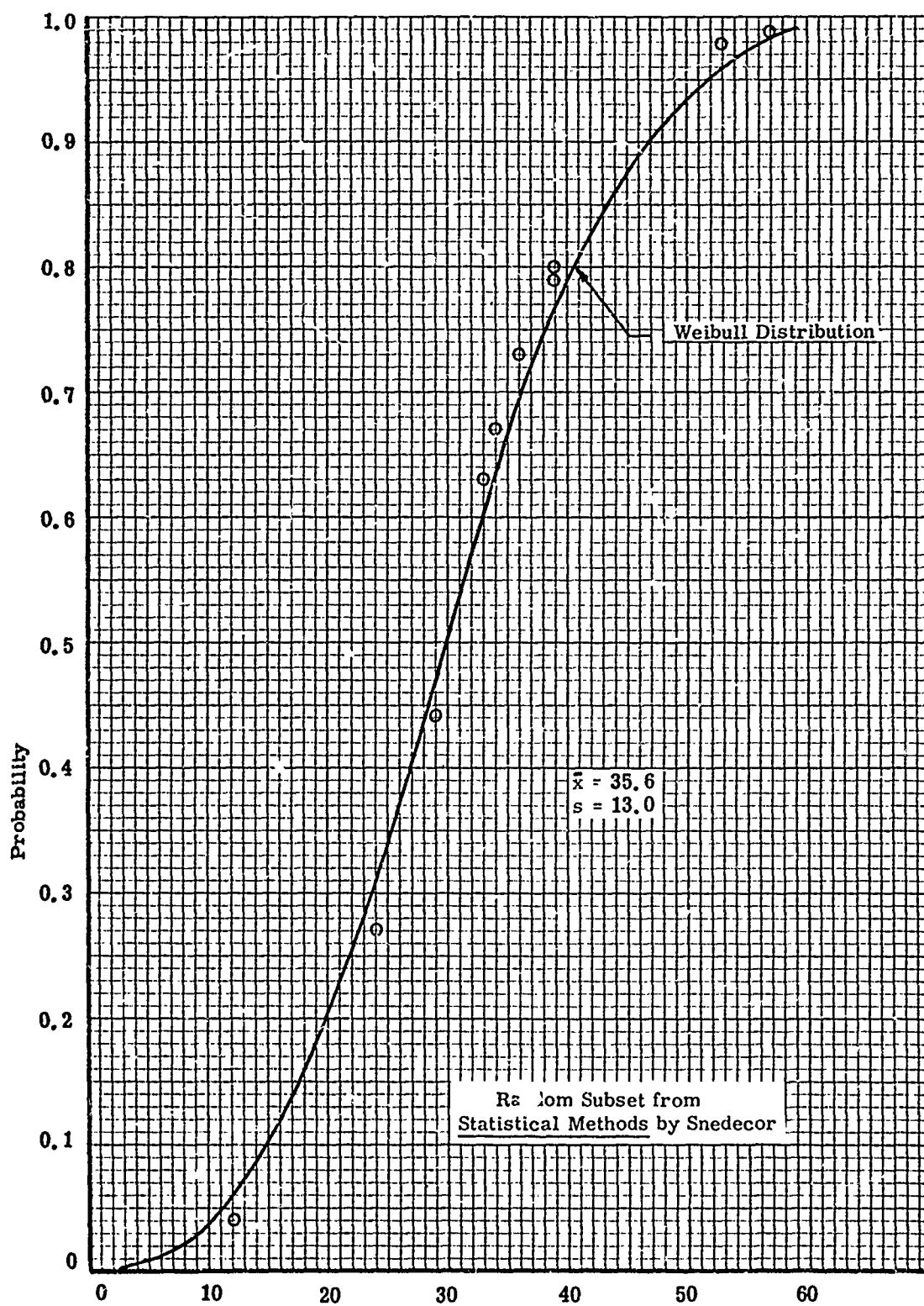
Figure 73. Random Subset No. 6 from Norm ally Distributed Population

123
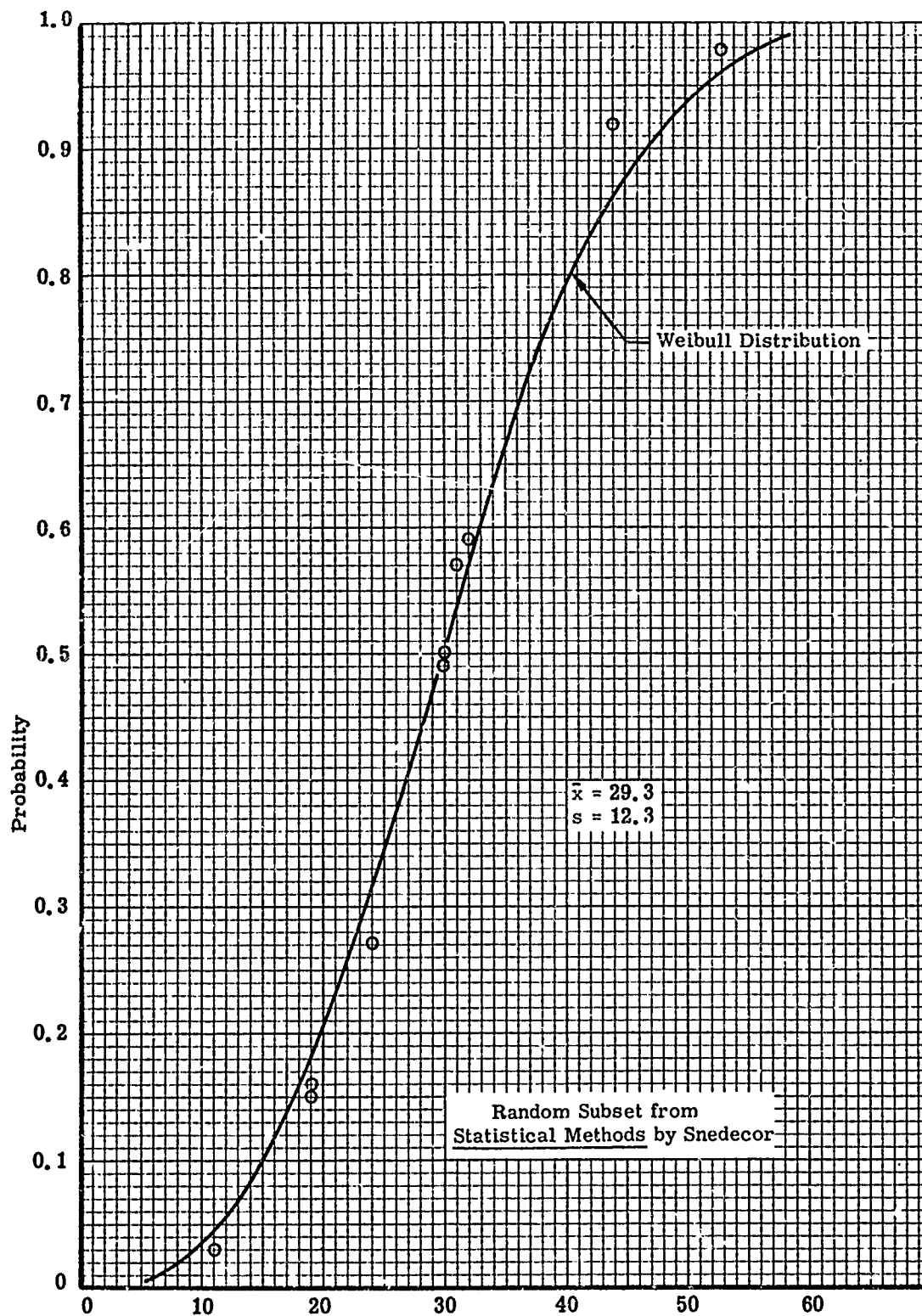
Figure 74. Random Subset No. 7 from Normally Distributed Population

124
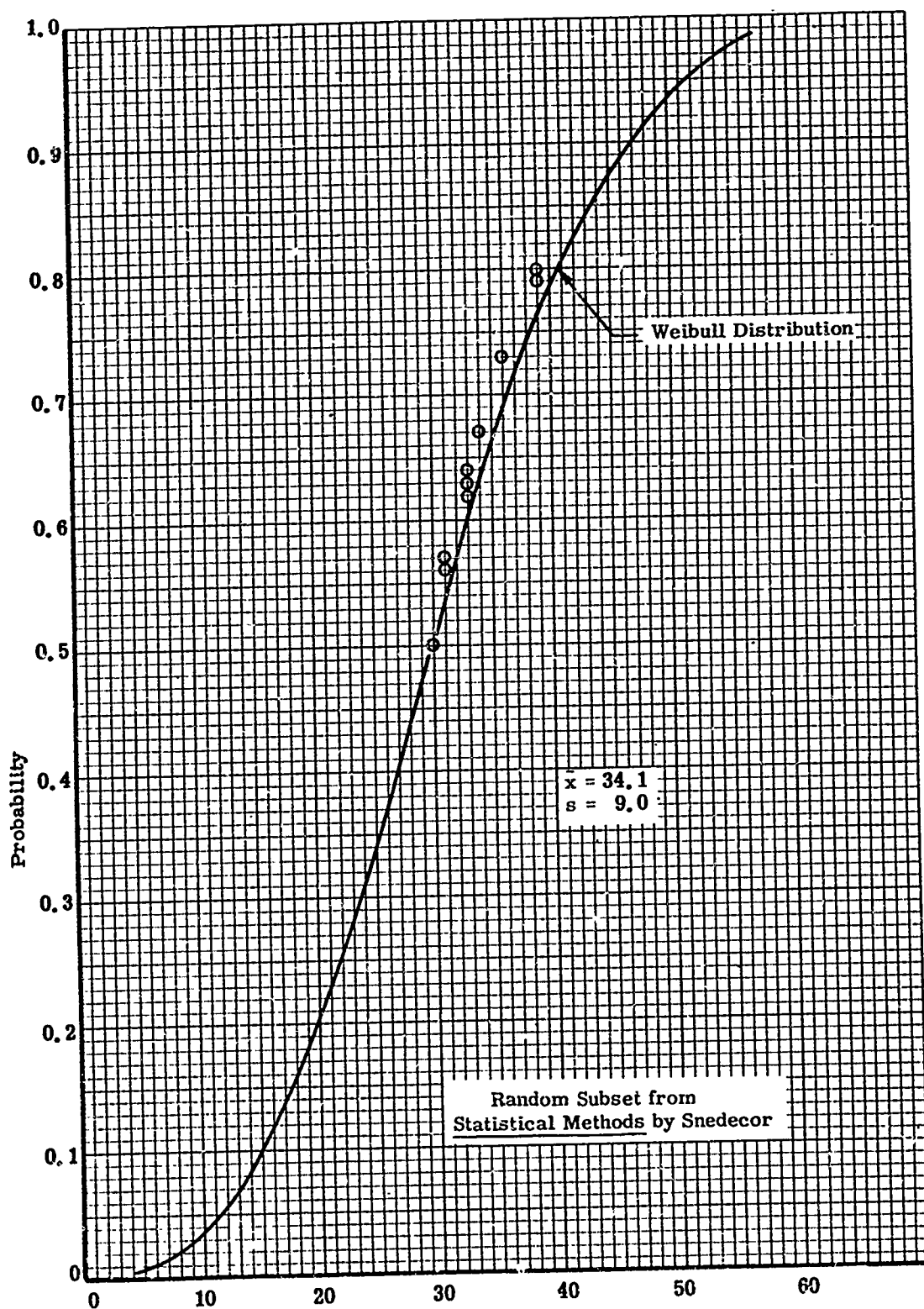
Figure 75. Random Subset No. 8 from Normally Distributed Population

125
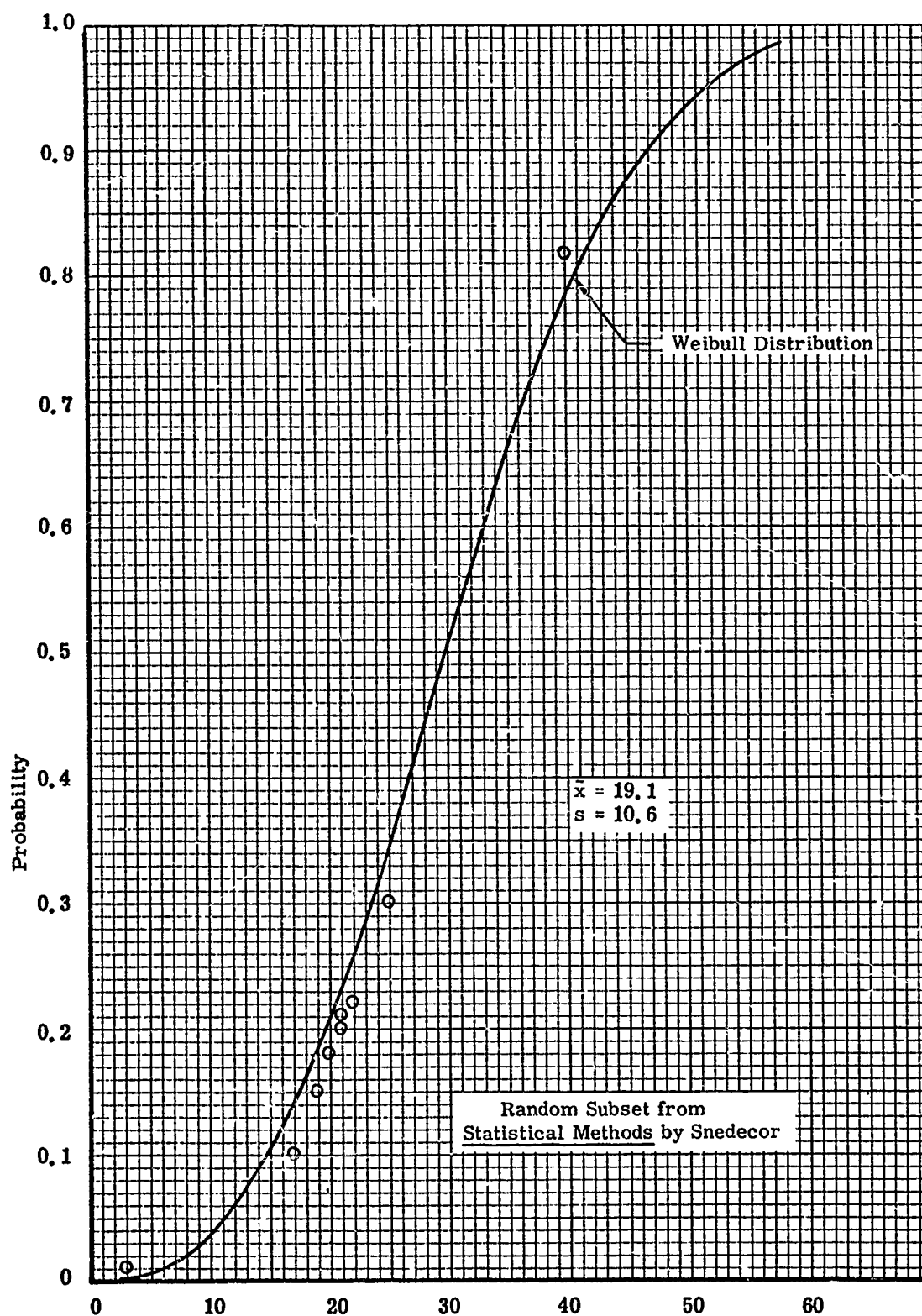
Figure 76. Random Subset No. 9 from Normally Distributed Population

126
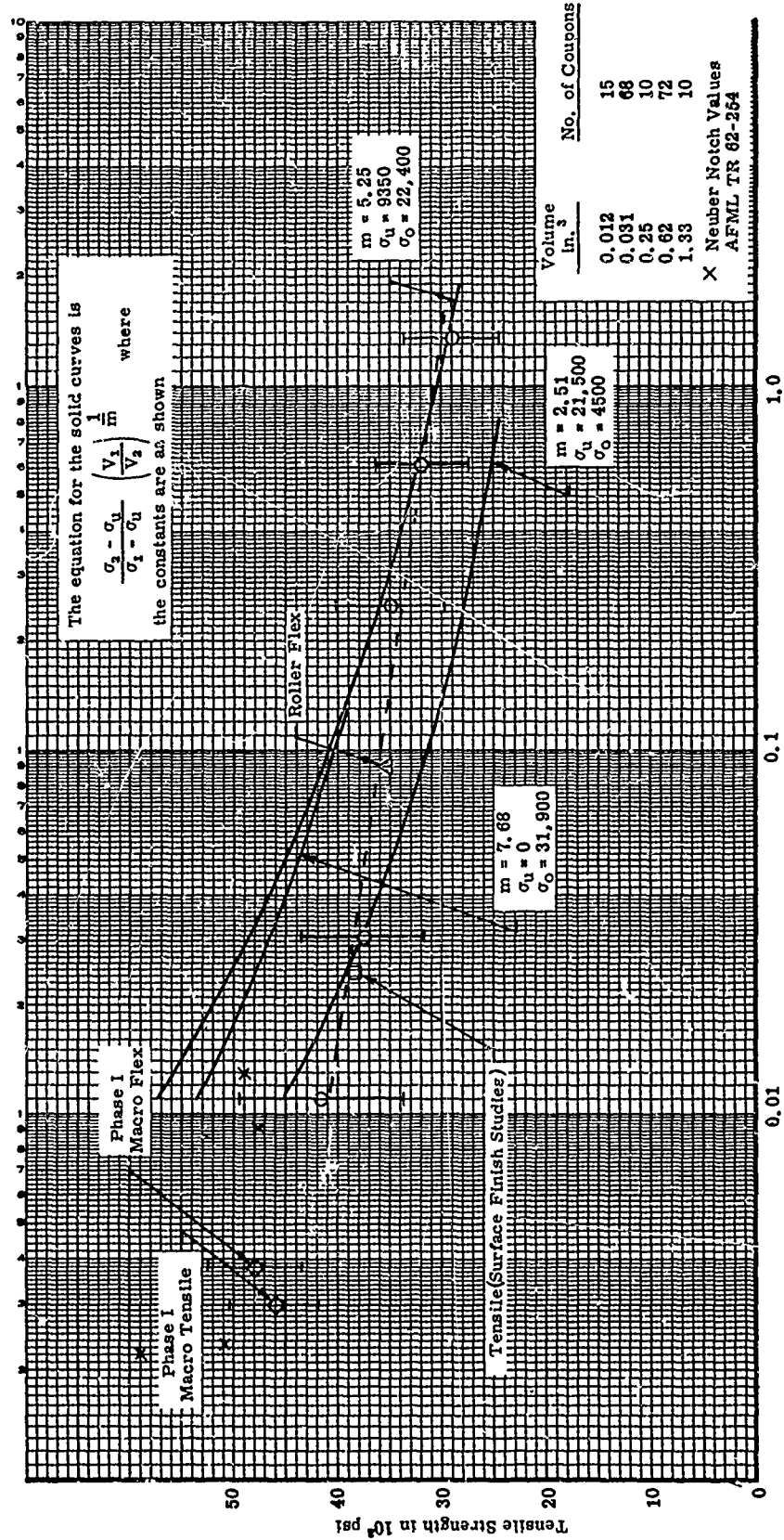
Figure 77. Average Ultimate Tensile Strength versus Volume, also Showing Standard Deviations, for the Culled Alumina Data from AFML-TR-66-228 and the Phase I Alumina Data on Macro Specimens

127

Figure 78. Flexural Specimen 1 of Table 10 (3A09-085-2F) Internal Longitudinal Profile, As Polished, 50X.
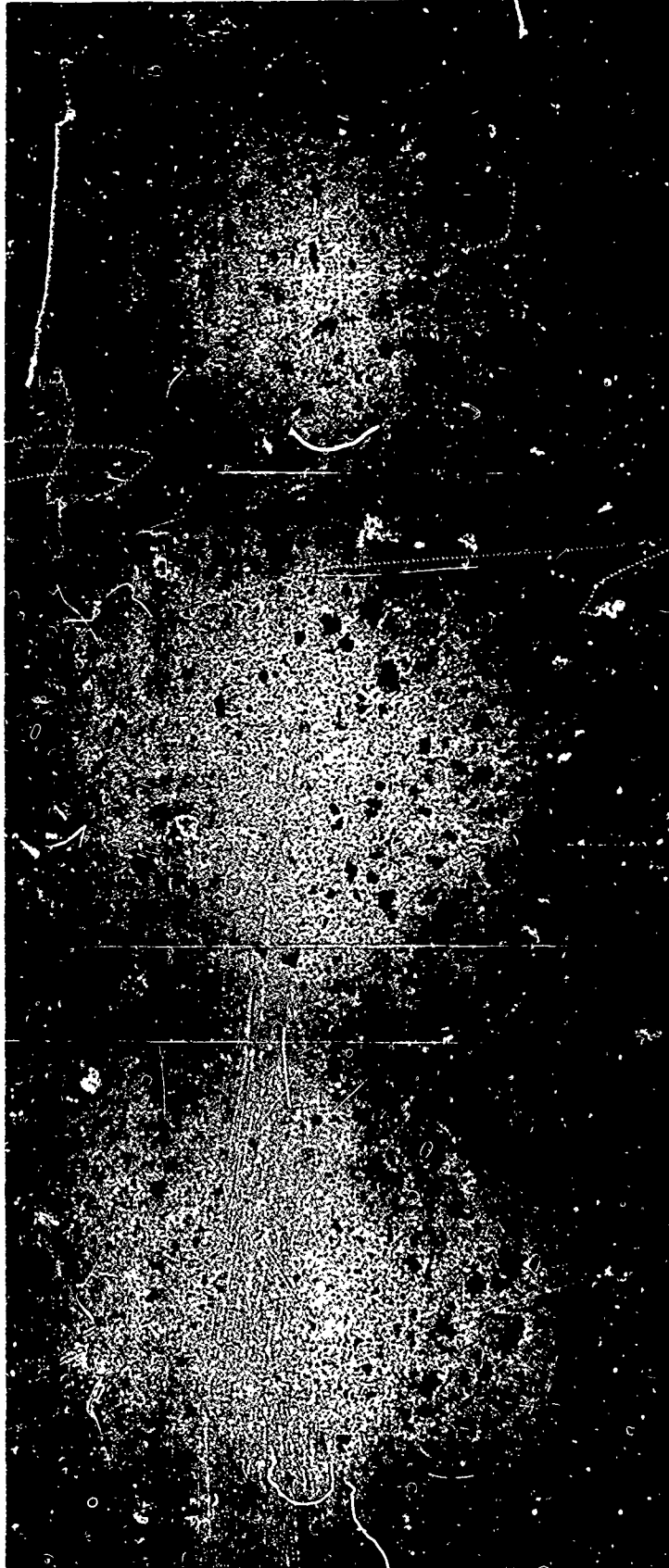
Figure 79. Flexural Specimen 2 of Table 10 (6A14-106-12F) Internal Longitudinal Profile, As Polished, 50X.

129
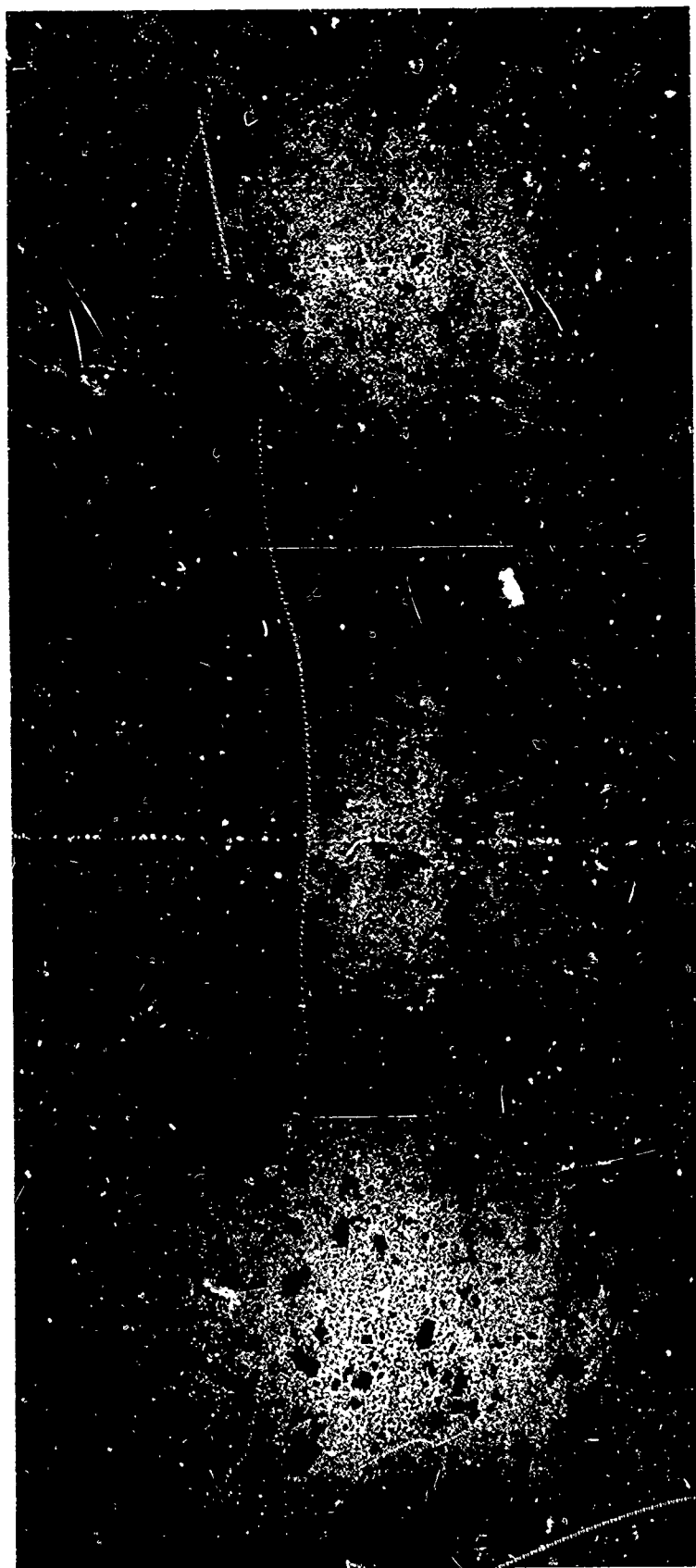
Figure 30.   Flexural Specimen 3 of Table 10 (6A14-104-7F) Internal Longitudinal Profile, As Polished, 50X.

130

Figure 81. Flexural Specimen 4 of Table 10 (5A13-102-6F) Internal Longitudinal Profile, As Polished, 50X.

Figure 82. Flexural Specimen 5 of Table 10 (2A12-096-12F) Internal Longitudinal Profile, As Polished, 50X.
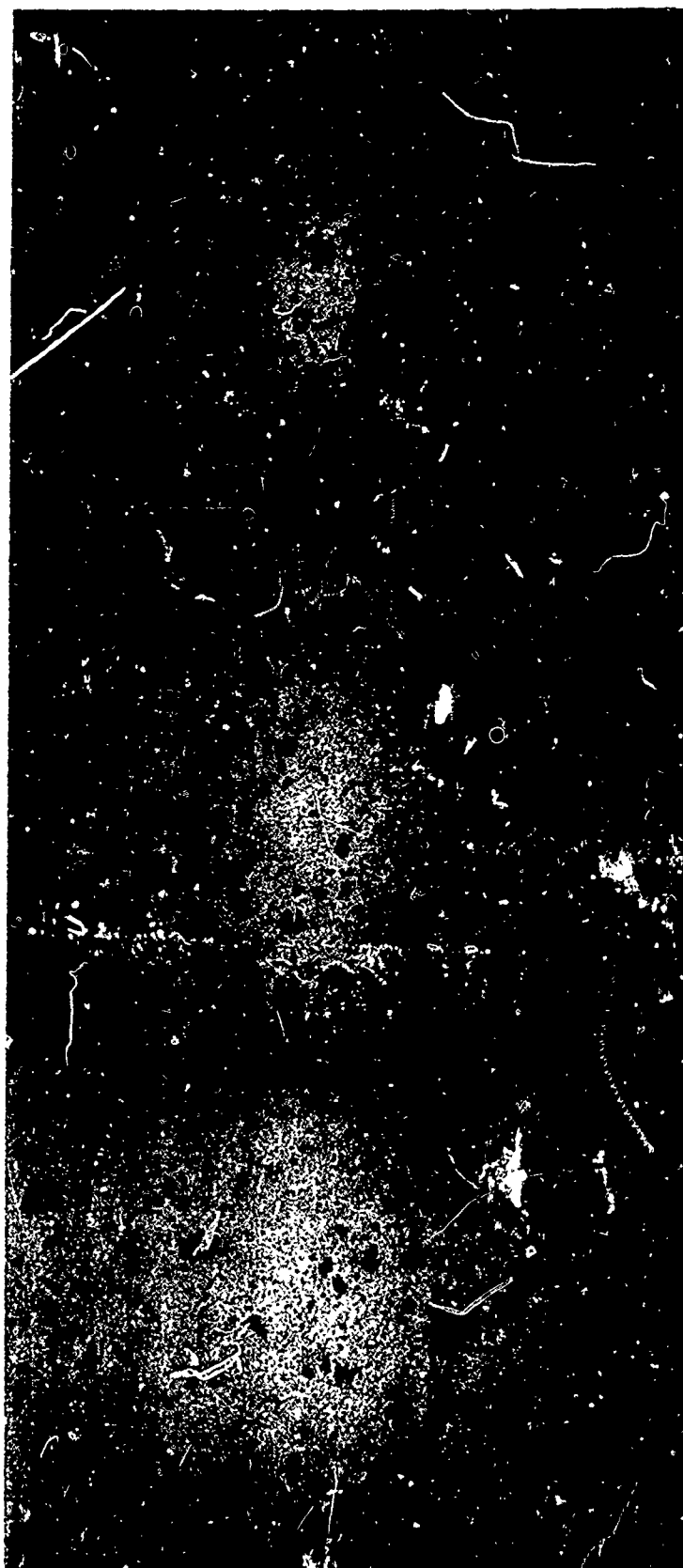
Figure 83. Flexural Specimen 6 of Table 10 (3A09-085-1F) Internal Longitudinal Profile, As Polished, 50X.

133

Figure 84. Flexural Specimen 7 of Table 10 (4A11-089-1F) Internal Longitudinal Profile, As Polished, 50X.

134
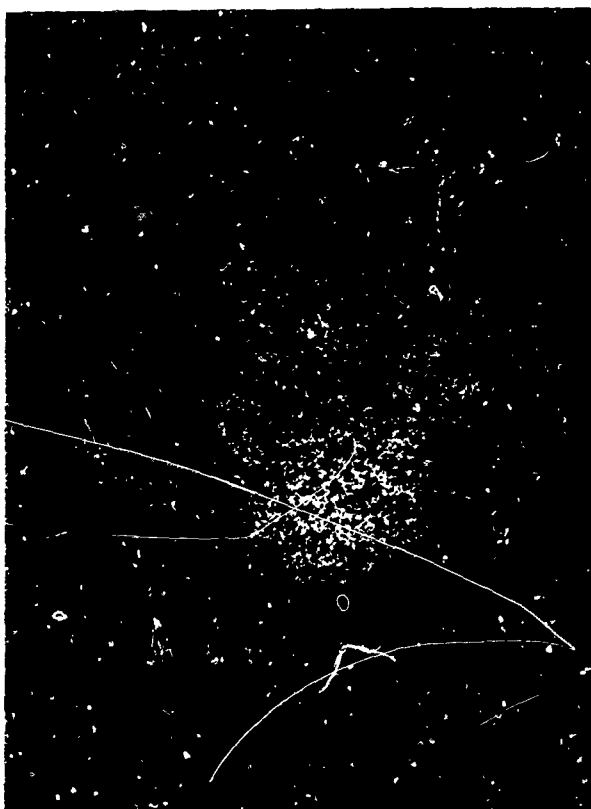
Figure 85a

Tensile Specimen 1 of Table 10
(5A13-101-4T) Transverse Section
at Fracture, As Polished, 50X.
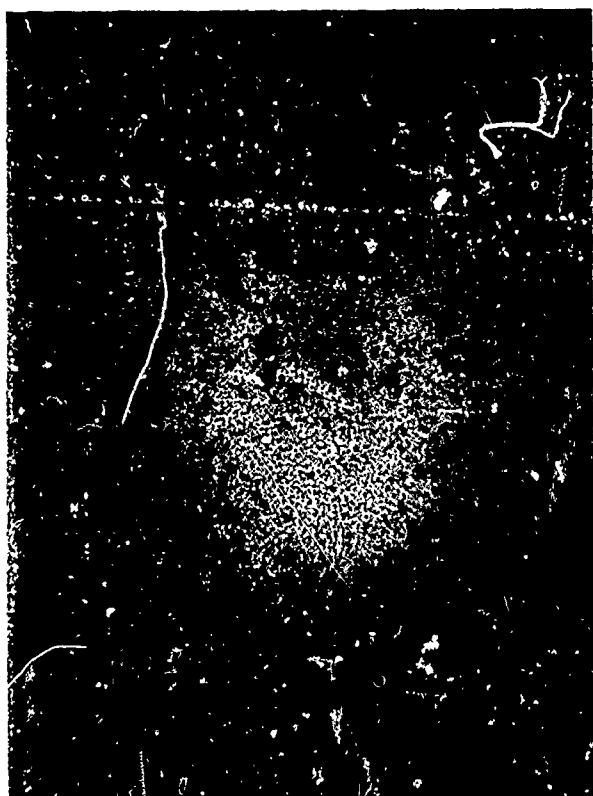
Figure 85b

Tensile Specimen 2 of Table 10
(2A12-095-3T) Transverse Section
at Fracture, As Polished, 50X.

(Large black areas-carbon film)

135
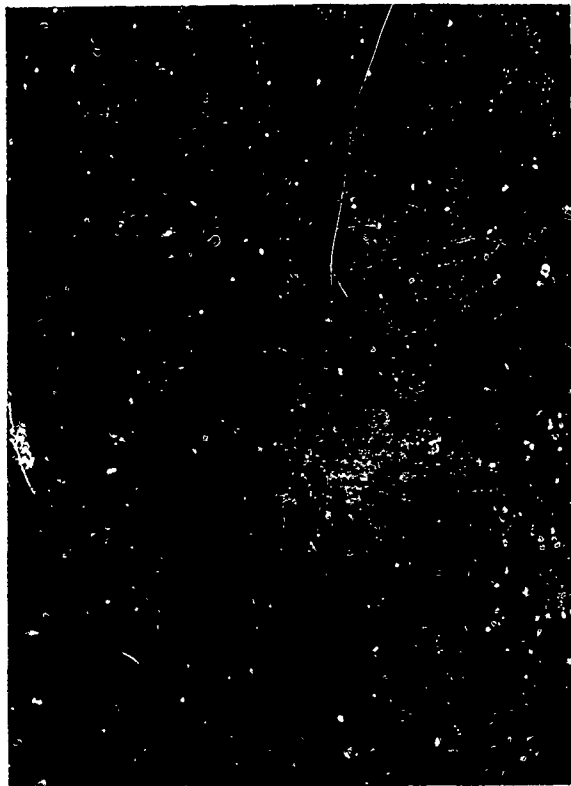
Figure 86a

Tensile Specimen 3 of Table 10
(2A05-047-2T) Transverse Section
at Fracture, As Polished, 50X.
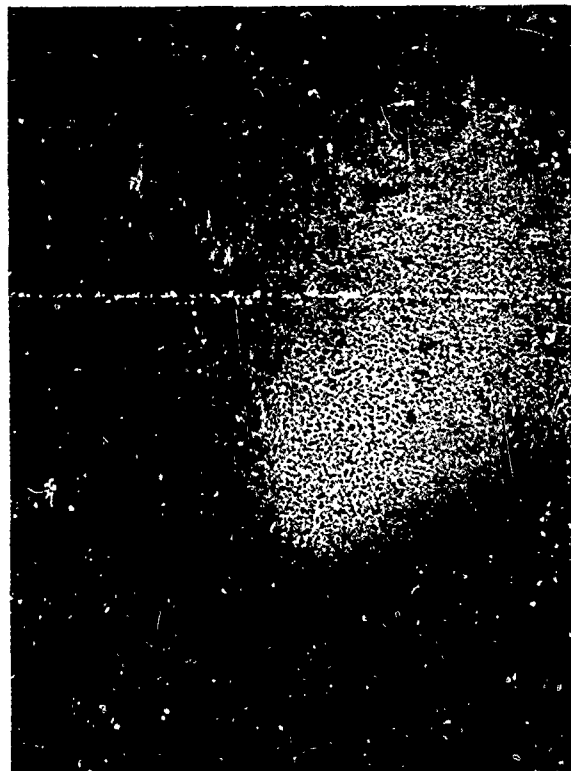
Figure 86b

Tensile Specimen 4 of Table 10
(2A05-047-1T) Transverse Section
at Fracture, As Polished, 50X.
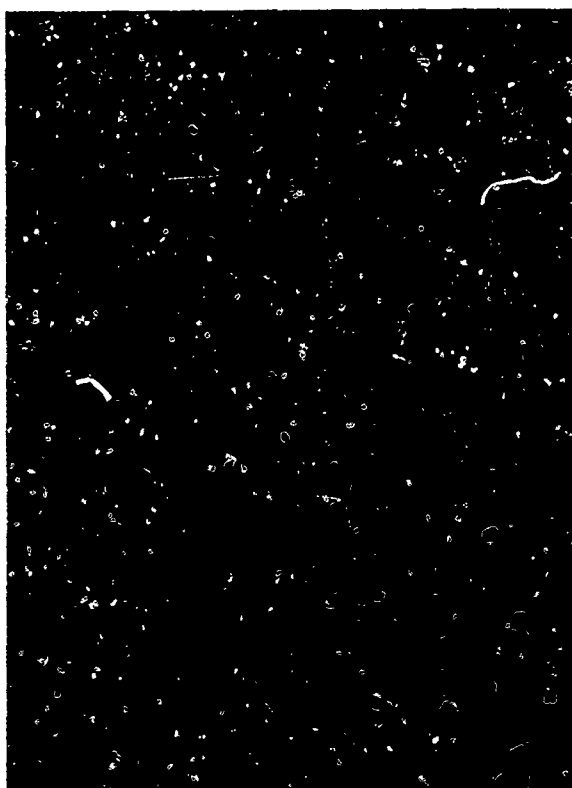
Figure 87a

Tensile Specimen 5 of Table 10
(4A11-089C-2T) Transverse Section
at Fracture, As Polished, 50X.
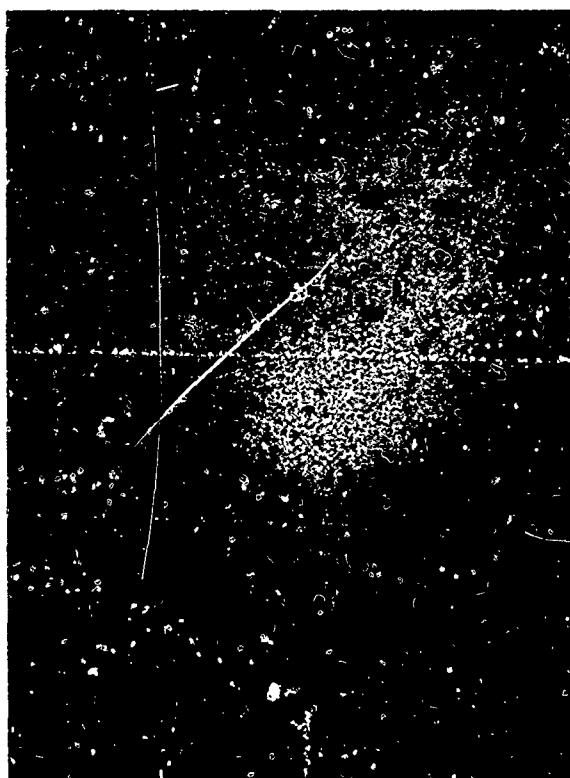
Figure 87b

Tensile Specimen 6 of Table 10
(3A09-085-2T) Transverse Section
at Fracture, As Polished, 50X.

Figure 88a

Tensile Specimen 7 of Table 10
(3A10-087-2T) Transverse Section
at Fracture, As Polished, 50X.
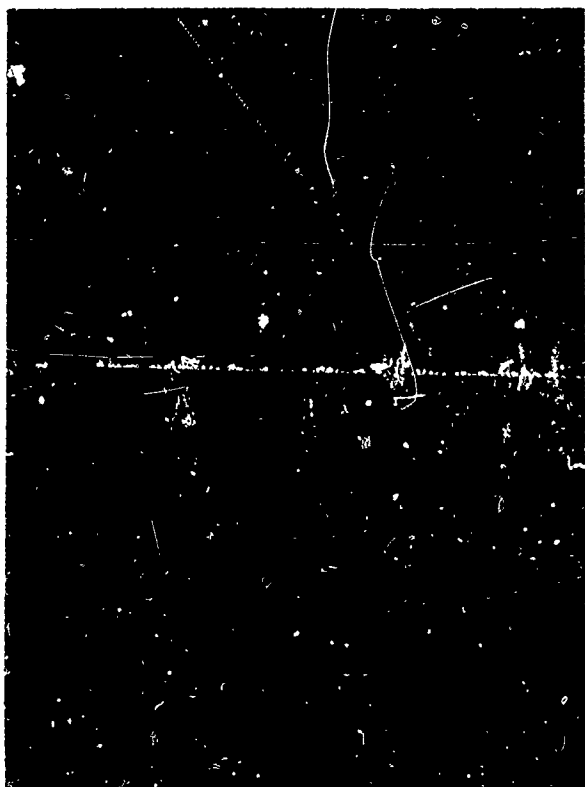
Figure 88b

Tensile Specimen 8 of Table 10
(4A11-089A-6T) Transverse Section
at Fracture, As Polished, 50X.

138

Frequency
Table 10

Pore Area in sq mils	Flexural Specimen Number			
	1	4	6	7
1-2	68	133	66	112
2-3	15	42	12	34
3-4	5	12	4	13
4-5	0	3	0	3
5-6		1		5
6-7		1		0
7-8		0		1
8-9				0
9-10				0
10-11				1
11-12				0
12-13				1

□ Specimen 4 50,000
■ Specimen 7 38,000

○ Specimen 1 52,000
● Specimen 6 35,000
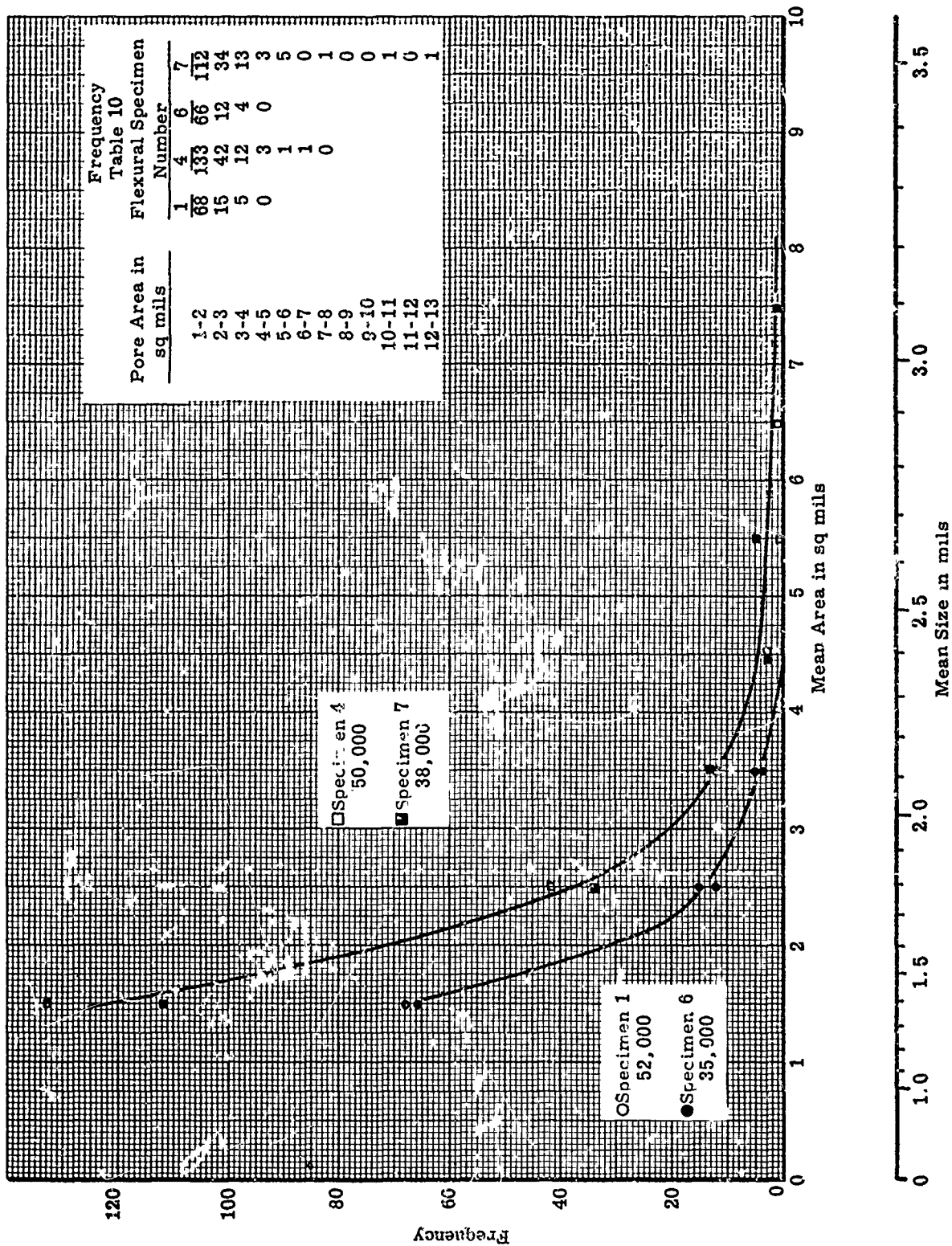
Figure 89 - Pore Size Distribution for Specific Flexural Macro Specimens of Table 10
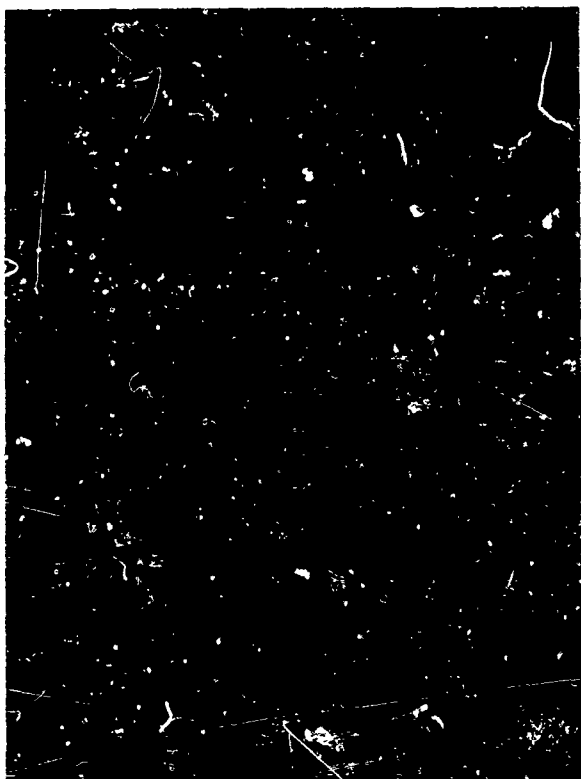
Figure 90a

Flexural Specimen 1 of Table 10
(3A09-085-2F) Internal Longitudinal
Profile, As Polished, Position 2, 500X.
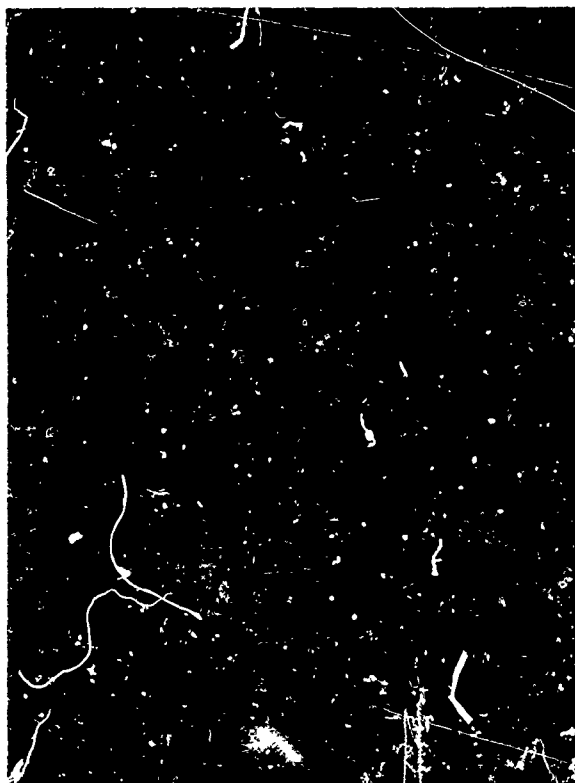
Figure 90b

Flexural Specimen 2 of Table 10
(6A14-106-12F) Internal Longitudinal
Profile, As Polished, Position 2, 500X.

Figure 91b

Flexural Specimen 4 of Table 10
(5A13-102-6F) Internal Longitudinal
Profile, As Polished, Position 2, 500X.
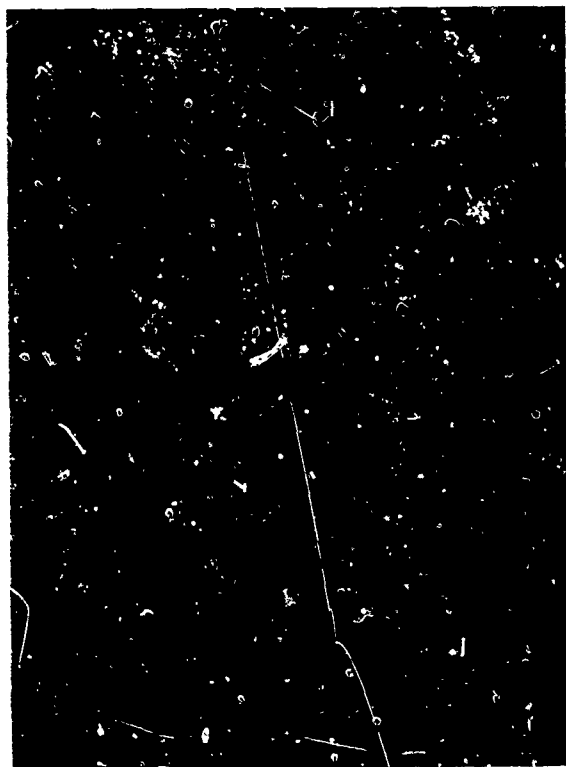
Figure 91a

Flexural Specimen 3 of Table 10
(3A09-085-2F) Internal Longitudinal
Profile, As Polished, Position 2, 500X.

Figure 92a

Flexural Specimen 5 of Table 10
(2A12-096-11F) Internal Longitudinal
Profile, As Polished, Position 2, 500X.
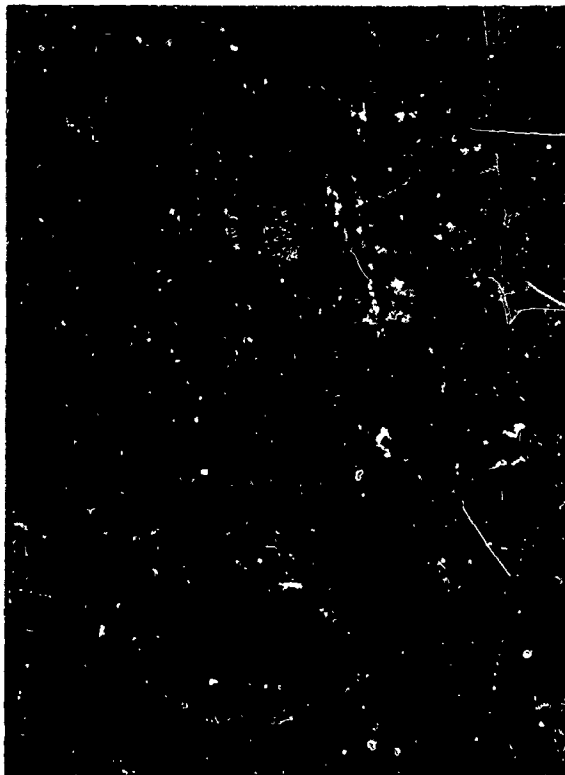
Figure 92b

Flexural Specimen 6 of Table 10
(3A09-085-1F) Internal Longitudinal
Profile, As Polished, Position 1, 500X.

142
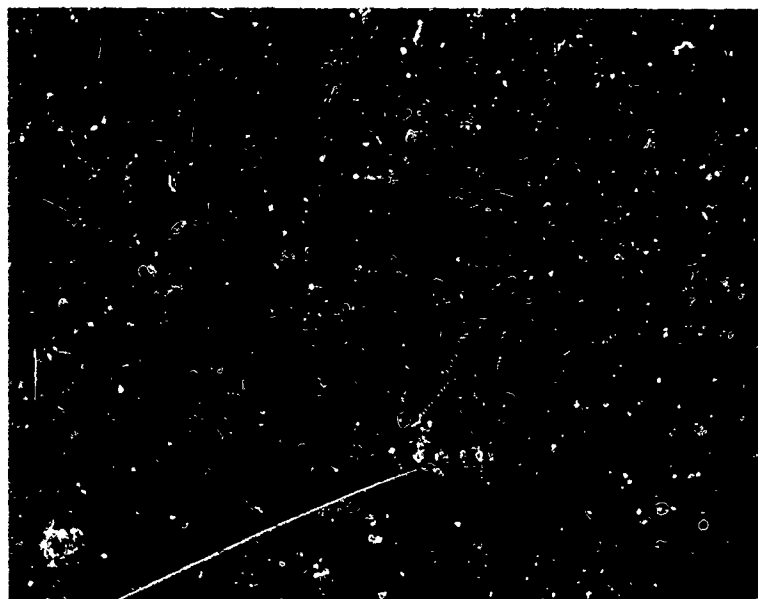
Figure 93. Flexural Specimen 7 of Table 10 (4A11-089D-1F) Internal
Longitudinal Profile, As Polished, Position 3, 500X.

143

Figure 94a

Flexural Specimen 2 of Table 10
(6A14-106-12F) Internal Longitudinal
Profile, H_3PO_4 Etch at 150°C, Position 2,
800X.
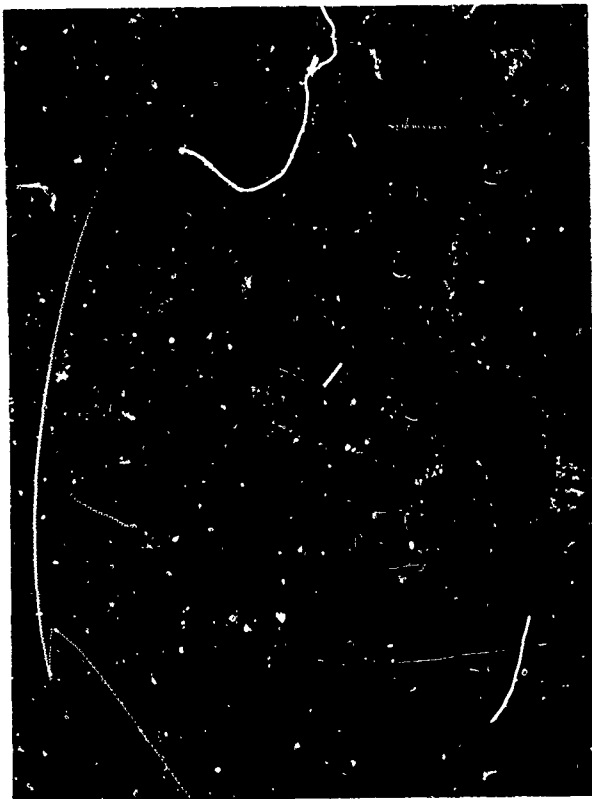
Figure 94b

Flexural Specimen 3 of Table 10
(6A14-104-7F) Internal Longitudinal
Profile, H_3PO_4 Etch at 150°C, Position 2,
800X.

144
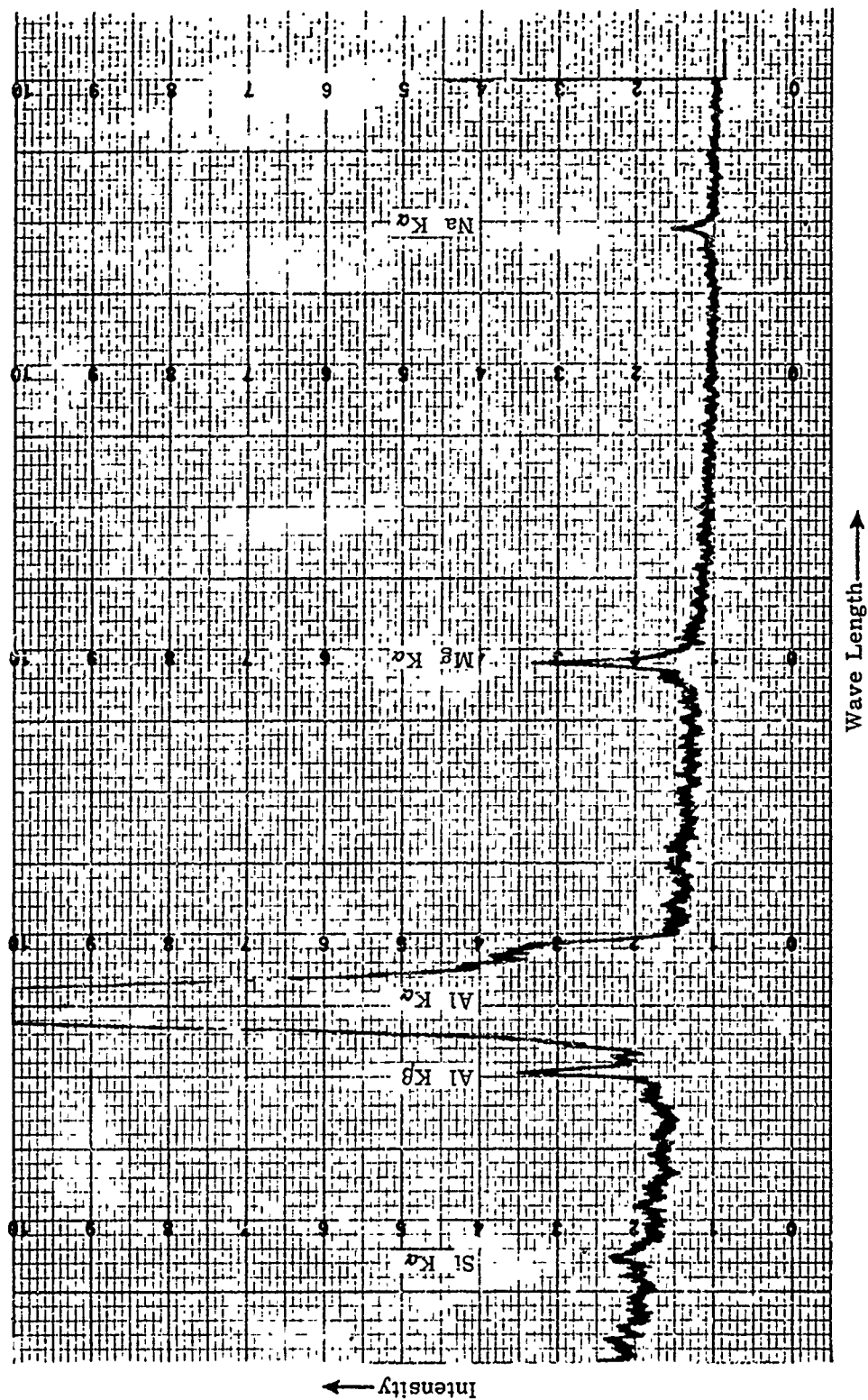
Figure 95. Microprobe Stationary Beam Spectral Scan Beam Focused on "Second Phase", Flexural Specimen 6 of Table 10 (3A09-085-1F), Relief Polished

145
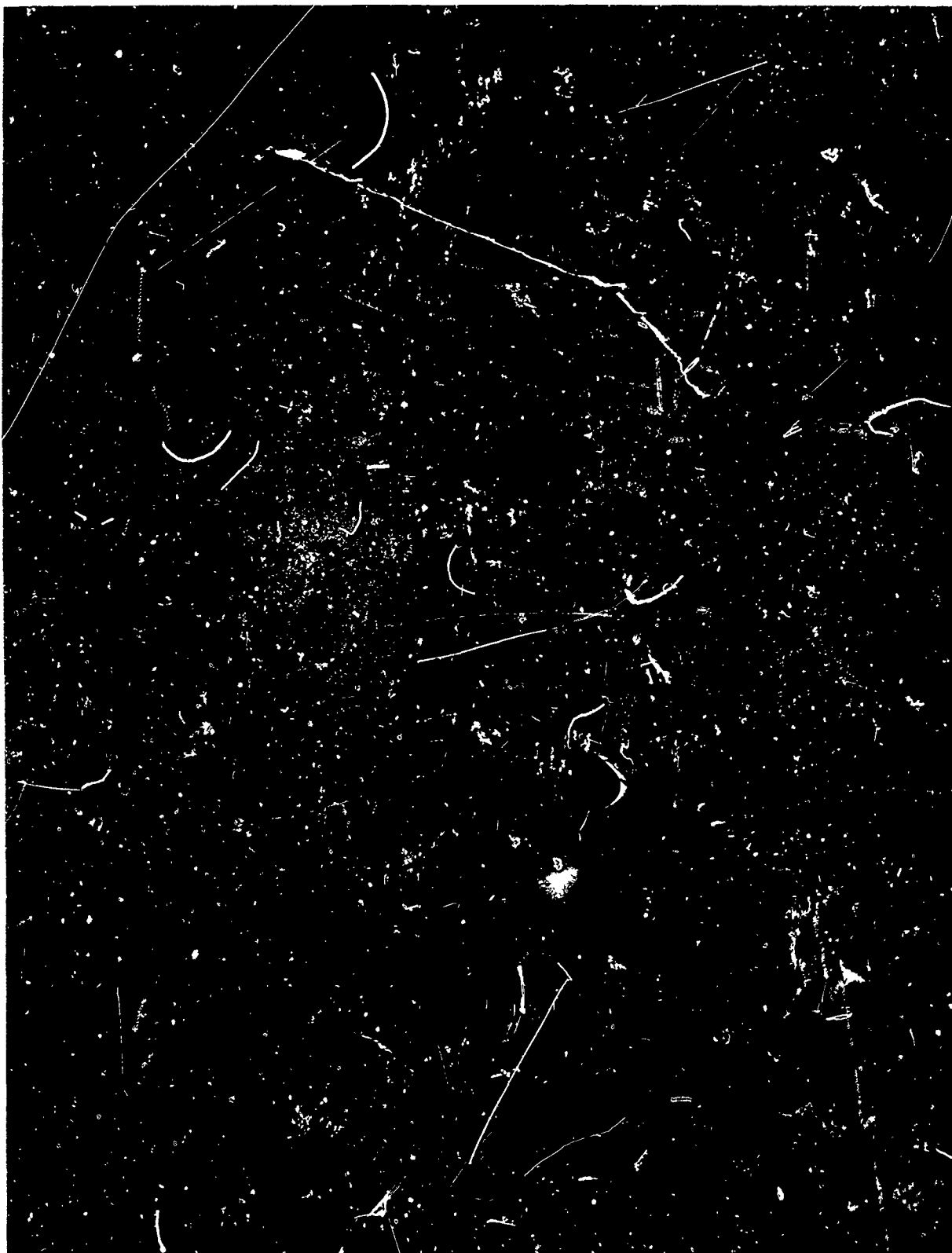
Figure 96. Tensile Specimen 3, Table 10 (2A05-047-2T) Two stage replication, Specimen polished and etched at 150°C with H_3PO_4
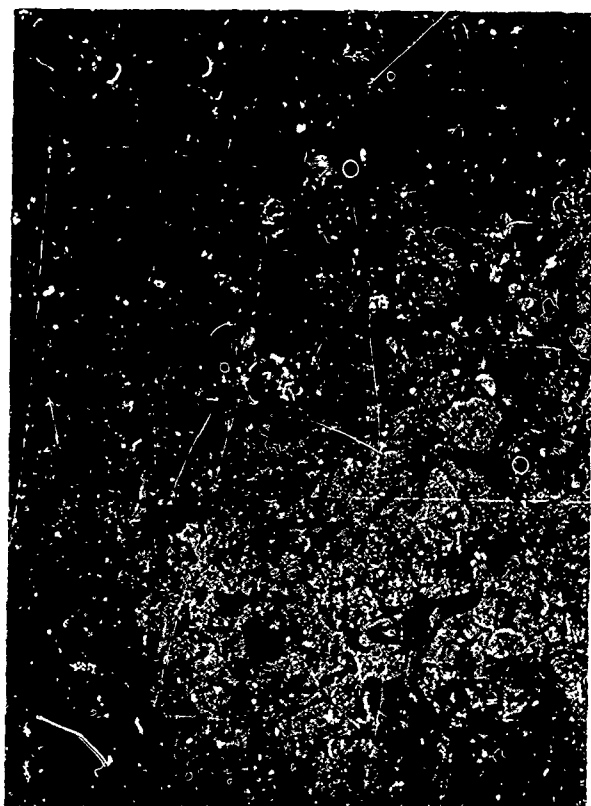
Figure 97a

Flexural Specimen 4 of Table 10
(5A13-102-6F) Internal Longitudinal
Profile, H_3PO_4Etch at 250°C, Position 2,
800X.
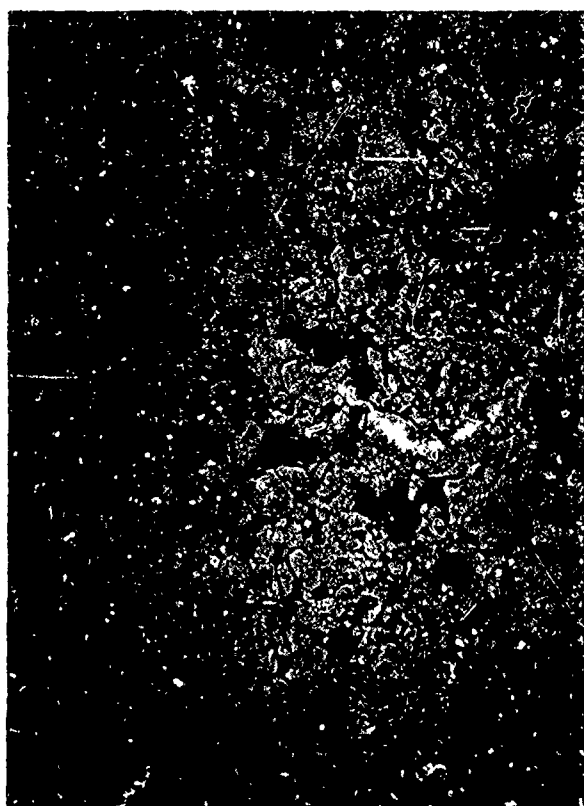
Figure 97b

Flexural Specimen 6 of Table 10
(3A09-085-1F) Internal Longitudinal
Profile, H_3PO_4Etch at 250°C, Position 2
800X.

Figure 98a

Flexural Specimen 1 of Table 10
(3A09-085-2F), 50X External Profile,
Compression Region at Top.
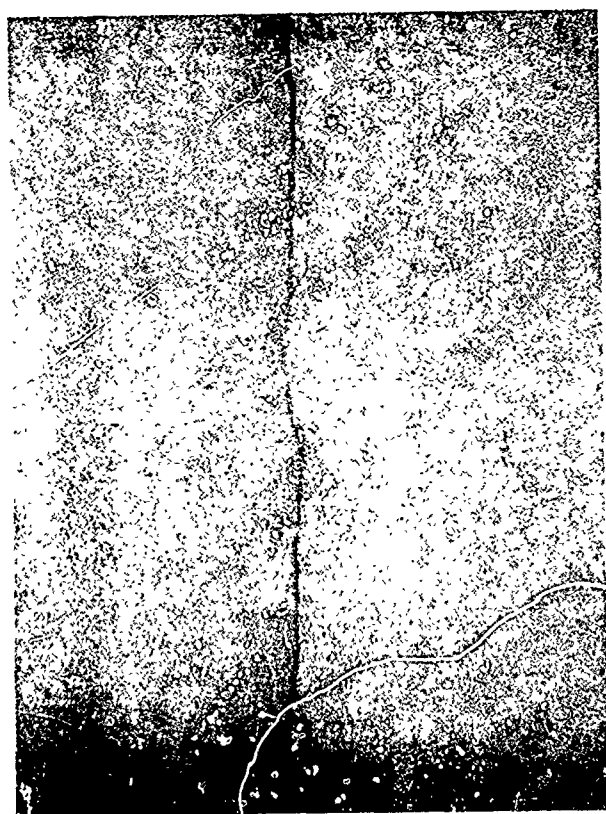
Figure 98b

Flexural Specimen 6 of Table 10
(3A09-085-1F), 50X External Profile,
Compression Region at Top.
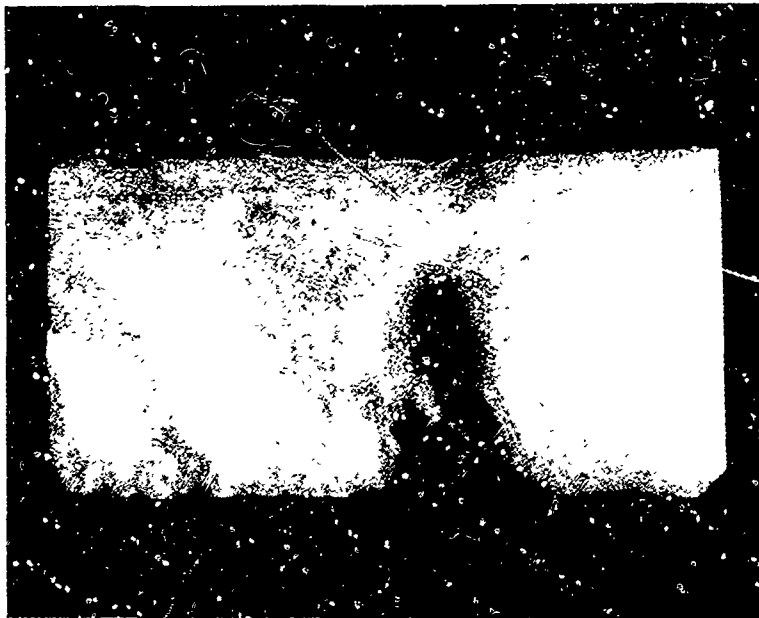
Figure 99a

Flexural Specimen 1 of
Table 10 (3A09-085-2F),
20X Fracture Face,
Compression Region at Top.
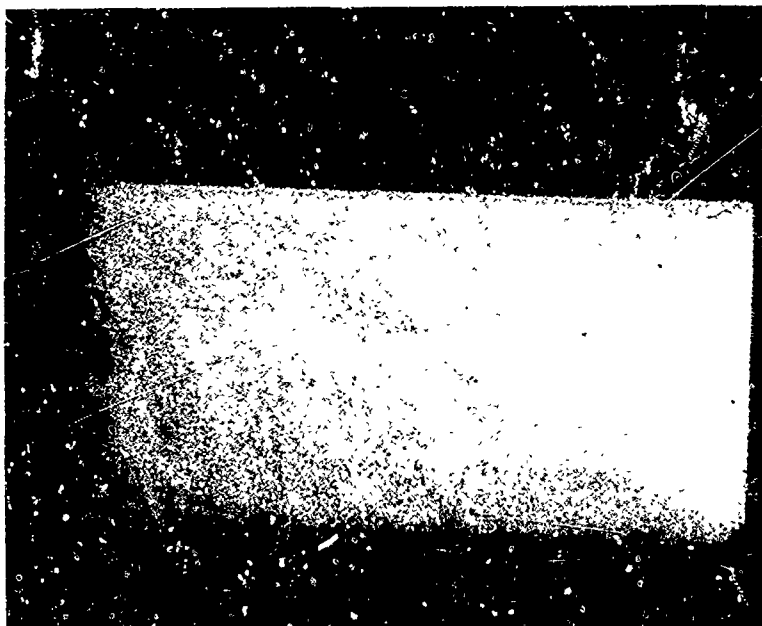
Figure 99b

Flexural Specimen 6 of
Table 10 (3A09-085-1F),
20X Fracture Face,
Compression Region at Top.

Figure 100. Electron Fractograph of Flexural Specimen 1 of Table 10 (3A09-085-2F)

150

Figure 101. Electron Fractograph of Flexural Specimen 1 of Table 10 (3A09-085-2F)

Figure 102. Electron Fractograph of Flexural Specimen 6 of Table 10 (3A09-085-1F)

152
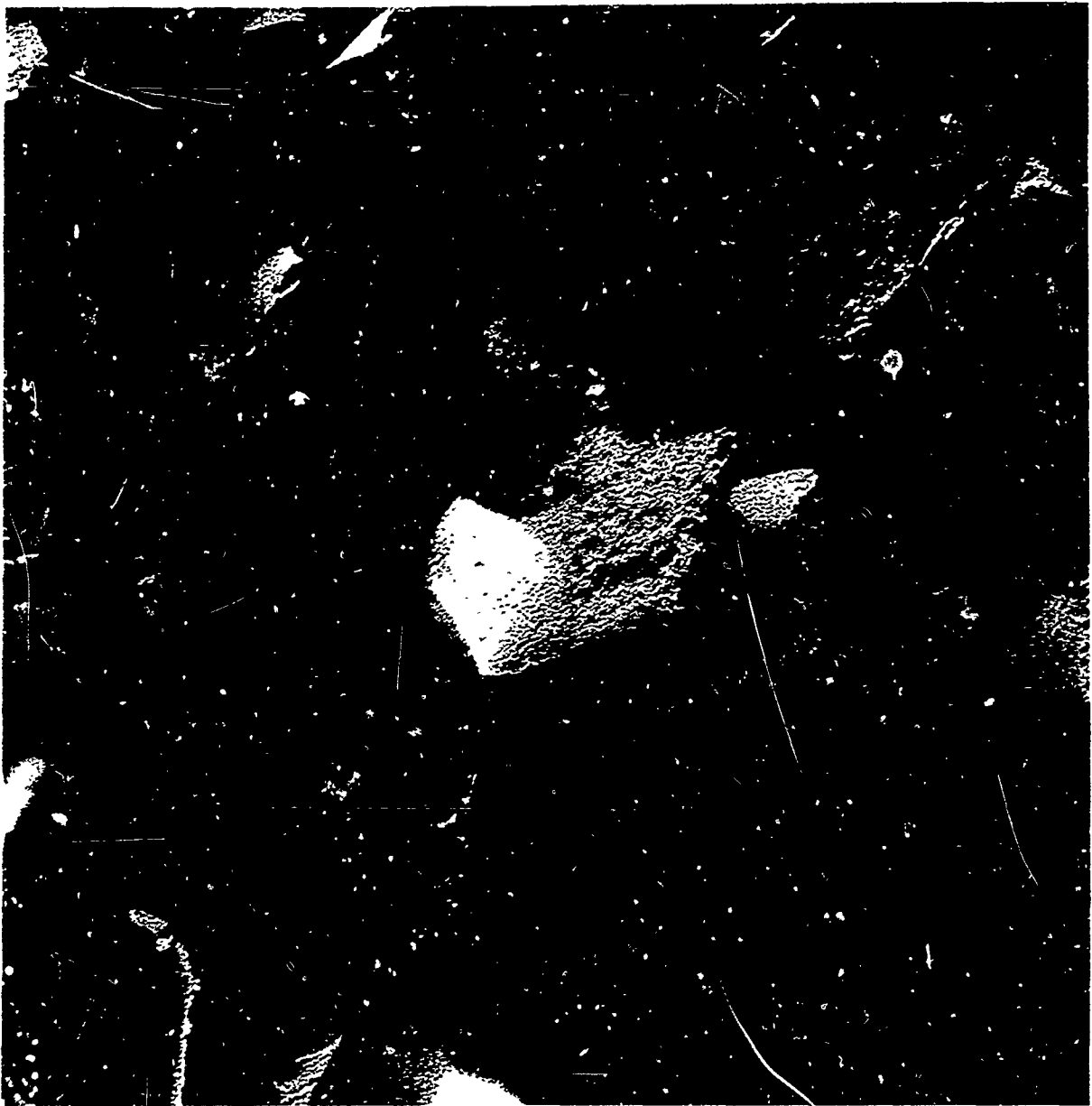
Figure 103. Electron Fractograph of Flexural Specimen 6 of Table 10 (3A09-085-1F)
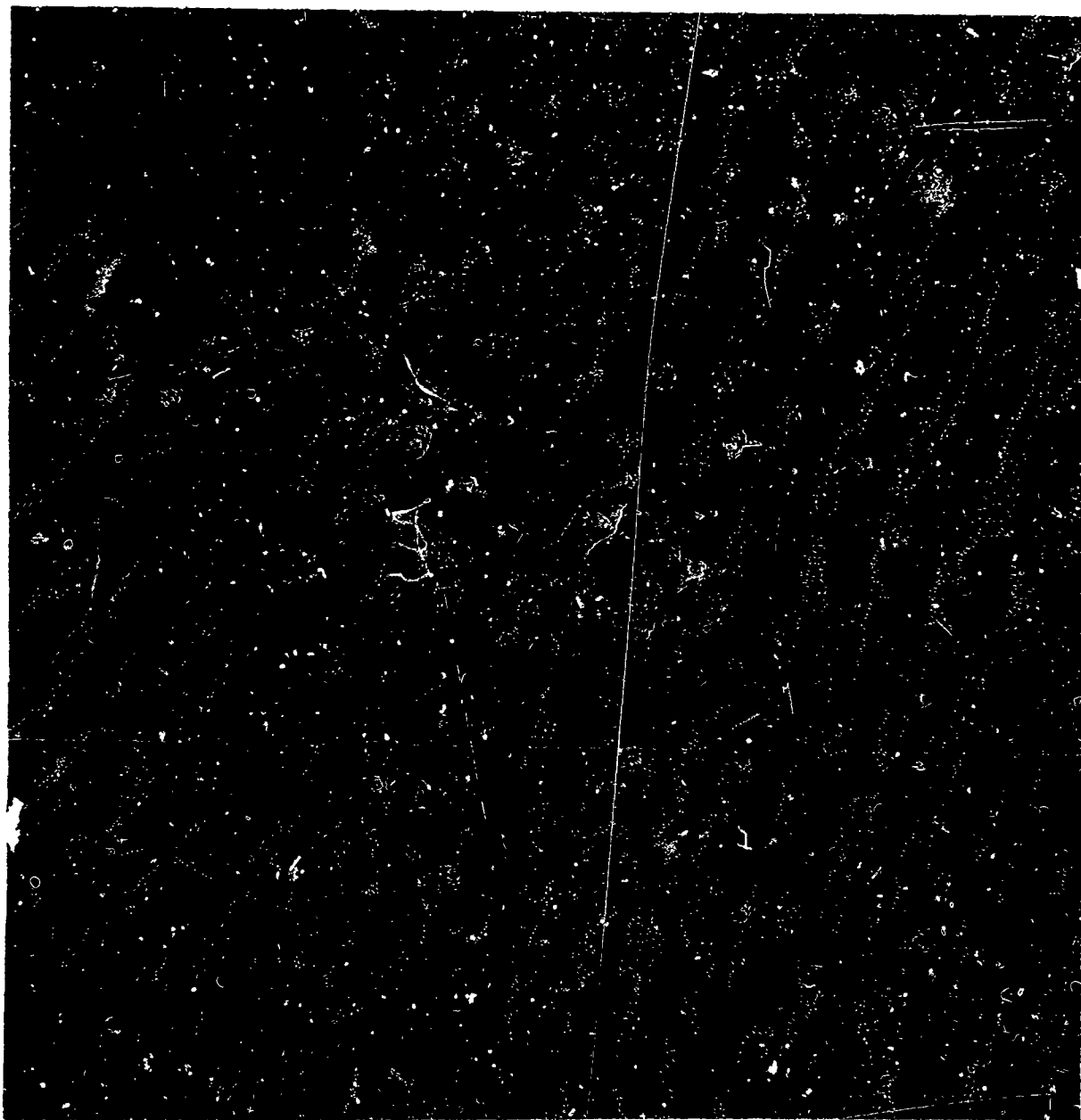
Figure 104. Electron Fractograph of Flexural Specimen 4 of Table 10 (5A13-102-6F) Compression Zone

Figure 105. Electron Fractograph of Flexural Specimen 5 of Table 10 (2A12-096-11F) Com ression Zone

155

Figure 106.   Electron Fractograph of Flexural Specimen 4 of Table 10 (5A13-102-6F)
Tension Zone.

156
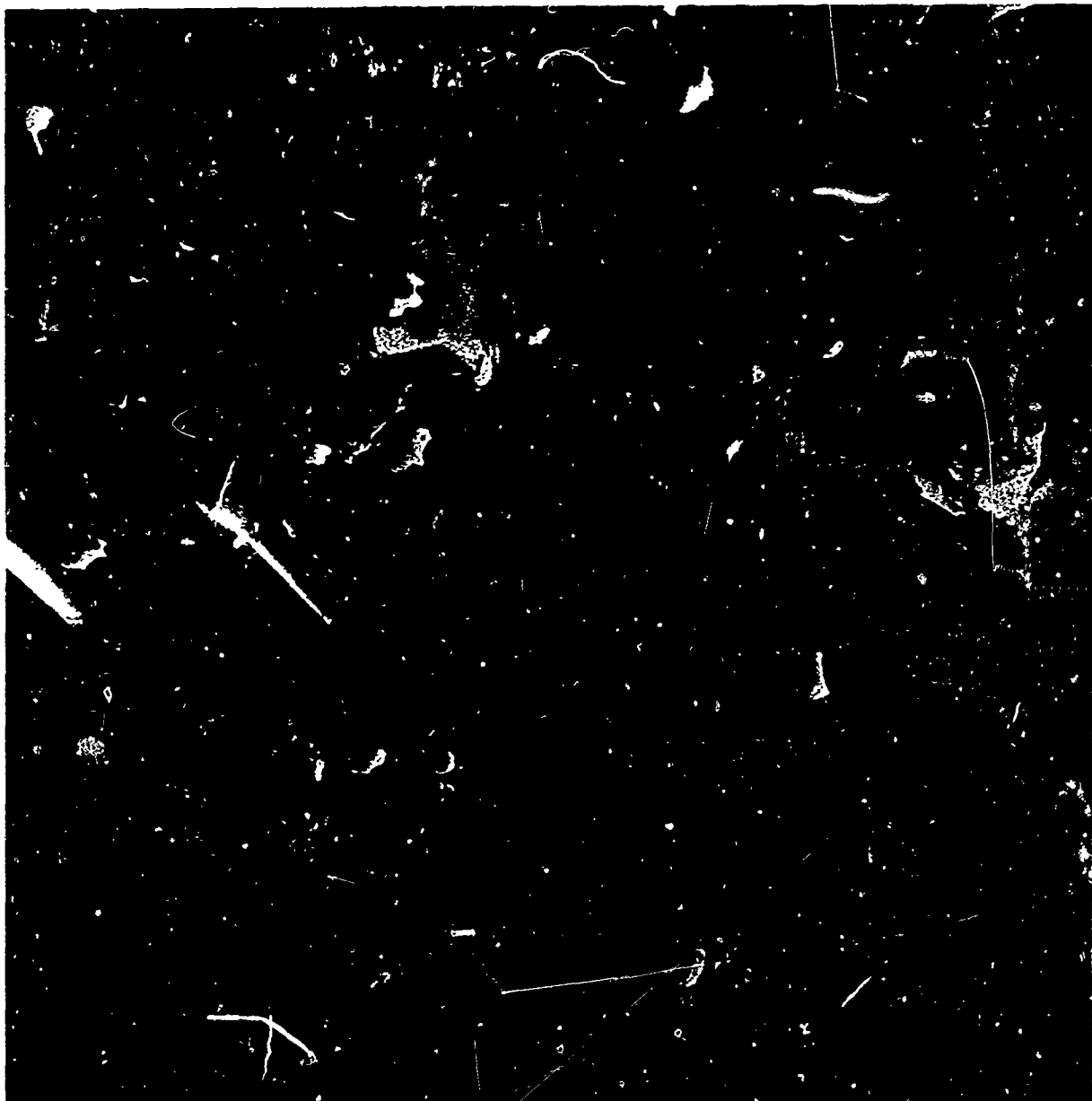
Figure 107. Electron Fractograph of Flexural Specimen 5 of Table 10 (2A12-096-11F) Tension Zone.
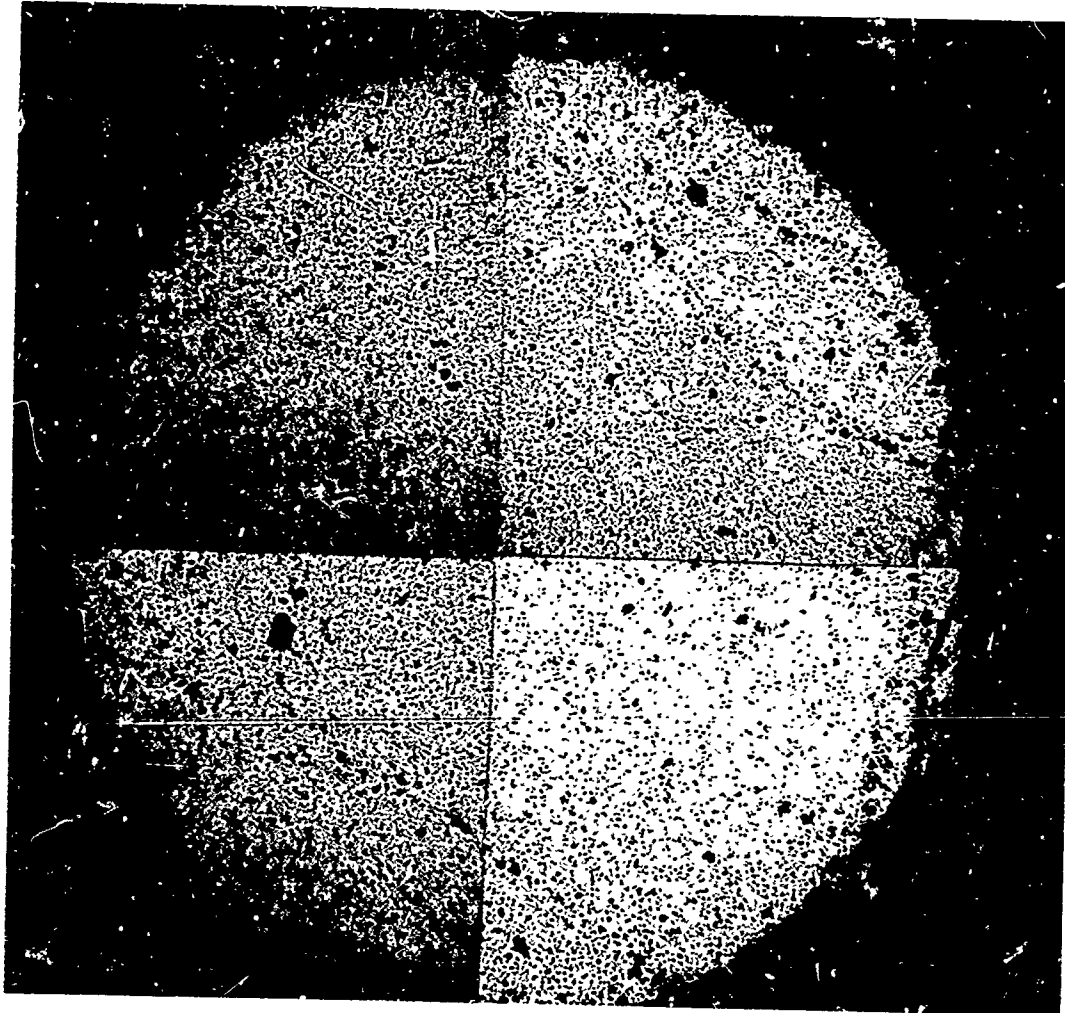
Figure 108. Tensile Specimen 3 of Table 10 (2A05-047-2T) Cross-section at Fracture, As Polished, 60X.
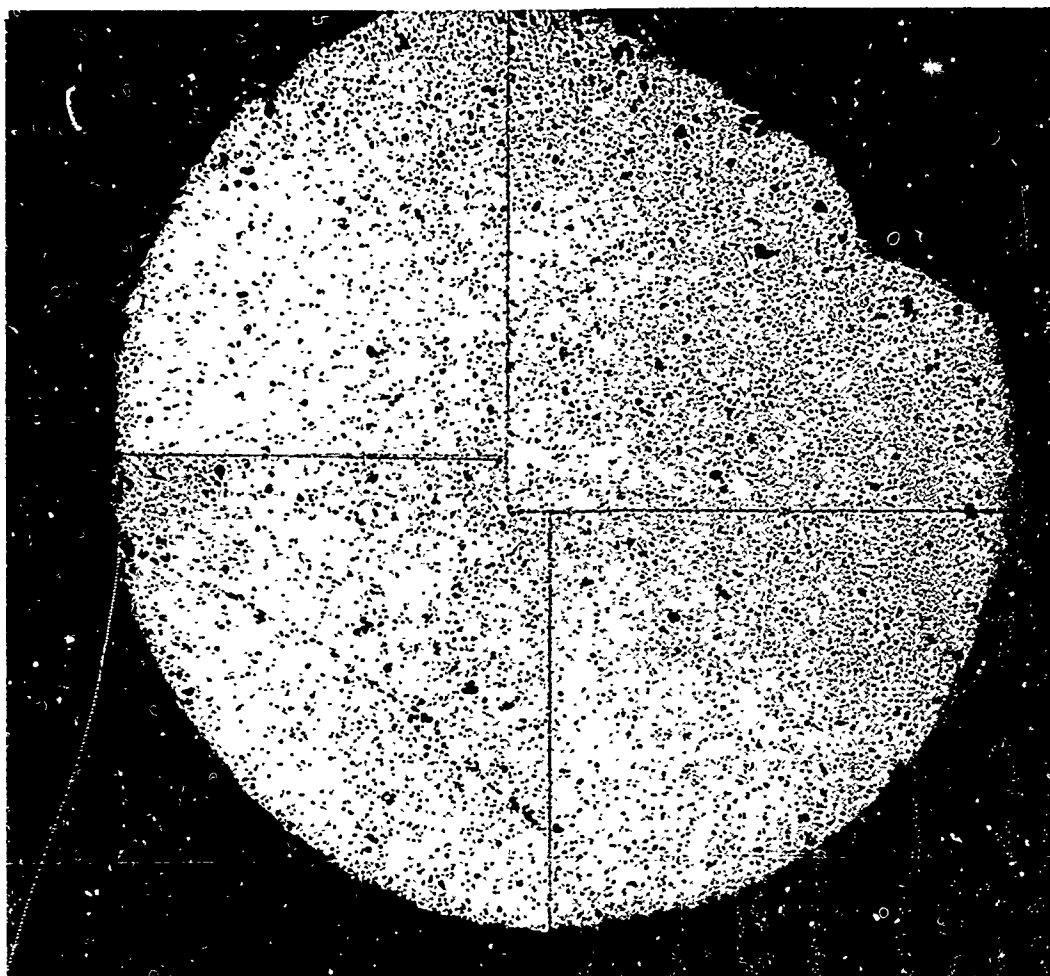
Figure 109. Tensile Specimen 4 of Table 10 (2A05-047-1T) Cross-section at Fracture, As Polished, 60X.

Figure 110a

Tensile Specimen 3 of Table 10
(2A05-047-2T) Cross-section at
Fracture, As Polished, 250X.
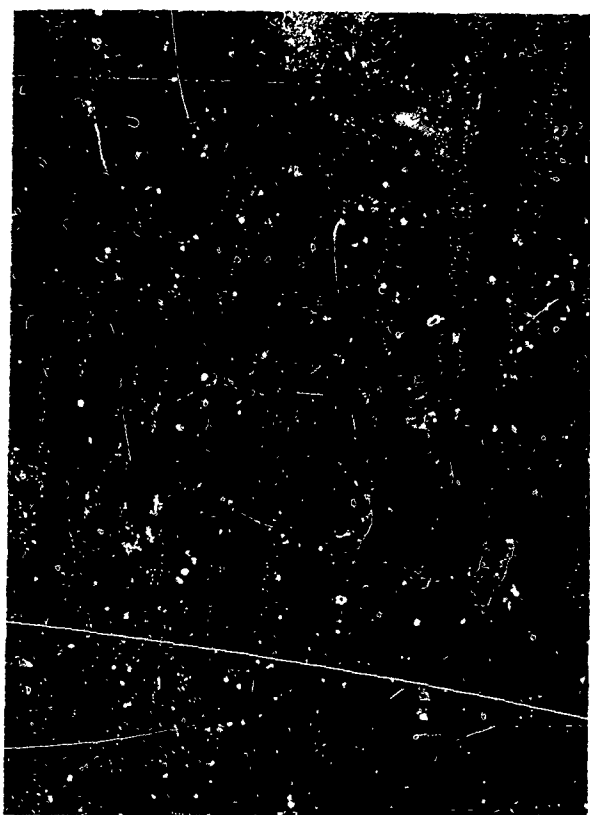
Figure 110b

Tensile Specimen 4 of Table 10
(2A05-047-1T) Cross-section at
Fracture, As Polished, 250X.
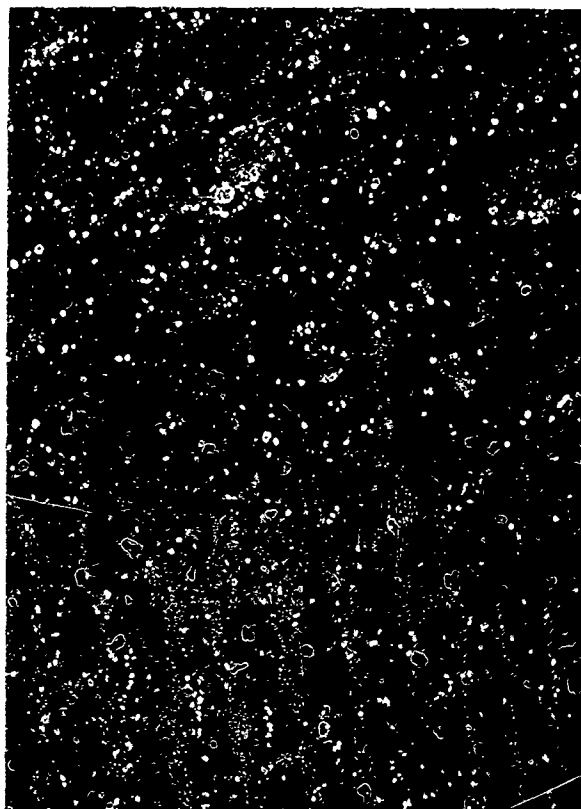
Figure 111a

Tensile Specimen 3 of Table 10
(2A05-047-2T) Cross-section at
Fracture, H_3PO_4 Etch at 150°C,
250X.
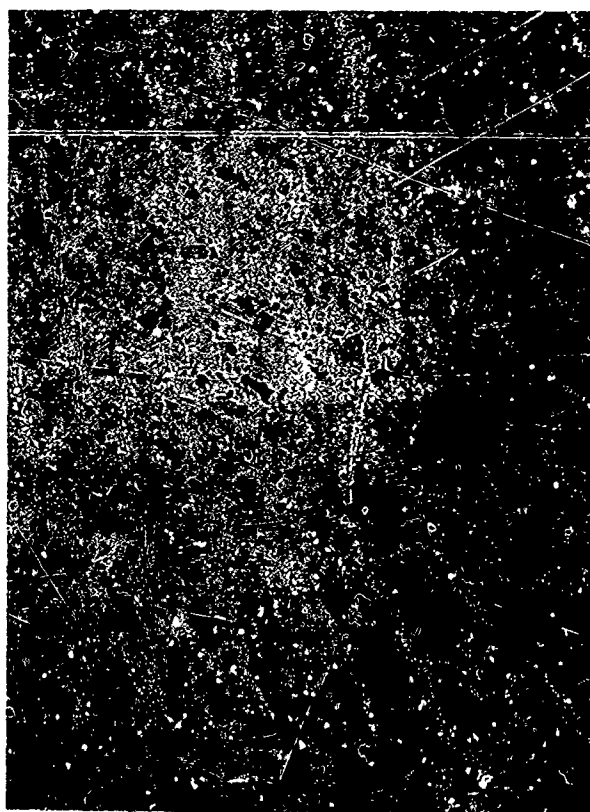
Figure 111b

Tensile Specimen 4 of Table 10
(2A05-047-1T) Cross-section at
Fracture, H_3PO_4 Etch at 150°C,
250X.

161

Figure 112a

Tensile Specimen 3 of Table 10
(2A05-047-2T) Cross-section at
Fracture, H_3PO_4 Etch at 250°C,
800X.

Figure 112b

Tensile Specimen 4 of Table 10
(2A05-047-1T) Cross-section at
Fracture, H_3PO_4 Etch at 250°C,
800X.

162

Figure 113. Electron Fractograph of Tensile Specimen 3 of Table 10 (2A05-047-2T)

163

Figure 114. Electron Fractograph of Tensile Specimen 3 of Table 10 (2A05-047-2T)

164

Figure 115. Electron Fractograph of Tensile Specimen 4 of Table 10 (2A05-047-1T)

Figure 116. Electron Fractograph of Tensile Specimen 4 of Table 10 (2A05-047-1T)
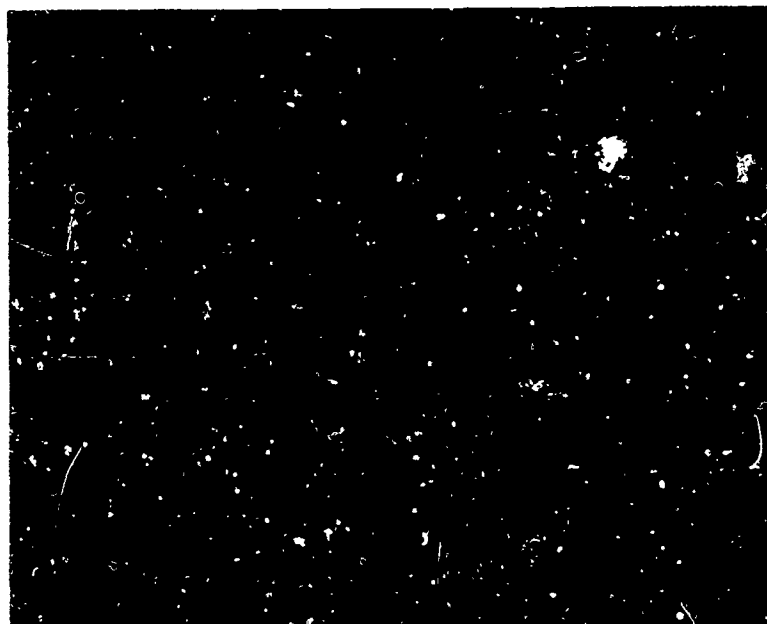
Figure 117. Flexural Specimen 2A05-043-3F External Profile, 50X,
Dash line-neutral axis.

167
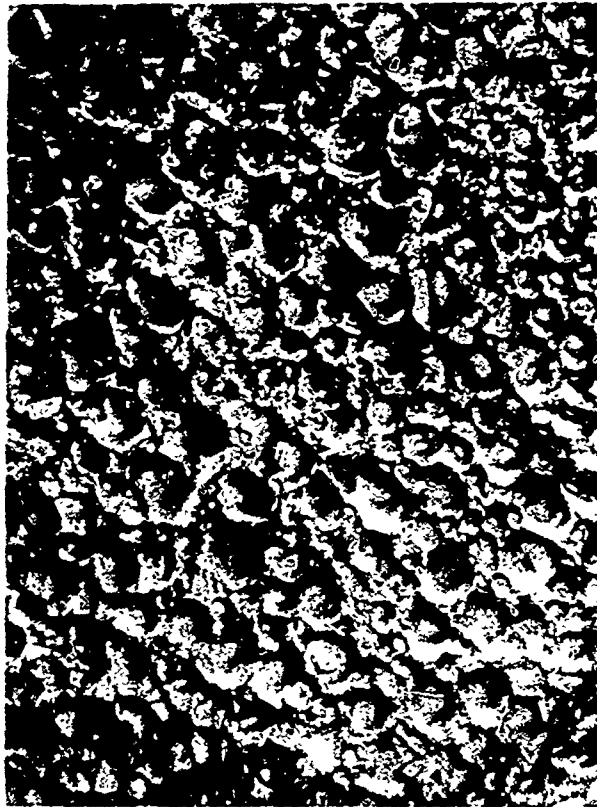
Figure 118a

"As received" pressed and
sintered surface Plastic replica-
transmitted light, 100X

Figure 118b

Standard shop ground surface,
15 RMS Plastic replica-
transmitted light 500X

Figure 119a

Standard shop grind plus shop lapping with diamond, 3 RMS Plastic replica-transmitted light 500X
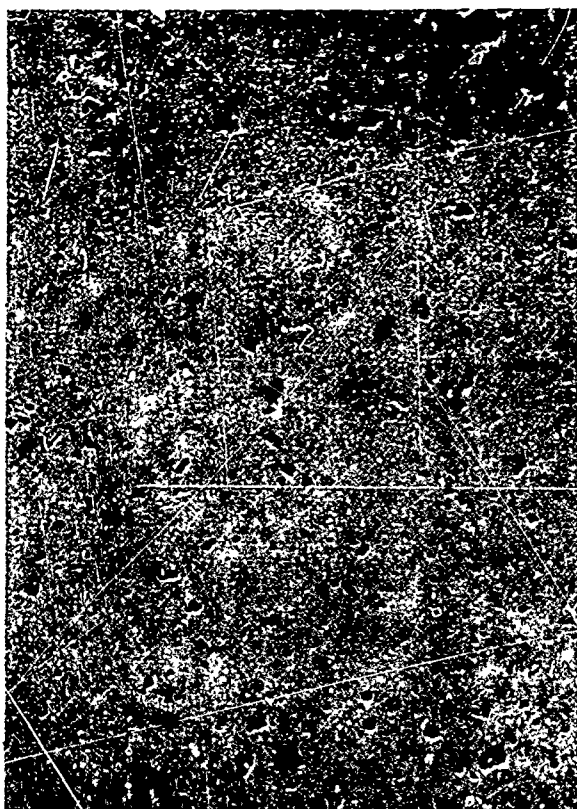
Figure 119b

Standard shop grind plus metallugrical lap with diamond Plastic replica-transmitted light 500X

169
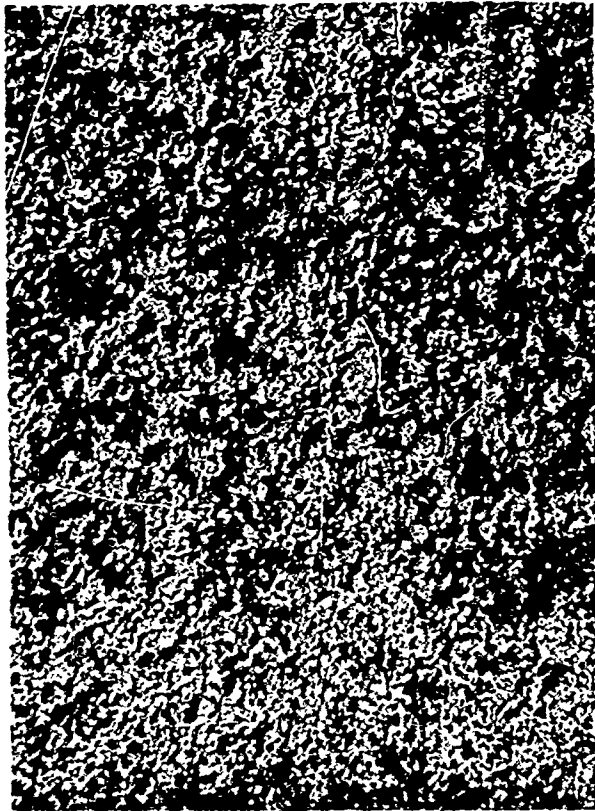
Figure 120a

"As received" pressed, green machined, and sintered surface Plastic replica-transmitted light 500X
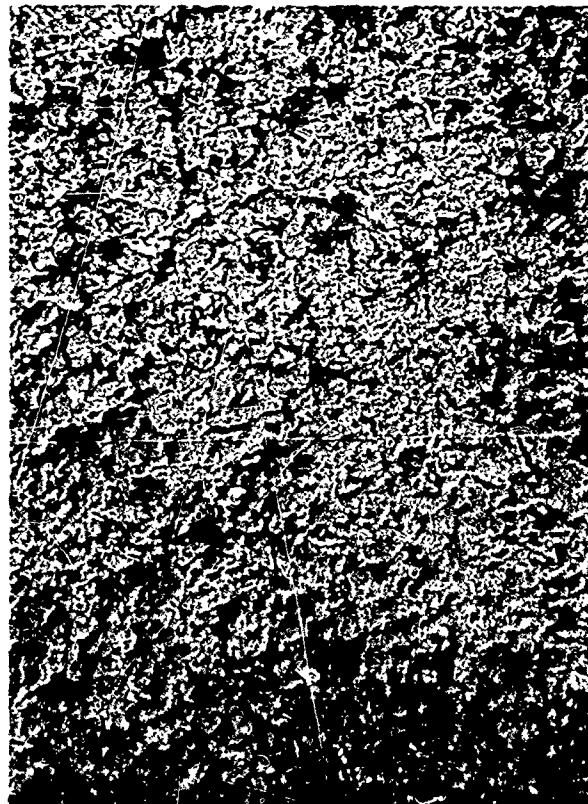
Figure 120b

Standard shop grind plus refire Plastic replica-transmitted light 500X

170

Figure 121. "As received", pressed and sintered surface

171

Figure 122. Standard shop grind

Figure 123. Standard shop grind plus lapping with 15 and $\frac{1}{4}$ micron diamond

Figure 124. Standard shop grind plus lapping with 15, 7, 1, and $\frac{1}{4}$ micron diamond

174

Figure 125. "As received", pressed, green machined and sintered

175

Figure 126. Standard shop grind and refined

176

Figure 127. Standard shop grind plus metallurgical lapping through 3 micron diamond
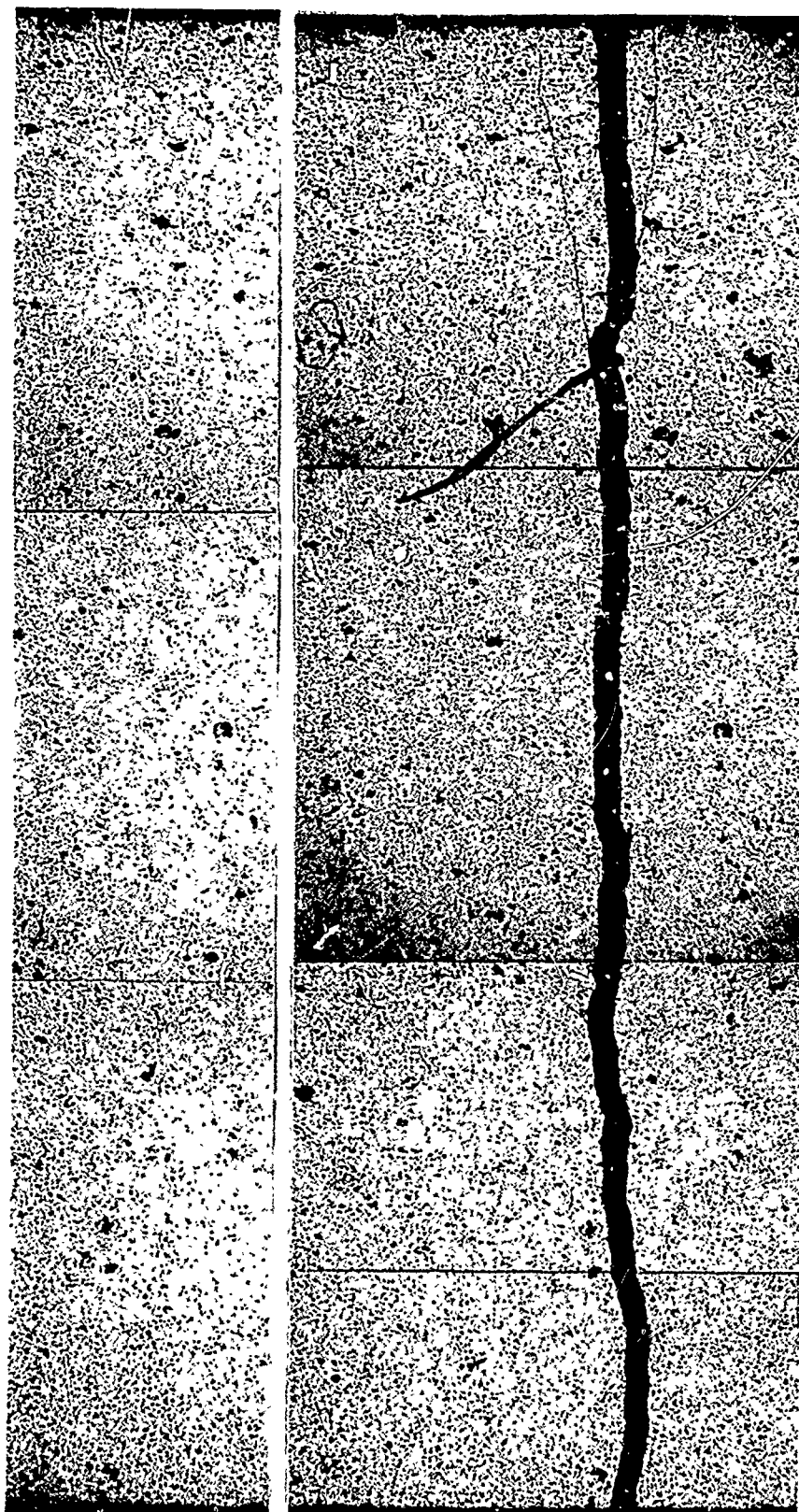
Figure 128. Tensile Face of Flexural Specimen 3A10-148-C12F-A, Shop ground and metallurgically lapped, 50X, before and after fracture. *Artifact-lint

178
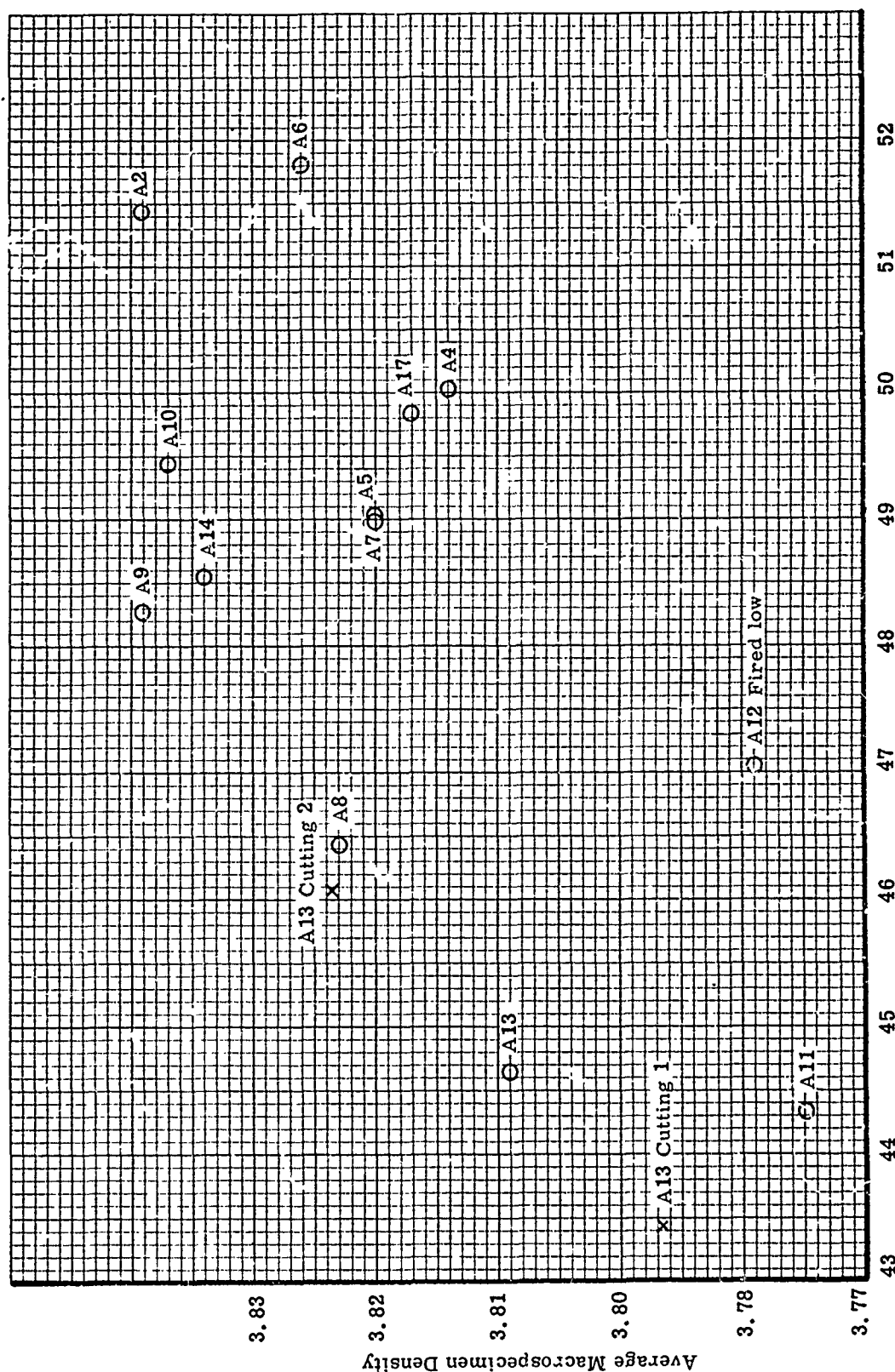
Figure 129. Average Density versus Average Flexural Strength for Macro Specimens

179
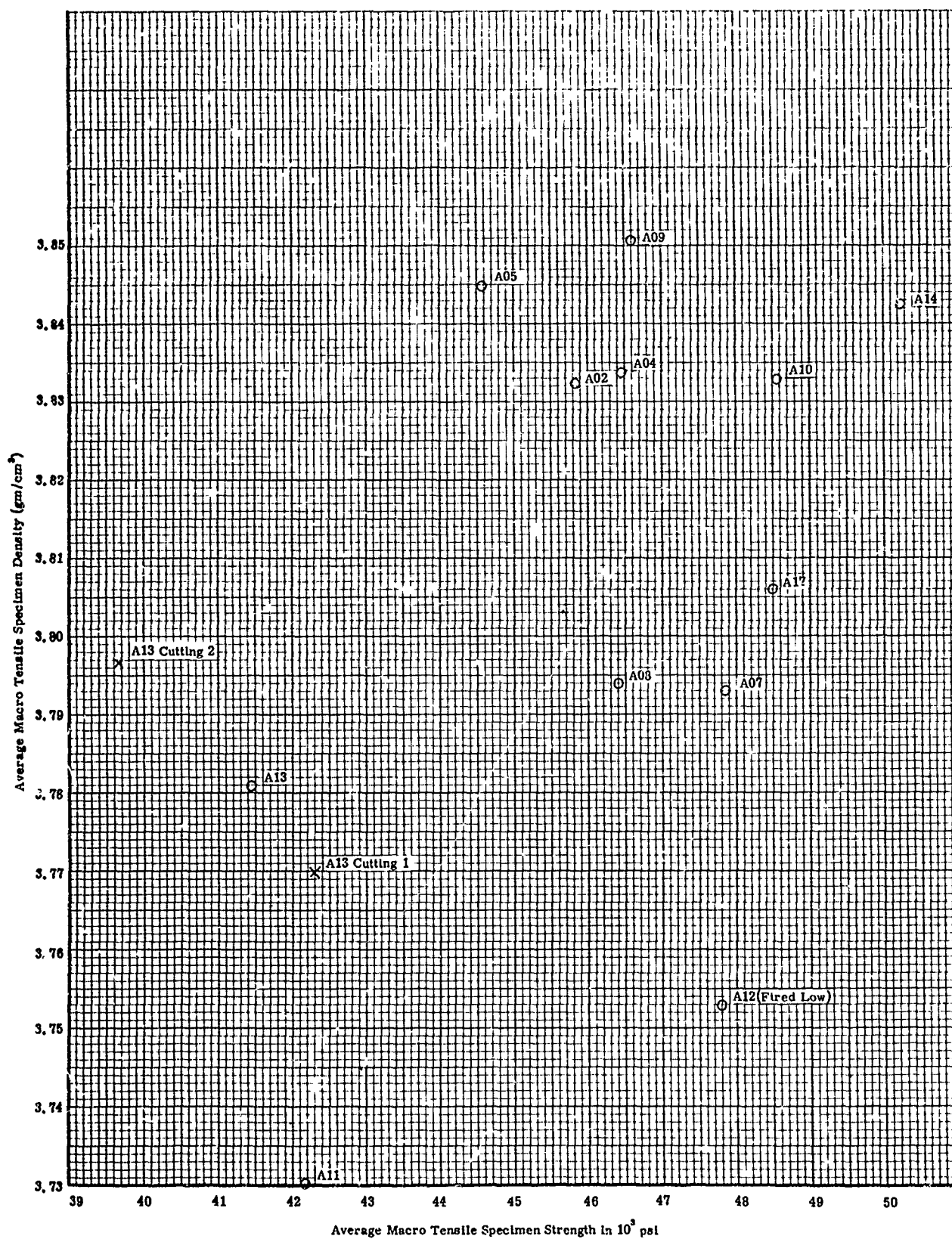
Figure 130. Average Density versus Average Tensile Strength for Macro Specimens

180
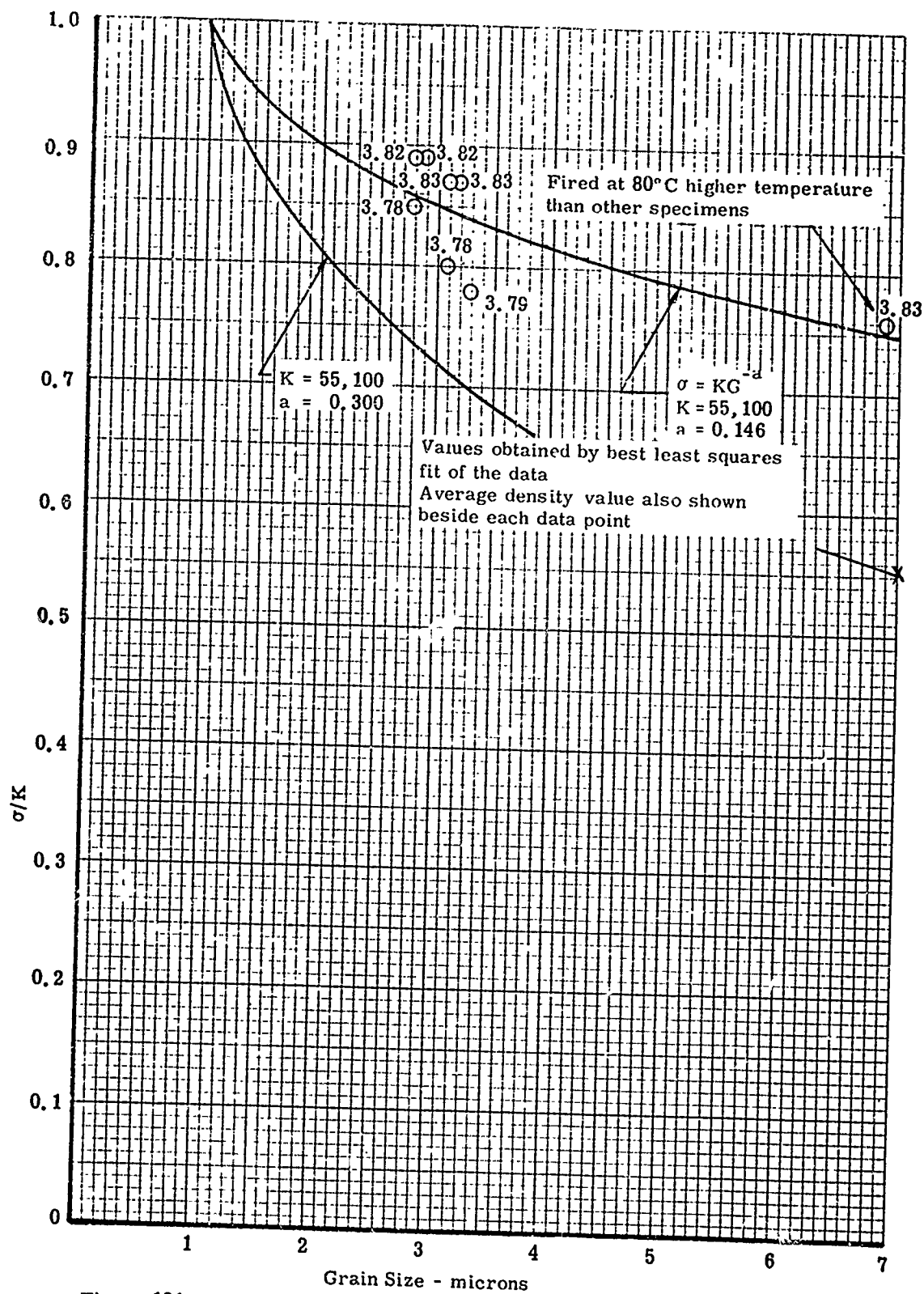
Figure 131. Average Flexural Strength versus Grain Size for Macro Flexural Specimen

181

σ = Ae^{bx}
$\sigma = Ae^{bx}$
A = 61,800
b = -5.4
Values obtained by best least
square fit of the data
(high fired piece deleted)

A = 61,800
b = -7.0

Volume Fraction of Porosity (based on density, ρ_{th} = 3.99 gm/cm^3)
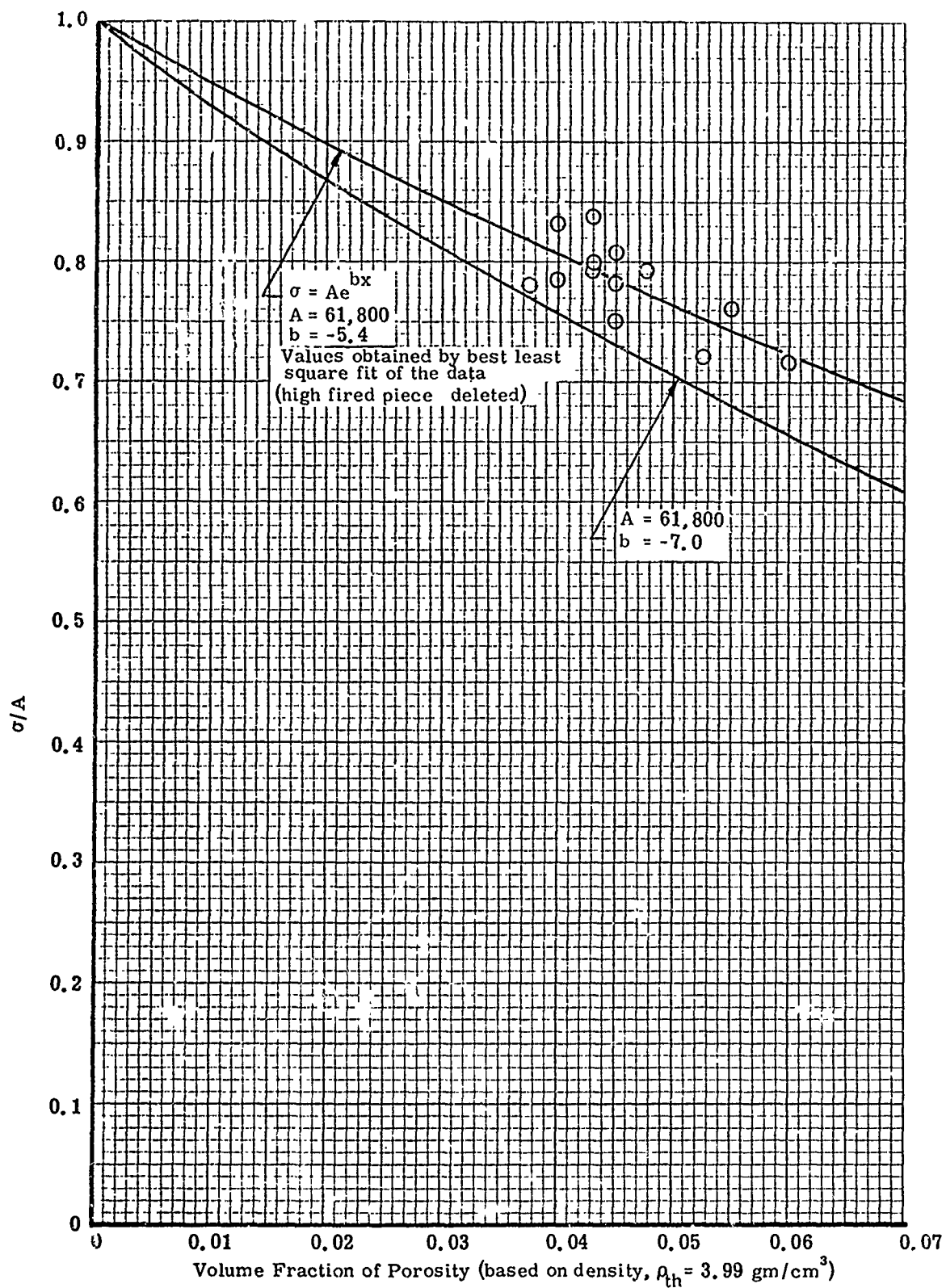
Figure 132. Average Flexural Strength versus Porosity for Macro Flexural Specimens

182

FIRING ANALYSIS DATA   Southern Research Institute   PO 16-07476

Table 1

Item No.	Coors Specimen Number	SRI Part No. (No./Order)	Date Fired	L-33 Kiln Car No.	Location on Kiln Car and Bung No.	No. of Flexural Specimens	No. of Tensile Specimens	Comments	Cone Deformatio(n)	Fired Density	X-Ray	Photomicrographs See Figure	Crystal Size Range	Crystal Size Average	Vacuum*	Pressing Steel Shell	Pressing Caps	Tool Set No.
1	53	1831-A-2 (20)	9/26	6	O R 28	2	2		△ B 31½ at 1:00	3.89	Good				No	Yes	Steel	1
2	61	"	"	"	R 29	2	2		(B 31½ at 1:00)		"				"	"	"	"
3	62	"	"	"	R 30	2			(B 31½ at 1:30)		Void				"	"	"	"
4	63	"	"	"	R 31	2			B 31½ at 2:00		Good				"	"	"	"
5	76	"	"	"	R 32	2			B 31½ at 2:30		"				"	"	"	"
6	79	"	"	"	R 33				B 31½ at 4:00		"				"	"	"	"
7	84	"	"	"	R 34				B 31½ at 5:00		"				"	"	"	"
8	86	"	"	"	RC 19		2		B 31½ at 1:00		"				"	"	"	"
9	90	"	"	"	RC 20	2			R 31½ at 1:00	3.87	Void				"	"	"	"
10	91	"	"	"	RC 21				B 31½ at 1:00		Good				"	"	"	"
11	92	"	"	"	RC 22				B 31½ at 12:30		"				"	"	"	"
12	93	"	"	"	RC 23				(B 31½ at 12:30)		"				"	"	"	"
13	94	"	"	"	RC 24				B 31½ at 12:30		"				"	"	"	"
14	95	"	"	"	RC 25				(B 31½ at 12:30)		"				"	"	"	"
15	103	"	"	"	LC 11	2			B 31½ at 1:00		"				"	"	"	"
16	104	"	"	"	LC 12	2			B 31½ at 1:00		"				"	"	"	"
17	105	"	"	"	LC 13				B 31½ at 1:30		"				"	"	"	"
18	125	"	"	"	LC 15	2	2		B 31½ at 1:30	3.89	"	38			"	"	"	"
19	126	"	"	"	LC 16				B 31½ at 3:00	3.87	"				"	"	"	"
20	127	"	"	"	L 5	2			B 31½ at 3:00		"				"	"	"	"
21	128	"	"	"	L 6				(B 31½ at 3:00)		"				"	"	"	"
22	130	"	"	"	L 7				B 31½ at 3:00		"				"	"	"	"
23	132	"	"	"	L 8	2			B 31½ at 3:00	3.88	Photo-micro		2-25	12	"	"	"	"
24	44	1831-A-4 (10)	9/14	13	R 31	2	2		B 31 at 6:00	3.86	"	37			"	"	"	2
25	107	"	"	"	L 8	2	2		B 31½ at 5:30	3.86	Low Den.		2-25	8	"	"	"	"
26	108	"	"	"	LC 11	4			B 31½ at 12:30	3.84	Good				"	"	"	"
27	110	"	"	"	LC 12	2	2		(B 31½ at 12:30)		"				"	"	"	"
28	111	"	"	"	LC 13	4			B 31½ at 12:30		Good				"	"	"	"
29	112	"	"	"	LC 14	2	2		(B 31½ at 1:00)		"				"	"	"	"
30	113	"	"	"	LC 15				B 31½ at 1:00		"				"	"	"	"
31	115	"	"	"	R 28				B 31½ at 3:00		"				"	"	"	"
32	116	"	"	"	R 29				(B 31½ at 4:00)		"				"	"	"	"
33	118	"	"	"	R 30				B 31½ at 5:00		"				"	"	"	"
34	139	"	"	"	LC 16				B 31½ at 1:30		"				"	"	"	"
35	161	"	9/28	35	L 2	4			B 31½ at 3:00		"				"	"	"	"

Table 1 (Continued)

Item No.	Coors Specimen Number	SRI Part No. (No./Order)	Date Fired	L-33 Kiln Car No.	Location on Kiln Car and Bung No.	No. of Flexural Specimens	No. of Tensile Specimens	Comments	Green Density	Cone Deformation	Fired Density by Coors	X-Ray	Vacuum*	Pressing Steel Shell	Pressing Caps	Tool Set No.
36	46	1831-A-5 (8)	9/12	13	O L2	2	2		2.57	∆B 31¼ at 5:00	3.94	Good	No	Yes	Steel	2
37	75	"	"	"	L3					(B 31¼ at 5:30)		"	"	"	"	"
38	80	"	"	"	L4					(R 31¼ at 6:00)		"	"	"	"	"
39	81	"	"	"	L5	2	2		2.53	B 31¼ at 6:30	3.84	"	"	"	"	"
40	83	"	"	"	L6					(B 31¼ at 5:00)		"	"	"	"	"
41	88	"	"	"	L7					B 31¼ at 4:00		"	"	"	"	"
42	89	"	"	"	L8					B 31¼ at 3:00		"	"	"	"	"
43	96	"	"	6	LC 11	4	2		2.65	B 31¼ at 1:00	3.88	"	"	"	"	"
44	158	"	"	"	LC 12	2				(B 31¼ at 3:00)		"	"	"	"	"
45	159	"	9/26	"	L3					B 31¼ at 3:00		"	"	"	"	"
46	160	"	"	"	L4	2	2		2.59	T 33 at 1:30	3.88	"	"	"	"	"
47	169	"	"	22	L6	2	2		2.59	B 33 at 2:00	3.87	"	"	"	"	"
48	170	"	10/2	"	LC 14					B 33 at 12:30 / B 33 at 1:30		"	"	"	"	"
49	171	"	"	"	R 32					T 33 at 1:30 / T 33 at 2:30		"	"	"	"	"
50	133-1	1831-A-6 (8)	9/12	13	RC 19	2			2.60	T 31¼ at 2:00	3.84	"	No	Yes	Steel	1
51	133-2	"	"	"	RC 19	2			2.60	T 31¼ at 2:00	3.84	"	"	"	"	"
52	133-3	"	"	"	RC 19	2			2.60	T 31¼ at 2:00	3.84	"	"	"	"	"
53	134-1	"	"	"	RC 19	2			2.57	B 31¼ at 1:45	3.86	"	"	"	"	"
54	134-2	"	"	"	RC 19	2			2.57	B 31¼ at 1:45	3.86	"	"	"	"	"
55	134-3	"	"	"	RC 20	2			2.57	(T 31¼ at 1:30)	3.86	"	"	"	"	"
56	135-1	"	"	"	RC 20					(T 31¼ at 1:30)		"	"	"	"	"
57	135-2	"	"	"	RC 20					(T 31¼ at 1:30)		"	"	"	"	"
58	135-3	"	"	"								"	"	"	"	"
59	119-1	1831-A-7 (10)	9/12	13	LC 14	4	3		2.61	(T 31¼ at 1:00)	3.84	"	No	Yes	Steel	2
60	119-2	"	"	"	LC 14				2.61	(T 31¼ at 1:00)	3.84	"	"	"	"	"
61	119-3	"	"	"	LC 14				2.61	(B 31¼ at 1:00)	3.84	"	"	"	"	"
62	120-1	"	"	"	LC 15	4	1		2.59	(B 31¼ at 1:00)	3.84	"	"	"	"	"
63	120-2	"	"	"	LC 15				2.59	(T 31¼ at 2:00)	3.84	"	"	"	"	"
64	121-1	"	"	"	LC 15	2			2.60	(T 31¼ at 2:00)	3.85	"	"	"	"	"
65	121-2	"	"	"	LC 15	4			2.60	(B 31¼ at 2:00)	3.85	"	"	"	"	"
66	121-3	"	"	"	LC 16	4			2.60	(B 31¼ at 2:00)	3.85	"	"	"	"	"
67	122-1	"	"	"	LC 16	4				T 31¼ at 3:00		"	"	"	"	"
68	122-2	"	"	"	LC 16	2	3			T 31¼ at 3:00		"	"	"	"	"
69	122-3	"	"	"	LC 16					(B 31¼ at 3:00)		"	"	"	"	"

184

Table 1 (Continued)

Item No.	Coors Specimen Number	SRI Part No. (No./Order)	Date Fired	L-33 Kiln Car No.	Location on Kiln Car and Bung No.	No. of Flexural Specimens	No. of Tensile Specimens	Comments	Green Density	Cone Deformation	Fired Density by Coors	X-Ray	Photomicrographs See Figure	Crystal Size Range	Crystal Size Average	Vacuum	Steel Shell	Caps	Tool Set No.
70	136-1	1851-A-8 (8)	9/12	12	R 31	3	3		2.62	T 31½ at 2:00	3.86	Good				No	Yes	Steel	2
71	136-2	=	=	=	R 31	6			2.62	T 31½ at 2:00	3.86	=				=	=	=	=
72	136-3	=	=	=	R 31	3	3		2.62	B 31½ at 1:30	3.86	=				=	=	=	=
73	137-1	=	=	=	R 32					B 31½ at 1:30		=				=	=	=	=
74	137-2	=	=	=	R 32					T 31½ at 2:30		=				=	=	=	=
75	137-3	=	=	=	R 32	3	3		2.65	T 31½ at 2:30	3.86	=				=	=	=	=
76	138-1	=	=	=	R 32				2.65	B 31½ at 2:00	3.86	=				=	=	=	=
77	138-2	=	=	=	R 33				2.65	T 31½ at 2:00		=				=	=	=	=
78	138-3	=	=	=	R 33					B 31½ at 5:30		=				=	=	=	=
79	141-1	=	=	=	R 33					B 31½ at 3:30		=				=	=	=	=
80	141-2	=	=	=	R 33					B 31½ at 3:30		=				=	=	=	=
81	146	1851-A-9 (5)	9/28	35	L 3	6	6		2.55	B 31½ at 3:00	3.87		39	2-25	12	=	=	=	3
82	147	=	=	=	L 4	8	2		2.55	B 31½ at 2:30	3.87					=	=	=	=
83	150-1	=	=	=	L 5	6			2.55	B 31½ at 2:30	3.86					=	=	=	=
84	150-2	=	=	=	L 6				2.55	B 31½ at 2:30						=	=	=	=
85	151-1	=	=	=	L 7					B 31½ at 2:00						=	=	=	=
86	151-2	=	=	=	L 8					B 31½ at 1:30						=	=	=	=
110	195	(24)	11/1	33	Center						3.86					=	=	=	=
87	143	1851-A-10 (2)	9/14	12	L 2		6		2.52	(L 31½ at 5:00)	3.86					=	=	=	=
88	148	=	=	=	L 4				2.57	(B 31½ at 5:03)	3.86					=	=	=	=
89	152	1851-A-11 (2)	9/22	25	Center		20		2.55	33 at 1:00	3.87	Crack	44	2-30	12			Rubber	4
90	153	=	9/28	35	Center				2.52		3.06	Crack						Rubber	=
91	178	=	10/17	7	Center				2.49		3.83	Crack	45, 54	2-20	6			Rubber	=
92	179	=	10/17	7	Center						3.84	Good	=					Rubber	=
93	180	=	10/19	7	Center						3.84	Crack						Rubber	=
94	181	=	10/19	7	Center						3.95	Good						Rubber	=
111	201	=	11/10	38	Center						T3.87, B3.87	Void						Rubber	
112	202	=	"	"	Center	20	20			33 at 1:30	T3.87, B3.87	Chip						Rubber	
113	203	=	"	"	Center						B3.87, B3.86	Void						Rubber	
114	204	=	"	"	Center						B3.85*, B3.85*	Void						Rubber	
95	166	1851-A-12 (3)	9/28	35	LC 11	7	7		2.60	B 31½ at 12:30	3.84	=	40	2-35	17	=	=	Steel	2
96	167	=	10/2	22	LC 12	13	1		2.57	(B 31½ at 12:30)	3.83	=				=	=	=	=
97	168	=	"	"	LC 5				2.66	B 34 at 1:30	3.88	=				=	=	=	=
98	172	=			LC 13				2.66	T 33 at 1:00	3.88	=				=	=	=	=
99	173	=	"	"	RC 22				2.62	T 33 at 3:00	3.88	=				=	=	=	=
100	174	=	"	"	R 31				2.58	B 33 at 5:00	T3.88, B3.88	=				=	=	=	=

Table 1 (continued)

Item No.	Coors Specimen Number	SRI Part No. (No./Order)	Date Fired	L-33 Kiln Car No.	Location on Kiln Car and Bung No.	No. of Flexural Specimens	No. of Tensile Specimens	Comments	Cone Deformation	Fired Density	X-Ray	Photomicrographs See Figure	Crystal Size Range	Crystal Size Average	Vacuum	Steel Shell	Caps	Tool Set No.
70	136-1	1831-A-8 (8)	9/12	13	O R 31	3	3		△ T 31½ at 2:00	3.86	Good				No	Yes	Steel	2
71	136-2	=	=	=	R 31	6			T 31½ at 2:00	3.86	=				=	=	=	=
72	136-3	=	=	=	R 31	3	3		(B 31½ at 1:30)	3.86	=				=	=	=	=
73	137-1	=	=	=	R 32				(B 31½ at 1:30)		=				=	=	=	=
74	137-2	=	=	=	R 32				(T 31½ at 2:30)		=				=	=	=	=
75	137-3	=	=	=	R 32				(T 31½ at 2:30)		=				=	=	=	=
76	138-1	=	=	=	R 32				(B 31½ at 2:00)	3.86	=				=	=	=	=
77	138-2	=	=	=	R 33				(B 31½ at 2:00)	3.86	=				=	=	=	=
78	138-3	=	=	=	R 33		3		T 31½ at 5:30		=				=	=	=	=
79	141-1	=	=	=	R 33	6			B 31½ at 3:30		=				=	=	=	=
80	141-2	=	=	=	R 33	3	3		B 31½ at 3:30		=				=	=	=	=

⊕ Fired in L-32 kiln (80° higher temperature than L-33).
* Vacuum was used with rubber shell only.
OR, RC, LC and L designate right, right center, left center, and left.
△B and M designate the bottom or middle of bungs.
( ) Designates estimated cone deformations from cones in same area.

Note: All parts were pressed at 30,000 psi.
Fired densities were taken on a 4AQL, Level II per MIL. Std. 105D.
Photomicrographs were made one per kiln car.
For defective X-rayed parts, see Figure 46, Specimens 63 and 93

47	"		107
48	"		152
49	"		153
50	"		178
51	"		180

186

TABLE 2

RESULTS OF FLEXURAL EVALUATIONS OF PHASE 1 MACRO SPECIMENS

SRI Run Number	Specimen	Temperature °F	Bulk Density (Mechanics Section) gm/cm³	Stress Rate psi/sec	Load at Fracture lbs	Fracture Stress psi	Fracture Location inches from midspan	Sonic Velocity in./μsec	Remarks
1	1A02-002-1	70	3.830	5000	96.25	54140	0.35-0.375		
2	-002-2		3.830		93.75	52730	0.45-0.375		
3	-004-1		3.827		93.75	52730	0.55		
4	-004-2		3.833		93.25	52450	0.2		
5	-005-1		3.825		82.25	46270	0.05		
6	-005-2		3.822		100.75	56670	0.0		
7	-006-1		3.824		99.00	55690	0.05		
8	-006-2		3.831		85.00	47810	0.35		
9	-007-1		3.828		84.00	47250	0.3		
10	-007-2		3.838		78.25	44020	0.05		
11	-011-1		3.827		86.75	48800	0.35		
12	-011-2		3.812		96.25	54140	0.0		
13	-016-1		3.822		81.50	45840	0.0		
14	-016-2		3.834		90.25	50770	0.25		
15	-017-1		3.814		92.00	51750	0.0		
16	-017-2		3.828		93.50	52590	0.35		
17	-020-1		3.849		95.75	53860	0.25		
18	-020-2		3.839		93.50	52590	0.25		
19	-023-1		3.833		92.75	52170	0.15		
20	-023-2		3.835		100.75	56670	0.2		
Mean Value						51450			
Standard Deviation						3640			
Coefficient of Variation						0.0706			
21	2A04-024-1		3.833		89.25	50200	0.3		
22	-024-2		3.825		99.25	55830	0.25		
23	-025-1		3.830		85.00	47810	0.25		
24	-025-2		3.830		86.25	48520	0.25-0.375		
25	-026-1		3.759		97.00	54560	0.375-0.375		
26	-026-2		3.760		80.50	45280	0.0		
27	-026-3		3.804		82.00	46130	0.3		
28	-026-4		3.797		93.00	52310	0.2		
29	-028-1		3.802		77.75	43730	0.05		
30	-028-2		3.805		85.75	48230	0.1		
31	-030-1		3.793		98.00	55130	0.3		
32	-030-2		3.794		78.50	44160	0.2		
33	-030-3		3.789		93.25	52450	0.375		
34	-030-4		3.811		91.50	51470	0.0		
35	-031-1		3.819		90.00	50630	0.1		
36	-031-2		3.816		95.00	53440	0.25		
37	-035-1		3.799		81.00	45310	0.35		Specimen length = 1.592
38	-035-2		3.794		75.00	42190	0.375		
39	-035-3		3.809		91.25	51330	0.2		
40	-035-4		3.804		102.00	57380	0.3-0.35		
Mean Value			3.804			49810			
Standard Deviation			0.020			4390			
Coefficient of Variation						0.0881			
41	2A05-043-1		3.786		87.25	49080	0.35-0.375	0.4355	
42	-043-2		3.753		92.25	51890	0.375	0.4509	
43	-043-3		3.797		95.50	53710	0.10	0.4591	
44	-043-4		3.797		94.00	52880	0.375-0.375	0.4398	
45	-036-1								Broken during grinding
46	-036-2		3.794		85.00	47810	0.25	0.4507	
47	-039-1		3.809		85.50	48090	0.25	0.4431	
48	-039-2		3.818		92.75	52170	0.375	0.4386	
49	-044-1		3.831		85.00	47810	0.375	0.4546	
50	-044-2		3.820		81.50	45840	0.375	0.4453	
51	-046-1		3.808		85.25	47950	0.20	0.4371	
52	-046-2		3.814		88.75	49920	0.25	0.4431	
53	-047-1		3.829		80.25	45140	0.20	0.4422	Fired at 80°C higher temperature
54	-047-2		3.840		80.75	45420	0.00	0.4496	Fired at 80°C higher temperature
Mean Value			3.810			49740			
Standard Deviation			0.017			2550			
Coefficient of Variation						0.0513			
167	1A06-051-1		3.781		88.75	49920	0.00	0.4147	
168	-051-2		3.803		91.25	51330	6.00	0.4136	
169	-052-1		3.815		89.75	50480	0.10	0.4122	
170	-052-2		3.821		93.25	52450	0.10	0.4130	
171	-053-1		3.811		78.50	44160	0.20	0.4204	
172	-053-2		3.809		101.25	56950	0.10	0.4188	
173	-054-1		3.822		96.00	54000	0.10	0.4193	
174	-054-2		3.839		78.75	44300	0.20	0.4206	
175	-055-1		3.805		100.25	56390	0.20	0.4237	
176	-055-2		3.802		98.25	55270	0.10	0.4241	
177	-056-1		3.824		101.00	56810	0.20	0.4237	
178	-056-2		3.823		96.50	54280	0.20	0.4309	
179	-057-1		3.832		94.50	53160	0.20	0.4191	
180	-057-2		3.834		82.00	46130	0.10	0.4173	
Mean Value			3.816			51830			
Standard Deviation			0.015			4390			
Coefficient of Variation						0.0846			

TABLE 2 (Continued)

SRI Run Number	Specimen	Temperature °F	Bulk Density (Mechanics Section) gm/cm³	Stress Rate psi/sec	Load at Fracture lbs	Fracture Stress psi	Fracture Location inches from midspan	Sonic Velocity in./µsec	Remarks
55	2A07-059-1	70	3.806	5000	86.00	48380	0.05	0.3964	
56	-059-2		3.813		78.50	43030	0.15	0.3861	
57	-059-3		3.810		92.50	52030	0.20	0.3932	
58	-059-4		3.805		85.00	47810	0.40	0.3913	
59	-062-1		3.803		91.00	51190	0.1	0.3925	
60	-062-2		3.805		93.50	52590	0.3	0.3893	
61	-062-3		3.814		92.50	52090	0.0	0.3979	
62	-062-4		3.802		91.00	45580	0.30	0.3904	
63	-064-1		3.802		87.75	49380	0.15	0.3964	
64	-064-2		3.811		91.75	51610	0.0	0.3911	
65	-065-2		3.813		93.50	52590	0.3	0.3830	
7	-065-3		3.810		91.00	51190	0.15	0.3941	
3	-065-4		3.819		81.75	45980	0.0	0.3953	
69	-066-1		3.819		89.00	50090	0.2	0.3963	
70	-066-2		3.817		89.75	50480	0.3	0.3955	
71	-066-3		3.813		83.25	46830	0.15	0.3861	
72	-066-4		3.820		89.75	50480	0.05	0.3916	
73	-067-1		3.818		85.25	47950	0.35	0.3965	
74	-067-2		3.811		74.75	42050	0.0	0.3967	
75	-067-3		3.806		80.00	45000	0.25-0.45	0.3928	
76	-067-4		3.808		86.00	48380	0.3	0.3935	
77	-068-1		3.787		94.50	53160	0.06	0.3966	
78	-068-2		3.751		93.00	52310	0.15	0.3953	
65	-065-1		3.821		82.00	46130	0.35	0.3926	
Mean Value			3.810			49010			
Standard Deviation			0.006			3170			
Coefficient of Variation						0.0647			
79	2A06-070-1		3.815		80.75	45420	0.375	0.3952	
80	-070-2		3.806		84.50	47530	0.3	0.3938	
81	-070-3		3.817		65.00	36580	0.3	0.3979	
82	-071-1		3.820		88.25	49640	0.15	0.3944	
83	-071-2		3.811		86.50	48660	0.15	0.3964	
84	-071-3		3.816		72.50	40780	0.3	0.3960	
85	-071-4		3.807		82.50	46410	0.25	0.4015	
86	-071-5		3.796		81.00	45560	0.3	0.4043	
87	-071-6		3.797		92.00	51750	0.25	0.4020	
88	-073-1		3.821		80.75	45420	0.25	0.3982	
89	-073-2		3.816		91.25	51330	0.2	0.3896	
90	-073-3		3.822		83.75	47110	0.05	0.3933	
91	-075-1		3.832		79.50	44730	0.3	0.3897	
92	-079-2		3.818		91.00	51190	0.3	0.3917	
93	-079-3		3.791		77.75	43730	0.35	0.3923	
94	-079-4		3.820		76.75	43170	0.05	0.3869	
95	-079-5		3.818		88.25	49640	0.05	0.3958	
96	-079-6		3.820		92.00	51750	0.25	0.3942	
97	-080-1		3.811		73.00	41060	0.06	0.3950	
98	-080-2		3.812		86.75	43800	0.1	0.3887	
99	-080-3		3.811		80.00	45000	0.3	0.3844	
Mean Value			3.813			46440			
Standard Deviation			0.010			4000			
Coefficient of Variation						0.0861			
100	3A09-083-1		3.834		81.25	45700	0.2	0.4020	14 RMS
101	-083-2		3.835		91.25	51330	0.06	0.4042	
102	-083-3		3.836		93.75	52730	0.1	0.4013	
103	-083-4		3.841		90.00	50630	0.1	0.4041	
104	-083-5		3.837		85.00	47810	0.15	0.4009	
105	-083-6		3.847		86.50	48660	0.15	0.4042	
106	-085-1		3.818		61.75	34730	0.0	0.4030	13 RMS
107	-085-2		3.845		92.50	52030	0.3	0.4117	
108	-085-3		3.840		81.50	45840	0.35	0.4120	
109	-085-4		3.822		81.75	45980	0.15	0.4085	
110	-085-5		3.819		78.50	43500	0.3	0.4063	
111	-085-6		3.819		83.00	48380	0.25	0.4086	
112	-085-7		3.824		92.75	52170	0.05	0.4066	
113	-085-8		3.838		80.00	50060	0.3	0.4153	
114	-086-1		3.832		85.00	47810	0.06	0.4771	
115	-086-2		3.826		92.25	51890	0.2	0.4352	
116	-086-3		3.821		91.00	51190	0.06	0.4290	
117	-086-4		3.820		90.75	51050	0.3	0.4340	
118	-086-5		3.842		79.00	44440	0.3	0.4425	
119	-086-6		3.820		84.25	49640	0.2	0.4333	
Mean Value			3.829			48233			
Standard Deviation			0.010			4210			
Coefficient of Variation						0.0873			
120	3A10-087-1		3.825		87.00	49230	0.35	0.4113	
121	-087-2		3.841		83.75	47110	0.2	0.4119	
122	-087-3		3.827		88.00	49500	0.375	0.4117	
123	-087-4		3.824		96.00	54410	0.375-0.375	0.4120	
124	-087-5		3.848		90.00	48660	0.1	0.4132	
125	-087-6		3.820		87.50	49230	0.3	0.4094	15 RMS
126	-087-7		3.823		95.25	53550	0.2	0.4106	
127	-087-8		3.832		92.25	51450	0.1	0.4101	
128	-087-9		3.811		84.50	47550	0.25	0.4072	
129	-087-10		3.816		83.25	46270	0.06	0.4119	
130	-087-11		3.816		83.50	48660	0.05	0.4119	
131	-087-12		3.809		73.50	41710	0.0	0.4120	
132	-087-13		3.822		81.75	45980	0.2	0.5084	
133	-087-14		3.843		75.00	42190	0.1	0.4170	
134	-087-15		3.826		86.00	43250	0.3	0.4102	
135	-087-16		3.824		74.25	41766	0.06	0.4094	
136	-087-17		3.816		77.75	43730	0.1	0.4099	
137	-087-18		3.817		91.50	51470	0.3	0.4119	

TABLE 2 (Continued)

SRI Run Number	Specimen	Temperature °F	Bulk Density (Mechanics Section) gm/cm³	Stress Rate psi/sec	Load at Fracture lbs	Fracture Stress psi	Fracture Location inches from midspan	Sonic Velocity in./μsec	Remarks
138	3A10-087-19	70	3.771	5C30	75.75	42810	0.25	0.3837	Weak back echo
139	-087-20		3.818		80.00	45000	0.15	0.4087	
140	-087-21		3.797		93.75	52730	0.35-0.35	0.4111	
141	-087-22		3.823		86.00	48380	0.05	0.4137	
142	-087-23		3.825		88.75	48920	0.25	0.4130	
143	-087-24		3.823		81.00	45530	0.15	0.4117	
144	-087-25		3.834		94.00	52880	0.1	0.4123	
145	-087-26		3.811		82.00	46150	0.05	0.4124	
261	-088-A1		3.841		101.00	56760	0.20	0.4037	
268	-088-A2		3.834		93.50	52550	0.00	0.3989	
266	-088-A3		3.817		94.50	53110	0.375-0.375	0.4029	
246	-088-A4		3.842		82.50	48450	0.375	0.4033	3 RMS
275	-088-A5		3.855		86.50	48510	0.30	0.4072	
262	-088-B1		3.837		104.75	58950	0.62	0.4057	
265	-088-B2		3.823		94.50	53110	0.00	0.4031	
274	-088-B3		3.835		100.00	56630	0.25	0.4037	
267	-088-B4		3.825		85.00	47770	0.375	0.4041	
287	-088-B5		3.830		88.00	50100	0.10	0.4034	4 RMS
283	-088-B6		3.852		94.75	53250	0.15	0.4048	
288	-088-B7		3.838		89.25	50180	0.375-0.375	0.4037	
269	-088-B8		3.805		84.25	47356	0.05	0.4022	
271	-088-B9		3.842		89.00	50023	0.30	6.4036	
279	-088-B10		3.841		93.25	53410	0.30	0.3995	
272	-088-B11		3.851		90.75	51000	0.375	0.4052	
277	-088-B12		3.841		94.00	52830	0.15	0.4046	
285	-088-B13		3.843		38.30	49740	0.10	0.4046	
281	-088-B14		3.844		100.50	56480	0.00	0.4019	
290	-088-B15		3.822		85.75	48190	0.375	0.4028	
292	-088-C1		3.842		89.75	51200	0.15	0.4050	4 RMS
296	-088-C2		3.831		79.50	45950	0.10	0.4051	3 RMS
294	-088-C3		3.836		82.50	47050	0.15	0.4051	3 RMS
289	-088-C5		3.850		85.50	36810	0.25	0.4074	
284	-088-C7		3.834		76.50	42990	0.10	0.4029	
282	-088-C8		3.831		92.50	51900	0.20	0.4021	
280	-088-C9		3.831		94.00	52830	0.10	0.4036	
276	-088-C10		3.834		94.25	52970	0.10	0.4033	
291	-088-D1		3.843		96.25	55050	0.20	0.4005	3 RMS
295	-088-D2		3.827		84.75	43100	0.20	0.4050	3 RMS
293	-088-D3		3.818		78.50	44500	0.10	0.4045	3 RMS
273	-088-D6		3.844		101.75	57180	0.09	0.4040	
270	-088-D7		3.835		91.50	51420	0.10	0.4037	
278	-088-D8		3.840		77.75	43700	0.00	0.4037	
264	-088-D9		3.841		94.50	53110	0.10	0.4019	
263	-088-D10		3.831		94.50	53110	0.10	0.4046	
Mean Value			3.837			49520			
Standard Deviation						4380			
Coefficient of Variation						0.0885			
213	4A11-089-A1		3.782		88.25	49840	0.2		
200	-089-A2		3.787		89.00	50060	0.05		
220	-089-A3		3.755		83.75	47110	0.375		
201	-089-A4		3.786		81.00	45560	0.25		
251	-089-A5		3.756		79.25	44580	0.33		
185	-089-A6		3.791		81.75	45900	0.1		
186	-089-B1		3.744		68.50	38530	0.3		
199	-089-C1		3.802		79.50	44720	0.2		
205	-089-C2		3.790		89.50	50340	0.15		
225	-089-C3		3.765		69.25	38950	0.45		
219	-089-C4		3.776		68.00	38250	0.1		
190	-089-C5		3.773		72.50	40780	0.3		
192	-089-C6		3.786		89.00	50080	0.2		
248	-089-D1		3.725		67.00	37690	0.0		
228	-089-E1		3.791		86.50	48680	0.1		
196	-089-E2		3.768		63.00	35440	0.05		
200	-089-E3		3.768		75.75	42810	0.15		
198	-089-E4		3.789		74.25	41770	0.2		
218	-089-E5		3.775		82.50	46410	0.25		
212	-089-E6		3.787		87.50	49220	0.35		
Mean Value			3.775			44320			
Standard Deviation			0.019			4780			
Coefficient of Variation			0.1079						
240	2A12-095-1		3.772		83.75	47110	0.3		
205	-095-2		3.792		87.50	49220	0.35		
250	-095-3		3.779		90.75	51050	0.2		
252	-095-4		3.783		94.00	52880	0.3-0.2		
343	-095-5		3.777		81.50	45840	0.5		
193	-095-6		3.783		79.75	44880	0.375		
204	-095-7		3.794		84.25	47390	0.2		
256	-096-1		3.770		85.50	48090	0.3		
234	-096-2		3.789		91.25	51330	0.35		
183	-096-3		3.774		80.00	45000	0.3		
182	-096-4		3.768		85.75	48230	0.1		
232	-096-5		3.773		85.50	48090	0.15		
262	-096-6		3.785		89.50	50340	0.05		
257	-096-7		3.771		83.00	46690	0.2		
208	-096-8		3.760		85.00	47810	0.0		
191	-096-9		3.781		87.75	49360	0.2		
211	-096-10		3.791		85.25	47950	0.0		
216	-096-11		3.796		53.00	29810	0.3		
223	-096-12		3.775		82.25	46270	0.1		
214	-096-13		3.778		77.50	43590	0.15		
Mean Value			3.779			47060			
Standard Deviation			0.009			4671			
Coefficient of Variation						0.0992			

TABLE 2 (Continued)

SRI Run Number	Specimen	Temperature °F	Bulk Density (Mechanics Section) gm/cm³	Stress Rate psi/sec	Load at Fracture lbs	Fracture Stress psi	Fracture Location inches from midspan	Sonic Velocity in./μsec	Remarks
224	5A13-101-1	70	3.802	5000	73.50	41340	0.05		
208	-101-2		3.807		71.50	40220	0.0		
236	-101-3		3.797		77.00	43310	0.0		
345	-101-4		3.800		76.00	42750	0.375		
195	-101-5		3.797		69.00	38810	0.3		
246	-101-6		3.800		78.50	44180	0.3-0.375		
227	-101-7		3.799		77.50	43590	0.375		
207	-102-1		3.775		75.50	42470	0.375		
239	-102-2		5.781		80.25	45140	0.3		
231	-102-3		3.768		63.25	35580	0.3-0.35		
215	-102-4		3.771		77.50	43590	0.35		
220	-102-5		2.767		77.75	43730	0.25		
254	-102-6		3.765		89.50	50340	0.0		
242	-102-7		3.773		75.50	42470	0.1		
300	-102-10		3.807		78.50	44130	0.20	0.4050	
313	-102-11		3.815		86.00	48330	0.375-0.375	0.4052	
312	-102-12		3.816		88.75	49680	0.15	0.4052	
311	-102-13		3.815		67.25	37800	0.375	0.4042	
310	-102-14		3.815		87.25	49040	0.05	0.4043	
308	-102-15		3.812		83.50	46930	0.10	0.4063	
305	-102-16		3.807		85.25	47910	0.10	0.4034	
302	-102-17		3.812		88.75	49680	0.05	0.4061	
298	-102-18		3.816		57.25	32180	0.05	0.4064	
187	-103-1		3.787		86.00	48380	0.3		
217	-103-2		3.788		77.00	43310	0.2		
182	-103-3		3.787		79.50	44720	0.15		
255	-103-4		3.786		80.00	45000	0.15		
259	-103-5		3.794		76.50	43030	0.2		
188	-103-6		3.785		81.25	45700	0.2		
238	-103-7		3.789		78.50	44160	0.05		
309	-103-10		3.819		81.75	45940	0.10	0.4049	
306	-103-11		3.819		78.50	44120	0.05	0.4055	
304	-103-12		3.826		88.00	49460	0.15	0.4092	
303	-103-13		3.817		89.00	50020	0.15	0.4065	
301	-103-14		3.817		82.75	46510	0.15	0.4045	
297	-103-15		3.817		87.50	49180	0.375	0.4065	
307	-103-16		3.816		85.00	47770	0.375-0.375	0.4068	
299	-103-17		3.807		79.50	44680	0.30	0.4054	
314	-103-18		3.811		81.50	45800	0.20	0.4036	
Mean Value			3.799			44650			
Standard Deviation						4020			
Coefficient of Variation						0.0900			
146	6A14-104-1		3.832		88.50	49780	0.20	0.4114	
147	-104-2		3.825		87.50	49220	0.10	0.4125	
148	-104-3		3.832		88.25	49640	0.20	0.4145	
149	-104-4		3.829		81.75	45980	0.30	0.4239	
150	-104-5		3.832		74.50	41910	0.10	0.4082	
151	-104-6		3.830		93.00	52310	0.20	0.4033	
152	-104-7		3.831		62.26	35020	0.10	0.4033	
153	-104-8		3.830		80.00	45000	0.375	0.4066	
154	-106-1		3.814		85.50	48090	0.10	0.4130	
155	-106-2		3.803		94.50	53160	0.375	0.4102	
156	-106-3		3.830		99.00	55680	0.05	0.4079	
157	-106-4		3.823		88.75	49920	0.10	0.4096	
158	-106-5		3.832		84.75	47670	0.05	0.4110	
159	-106-6		3.823		85.00	47810	0.10	0.4070	
160	-106-7		3.802		88.50	49780	0.20	0.4117	
161	-106-8		3.817		88.50	49780	0.375	0.4091	
162	-106-9		3.812		74.00	41630	0.20	0.4118	
163	-106-10		3.812		93.00	52310	0.05	0.4073	
164	-106-11		3.821		90.25	50770	0.05	0.4074	
165	-106-12		3.830		100.50	56530	0.375-0.375	0.4099	
166	-106-13		3.836		85.50	48090	0.35	0.4098	Spare from scrap
Mean Value			3.824			48580			
Standard Deviation			0.010			4860			
Coefficient of Variation						0.1001			
244	6A17-107-1		3.819		91.50	55410	0.25		
181	-107-2		3.812		85.50	48090	0.2		
256	-107-3		3.811		90.25	50770	0.3		
165	-107-4		3.812		85.00	47810	0.35		
249	-107-5		3.814		90.25	50770	0.375		
197	-107-6		3.812		93.50	52590	0.2		
247	-107-7		3.813		94.75	53300	0.375-0.375		
261	-108-1		3.799		93.50	52590	0.3		
253	-108-2		3.796		83.50	46790	0.15		
206	-108-3		3.803		80.50	45280	0.25		
194	-108-4		3.803		90.50	50910	0.25		
233	-108-5		3.803		87.50	49220	0.3		
210	-108-6		3.801		94.75	53300	0.375		
203	-108-7		3.803		90.00	50630	0.35		
212	-109-1		3.808		90.25	50770	0.1		
236	-109-2		3.802		88.00	49500	0.3		
241	-109-3		3.806		85.50	48090	0.2		
237	-109-4		3.803		83.50	46970	0.2		
221	-109-5		3.808		79.50	44720	0.1		
235	-109-6		3.806		94.25	53020	0.375 0.375		
230	-109-7		3.813		82.75	46550	0.1		
Mean Value			3.807			49670			
Standard Deviation			0.006			2910			
Coefficient of Variation						0.0583			

190

Table 3

Table of Mean Stresses, Standard Deviations, and Coefficients of
Variation for Phase I Flexural Data on Macro Specimens

Specimen Blank Type	Number of Specimens	Mean Fracture Stress	Standard Deviation	Coefficient of Variation
A2	20	51450	3640	0.0706
A4	19	49810	4390	0.0881
A5	13	49050	2870	0.0585
A6	14	51830	4390	0.0846
A7	24	49010	3170	0.0647
A8	21	46440	4000	0.0861
A9	20	48280	4210	0.0873
A10	62	49520	4380	0.0885
A11	20	44320	4780	0.1078
A12	20	47060	4670	0.0992
A13	39	44650	4020	0.0900
A14	21	48580	4860	0.1001
A17	21	49870	2910	0.0583
Total Population	314	48290	4160	0.0954

Note: The mean sonic modulus of the flexural specimens was 53.6×10^6
psi. The engineering modulus for this material will be determined
during the next phase of this program.

191

TABLE 4

RESULTS OF TENSILE EVALUATIONS OF PHASE I MACRO SPECIMENS

SRI Run Number	Specimen	Temperature °F	Bulk Density (Mechanize Section) gm/cm³	Stress Rate psi/sec	Load at Fracture lbs	Fracture Stress psi	Fracture Location inches from midspan	Sonic Velocity in./µsec	Remarks
T-15	1A02-001-1T	70	3.845	5000	342.8	48390	R	0.3788*	Fracture stress base on gage diameter
T-5	-001-2T		3.849		282.5	47370	G	0.3800*	0.004 diameter
T-6	-003-1T		3.831		303.8	43770	G	0.3793*	
T-10	-003-2T		3.827		279.0	40200	G	0.3776*	
T-11	-010-1T		3.815		306.0	44090	G	0.3750*	
T-9	-010-2T		3.818		324.8	46790	G	0.3762*	
T-13	-021-1T		3.832		330.0	47550	G	0.3778*	
T-16	-021-2T		3.836		329.3	47440	R-0.1010	0.3779*	
Mean Value			3.832			45830			
Standard Deviation						2940			
Coefficient of Variation						0.0641			
T-18	2A04-024-1T		3.945		351.0	50580	G	0.3741*	
T-2	-024-2T		3.845		241.0	34730	R-0.1065	0.3950*	
T-17	-025-1T		3.827		335.3	48310	G	0.3906*	
T-4	-025-2T		3.808		348.0	50140	G	0.3871*	
T-20	-028-1T		3.823		313.5	45170	R-0.0876	0.3935*	
T-7	-028-2T		3.827		303.8	43770	R-0.1080	0.3921*	
T-22	-031-1T		3.842		336.8	48520	G	0.3942*	
T-14	-031-2T		3.851		348.8	50250	G	0.3963*	
Mean Value			3.834			46430			
Standard Deviation						5330			
Coefficient of Variation						0.1148			
T-21	2A05-036-1T		3.821		305.3	43980	G	0.3938*	
T-82	-036-2T		3.818		240.0	34580	R-0.0985	------	
	-039-1T		----		----	----	G	------	Broken in handling
T-83	-039-2T		3.832		342.8	49390	G	------	
T-80	-044-1T		3.784		223.3	46580	G	0.3943*	
T-3	-044-2T		3.841		309.0	44520	G	0.3961*	
T-8	-046-1T		3.835		330.0	47550	G	0.3921*	
T-19	-046-2T		3.846		317.3	45710	G	0.3928*	
T-12	-047-1T		3.869		158.3	22800	G	0.3955*	Fired at 80°C higher temperature
T-1	-047-2T		3.846		323.0	46540	G	------	Fired at 80°C higher temperature
Mean Value			3.845			44620			
Standard Deviation						4790			
Coefficient of Variation						0.1070			
T-94	2A07-060-1T		3.786		364.5	52520	G	0.4063	
T-88	-060-2T		3.787		317.3	45710	G	0.4100	
T-71	-060-3T		3.786		360.0	51870	G	0.4107	
T-78	-060-4T		3.786		330.0	47550	G	0.4099	Spare
T-95	-064-1T		3.787		338.3	48740	G	0.4120	
T-107	-064-2T		3.798		327.0	47120	R-0.1065	0.4159	Spare
T-75	-068-1T		3.786		307.5	44310	G	0.4098	
T-29	-068-2T		3.783		306.0	44090	G	0.4115	Spare
T-47	-068-1T		3.796		318.5	45810	G	0.4086	
T-113	-068-2T		3.801		348.0	50140	G	0.4061	
T-27	-068-3T		3.797		339.8	48960	R-0.0096	0.4055	
-----	-068-4T		3.802		-----	-----		0.4058	Spare broken during gluing
Mean Value			3.793			47870			
Standard Deviation						2870			
Coefficient of Variation						0.0598			
T-59	2A08-070-1T		3.801		292.5	42150	G	0.4144	
T-72	-070-2T		3.801		339.8	48960	G	0.4128	
T-49	-070-3T		3.749		321.0	46280	G	0.4139	
T-79	-073-1T		3.794		346.5	49930	G	0.4076	
T-101	-073-2T		3.800		348.8	50250	G	0.4151	
T-108	-073-3T		3.803		300.0	43230	G	0.4111	
T-87	-080-1T		3.800		344.3	49610	G	0.4114	
T-31	-080-2T		3.799		291.8	42040	R-0.0985	0.4094	
T-115	-080-3T		3.798		315.0	45390	G	0.4112	
Mean Value			3.794			46420			
Standard Deviation						3400			
Coefficient of Variation						0.0731			
T-70	3A09-063-1T		3.842		338.3	48740	G	0.4136	
T-112	-063-2T		3.858		284.3	40960	G	0.4156	
T-97	-063-3T		3.841		309.8	44630	G	0.4149	
T-29	-063-4T		3.861		364.3	52530	G	0.4177	
T-50	-063-5T		3.849		343.5	49500	G	0.4163	
T-65	-063-6T		3.843		309.0	44530	G	0.4120	
T-24	-065-1T		3.857		300.8	43340	G	0.4151	
T-34	-065-2T		3.855		336.0	48420		0.4175	
Mean Value			3.851			46590			
Standard Deviation						3840			
Coefficient of Variation						0.0824			
	3A10-067-1T		3.823		-----	-----		0.4124	Broken in handling
T-120	-067-2T		3.824		331.5	47770	R-0.125	0.4088	
T-116	-067-3T		3.835		342.8	49390	G	0.4143	
T-121	-067-4T		3.831		322.5	46470	G	0.4158	
T-35	-067-5T		3.824		322.5	46470	G	0.4118	
T-96	-067-6T		3.837		339.0	48850	G	0.4126	
T-98	-067-7T		3.847		375.0	54040	R-0.1002	0.4145	
T-77	-067-8T		3.840		304.5	43880	G	0.4302	
T-61	-067-9T		3.837		345.8	49830	G	0.4118	
T-56	-067-10T		3.833		336.8	48520	G	0.4118	
T-93	-067-11T		3.852		381.0	54900	G		Spare
T-26	-067-12T		3.818		306.0	44090	G	0.4119	Spare
Mean Value			3.833			48580			
Standard Deviation						3520			
Coefficient of Variation						0.0734			

TABLE 4 (Continued)

SRI Run Number	Specimen	Temperature °F	Bulk Density (Mechanics Section) gm/cm³	Stress Rate psi/sec	Load at Fracture lbs	Fracture Stress psi	Fracture Location Inches from midspan	Sonic Velocity in./μsec	Remarks
	4A11-089-A1T	70	3,726	5000	--- -	------			Broken during gluing
T-37	-089-A2T		3,776		285.8	41190	G		
T-44	-089-A3T		3,743		309.0	44530	G		
T-129	-089-A4T		3,699		244.5	35230	G		
T-130	-089-A5T		3,738		280.5	40420	G		
T-131	-089-A6T		3,716		342.8	49390			
T-133	-089-B1T		3,668		309.0	44530	G		
T-51	-089-C1T		3,624		306.8	44200	G		
T-134	-089-C2T		3,714		279.0	40200	L		
T-103	-089-C3T		3,726		273.0	39340	G		
T-90	-089-C4T		3,693		276.8	39880	G		
T-119	-089-C5T		3,722		270.0	38910	G		
T-62	-089-C6T		3,714		302.3	43550	G		
T-132	-089-C7T		3,725		240.0	34580	G		Spare
T-55	-089-D1T		3,678		264.0	38040	C		
T-66	-089-E1T		3,739		313.5	45170	R-0.1009		
	-089-E2T		3,783		-----	-----			Broken during grinding
T-48	-089-E3T		3,725		318.0	45820	R-0.1035		
T-75	-089-E4T		3,780		277.5	3 790	G		
T-42	-089-E5T		3,742		346.5	4,930	R-0.2053		
T-128	-089-E6T		3,706		321.8	46360	G		
Mean Value			3,730			42170			
Standard Deviation						4270			
Coefficient of Variation						0.1013			
T-84	2A12-095-1T		3,757		324.0	46690	R-0.1000		
T-125	-095-2T		3,760		346.5	49930	G		
T-117	-095-3T		3,762		344.3	49610	G		
T-87	-095-4T		3,761		342.8	49390	G		
T-109	-095-5T		3,759		329.3	47440	G		
T-123	-095-6T		3,759		325.5	46900	G		
	-095-7T		3,754		-----	-- --			Broken in handling
T-40	-096-1T		3,714		312.8	45070	G		
Mean Value			3,755			47860			
Standard Deviation						1820			
Coefficient of Variation						0.0380			
T-90	5A13-101-1T		3,767		292.5	42150	R-0.1036		
T-111	-101-2T		3,677		301.5	43450	R-0.1046		
T-126	-101-3T		3,764		298.5	43010	G		
T-03	-101-4T		3,760		271.5	39120	G		
-----	-101-5T		3,747		-----	-----			Broken in handling
T-85	-102-1T		3,733		298.5	43010	R-0.1044		
T-92	-102-2T		3,788		291 8	42040	G		
T-104	-102-3T		3,781		307.5	44310	G		
T-105	-102-4T		3,786		299.3	43120	R-0.1000		
T-110	-102-5T		3,763		272.3	39230	R-0.0985		
T-148	-102-6T		3,794		292.5	42150	G		
-----	-102-7T		3,794		-----	-----			Broken
T-146	-102-8T		3,791		288.0	41500	G		
T-145	-102-9T		3,796		252.8	36420	G		
T-147	-102-10T		3,794		281.5	40530	G		
T-60	-103-1T		3,791		296.3	42690	G		
T-118	-103-2T		3,810		339.8	48960	G		
T-64	-103-3T		3,788		308 3	44420	G		
T-124	-103-4T		3,808		237.8	34260	G		
T-61	-103-5T		3,767		296.3	42960	G		
T-139	-103-6T		3,800		278.3	40090	G		
T-138	-103-7T		3,802		240.9	34700	G		
T-137	-103-8T		3,802		295.5	42580	G		
----	-103-9T		3,794		-----	---			Broken in grinder
- --	-103-10T		3,801		- --	- --			Broken in grinder
Mean Value			3,781			41450			
Standard Deviation						3360			
Coefficient of Variation						0.0811			
T-58	6A14-104-1T		3 837		321.8	46360	G	0.4544	
T-45	-104-2T		3,821		354.0	51010	G	0.4140	
T-43	-104-3T		3,840		323.3	46580	G	0.4083	
T-36	-104-4T		3,838		351.0	50580	G	0.4112	
T-30	-104-5T		3,828		366.0	52740	G	0.4067	
T-23	-104-6T		3,836		. 8	54580	G	0.4101	
T-25	-104-7T		3,839		.0	51010	G	0.4120	
T-28	-104-8T		3,835		345.0	49710	G	0.4096	
T-63	-106-1T		3,857		345.0	49710	G	0.4056	
T-57	-106-2T		3,861		327.8	47230	R-0.1004	0.4106	
T-54	-106-3T		3,863		374 3	53930	G	0.4089	
T-52	-106-4T		3,862		344.3	49610	R-0.1033	0.4005	
Mean Value			3,843			50250			
Standard Deviation						2670			
Coefficient of Variation						0.0531			

193

TABLE 4 (Continued)

SRI Run Number	Specimen	Temperature °F	Bulk Density (Mechanical Section) gm/cm³	Stress Rate psi/sec	Load at Fracture lbs	Fracture Stress psi	Fracture Location inches from midspan	Sonic Velocity in./μsec	Remarks
T-38	6A17-107-1T	70	3.806	5000	286.5	41282	G		
T-127	-107-2T		3.804		351.8	50690	G		
T-138	-107-3T		3.807		384.0	55330	G		
T-138	-107-4T		3.807		309.0	44530	G		
T-106	-107-5T		3.806		328.5	47340	R-0.1000		
T-74	-107-6T		3.803		351.0	50580	G		
T-32	-107-7T		3.806		342.8	49390	G		
T-114	-108-1T		3.819		339.0	48850	G		
T-122	-108-2T		3.810		362.3	53200	G		
-----	-108-3T		3.837		-----	-----			Broken during gluing
T-102	-108-4T		3.832		314.3	45280	G		
T-100	-108-5T		2.832		309.8	44630	G		
T-76	-108-6T		3.814		338.3	48740	G		
T-86	-108-7T		3.807		330.8	47660	G		
T-33	-109-1T		3.788		352.5	50790	R-0.1157		
T-39	-109-2T		3.784		351.8	50690	G		
T-46	-109-3T		3.791		345.0	49710	G		
T-41	-109-4T		3.797		346.5	49930	G		
T-62	-109-5T		3.789		345.0	49710	G		
T-99	-109-6T		3.789		311.3	44850	G		
T-53	-109-7T		3.793		331.6	47770	G		
Mean Value			3.806			48500			
Standard Deviation						3200			
Coefficient of Variation						0.0659			

* Specimen ends cantered (Signal weak due to reduced area causing difficulty in reading output.
The values shown should not be used to compare with uncamfered specimens).

** G denotes specimen fractured within the uniform diameter gage section.
R-0.1010 denotes that the specimen failed in the breakdown radius and the fracture cross section was 0.1010 inches in diameter.

Table 5

Table of Mean Stresses, Standard Deviations, and Coefficients of
Variation for Phase I Tensile Data on Macro Specimens

Specimen Blank Type	Number of Specimens	Mean Fracture Stress	Standard Deviation	Coefficient of Variation
A2	8	45830	2940	0.0641
A4	8	46430	5330	0.1148
A5	9	42410	8470	0.1996
A6	--	-----	-----	------
A7	11	47870	2870	0.0598
A8	9	46420	3400	0.0731
A9	8	46590	3840	0.0824
A10	11	48560	3520	0.0724
A11	19	42170	4270	0.1013
A12	7	47860	1820	0.0380
A13	21	41450	3360	0.0811
A14	12	50250	2670	0.0531
A17	20	48500	3200	0.0659
Total Population	143	46300	4330	0.0935

Note: The mean sonic modulus of the tensile specimens was 54.7×10^6
psi. The engineering modulus for this material will be determined
during the next phase of this program.

195

Table 6

Results of Flexural Evaluations on Macro Specimens from SRI Part No. A10 (Surface Finish)

SRI Run Number	Specimen	Temp. °F	Bulk Density (Mechanics Section) gm/cm³	Stress Rate psi/sec	Load at Fracture lbs.	Fracture Stress psi	Fracture Location in. from midspan	Sonic Velocity in./μsec	Remarks
316	3A10-088-C11F-A	70		5000	166.3	49220	0.19	} 0.4012	Polished
315	-C11F-B				180.0	53290	0.19		Polished
318	-C12F-A				167.0	49440	0.0	} 0.4010	Polished
317	-C12F-B				166.0	49150	0.0		
320	-C13F-A				181.8	53810	0.06	} 0.4040	Polished
319	-C13F-B				180.3	53360	0.09		
286	-A4		3.842		82.5	48450	0.375	0.4033	3 RMS
287	-B5		3.830		88.0	50100	0.10	0.4024	4 RMS
292	-C1		3.842		89.8	51200	0.15	0.4050	4 RMS
296	-C2		3.831		79.5	45950	0.10	0.4051	3 RMS
294	-C3		3.836		82.5	47050	0.15	0.4051	3 RMS
291	-D1		3.843		96.3	55050	0.20	0.4055	3 RMS
295	-D2		3.827		84.8	45050	0.20	0.4030	3 RMS
293	-D3		3.818		78.5	44500	0.10	0.4045	3 RMS
321	-A6		3.856		69.3	38953	0.1	0.4092	Tension Surface as fired
322	-A7		3.765		72.3	40641	0.15	0.4048	
323	-A8		3.808		81.3	45703	0.375-0.375	0.4045	
324	-A9		3.778		67.5	37989	0.375-0.375	0.4066	

196

Table 7

Results of Tensile Evaluations of Polished Macro Specimens removed from SRI Part 1831-A-10

SRI Run Number	Specimen	Temperature °F	Bulk Density gm/cm³	Stress Rate psi/sec	Load at Fracture lbs	Fracture Stress psi	Fracture Location in.	Sonic Velocity in./microsec	Remarks
141	3A10-088-C4	70	3.809	5000	—	—	—	0.4004	3-4 rms
140	-C5		3.812		315.0	45880	0.1	0.4028	"
142	-C14		3.774		319.5	46040	0.1	0.4032	"
144	-C15		3.791		338.0	49760	0.15	0.4004	"
143	-D4		3.808		298.5	43480	0.1	0.3979	"
	-D5		3.815		318.8	45930	0.1	0.3979	

Mean Stress = 46220
Standard Deviation = 2250
Coefficient of Variation = 0.0487

197

Table 8

Results of Surface Finish Study on Macro Specimens

Surface Condition	Remarks	Flexure psi	Tension psi
pressed and fired (150-175 rms)	Blank 3A10-088	40,820	——
pressed, green machined, and fired	No data	——	——
Ground surface (15 rms) (shop ground)	Blank 3A10-087 Blank 3A10-088	47,890 50,620	48,560
Polished surface (3-4 rms) (shop polish)	Blank 3A10-088	48,420	46,220
Polished surface (lapped) (Metallurgically Lapped)	Blank 3A10-088 One-inch specimens taken fro: o-inch specimen. Alternate ends were evaluated as ground. MOR = 51,930 psi.	50,820	——

198

Table 9

Summary of Tensile and Flexural Results on Macro Specimens

Specimen Type	Blank Type or Drawing No. (Tool Set)	Sonic Velocity in./microsec	No. of Tensile Specimens	Mechanics Bulk Density of Tensile Specimens gm/cm³	Tensile Strength; Standard Deviation; Coefficient of Variation psi	Extreme Values Low and High psi	No. of Flexural Specimens	Mechanics Bulk Density of Flexural Specimens gm/cm³	Modulus of Rupture; Standard Deviation; Coefficient of Variation psi	Extreme Values Low and High psi
I-Tensile	A2 (1)	0.3778[1]	8	3.83	45,830 / 2,240 / 0.064	40,200 / 49,390	20	3.838	51,450 / 3,640 / 00.071	44,020 / 56,670
II-Tensile	A4 (2)	0.3905[1]	8	3.83	46,340 / 5,330 / 0.115	34,730 / 50,580	19	3.80	50,040 / 4,380 / 0.087	42,190 / 57,380
III-Tensile	A5* (2)	0.4287[2]	7	3.85	44,620 / 4,790 / 0.107	34,580 / 49,390	11	3.81	49,740 / 2,550 / 0.051	45,840 / 53,710
I-Compressive	A6 (1)	0.4194[2]	-	....	.....	-----	14	3.82	51,830 / 4,390 / 0.085	44,160 / 56,950
II-Compressive	A7 (2)	0.3981	11	3.79	47,870 / 2,870 / 0.090	44,090 / 52,520	24	3.81	49,010 / 3,170 / 0.065	42,050 / 53,160
III-Compressive	A8 (2)	0.3997	9	3.79	46,420 / 3,400 / 0.073	42,040 / 50,250	21	3.81	46,440 / 4,000 / 0.086	36,560 / 51,750
I-Flexural	A9 (3)	0.4132	8	3.85	46,590 / 3,840 / 0.082	40,960 / 52,630	20	3.83	48,280 / 4,210 / 0.087	34,730 / 52,730
II-Flexural	A10 (3)	0.4110	11	3.83	48,560 / 3,520 / 0.072	43,880 / 54,900	62	3.83	49,470 / 4,420 / 0.089	41,770 / 58,950
III-Flexural	A11 (4)	-----	19	3.73	42,170 / 4,270 / 0.101	34,330 / 49,930	20	3.78	44,320 / 4,720 / 0.106	33,440 / 50,340
II-Diametral Compression	A12 (2)	-----	7	3.75	47,860 / 1,820 / 0.038	45,070 / 49,930	20	3.78	47,060 / 4,670 / 0.099	29,810 / 52,880
III-Diametral Compression	A13 (5)	-----	21	3.78	41,450 / 3,350 / 0.081	35,250 / 48,960	39	3.80	44,650 / 4,020 / 0.090	32,180 / 50,020
Thin Ring	A14 (6)	0.4109	12	3.84	50,250 / 2,670 / 0.053	46,380 / 54,680	21	3.82	48,880 / 4,860 / 0.100	35,030 / 56,530
Thick Ring	A17 (6)	-----	20	3.81	48,500 / 3,200 / 0.066	41,280 / 55,330	21	3.81	49,870 / 2,810 / 0.058	44,720 / 55,410
			141		46,300 / 4,330 / 0.0935	34,280 / 55,330	312		48,390 / 4,610 / 0.0954	29,810 / 57,380

* Tensile specimens only. Specimen ends were cambered. The reduced ar.. weakened the signal causing difficulty in reading in output.
* The value shown should not be compared with other groups.
* Tensile and Flexural Specimens, but the ends of the tensile specimens were cambered. See Note 1
* Flexural specimens only
* Two Tensile and two Flexural specimens fired at 80°C higher temperature are not included in values shown. One of the Tensile specimens had a strength of 22,800 psi. Other strength values were nominal

199

TABLE 10

FRACTURE STRESS, DENSITY, AND MICROSTRUCTURAL DATA FOR SELECTED HACLO SPECIMENS

FLEXURAL SPECIMENS

Specimen No.	Description	Fracture Stress, psi x10³ Individual	Average for Group	Low, High for Group	Density, g/cc Average for Group	Low, High for Group	Individual	Individual Small Piece Vol. Measured	Coors	Grain Size Average Micron	Largest Grain Micron	Second Phase % Area Fraction	Average Size Micron	Porosity Features % Area Fraction	Average Pore Size Micron	Medium Linear Micron	Maximum Pore Size Areal Micron²
				Mechanics Section Data				Ceramics									
1	2A09-085-3F	53	46	35,53	3.83	3.92 / 3.88	3.63	3.96	3.88	3.1	15-20	5.1	1.9	5.0	1.6	27	220
2	6A14-106-11F	57	49	35,57	3.83	3.90 / 3.84	3.63	3.87	3.84	2.8	15-20	6.6	2.0	5.0	1.1	59	835
3	6A14-104-7F	35	49	35,57	3.82	3.90 / 3.94	3.83	3.87	3.88	2.9	10-15	6.7	2.0	5.8	1.3	43	430
4	5A13-102-6F	50	43	35,60	3.76	3.77 / 3.61	3.77	3.83	3.84	3.3	20-25	4.9	1.9	10.6	1.8	43	1660
5	2A12-096-11F	30	47	30,53	3.78	3.77 / 3.80	3.80	3.84	3.83	2.8	10-15	7.7	2.3	6.0	1.1	16	800
6	3A09-085-1F	35	44	35,53	3.83	3.82 / 3.85	3.82	3.87	3.86	3.2	20-25	6.4	3.4	6.4	1.2	54	1100
7	411-089D-1F	38	44	35,50	3.78	3.72 / 3.80	3.73	3.80	3.80*	3.1	10-15	7.2	1.7	10.4	1.4	32	420

TENSILE SPECIMENS

Specimen No.	Description	Individual	Average for Group	Low, High for Group	Average for Group	Low, High for Group	Individual	Individual Small Piece	Coors	Average Micron	Largest Grain Micron						
1	5A13-101-4T	39	43	34,49	3.77	3.68 / 3.81	3.76	-	3.85	3.4	20-25						
2	2A12-095-3T	50	49	45,50	3.76	3.72 / 3.76	3.76	-	3.84	3.1	15-20						
3	2A05-047-2T	47	45*	33,49	3.83	3.78 / 3.87	3.87	-	3.03	6.0***	30-35						
4	2A05-047-1T	33	45*	33,49	3.83	3.78 / 3.87	3.87	-	3.88	6.0***	30-25						
5	4A11-089C-2T	40	43	35,50	3.73	3.67 / 3.81	3.71	-	3.82*	-	16-20						
6	3A09-085-2T	48	47	41,53	3.85	3.84 / 3.76	3.66	-	2.85	-	-						
7	3A10-087-2T	46	49	44,55	3.83	3.82 / 3.85	3.82	-	3.86	-	-						
8	4A11-089A-6T	49	42	35,50	3.73	3.67 / 3.81	3.72	-	3.60*	-	-						

NOTES:
* Values taken from Coor's final report, 11-7-67, Figure 33, Item 154.
** Does not include 25,000 psi specimen.
*** Higher-than-normal firing technique.

APPENDIX A

Weibul Distribution Program

```
*DELETE              MINIM
CART ID 2571    DB ADDR  3472    DB CNT    0036
*EXTENDED PRECISION
*ONE WORD INTEGERS
*LIST SOURCE PROGRAM
      SUBROUTINE MINIM (N,SIGMU,SLOPE,SEPT,L)
      COMMON SIGMA(250), X(250),Y(250),DEVSQ(11),SIGU(12),SIGIN(5)
      WRITE(3,1)
    1 FORMAT(///43X,'LEAST SQUARE SELECTION OF SIGMA U',//)
      WRITE(3,2)
    2 FORMAT (10X, 'ZERO STRENGTH',20X, 'SLOPE',20X,'INTERCEPT',20X, 'SU
     1M OF DEV. SQ.'/)
      BASTN=ALOG(10.)
      TOTAL=N
      Q=0.
      IF(L-2)8,3,3
    8 DO 9 I=1,N
      Q=Q+1.
    9 Y(I)=(ALOG((ALOG((TOTAL+1.)/(TOTAL+1.-Q)))/BASTN))/BASTN+((ALOG(SI
     1GMA(I)))/BASTN)
      GO TO 5
    3 DO 4 I=1,N
      Q=Q+1.
    4 Y(I)=ALOG(ALOG((TOTAL+1.)/(TOTAL+1.-Q))/BASTN)/BASTN
    5 SIGU(1)=0.
      SIGIN(1)=SIGMA(1)/10.-1.
      DO 6 I=1,4
    6 SIGIN(I+1)=SIGIN(I)/10.
      DO 100 K=1,5
      DO 21 J=1,11
      DO 12 I=1,N
      IF(SIGMA(I)-SIGU(J))11,11,12
   11 SIGU(J)=SIGU(J)-(SIGIN(K)/2.)
   12 X(I)=ALOG(SIGMA(I)-SIGU(J))/BASTN
      A=0.
      B=0.
      C=0.
      D=0.
      DO 10 I=1,N
      A=A+Y(I)
      B=B+X(I)
      C=C+X(I)*Y(I)
   10 D=D+X(I)**2
      SEPT=(A*D-B*C)/(TOTAL*D-B**2)
      SLOPE=(TOTAL*C-A*B)/(TOTAL*D-B**2)
      DEV=0.
      DO 20 I=1,N
   20 DEV=DEV+(Y(I)-SLOPE*X(I)-SEPT)**2
      DEVSQ(J)=DEV
      SIGU(J+1)=SIGU(J)+SIGIN(K)
   21 CONTINUE
      IF(DEVSQ(1)-DEVSQ(2)) 22,22,23
   22 DVMIN=DEVSQ(1)
      NUMBR=1
      GO TO 25
   23 DVMIN=DEVSQ(2)
      NUMBR = 2
   25 DO 30 M=3,11
      IF(DVMIN-DEVSQ(M)) 30,27,27
   27 DVMIN=DEVSQ(M)
```

202

```
      NUMBR=M
   30 CONTINUE
      IF(NUMBR-1)35,35,99
   35 SIGU(1)=SIGU(NUMBR)
      GO TO 100
   99 SIGU(1)=SIGU(NUMBR)-SIGIN(K)/2.
  100 CONTINUE
      WRITE(3,300)SIGU(NUMBR),SLOPE,SEPT,DVMIN
  300 FORMAT (8X,E16.8,13X,E16.8,11X,E16.8,16X,E16.8)
      SIGMU=SIGU(NUMBR)
      RETURN
      END
```

FEATURES SUPPORTED
 ONE WORD INTEGERS
 EXTENDED PRECISION

CORE REQUIREMENTS FOR MINIM
 COMMON   2334 VARIABLES   50 PROGRAM   762

 END OF COMPILATION

*STORE   WS UA MINIM

```
CART ID 2571    DB ADDR  360E    DB CNT   000E

#DELETE               SWAP
CART ID 2571    DB ADDR  3472    DB CNT   000F
*EXTENDED PRECISION
*ONE WORD INTEGERS
*LIST SOURCE PROGRAM
      SUBROUTINE SWAP(N,XMEAN,SUMDV,STDEV,COVAR,TOTAL)
      COMMON SIGMA(250), X(250),Y(250),DEVSQ(11),SIGU(12),SIGIN(5)
      LESS=N-1
      DO 30 I=1,LESS
      MORE=I+1
      DO 30 J=MORE,N
      IF(SIGMA(I)-SIGMA(J)) 30,30,28
   28 SWAPX=SIGMA(I)
      SIGMA(I)=SIGMA(J)
      SIGMA(J)=SWAPX
   30 CONTINUE
      TOTAL=N
      SUM=0.
      DO 40 I=1,N
   40 SUM=SUM+SIGMA(I)
      XMEAN=SUM/TOTAL
      SUMDV=0.
      DO 44 I=1,N
   44 SUMDV=SUMDV+(SIGMA(I)-XMEAN)**2
      STDEV=SQRT(SUMDV/(TOTAL-1.))
      COVAR=(STDEV/XMEAN)
      RETURN
      END

FEATURES SUPPORTED
 ONE WORD INTEGERS
 EXTENDED PRECISION

CORE REQUIREMENTS FOR SWAP
 COMMON   2334  VARIABLES      16  PROGRAM    212

 END OF COMPILATION

*STORE      WS  UA  SWAP
```

204

```
CART ID 2571    DB ADDR  35E6    DB CNT    0036

*DELETE              HEAD
CART ID 2571    DB ADDR  3472    DB CNT    000E
*ONE WORD INTEGERS
*EXTENDED PRECISION
*LIST SOURCE PROGRAM
     SUBROUTINE HEAD(SIGO,SIGMU,XM,L)
     COMMON SIGMA(250), X(250),Y(250),DEVSQ(11),SIGU(12),SIGIN(5)
  65 WRITE(3,70) SIGO,SIGMU,XM
  70 FORMAT(/18X,'SIGMA O = ',E16.8,9X,'SIGMA U = ',E16.8,9X,'M = ',E12
    1.5)
     IF(L-2)80,90,90
  80 WRITE(3,85)
  85 FORMAT(/63X,'LOG LOG',17X,'LOG'/20X,'STRENGTH',14X,'N /',15X,'(TOT
    1AL + 1) /',11X,'(SIGMA -',/9X,'N',12X,'DATA',12X,'(TOTAL + 1)',10X
    2,'(TOTAL + 1 - N)',10X,'SIGMA U)',15X,'S',/60X,'+ LOG SIGMA',//)
     GO TO 103
  90 WRITE(3,102)
 102 FORMAT(/63X,'LOG LOG',17X,'LOG'/20X,'STRENGTH',14X,'N /',15X,'(TOT
    1AL + 1) /',11X,'(SIGMA -',/9X,'N',12X,'DATA',12X,'(TOTAL + 1)',10X
    2,'(TOTAL + 1 - N)',10X,'SIGMA U)',15X,'S'//)
 103 CONTINUE
     RETURN
     END

UNREFERENCED STATEMENTS
 65

FEATURES SUPPORTED
 ONE WORD INTEGERS
 EXTENDED PRECISION

CORE REQUIREMENTS FOR HEAD
 COMMON   2334  VARIABLES        0  PROGRAM    224

 END OF COMPILATION

*STORE       WS  UA  HEAD
```

```
*EXTENDED PRECISION
*ONE WORD INTEGERS
*IOCS(CARD,1132 PRINTER)
*LIST SOURCE PROGRAM
      DIMENSION SIGMA(250),X(250),Y(250),DEVSQ(11),SIGU(12),SIGIN(5),TIT
     1LE(20)
      COMMON SIGMA,X,Y,DEVSQ,SIGU,SIGIN
      BASTN=ALOG(10.)
    4 READ(2,5)N,L
    5 FORMAT(2I4)
      IF(N) 252,252,7
    7 READ(2,8)TITLE
    8 FORMAT(20A4)
      WRITE(3,10)TITLE
   10 FORMAT('1',1X,20A4,/////)
      IF(L-2) 12,16,16
   12 WRITE(3,14)
   14 FORMAT(' ',37X,'WEIBULL DISTRIBUTION PARAMETERS--FLEXURE DATA')
      READ(2,15)WIDTH,XLNGH,DEPTH
   15 FORMAT(3F8.4)
      GO TO 20
   16 WRITE(3,18)
   18 FORMAT(' ',37X,'WEIBULL DISTRIBUTION PARAMETERS--TENSION DATA')
      READ(2,19)VOL
   19 FORMAT(F10.0)
   20 READ(2,22)(SIGMA(I),I=1,N)
   22 FORMAT(10F8.0)
      CALL SWAP(N,XMEAN,SUMDV,STDEV,COVAR,TOTAL)
      CALL MINIM (N,SIGMU,SLOPE,SEPT,L)
      IF(L-2)50,60,60
   50 DMNSN=DEPTH*(XMEAN-SIGMU)/(2.*XMEAN)
      VOL=WIDTH*XLNGH*DMNSN
      WRITE(3,54)VOL
   54 FORMAT(/,' VOLUME = ',E16.8)
      SIGO=10.**((-SEPT-(ALOG(2.*SLOPE)-ALOG(VOL))/BASTN-0.36221568)/(SL
     1OPE-1.))
      XM=SLOPE-1.
      GO TO 65
   60 SIGO=10.**((-SEPT+ALOG(VOL)/BASTN-0.36221568)/SLOPE)
      XM=SLOPE
   65 CALL HEAD(SIGO,SIGMU,XM,L)
      COUNT=1.
      DO 140 I=1,N
      PROBA=COUNT/(TOTAL+1.)
      THIRD=SLOPE/3.
      IF(L-2)110,120,120
  110 CONTINUE
      XLLOG=(ALOG((ALOG((TOTAL+1.)/(TOTAL+1.-COUNT)))/BASTN))/BASTN+ALOG
     1(SIGMA(I))/BASTN
      XLOG=ALOG(SIGMA(I)-SIGMU)/BASTN
      PART1=(VOL*(SIGMA(I)-SIGMU)**THIRD)/(2.*SLOPE*SIGO**(THIRD-1.)*SIG
     1MA(I))
      PART2=((SIGMA(I)-SIGMU)**THIRD)/(SIGO**THIRD)
      RISK=PART1*PART2*PART2
      GO TO 122
  120 PART1=VOL*((SIGMA(I)-SIGMU)/SIGO)**THIRD
      PART2=((SIGMA(I)-SIGMU)/SIGO)**THIRD
      RISK=PART1*PART2*PART2
      XLLOG=(ALOG((ALOG((TOTAL+1.)/(TOTAL+1.-COUNT)))/BASTN))/BASTN
      XLOG=ALOG(SIGMA(I)-SIGMU)/BASTN
```

206

PAGE   2

```
  122 S=1.-1./EXP(RISK)
      ICNT=COUNT
      WRITE(3,124)ICNT,SIGMA(I),PROBA,XLLOG,XLOG,S
  124 FORMAT('N',6X,I3,9X,F8.0,14X,F6.4,16X,F8.5,13X,F8.4,10X,F10.4)
  130 COUNT=COUNT+1.
      WRITE(3,150)XMEAN,STDEV,COVAR
  150 FORMAT(///,1X,'MEAN STRESS = ',F9.1,/,1X,'STANDARD DEVIATION OF ST
     1RESS = ',F9.2,/,1X,'COEFFICIENT OF VARIATION = ',F6.4)
      GO TO 4
  252 CALL EXIT
      END

FEATURES SUPPORTED
 ONE WORD INTEGERS
 EXTENDED PRECISION
 IOGS

CORE REQUIREMENTS FOR
 COMMON    2334  VARIABLES    156  PROGRAM    730

 END OF COMPILATION
```

Security Classification

DOCUMENT CONTROL DATA - R & D

(Security classification of title, body of abstract and indexing annotation must be entered when the overall report is classified)

1. ORIGINATING ACTIVITY (Corporate author)	2a. REPORT SECURITY CLASSIFICATION
Southern Research Institute	Unclassified
2000 Ninth Avenue South	2b. GROUP
Birmingham, Ala. 35205	

3. REPORT TITLE

A QUANTITATIVE EVALUATION OF TEST METHODS FOR BRITTLE MATERIALS

4. DESCRIPTIVE NOTES *(Type of report and inclusive dates)*

Interim Report   15 April 1966 to 1 July 1969

5. AUTHOR(S) *(First name, middle initial, last name)*

C. D. Pears, H. S. Starrett, Roy E. Bickelhaupt, and Dan W. Braswell

6. REPORT DATE	7a. TOTAL NO. OF PAGES	7b. NO. OF REFS
February 1970	228	

8a. CONTRACT OR GRANT NO.	9a. ORIGINATOR'S REPORT NUMBER(S)
AF 33(615)-3265	
b. PROJECT NO. 7350	
c. TASK NO. 735003	9b. OTHER REPORT NO(S) *(Any other numbers that may be assigned this report)*
d.	AFML-TR-69-224, Part I

10. DISTRIBUTION STATEMENT This document is subject to special export controls and each transmittal to foreign governments or foreign nationals may be made only with prior approval of the Metals and Ceramics Division (MAM), Air Force Materials Laboratory, Wright-Patterson Air Force Base, Ohio 45433.

11. SUPPLEMENTARY NOTES	12. SPONSORING MILITARY ACTIVITY
	Air Force Materials Laboratory (MAMD)
	Air Force Systems Command
	Wright-Patterson AFB, Ohio 45433

13. ABSTRACT

This report covers the work completed under a preliminary phase of a program to perform a quantitative evaluation of test methods for brittle materials. This phase involved a production control study to demonstrate that a ceramic material produced in a variety of specimen configurations has uniform strength, microstructure, and density. This report includes most of the data generated to date and some preliminary analysis. More extensive analyses will be conducted and additional data generated where required.

Of the 13 blank types investigated, 10 demonstrated acceptable uniformity and reproducibility, one requires minor modifications, and two require additional work.

The only variables which correlated with strength on first inspection were fired density and a production figure of merit. There was not sufficient data to determine whether a strength-grain size correlation existed. Micro specimen fractology showed that the stronger specimens usually had the rougher, more undulating fracture surfaces.

With this material it should be possible to conduct an effective analysis of test methods; however, some additional definition of the material is required.

This abstract is subject to special export controls and each transmittal to foreign governments or foreign nationals may be made only with prior approval of the Metals and Ceramics Division (MAM), Air Force Materials Laboratory, Wright-Patterson Air Force Base, Ohio 45433.

DD FORM 1473
1 NOV 65

14. KEY WORDS	LINK A		LINK B		LINK C	
	ROLE	WT	ROLE	WT	ROLE	WT